The Geological History of the Metchosin Igneous Complex

by

Sean Timpa
B.Sc., Acadia University, 2000.

A Thesis Submitted in Partial Fulfillment of the
Requirements for the Degree of

MASTER OF SCIENCE

In the School of Earth and Ocean Sciences

Supervisors: Dr. Dante Canil and Dr. Kathy M. Gillis

ABSTRACT

The Metchosin Igneous Complex, a partial ophiolite exposed on southern Vancouver Island, is the most northerly exposure of the Eocene Crescent Terrane. The role of the Crescent Terrane in crustal genesis and Cordilleran tectonics would be affected by its tectonic setting, however that setting is in debate. Analysis of trace element compositions of basalt from the Metchosin Igneous Complex by ICP-MS was used to determine the tectonic setting in which the complex formed. REE and HFSE compositions are transitional between N-MORB and E-MORB and do not suggest a unique tectonic setting. Strong enrichments of Nb and Ta relative to N-MORB are contrary to formation in a subduction zone. In conjunction with existing plate motion data, this makes a rifted-margin origin unlikely. Interaction at a distance between the Yellowstone hot spot and the Kula-Farallon ridge is proposed to satisfy all the geological and geochemical data.

Many studies of ophiolites have interpreted high-temperature phases as hydrothermal in origin despite high permeability and low temperatures in sea floor volcanics. Metamorphic assemblages and compositions of metamorphic minerals were used to determine if alteration in the Metchosin Igneous Complex was related to sea floor alteration or obduction. Chlorite geothermometry and amphibole compositions show that peak metamorphic temperatures increase from east to west across the complex. The metamorphic facies increase from prehnite-actinolite and greenschist in the east to amphibolite in the west, corresponding with the temperatures inferred from mineral compositions. The temperature gradient is perpendicular to stratigraphy, whereas

hydrothermal patterns are expected to be parallel to stratigraphy. Therefore the pattern of alteration in the Metchosin Igneous Complex is unrelated to sea floor alteration. Metamorphism during obduction has overprinted any hydrothermal alteration patterns. The east-west thermal gradient is attributed to tilting of the complex, either by tectonic forces or by unequal exhumation due to orographic effects.

Table of Contents

List of Tables

List of Figures

Acknowledgements

First and foremost, I would like to thank my thesis supervisors, Dr. Dante Canil and Dr. Kathy Gillis for their guidance, encouragement and understanding. This project would never have been possible without their experience and insight and would never have been finished without their support and patience. I am forever grateful to both of them for their assistance with this work.

I would also like to thank Alison Hartley and Glen Nevokshonoff for early work on the complex. Dr. Steve Johnston has my gratitude for the helpful discussions on the regional tectonics. Emily Delahaye, Ikuko Wada, Tyler Rucks, and Erica Beauchamp deserve thanks for their invaluable field assistance. J. Fan, Mati Raudsepp, Rob Marr, and Bob MacKay deserve my thanks for their help with analytical equipment. Lastly, I would like to thank my mother, Jean Timpa, for her encouragement and for proof reading innumerable pages of various incarnations of this text.

Chapter 1: Introduction

1.1. Introduction

Continental growth has been ascribed to the accretion of island arcs and oceanic plateaus at convergent margins (Albarede, 1998; Condie and Abbott, 1999). Most of the Phanerozoic orogens along the western margin of North America have been attributed to the accretion of these types of terranes (Monger et al., 1982). Oceanic plateaus are hotter and composed of more buoyant material, making it easier for them to be obducted or accreted onto the continent. These oceanic terranes have been interpreted by some (Lapierre et al., 2003) to have begun evolving into continental crust prior to, or just after their accretion. Similar mechanisms have been proposed for the formation of Archean crust.

Oceanic plateaus form due to the eruption of partial melts above the heads of mantle plumes. Consequently they have large surface areas and thicknesses approaching that of continental crust. The amount of oceanic crust generated by oceanic plateaus in the last 100 Ma is 4.9% of the volume of the continental crust, equivalent to an accretion rate of 3.7 km^3/yr (Schubert and Sandwell, 1989). At this rate, all of the continental crust could have been formed by accretion of oceanic plateaus alone in less the 2 billion years (Putchel et al., 1998).

The Crescent Terrane which underlies the Olympic Mountains of northwest Washington State and the Coast Ranges of western Washington and Oregon has been interpreted as an obducted oceanic plateau (Duncan, 1982; Murphy et al., 2003). Whereas the Crescent Terrane is one of the most recent of several terranes to have accreted to the

western margin of North America (Monger et al., 1982), the origin of this terrane is fundamental to our understanding of cordilleran tectonics and continental growth. However, the origin and tectonic setting of the Crescent Terrane are still debated. Early studies suggested that it formed as seamounts offshore in a ridge-centered plume setting (Duncan, 1982; Glassley, 1974; Snavely et al., 1968). Other work has suggested that it formed by rifting of the continental margin in a transtensional setting during the early Tertiary (Babcock et al., 1992; Engebretson et al., 1985; Wells et al., 1984).

After its eruption oceanic crust may be altered by interaction with hydrothermal fluids on the ocean floor, and later by the P-T conditions generated during obduction. Alteration patterns documented for ophiolites and modern oceanic crust record the history of fluid-rock interaction associated with oceanic hydrothermal systems and, in some cases, their obduction onto land. Early ophiolite studies reported a progressive increase of metamorphic grade with depth, with most volcanic sequences being altered to zeolite to greenschist facies assemblages (Gillis and Banerjee, 2000). These patterns were generally attributed to seafloor alteration, even though thermal gradients were more typical of burial metamorphism. Exploration of the ocean floor by the Deep Sea Drilling Program (DSDP) and Ocean Drilling Program (ODP) has revealed that volcanic sequence on the ocean floor is highly permeable, permitting seawater circulation (Fisher, 1998). With the exception of tightly focused upflow zones, this circulation keeps temperatures in the volcanic sequence low (<50°C) resulting in low temperature assemblages (Alt, 1995). As a consequence, the temperatures required to form the mineral assemblages typical of many ophiolites, such as chlorite, prehnite, pumpellyite, epidote, or actinolite, cannot be attained except in localized zones of high temperature upflow. If prehnite-pumpellyite

and lower greenschist assemblages are the result of seafloor hydrothermal alteration, then either our understanding of the physical properties of the ocean crust is fundamentally flawed, or the thermal structure of the ocean floor has changed radically within the last few million years. Conversely, if these assemblages are not the result of seafloor hydrothermal alteration, then they must have been formed during subsequent metamorphic events related to the obduction of ophiolites and cannot be used to examine seafloor processes.

1.2. Reason for Study

The Metchosin Igneous Complex on southern Vancouver Island is the most northerly exposure of the Crescent Terrane (Figure 1) and is an ideal location to determine the tectonic setting in which the Crescent Terrane formed. Geophysical information provided by the LITHOPROBE project (e.g. Clowes et al., 1987; Yorath et al., 1999) and more recent analysis of surface geology (Johnston and Acton, 2003) have revealed the deep crustal structure and the processes and possible consequences of accretion of the complex beneath southern Vancouver Island. Furthermore, the tectonic setting in which the Metchosin Igneous Complex formed may be used to constrain the location and interaction of the Yellowstone hot spot with the Kula-Farallon spreading center during the early Eocene. Subduction of the Kula-Farallon ridge may have modified the characteristics of the Laramide orogeny (Murphy et al., 2003). Accretion of the Crescent terrane affected the shape of Vancouver Island and the Olympic Peninsula (Johnston and Acton, 2003).

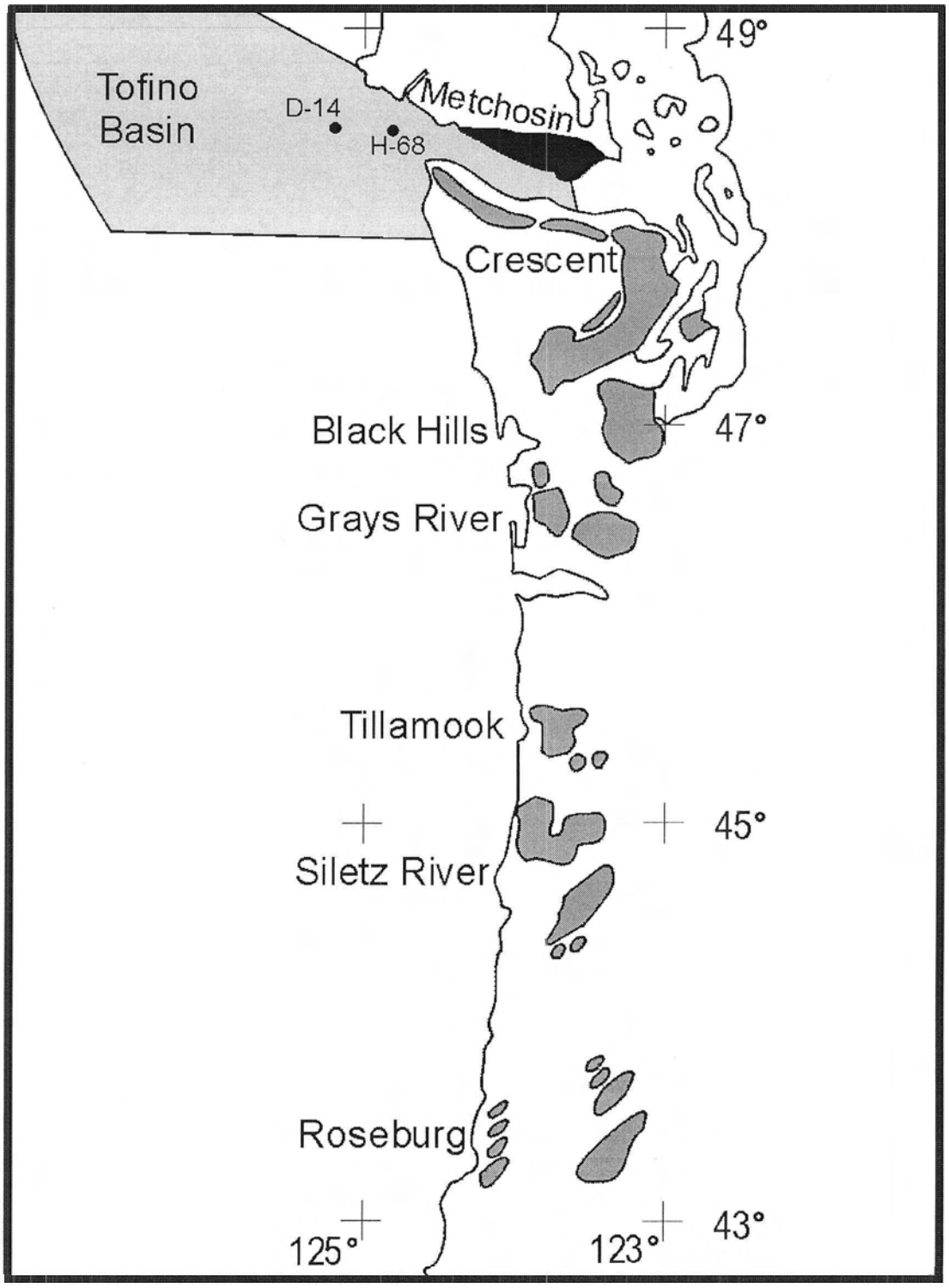

Figure 1: Location of the Metchosin Igneous Complex, Crescent Terrane and Coast Range Basalts (after Duncan, 1982). Points D-14 and H-68 are the location of the Shell Anglo Zeus D-14 and Prometheus H-68 test wells in the Tofino Basin.

The metamorphism of the Metchosin Igneous Complex has not been previously documented. Our understanding of the effects of emplacement on the metamorphic history of the complex and how emplacement-related metamorphism may obscure seafloor hydrothermal alteration may influence the interpretation of alteration patterns in other ophiolites. The presence of high-temperature assemblages in ophiolites should be viewed as suspicious because the temperatures required to produce them cannot be achieved in a normal seafloor environment.

1.3. Geological Background

The Metchosin Igneous Complex is the most northerly exposure of the Crescent Terrane which includes the Crescent Formation and the Coast Range Basalts of western Washington and Oregon states (Babcock et al., 1992). The complex is bounded to the north and west by the Leech River Fault which separates it from the Pacific Rim and Wrangel terranes (Figure 2), beneath which it was emplaced circa 42 Ma (Yorath et al., 1999). The Leech River fault has been imaged by seismic reflection and interpreted as a thrust fault dipping 35° to 45° to the northwest and extending to a depth of 10 km (Clowes et al., 1987). The Metchosin Igneous Complex is unusual in that it is thrust beneath the Pacific Rim terrane and Wrangellia, whereas most ophiolites are thrust over older terranes. The complex is locally overlain by clastic sedimentary rocks of the Oligocene Sooke Formation and Pleistocene glacial sediment (Muller, 1980). Exposure is limited to the south, east and west by the Juan de Fuca Strait. The Crescent Terrane continues offshore to the north and west of the Metchosin Igneous Complex, where it forms the basement of the Tofino Basin (Yorath et al., 1999).

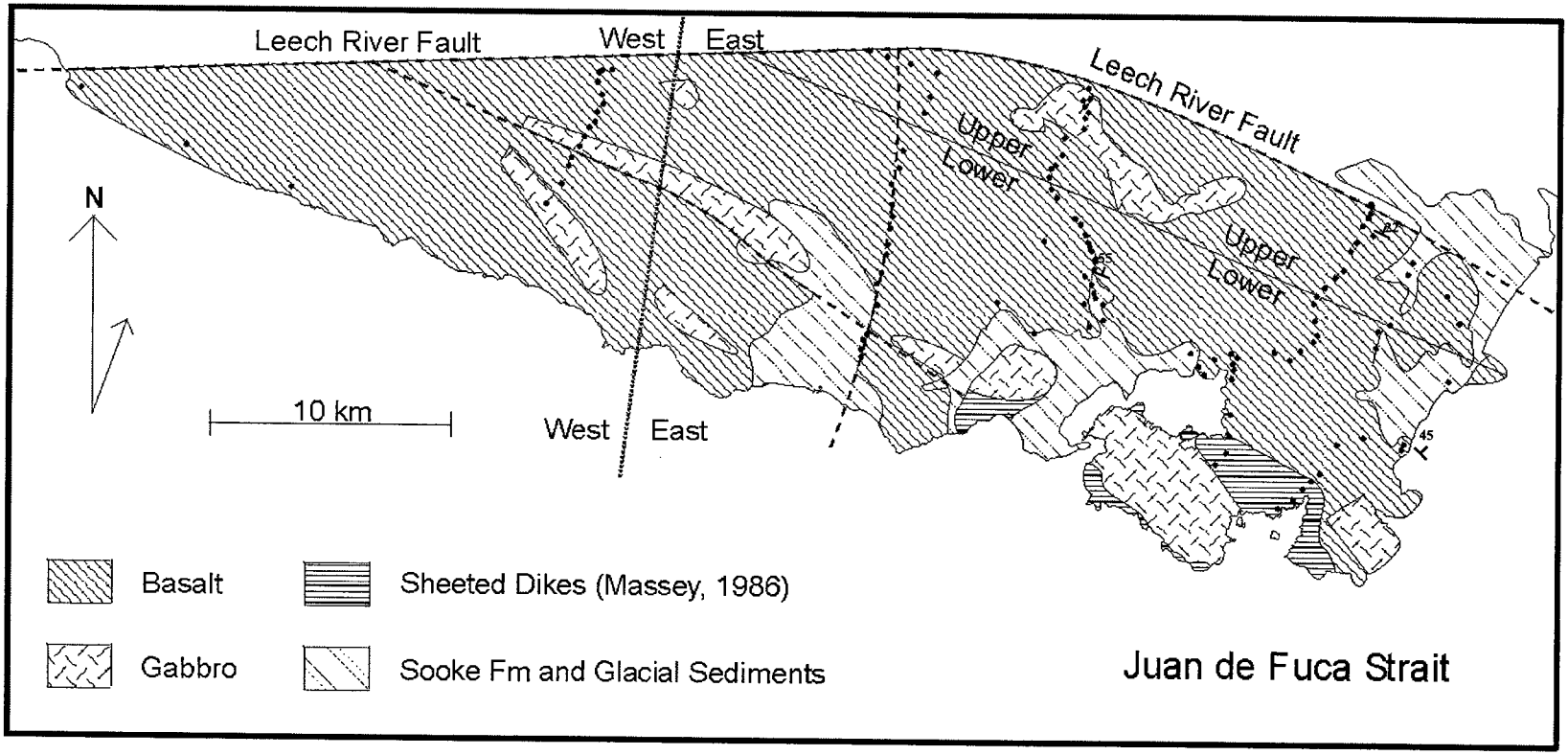

Figure 2: Geology of the Metchosin Igneous Complex (adapted from Muller, 1983). Dashed lines represent major faults, whereas the dotted line is the boundary between the east and west of the complex. The solid line is the boundary between the upper and lower volcanic sequences, and dots indicate sample locations.

The Metchosin Igneous Complex was originally described as two separate formations, the Metchosin Volcanics and Sooke Gabbro (Clapp and Cooke, 1917) but was later recognized as an ophiolite by Massey (Massey, 1986). The complex is composed of a 3 to 5 km thick volcanic sequence overlying a 500 to 1500 m thick sheeted dike complex and thin gabbroic sequence. The volcanic sequence is intruded bygabbro and tonalite sills which are several hundred meters thick and yield U-Pb ages of 58 to 52 Ma (Yorath et al., 1999). The basal mafic and ultramafic cumulates or mantle section of the ophiolite are not exposed. If present, these lithologies are either beneath the Juan de Fuca Strait or located at depth (Clowes et al., 1987; Ramachandran, 2001).

The Metchosin Igneous Complex volcanic sequence may be subdivided into upper and lower units based on morphology (Muller, 1977). The lower unit consists primarily of pillow basalt with occasional massive flows and rare interbedded chert layers. By contrast, the upper unit is almost entirely massive flows 0.5 m to 5 m thick with rare volcaniclastic deposits. The upper unit is commonly interpreted to have erupted subaerially due to the absence of submarine morphologies (Muller, 1977); however detailed mapping and sampling in this study did not reveal decisive evidence for its eruptive environment. Babcock et al. (1992) found that the Crescent Formation may be divided into lower and upper members, with strong evidence for subaerial eruption and distinct chemical trends between the two members. Similar differences in chemistry between the upper and lower units are observed in all of the Coast Range Basalts (Pyle, 1988).

The volcanic stratigraphy of the Metchosin Igneous Complex is disrupted by numerous faults, making it difficult to establish the extent of tectonic thickening (Massey,

1986; Muller, 1977). The only distinctive stratigraphic feature, the transition from the lower to upper unit, is not repeated by faulting which suggests limited tectonic thickening of the complex. The most complete stratigraphy is observed in the east where volcanic morphologies are well-preserved and are only rarely cut by brittle faults. By contrast, a greater degree of brittle deformation, a larger number of small faults and joint planes, and an overprint of primary basalt morphologies make it difficult to determine stratigraphic location in the west of the complex.

1.4. Analytical Approach and Sampling Strategy

The trace element geochemistry of basalts is a useful tool for determining the tectonic environment in which they formed (Pearce, 1996). Only limited studies have been done on the trace element geochemistry of basaltic rocks in the Metchosin Igneous Complex . Trace element geochemistry was used in this study in order to determine the tectonic setting in which the Metchosin Igneous Complex formed and to address its significance for the tectonic setting of oceanic plateau accretion.

Few attempts have been made to distinguish between seafloor hydrothermal alteration and regional metamorphism in ophiolites. Isotopic systems have been used to distinguish between the effects of seawater-derived and regional metamorphic fluids (Harper et al., 1988). Major and trace element compositions of metamorphic minerals have also proven useful in determining their environment of formation (Hannington et al., 2003).There is, however, no single proven method for distinguishing between these two metamorphic environments. Mineral assemblages and compositions were used to

constrain the P-T conditions under which the Metchosin Igneous Complex was metamorphosed.

Samples were collected along four strike-normal transects from the terrane-bounding Leech River Fault in the north to the southernmost exposure of the volcanic sequence in the south (Figure 2). Transect locations were designed to yield maximum coverage along strike, and samples were collected to give the greatest stratigraphic coverage on each transect. A major intra-terrane fault cuts the southern extent of the Tugwell Creek transect (Figure 2), and the resulting brecciation makes it difficult to determine stratigraphic location below this fault. The original basalt morphologies along the westernmost transect have been completely obscured by deformation, so it was not possible to distinguish between lava units.

Only samples collected along the two easternmost transects of the complex, where the stratigraphy is most complete and un-interrupted by faults (Figure 2), were used for geochemical analysis. Samples collected from the west of the complex were not used for geochemical analysis as a consequence of the higher degree of alteration and lack of stratigraphic control. For the easternmost transect, samples were collected from the terrane bounding Leech River Fault to the top of the sheeted dike complex. On a second transect, 20 km to the west, samples were collected along the Sooke River from the Leech River Fault to the southernmost extent of the pillow basalt exposure. In addition, four samples of drill cuttings from the Shell Anglo Zeus D-14 and Prometheus H-68 drill holes in the Tofino Basin were analyzed to determine their trace element compositions (Figure 1) to test inferences that these basement rocks belong to the Crescent Terrane.

Stratigraphic location in the Metchosin Igneous Complex is poorly constrained. In the east of the complex the boundary between the upper and lower units of the volcanic sequence provides the only good constraint on stratigraphy. This boundary has been reported from one location (Massey, 1986) and mapped at three others. It does not deviate from its predicted position by more than 100 m. The stratigraphic location of all samples was calculated based on their distance from this boundary and corrected for a 30 degree dip (Muller, 1977). The lower unit of the volcanic sequence consists largely of pillow basalt which makes it necessary to use occasional massive flows and sedimentary layers to obtain orientation of the stratigraphy. In the upper member, the orientation may be taken from the tops of massive flows. In both of these cases flat surfaces are rarely exposed and are commonly weathered to form irregular surfaces, making strike and dip unreliable. Small scale deformation has also altered the orientation of the stratigraphy in several outcrops. Dip angle in the east of the complex varies from ten to sixty degrees. Dip direction, however, remains relatively constant at ~030 degrees. The consistency of dip direction and location of the boundary between upper and lower volcanic units suggests that the stratigraphic position of samples relative to one another is relatively well constrained in the east.

In the west of the complex basalt morphologies have been totally destroyed, making stratigraphic location less accurate. Stratigraphy may be extrapolated from the east of the complex, however this may not be valid, especially due to the presence of two large intraterrane faults. The presence of volcaniclastics in the westernmost transect and seafloor sediment in one of the westernmost outcrops demonstrates that the sheeted dikes have not been reached, but otherwise stratigraphy is unconstrained.

Chapter 2: Origin of the Metchosin Igneous Complex

2.1. Igneous Petrography

The basalt in the Metchosin Igneous Complex varies in texture from hypohyaline, with up to 70% glass, to fine-grained, with generally less than 5% glass. Glass has been completely replaced in all samples and is inferred from patches of chlorite or prehnite that are not associated with other igneous phases. Samples vary from aphyric to slightly phyric basalt containing up to 15% phenocrysts. Hypohyaline samples exhibit variolitic and spherulitic quench textures with dendritic plagioclase and branching clinopyroxene. Plagioclase is acicular and commonly displays swallowtail and hopper structures. Pilotaxitic alignment of plagioclase laths is observed in four samples. By contrast, fine-grained basalt flows are more granular, indicative of a slower cooling rate. Clinopyroxene grains in fine-grained basalt are subophitic, and plagioclase is intersertal. Ilmenite is the primary opaque phase and forms up to 20% of the modal mineralogy. Most basalts are vesicular with up to 20% vesicles in some samples. The vesicle walls in five samples show much more rapid quenching than the surrounding groundmass and show collapse textures formed during cooling.

Medium-grained glomerocrysts of intergrown plagioclase and clinopyroxene occur in six samples. In the glomerocrysts, plagioclase exhibits sieve textures, and both plagioclase and clinopyroxene exhibit strong zoning, undulatory extinction, numerous fractures, and dissolution rims. The spatial relationships of these glomerocrysts and their disequilibrium and stress textures suggest that they are entrained portions of gabbro and not necessarily cognate (Dick and Johnson, 1995). Large crystals of plagioclase and

clinopyroxene that are not intergrown are interpreted to have formed by the same mechanism based on the occurrence of similar stress and disequilibrium textures. Olivine microphenocrysts (50 μm) are inferred from the presence of hexagonal chlorite pseudomorphs.

2.2. Whole-Rock Geochemistry

2.2.1. Methods

Twenty-nine samples were analyzed for major, minor, trace, and rare earth elements. Samples were selected to provide complete stratigraphic coverage of the transects and, where possible, from near pillow rims or flow margins to represent liquid compositions. Samples were crushed using a steel jaw crusher and powdered using a steel ring mill. Vesicle filling minerals were not removed from the basalt. Major and minor elements were determined by x-ray fluorescence (XRF) at the Geochemical Laboratories of McGill University (Appendix 1). Analyses were performed with a Philips PW2400 XRF spectrometer on 32 mm diameter beads prepared by lithium tetraborate fusion. An assessment of accuracy was provided by the laboratory and precision was determined by duplicate analysis of sample ST-43. The accuracy for SiO_2 is ±0.5%, and for all other major elements is within ±1%. Precision is better than ±2% for all elements except K_2O which is ±7.5%. The low precision of K_2O is a result of its low concentrations. Three analyses were discarded on the basis that they consistently plotted as outliers and showed extensive alteration in thin section. Two of these samples were collected from near a gabbroic intrusion, and the third was from near the Leech River Fault.

Two hundred mg of rock powder from each sample was dissolved using the HF-nitric dissolution technique outlined in Jenner et al. (1990). Trace element compositions were determined by solution nebulization inductively coupled plasma mass spectrometry (ICP-MS) at the University of Victoria (Appendix 2). Accuracy and precision were determined by replicate analysis of USGS BCR-2 standard. Accuracy was better than 10% for all elements except Nb (18%), Hf (18%) and Lu (16%), and precision was better than 10% for all elements except for Sm (11%). BCR-2 does not have an accepted value for Nb concentration, so the unofficial value of 14 ppm used in this study may be systematically in error. Accuracy and precision for the Tofino Basin drill cuttings is better than 5% for all trace elements except Zr and Nb which had precisions of 6.5% and 8.3% respectively and Sm which had an accuracy of 6.1%.

2.2.2. Results

2.2.2.1. Element Mobility

The Metchosin Igneous Complex is metamorphosed and may have undergone chemical modification as a result (see Chapter 3). It is therefore necessary to demonstrate that the primary igneous geochemistry in these rocks has not been changed by element remobilization (Pearce, 1996). For trace elements, this was accomplished simply by plotting one trace element against another. If both elements are immobile, then they should plot as a straight line with little scatter, whereas plotting a mobile element against an immobile element produces a random scatter of points (Figure 3) (Cann, 1970). If both elements are mobile but have similar chemical behavior, such as K and Rb, they may plot as a straight line when compared against each other; but plotting them against an element

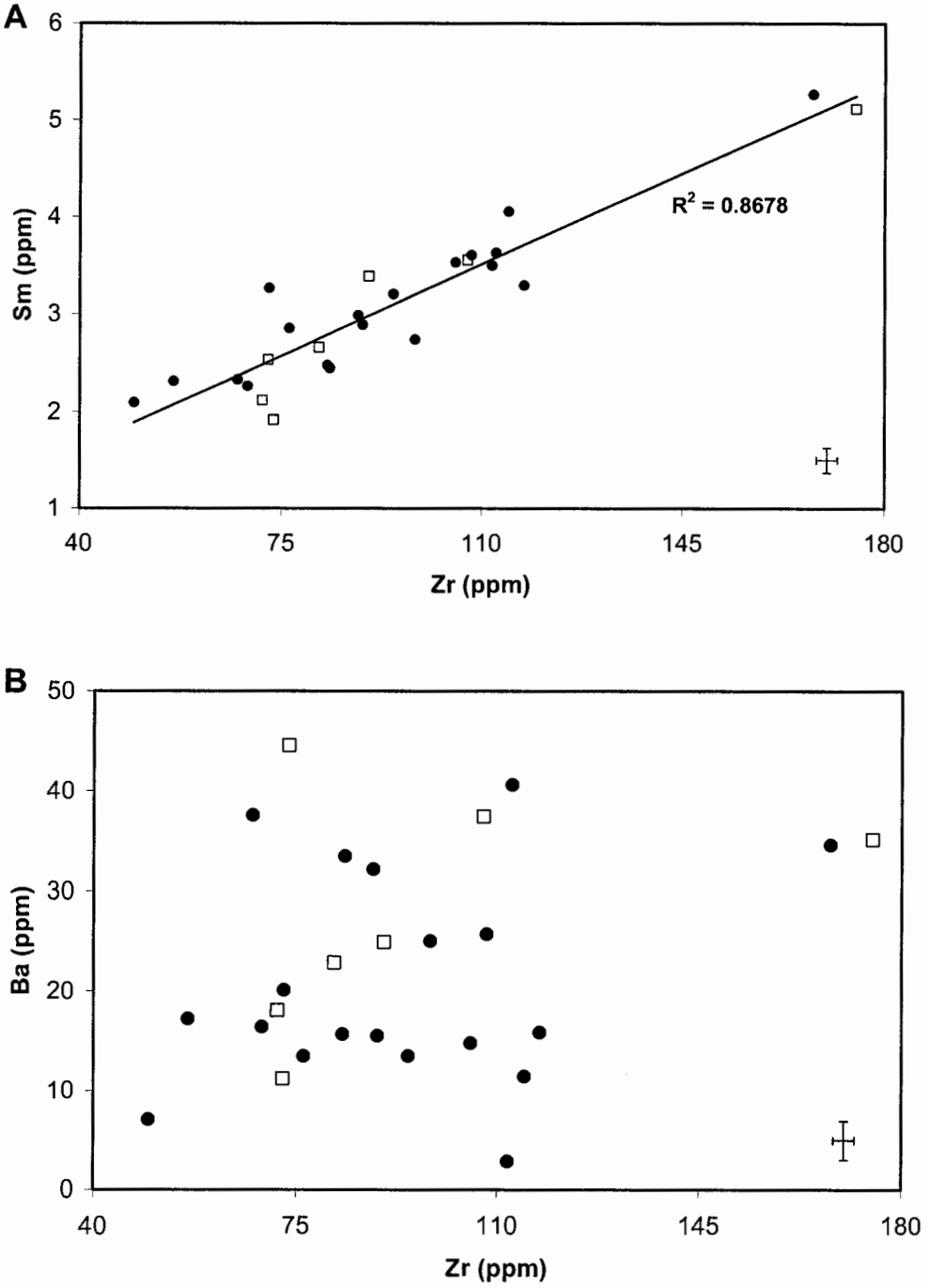

Figure 3: Diagrams of A) two conserved trace elements (Zr and Sm) showing strong correlation and B) a conserved trace element (Zr) and a mobile element (Ba) which show no correlation. Filled circles represent aphyric samples, whereas open squares represent glomerocryst-bearing samples. Sample error bars represent the maximum 2σ error.

which has a different chemical behavior produces a scatter of points. Using this approach, only K, Ba, and Sr were found to be mobile in the basalt samples analyzed in this study.

Pearce element ratios (Pearce, 1968) were used to determine the mobility of the major elements. The stoichiometric equivalent of the fractionating assemblage divided by a conserved element, was plotted against Si divided by the same conserved element (Stanley and Madeisky, 1996). Conserved elements are elements which are incompatible during magmatic differentiation and have not been subsequently remobilized. If the major elements are immobile and the fractionating assemblage has been correctly identified, the Pearce element ratios should ideally all plot along a line with a slope of 1.

Phenocryst assemblages in Metchosin Igneous volcanics suggest the fractionating assemblage is olivine + clinopyroxene + plagioclase. This is consistent with the presence of clinopyroxene, plagioclase and olivine in the gabbros underlying the volcanics in the complex (Yorath et al., 1999). Using Zr as the conserved element in the denominator yields a best fit line with a slope of 1.05 and an R^2 value of 0.98 (Figure 4), which is well within the variation expected from a natural system. These tests for element mobility assume a closed magmatic system and constant source composition. A constant source composition is not a strictly valid assumption and may account for the scatter around the observed trends. The degree of scatter between Na_2O and Mg# (Mg/(Mg+Fe))suggests that sodium may be mobile; however, due to the low concentrations of sodium, its mobility only generates a small degree of scatter on the Pearce fractionation plot and is not easily determined. The fit and slope of the regression in Figure 4 demonstrates that all other major elements have remained immobile during alteration, and that Pearce element ratios are consistent with the fractionating assemblage determined by petrography.

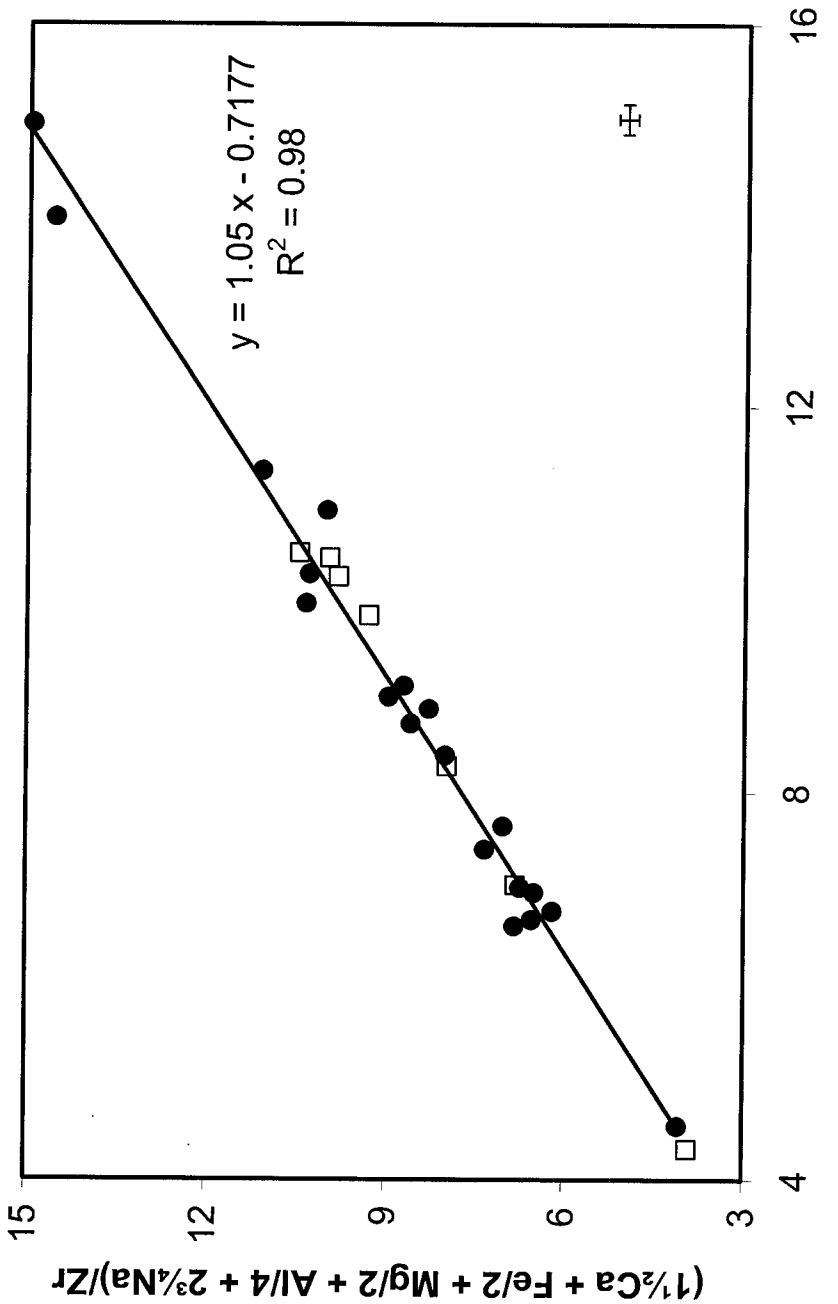

Figure 4: Pearce element diagram of fractionation of olivine, clinopyroxene, and plagioclase, represented by the equation (1½Ca + Fe/2 + Mg/2 + Al/4 + 2¾Na)/Zr, plotted against Si/Zr. Symbols are the same as those used in Figure 3. Sample error bars represent the maximum 2σ error.

2.2.2.2. Major and Trace Elements

The Mg# in samples from this study ranges from 0.65 to 0.42 and correlates with MgO, CaO and Al_2O_3 FeO and MnO (Figure 5). The conserved elements TiO_2, P_2O_5, and all rare earth elements (REE) increase with decreasing Mg# (Figure 6). SiO_2, Na_2O and K_2O are not correlated with Mg#. Glomerocryst-bearing and aphyric samples do not follow statistically different trends.

Basalts in the Metchosin Igneous Complex have flat chondrite-normalized REE patterns with only slight enrichment or depletion in the light REE ($(La/Sm)_N$ of 1.13 - 0.65) (Figure 7). A slight negative Eu anomaly ($Eu/Eu^* = Eu_N/(Sm_NGd_N)^{½}$) varies between 0.74 and 1.06.When normalized to normal mid-ocean ridge basalt (N-MORB), Nb is more enriched than Zr or Y (Figure 8).

2.3. Discussion

2.3.1. Major Elements

The immobility of the major elements during alteration, as demonstrated by Pearce element ratios, means that Mg# can be reliably used as a measure of magmatic evolution in the Metchosin Igneous Complex. The distribution coefficients of Fe and Mg between olivine and melt (Roeder and Emslie, 1970) can be used to show that mantle olivine with a composition of Fo_{90} equilibrates with melt with an Mg# of 0.73. The Mg#s of the basalt in the complex are all lower than 0.73, which demonstrates that they are not primary mantle-derived melts. The basalt compositions are most likely the product of mantle-derived melts which have subsequently undergone crystal fractionation. The

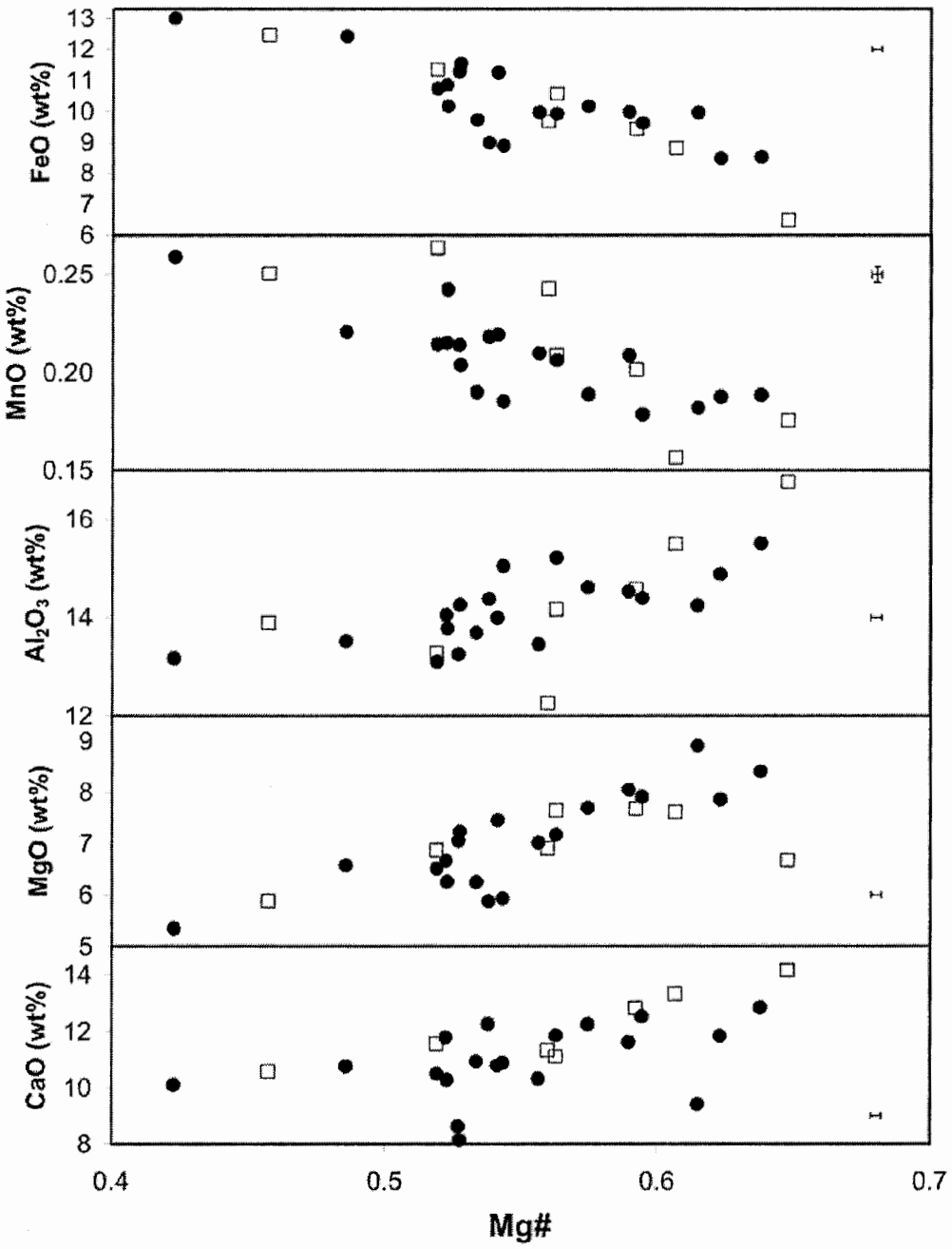

Figure 5: Diagrams of FeO, MnO, Al_2O_3, MgO, and CaO as wt% oxides plotted against Mg# (Mg/(Mg+Fe). Symbols are the same as those used in Figure 3. Errors in the wt% oxides are too small to display, with the exception of MnO. Sample error bars represent the maximum 2σ error.

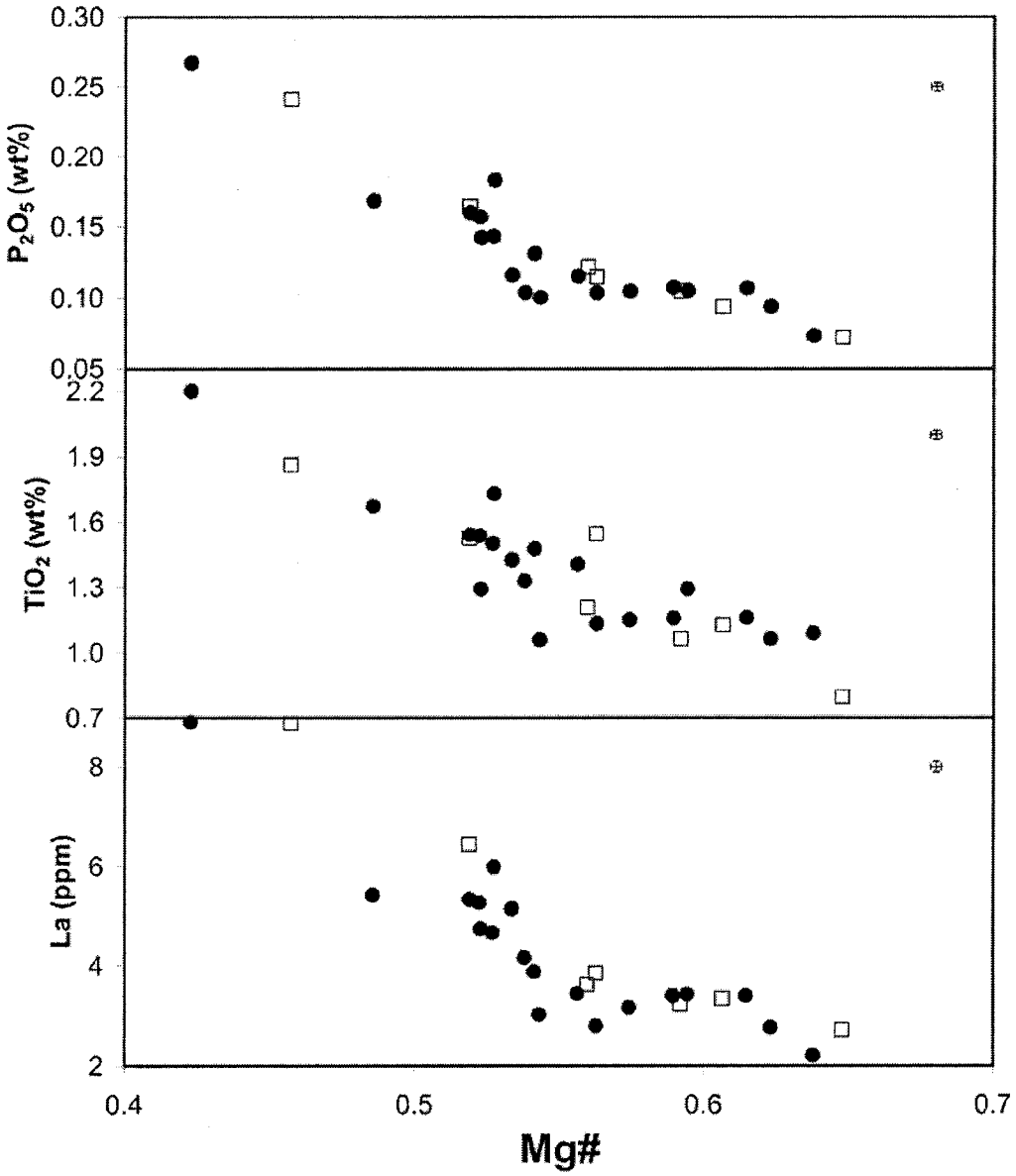

Figure 6: Diagrams of TiO_2, P_2O_5 and La plotted against Mg# (Mg/(Mg+Fe). Symbols are the same as Figure 3. Sample error bars represent the maximum 2σ error.

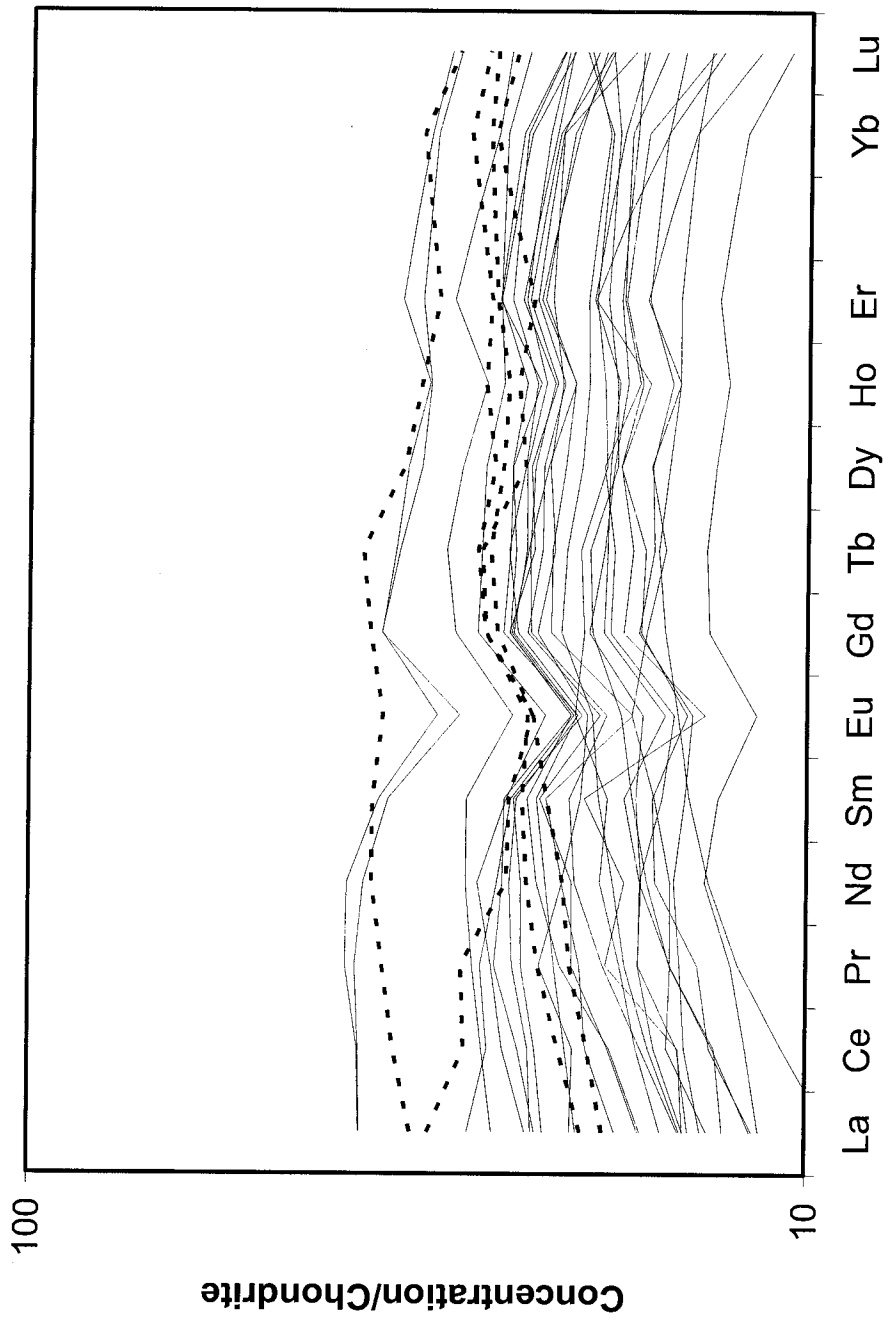

Figure 7: Chondrite normalized rare-earth element patterns for samples from the Metchosin Igneous Complex (solid lines) and the Tofino Basin (dashed lines). Chondrite values from McDonough and Sun (1995).

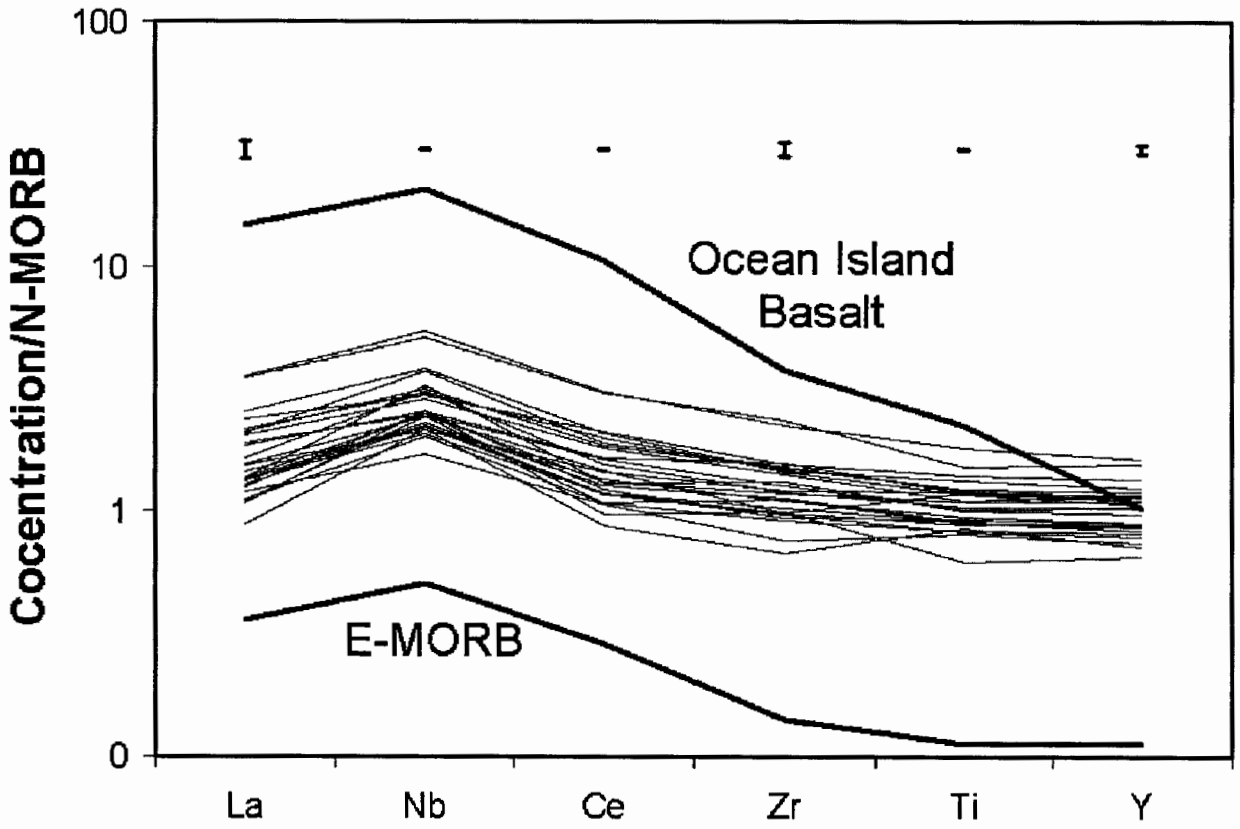

Figure 8: Trace element diagram of Metchosin Igneous Complex samples, Ocean Island Basalt and E-MORB normalized to N-MORB (Sun and McDonough, 1989). Values for E-MORB have been decreased by a factor of 7 for clarity. Unmodified values for E-MORB overlap those of the samples from the Metchosin Igneous Complex. Sample error bars represent the maximum 2σ error for each element.

tightness of fit of the major element data in the Pearce element ratio diagram (Figure 4) demonstrates that fractional crystallization is the cause of most of the variations in major element chemistry in the complex.

2.3.2. Trace Elements

Enrichment in the abundance of REE in the Metchosin Igneous Complex basalts, between 10 and 40 times chondrite (Figure 7), is most likely the product of crystal fractionation rather than a source characteristic, as demonstrated by the negative correlation between La and Mg# (Figure 6). The amount of crystal fractionation needed to produce the most REE-enriched composition from the least REE-enriched composition can be calculated by pure Rayleigh fractionation ($C_L/C_0=F^{D-1}$). Distribution coefficients for La in olivine, clinopyroxene and plagioclase of 0.0004, 0.054 and 0.27 respectively have been determined from melt inclusions in basalt (McKenzie and O'Nions, 1991). Using these distribution coefficients and assuming 50% of the fractionating minerals are plagioclase and 50% are clinopyroxene, the sample with the highest concentration of La (8.91 ppm) can be generated by fractional crystallization of 70-80% of a melt having a starting composition of the sample with the lowest La concentration (2.20 ppm). These compositions represent the most extreme cases, and only 50-60% fractional crystallization of a melt with a starting composition of 2.20 ppm La is required to produce the mean composition of 4.35 ppm. Variations in the concentrations of HFSE can be attributed to similar degrees of crystal fractionation.

These calculations are relatively insensitive to variations in the fractionating assemblage, because the distribution coefficient for plagioclase dominates the bulk distribution coefficient. Olivine has been ignored, because REEs are highly incompatible

in olivine, but assuming as much as 50% of the fractionated assemblage is olivine decreases the required amount of fractionation by less than 5%. Similarly, increasing the amount of plagioclase or clinopyroxene fractionated to as much as 70% of the fractionating assemblage causes similarly negligible differences in the total fractionation required. This calculation is also insensitive to the values used for the distribution coefficients. Decreasing the distribution coefficients by as much as an order of magnitude reduces the amount of fractionation required by only ~7%. Increasing the distribution coefficient of La in plagioclase by a factor of 2 requires ~8% more fractionation.

Basalts from the Metchosin Igneous Complex have REE profiles which are essentially flat, transitional between N- and E-MORB (Figure 7). The ratios of the HFSE Zr, Y, and Nb also fall between N- and E-MORB (Figure 8). Fitton et al (1997) used the ΔNb values in basalts:

$$\Delta Nb = 1.74 + \log(Nb/Y) - 1.92 \log(Zr/Y)$$

to distinguish between depleted and enriched MORB (Fitton et al., 1997). Values of ΔNb for the Metchosin basalts vary between 0.4 and –0.1, transitional between E- and N-MORB. Slight to moderately enriched patterns in REE and HFSE in basalt can be attributed to a wide variety of reasons including plume-ridge interaction (Robillard et al., 1992), source heterogeneity (Cousens et al., 1995), variations in partial melting (Klein et al., 1991), and thermal anomalies in the underlying mantle (Rhodes et al., 1990). Both $(La/Sm)_N$ and $(La/Yb)_N$ are negatively correlated with Mg# (Figure 9), suggesting that at least part of the LREE enrichment is due to crystal fractionation. The greater degree of scatter around these trends than around trends between La and Mg# (Figure 6) suggests

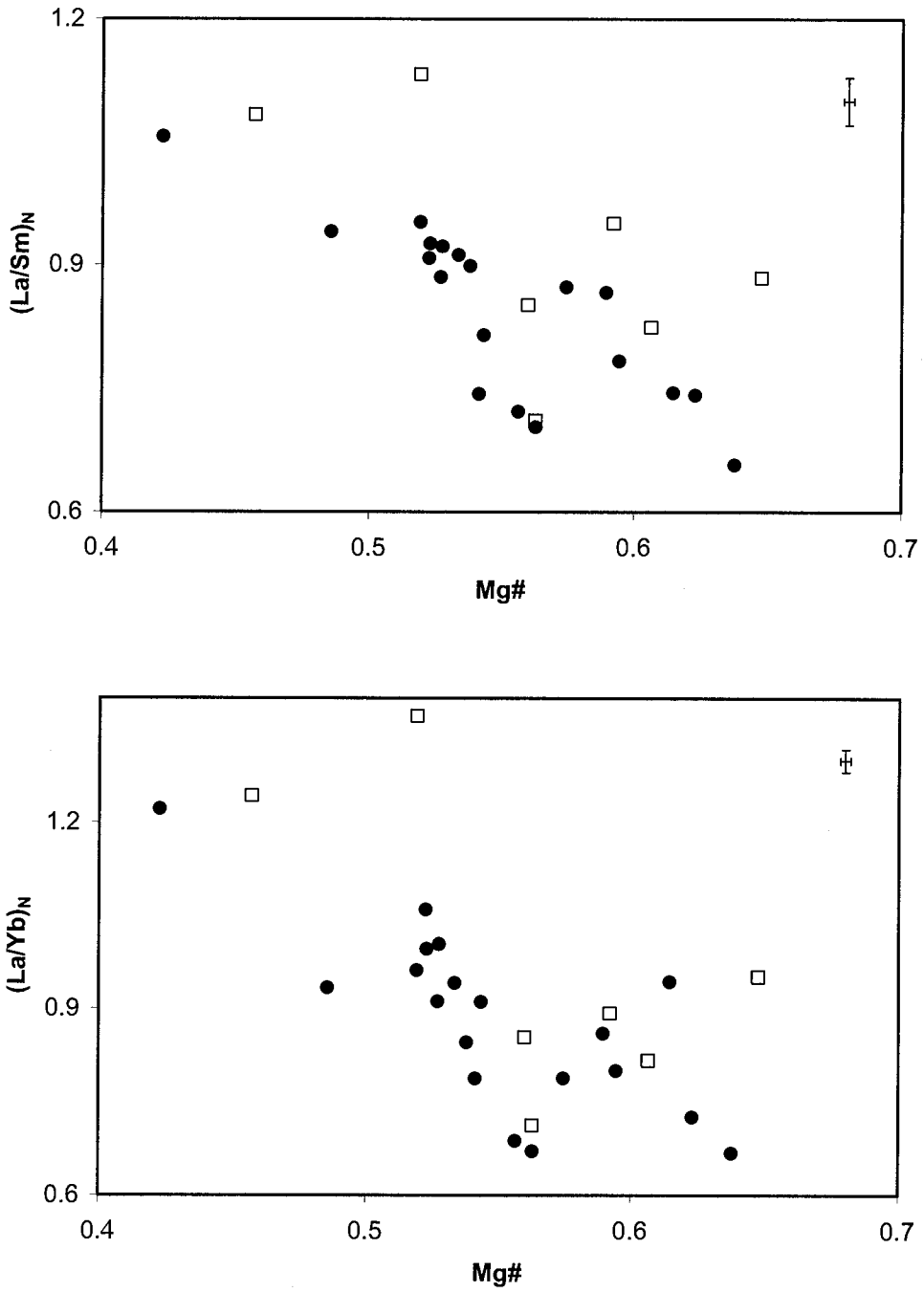

Figure 9: Diagrams of $(La/Sm)_N$ and $(La/Yb)_N$ plotted against Mg# (Mg/(Mg+Fe). Symbols are the same as Figure 3. Sample error bars represent the maximum 2σ error.

that variations in LREE enrichment are not entirely due to magmatic evolution and may in part be ascribed to mantle source heterogeneities. These variations in enrichment do not vary systematically either with stratigraphic height or laterally across the complex. The lack of systematic enrichment suggests that the source heterogeneities must have been relatively small, but not so small that they were averaged out during melting (Meibom and Anderson, 2003). Although these data permit a variety of tectonic settings for the complex, the lack of a negative Nb anomaly (Figure 8) indicates that the complex was not produced by subduction-related magmatism. A positive Nb anomaly is still present after correcting for a possible 18% excess indicated by analysis of the USGS BCR-2 standard. Ta, which is geochemically similar to Nb, also exhibits a positive anomaly on trace element diagrams.

Unlike other formations in the Crescent Terrane (Babcock et al., 1992; Pyle, 1988), upper and lower basalts of the Metchosin Igneous Complex are indistinguishable on a geochemical basis. Kilometer scale variations in geochemistry with stratigraphy are observed (Figures 10 and 11) which suggest periodic enrichment of the source region, however these variations are the same in both the upper and lower members of the volcanic sequence. Compared to other formations in the Crescent Terrane, the Metchosin Igneous Complex shows the least amount of enrichment in incompatible and rare earth elements (Figure 12). Pyle (1988) documented an increase of enrichment from north to south in the various components of the Crescent Terrane (Figure 12), and this study confirms that trend. Basalt from the Metchosin Igneous Complex and the basement of the Tofino Basin have similar REE patterns and HFSE enrichments. This suggests that the complex extends offshore to the west beneath the Tofino Basin. Based on Y, Zr and Nb

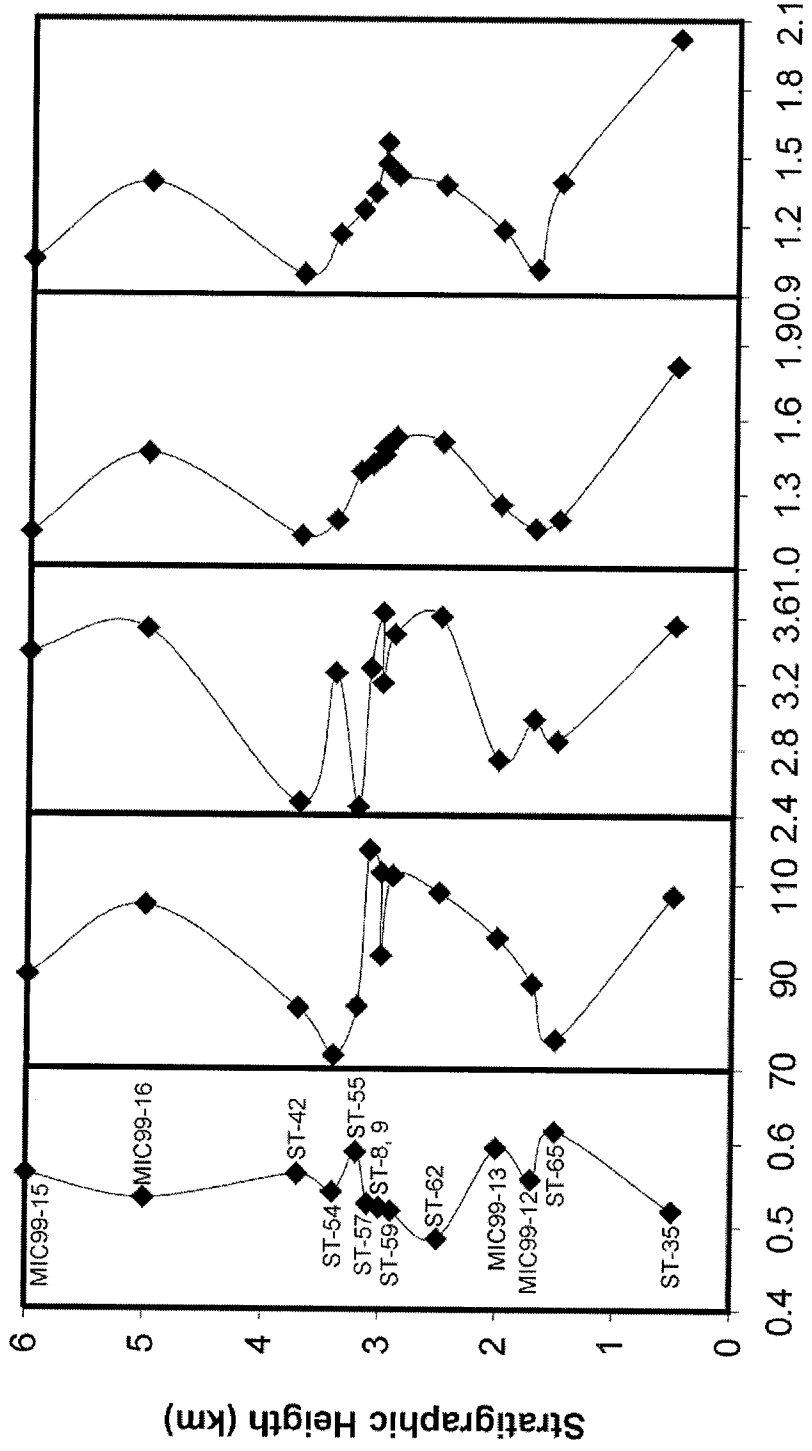

Figure 10: Diagram of Mg#, Zr and Sm concentrations, and La/Sm and La/Yb as a function of straatigraphic height (height above the top of the sheeted dike complex). Samples are from the easternmost transect (Humpback, Sooke and Happy Valley Roads).

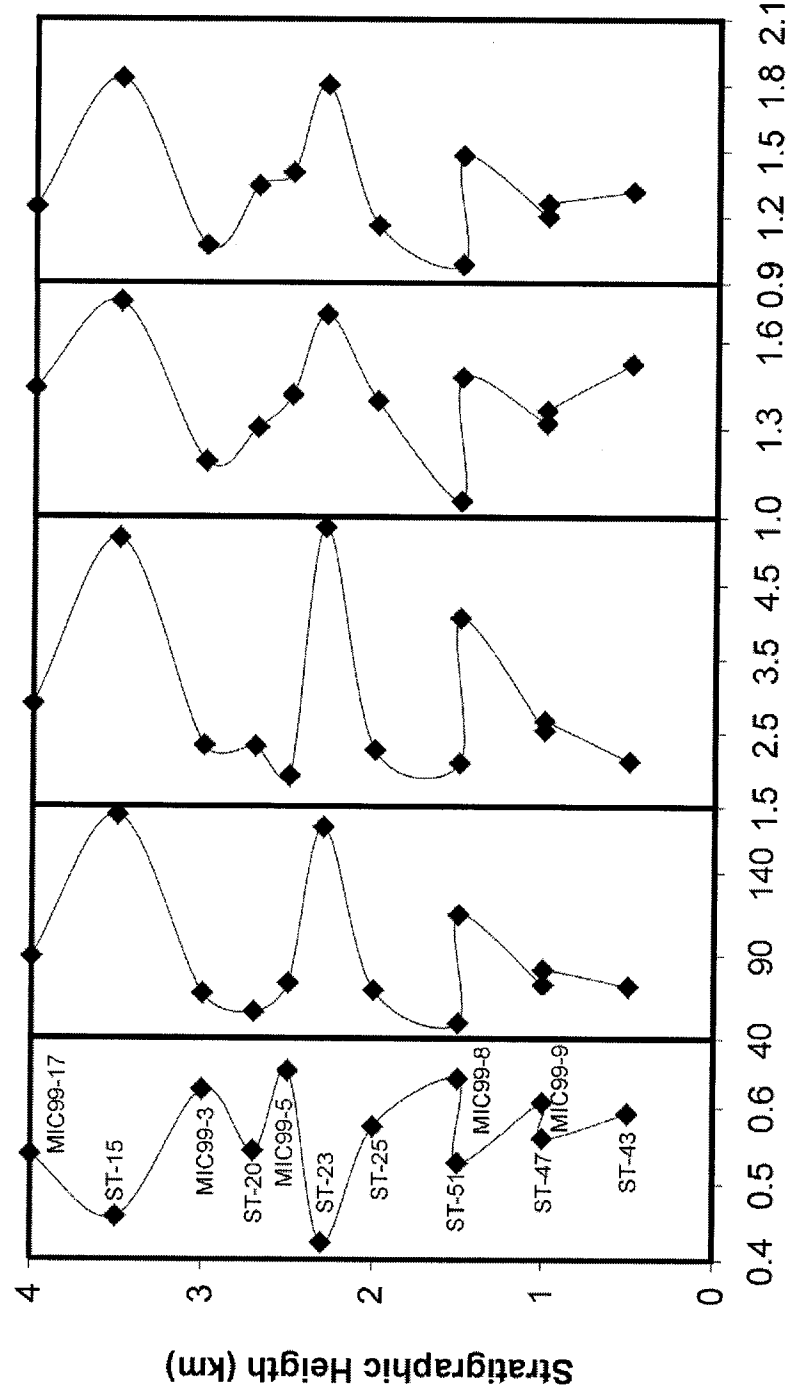

Figure 11: Diagram of Mg#, Zr and Sm concentrations, and La/Sm and La/Yb as a function of straatigraphic height (height above the top of the sheeted dike complex). Samples are from the second eastern transect (Sooke River).

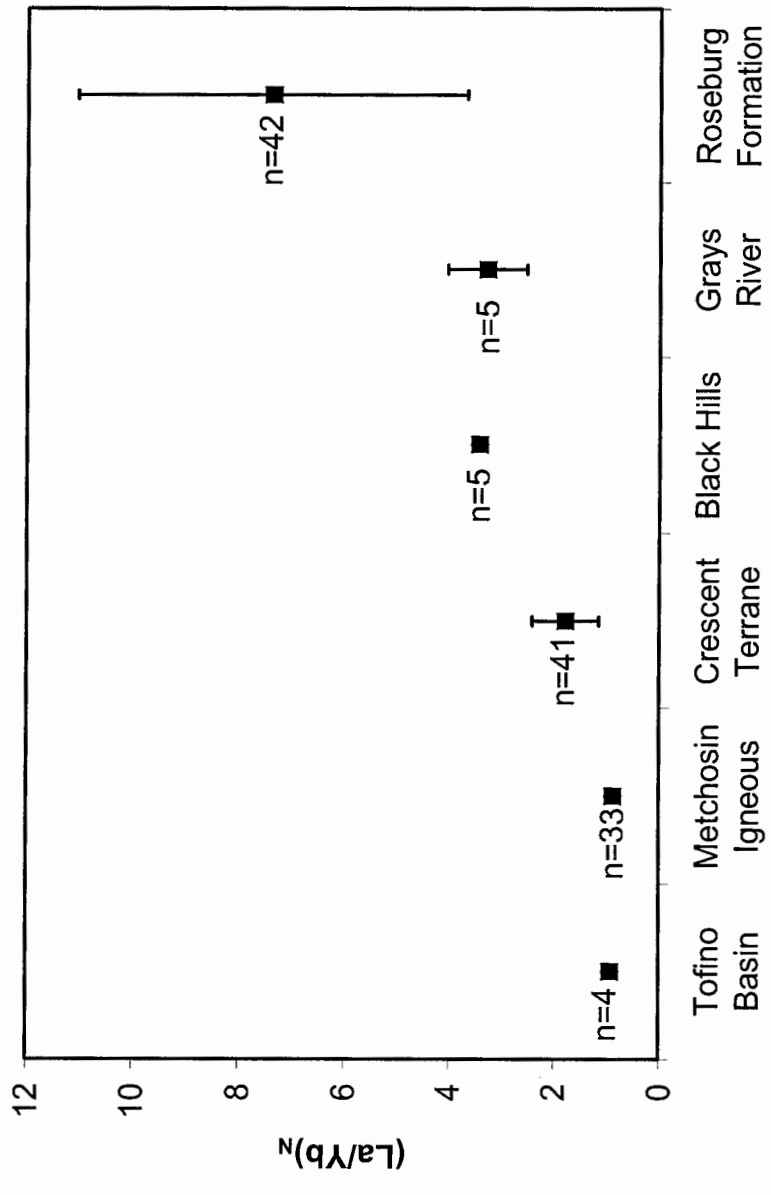

Figure 12: Diagram of $(La/Yb)_N$ for members of the Crescent Terrane (Pyle, 1988) and the Metchosin Igneous Complex demonstrating enrichment in light rare-earth elements from north to south. The Tofino Basin shows enrichment in LREE similar to the Metchosin Igneous Complex. Symbols represent the mean La/Yb_N and bars represent one standard deviation. Variations in the Metchosin Igneous Complex and Black Hills are less than the size of the symbols.

the Metchosin Igneous Complex is similar to the Lower Crescent member (Figure 13), but the latter is more enriched in LREE. There may be several eruptive depocenters within the Crescent Terrane, and the Metchosin Igneous Complex may more accurately correlate with the volcanics of Crescent Bay than those of the Dosewallips River section (Babcock, 2002 per. comm.).

2.3.3. Tectonic Setting

Several proposed tectonic settings for the Metchosin Igneous Complex and the Crescent Terrane are examined in light of the new data.

2.3.3.1. Ridge-Centered Plume Model

A mantle plume beneath the Kula-Farallon spreading center has been proposed as an origin for the Crescent Terrane because of the favorable position of the Yellowstone hot spot offshore of southern Oregon during the early Eocene (Duncan, 1982). Duncan (1982) showed that members of the Crescent Terrane become progressively older to the north and south of an age minima near the Columbia River. This trend has been interpreted as the obduction of a v-shaped chain of seamounts which formed by ridge-centered plume magmatism on the Kula and Farallon plates. The Roseburg Formation basalts, the most southerly extent of the Crescent Terrane, are geochemically similar to Hawaiian basalts (Pyle, 1988).

A ridge-centered mantle plume, analogous to Iceland, has the capacity to generate large thicknesses and similar chemistry to flows exposed in the Crescent Terrane on the Olympic peninsula, (Duncan, 1982; Muller, 1980; Pyle, 1988). The greatest difficulty for a ridge-centered mantle plume model is that it requires the Yellowstone hot spot to have been centered beneath the rapidly moving Kula-Farallon spreading center for the duration

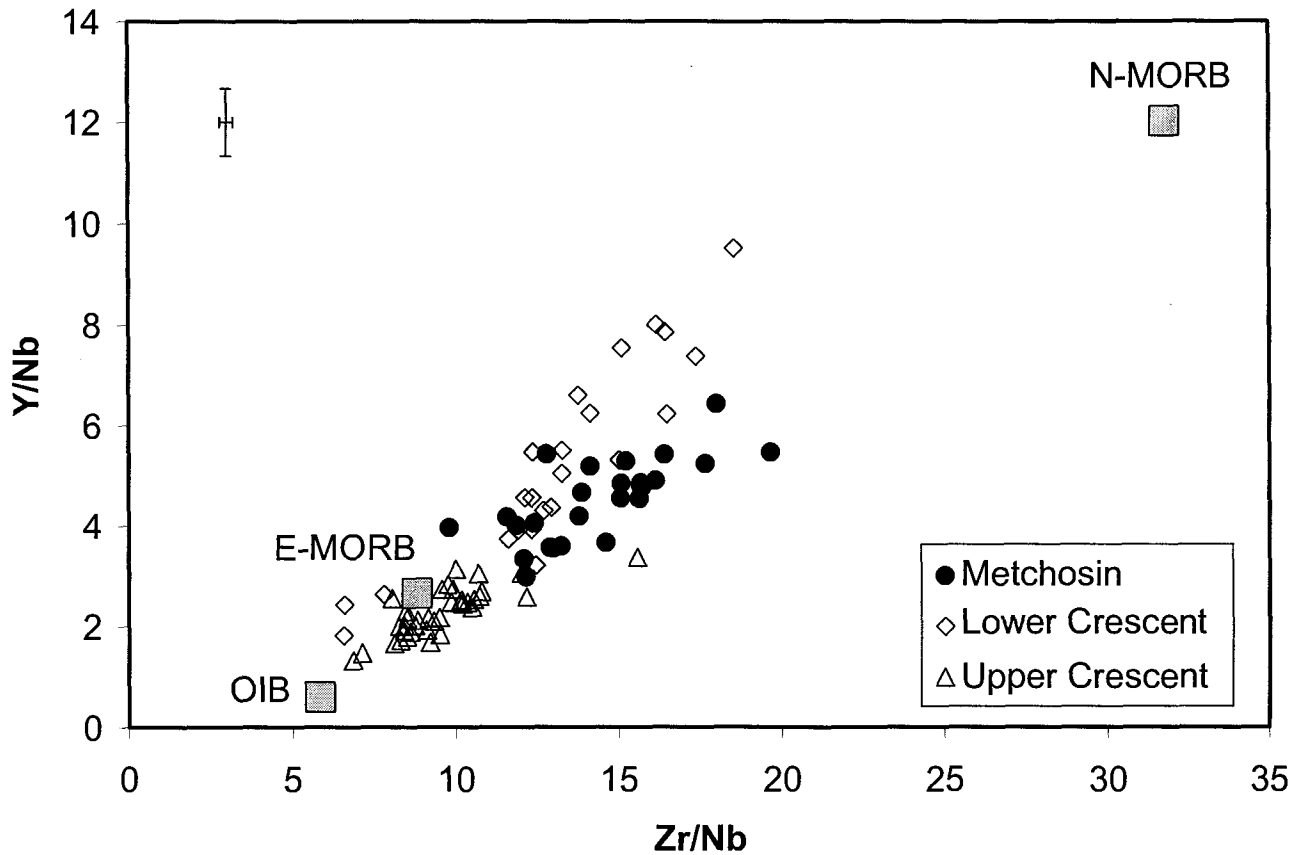

Figure 13: Comparison of Metchosin Igneous Complex basalts with Upper and Lower members of the Crescent Terrane (Babcock et al., 1992) on the basis of Y, Zr, and Nb. Grey squares are reference points for Ocean Island Basalt (OIB), N-MORB, and E-MORB (Sun and McDonough, 1989). Sample error bars represent the maximum 2σ error.

of the formation of the Crescent Terrane. Wells et al. (1984) calculated the motions of the Kula and Farallon plates at 100 mm/yr, which would produce seamount chains with a total length of 2600 km over the 13 Ma range of ages in the Crescent Terrane (Duncan, 1982). The present day length of the Crescent Terrane is roughly 600 km, which means that the majority of the seamounts would have to have been subducted (Wells et al., 1984). Paleomagnetic data demonstrate that different parts of the Crescent Terrane have undergone little or no poleward displacement or rotation since their formation (Babcock et al., 1992; Engebretson et al., 1985). Analysis of the plate motions shows that, if the Crescent Terrane were a large oceanic plateau, it would likely have undergone complex rotation and fragmentation during accretion, which contradicts the paleomagnetic data (Babcock et al., 1992).

The velocities of the Kula and Farallon plates relative to North America require a ridge-centered hot spot to initiate volcanism more than 600 km offshore. In contrast, clastic sediments derived eastward from the Cascades, San Juan Islands, and Coast Plutonic Complex are interbedded with the Crescent Terrane volcanics (Babcock et al., 1992), suggesting eruption much closer to continental North America. An Eocene Yellowstone hot spot beneath the Kula-Farallon spreading center so close in proximity to North America seems unlikely in light of the recent analysis of Murphy et al. (2003), who suggest an Eocene location 750 km west of the continental margin on a separate plate.

2.3.3.2. Rifted Margin Model

A rifted margin setting has been proposed for the Crescent Terrane because of the sedimentological evidence for the terrane in proximity to the continent for the duration of

its formation (Babcock et al., 1992; Massey, 1986; Wells et al., 1984; Yorath et al., 1999). A rifted margin setting, similar to the modern-day Andaman Sea, is appealing, because it satisfies the paleomagnetic data, does not contradict plate motion models, and allows eruption of the volcanics near the source of continental sediments (Babcock et al., 1992). The interaction of this rifted margin with the Kula-Farallon spreading center was invoked to explain the large volume of basalt in the Crescent Terrane (Yorath et al., 1999). Mixing of MORB, subduction, continental, and plume-derived sources have been used to explain the geochemical variation of Crescent Terrane basalts when plotted on basalt discrimination diagrams (Yorath et al., 1999).

The rifted margin model fails to explain the enrichment of light rare earth elements, Zr, Nb, and Ta in many of the formations of the Crescent Terrane. Although it is possible to form transitionally enriched MORB, such as is observed in the Metchosin Igneous Complex in such an environment, no mechanism exists for generating the more enriched basalts such as those that form the Upper Crescent member (Babcock et al., 1992) or the Roseburg Basalts (Pyle, 1988). Unlike the Andaman Sea which has formed along a transtensional boundary along the old, cold Indian Ocean plate, the proposed rifted margin setting for the Crescent Terrane would have formed in a transpressional setting adjacent to the young, hot, buoyant Kula and Farallon plates. The relative plate motions calculated by Engebretson et al. (1985) give an oblique northeast convergence of the North America and Kula plates at rates between 113 and 209 mm/yr and an oblique northeast convergence of the North America and Farallon plates at rates between 125 and 152 mm/yr in the timeframe and location in which the Crescent terrane formed. The lack of transpressional deformation and occurrence of extensional deformation in the Crescent

Terrane (Babcock et al., 1992) suggests that it was not formed at the boundary of the North American plate.

The convergence rates between North America and either the Kula or Farallon plate would produce subduction rather than rifting, and the subduction of oceanic lithosphere beneath the erupting Crescent Terrane would influence its geochemistry. Volcanic activity associated with the Laramide orogeny, between 75 and 40 Ma, is interpreted as the result of shallow angle subduction of the young Farallon plate beneath North America (Engebretson et al., 1985). The rifted margin model requires large volumes of basaltic magma to be generated from directly above this subducted plate, but neither the basalt from the Metchosin Igneous Complex nor any of the Crescent Terrane basalts exhibit negative Nb or Ta anomalies which are characteristic of subduction-related magmatism (Pearce, 1996). The lack of negative Nb or Ta anomalies suggests that the Crescent Terrane did not form in a rifted margin above a subduction zone and instead must have formed on the Kula or Farallon plates.

2.3.3.3. Off-Axis Plume Model

Most mantle plumes are not centered beneath ocean ridges and either cause intraplate magmatism or interact with ocean ridges at a distance (Kincaid et al., 1996). Buoyant plume material may flow subhorizontally from the plume center toward an adjacent spreading center along the upward sloping base of oceanic lithosphere (Figure 14). Plumes as far as 1200 km away can provide enriched mantle material to mid-ocean ridges on a steady state or transient basis (Schilling, 1991). The flow of plume material to the mid-ocean ridge is driven by the buoyancy of the hot plume material and the slope of the underside of the oceanic plate and opposed by the motion of the overlying oceanic

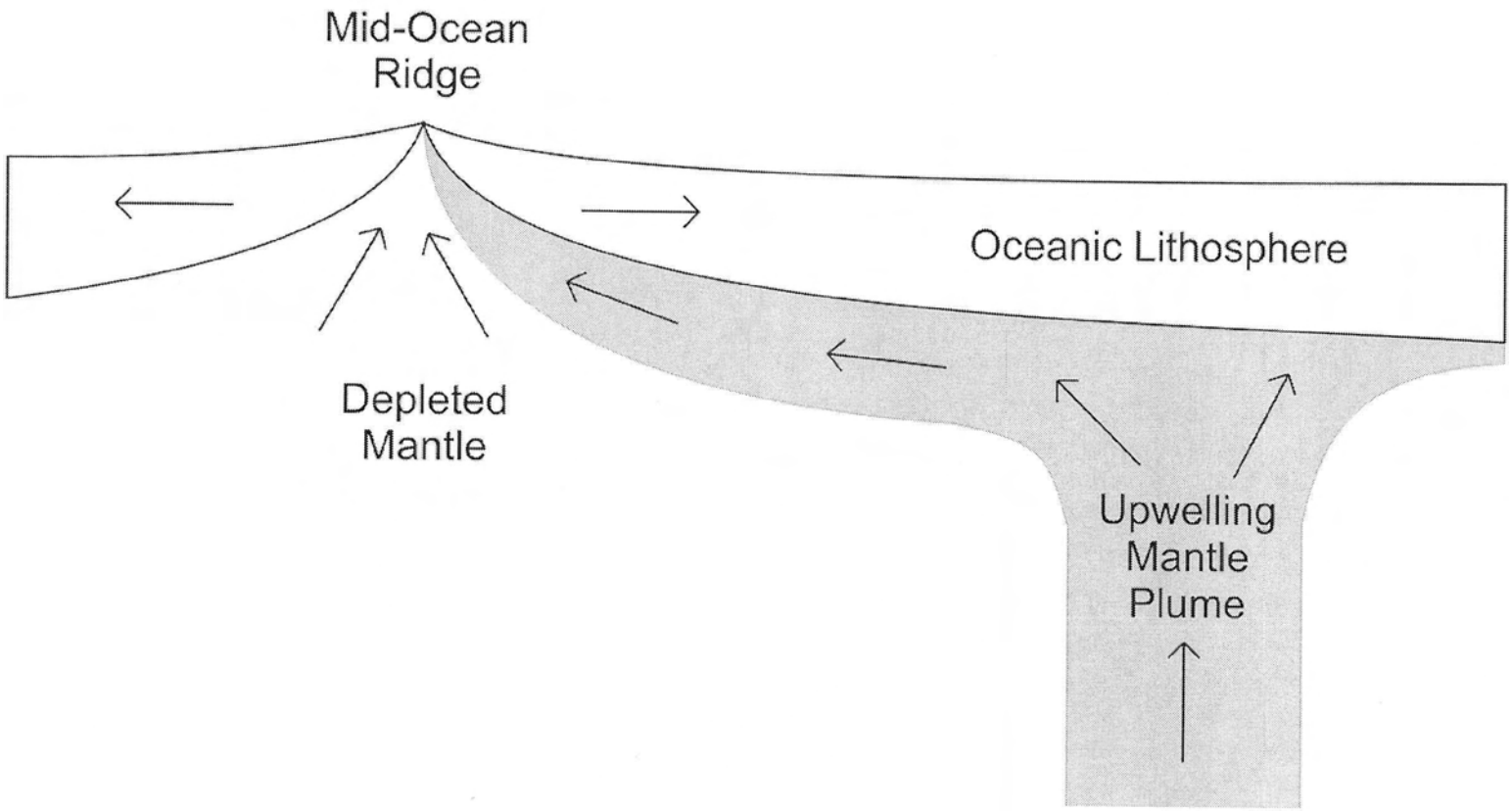

Figure 14: Schematic diagram of off-axis plume-ridge interaction (after Kingsley and Schilling, 1998). Buoyant plume material ascends along the sloping underside of the oceanic crust toward the mid-ocean ridge. The motion of the oceanic crust away from the ridge opposes the flow of plume material. At the ridge, plume material and depleted mantle material mix and melt, generating compositions transitional between N-MORB and Ocean Island Basalt.

plate away from the ridge (Kincaid et al., 1996). Mantle material flowing toward the mid-ocean ridge thermally erodes the base of the overlying lithosphere, generating a conduit in which it can travel and become progressively cooler and more diluted with distance from the plume (Kincaid et al., 1996; Kingsley and Schilling, 1998).

Although the location of the Kula-Farallon spreading center is poorly constrained during the early Tertiary, the range of possible locations is near the Yellowstone hot spot (Engebretson et al., 1985) and thus favorable for the formation of off-axis plume-ridge interactions. Unlike most off-axis plume-ridge settings, the rapid northeast motion of the Kula and Farallon plates (Engebretson et al., 1985) would deflect plume material toward the spreading center. The motion of the oceanic plates would thus enhance plume-ridge interaction while conversely decreasing the time span during which the interactions could occur. If the Yellowstone hot spot was relatively close to the Kula-Farallon spreading center, plume material could travel directly to the spreading center, where it would mix with depleted mantle material prior to eruption (Figure 15a). The effects of plume-ridge interaction would be to increase the volume of enriched heterogeneities in the mantle beneath a ridge segment, generating a more enriched mantle source which would produce a more enriched basalt.

Alternately, if the Yellowstone hot spot was further from the Kula-Farallon spreading center, plume material would encounter the subduction zone first and be deflected northward by the down-warped subducting plate. The buoyant plume material would be unlikely to travel downward along the base of the subducting plate. The plume material would be more likely to travel along the forebulge until it reached the Kula-Farallon-North America triple point, where it could erupt adjacent to the continent (Figure 15b).

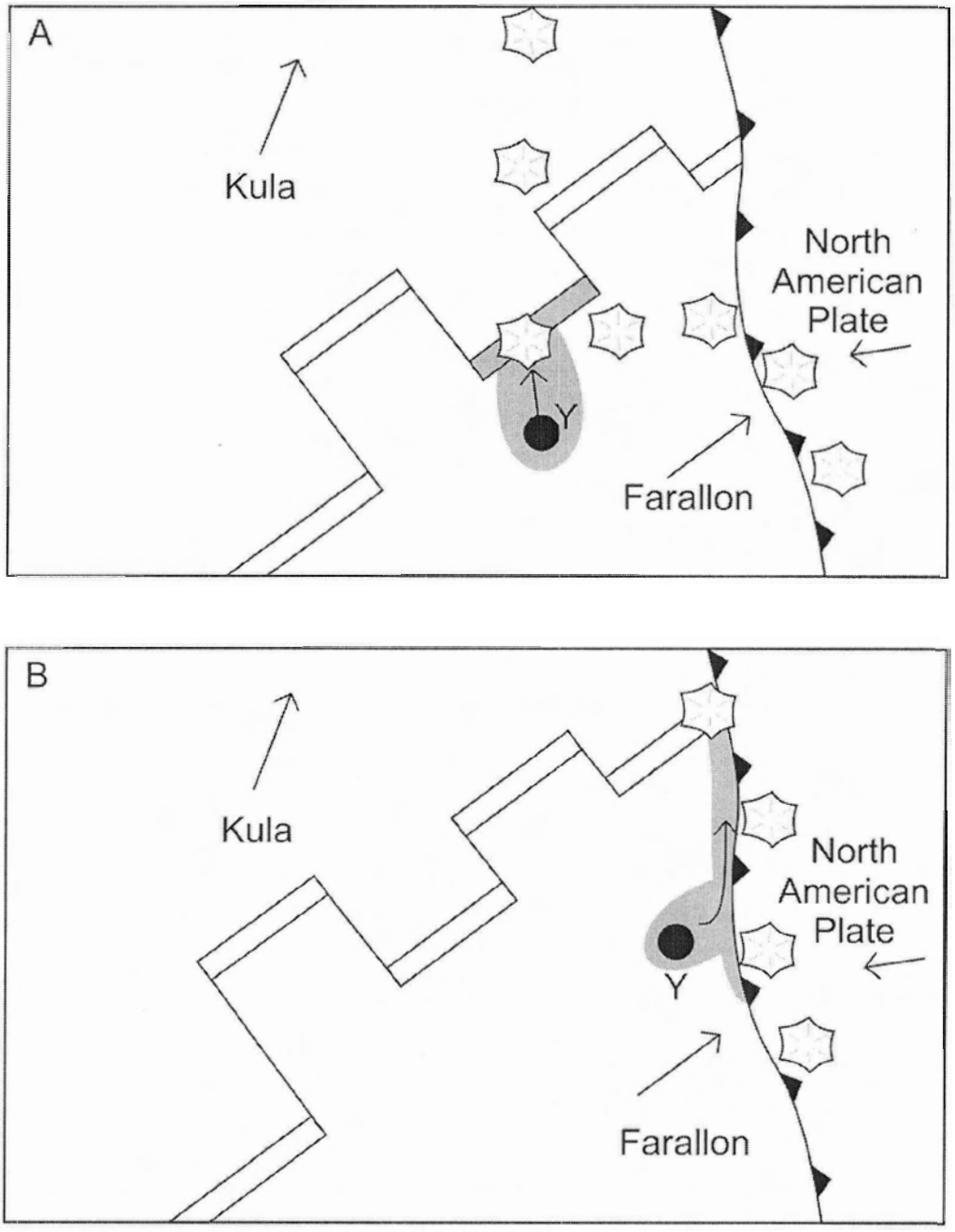

Figure 15: Schematic diagram of possible plume-ridge interactions between the Yellowstone hot spot (Y) and the Kula-Farallon spreading center: A) Direct interaction between the plume and the ridge when the plume is close to the ridge. B) Deflection of plume material (grey) toward the subduction zone by the motion of the Farallon plate followed by plume material traveling up the forebulge to the Kula-Farallon-North America triple point. Arrows indicate plate motions relative to the fixed Pacific hot spot reference frame (Engebretson et al., 1985).

Material erupted on the Farallon plate would move northeast into the subduction zone and be accreted to the margin of North America, whereas material erupted on the Kula plate would experience more northerly translation and could form the correlative Chugach and related terranes (Wells et al., 1984) in the Yukon and Alaska.

Unlike the ridge-centered plume model, the off-axis plume model is constrained only by the location of the Kula-Farallon spreading center and its distance from the Yellowstone hot spot. Neither of these values is well constrained (Engebretson et al., 1985), but the range of possible locations for the spreading center places it well within the limits of plume-ridge interaction. The northeast motion of the Kula-Farallon spreading center (Engebretson et al., 1985) would have lead to an increasing separation between the spreading center and the plume, resulting in increasing dilution of the plume material by depleted mantle material (Kingsley and Schilling, 1998) and the observed trend in enrichment from south to north in the Crescent Terrane (Figure 12). Variations in the rate of supply of plume material to the ridge (Kincaid et al., 1996) would explain the variations in trace element enrichment (i.e. La/Sm, ΔNb) observed in the Metchosin Igneous Complex. The off-axis plume model is most attractive because it allows production of large quantities of magma of the observed compositions in close proximity to the continental margin over the13 Ma (Duncan, 1982) during which the Crescent Terrane was formed.

Chapter 3: Metamorphism of the Metchosin Igneous Complex

3.1. Analytical Methods

The metamorphic mineral assemblages were determined for sixty samples from the Metchosin Igneous Complex. Metamorphic mineral compositions were determined by electron microprobe for nineteen of these samples using the JEOL-8200 SuperProbe at the University of Calgary. Wavelength-dispersive spectroscopy (WDS) analyses were performed at a 15 keV accelerating potential and 10 nA current, except for garnet which was analyzed using a 20 nA current. Zeolite and carbonate were analyzed using a beam defocused to 10 μm, whereas all other minerals were analyzed with a focused beam. Opaque phase mineralogy and the replacement of primary plagioclase by albite were confirmed by energy-dispersive spectroscopy (EDS). Fourteen additional samples were analyzed using the JEOL-8200 SuperProbe at Dalhousie University. Mineral compositions were determined by WDS using the same conditions described above. The mineral assemblages in fracture fill from six samples, vesicle fill from two samples, and one sample of interflow sediment were determined by X-ray powder diffraction at the University of Alberta.

3.2. Observations

3.2.1. Metamorphic Petrography

The volcanic sequence of the Metchosin Igneous Complex is altered to sub-greenschist to amphibolite facies assemblages. The degree of alteration of igneous minerals varies from a few percent to 100%. For the purposes of this study, the east and

west of the Metchosin Igneous Complex are considered separately due to the differences in alteration between the two areas (Table 1).

3.2.1.1. Eastern Area

In the east of the complex, investigations along the three easternmost transects (Figure 2) show that the original basalt morphologies are well preserved, except immediately adjacent to the Leech River Fault. Interstitial material in the groundmass is partially (<20%) replaced by the common assemblages (1) chlorite + albite ± epidote ± amphibole or (2) chlorite + prehnite + albite ± epidote ± amphibole. Assemblage (1) occurs in the upper and lower lavas of all three transects, with the exception of the upper lavas of the easternmost transect where assemblage (2) occurs. Chlorite is the most common alteration mineral, replacing interstitial material, filling microfractures, and lining grain boundaries. Prehnite is restricted to the upper volcanic unit where it replaces interstitial material and is intergrown with chlorite. Amphibole and prehnite occur with chlorite and epidote in four samples at the southernmost limit of prehnite occurrence.

Amygdule assemblages are similar to those of the groundmass (Table 1), except that epidote and amphibole are proportionally more abundant, and that the prehnite + chlorite ± quartz ± epidote assemblage is only observed in samples from the upper volcanic sequence of the easternmost transect. Vesicles containing chlorite have a thin outermost shell of chlorite and may be intergrown with minor amounts of amphibole. These vesicles are dominantly filled with epidote± quartz (Figure 16). Amphibole is typically a minor phase and occurs intergrown with epidote in approximately half the epidote-bearing samples. Anhedral grains of pyrite occur near the centers of epidote-bearing vesicles. In three samples, subhedral grains of andradite were observed within the

Feature	East Metchosin Igneous Complex	West Metchosin Igneous Complex
Metamorphic facies	Prehnite-Actinolite to Greenschist	Upper Greenschist to Amphibolite
Groundmass alteration assemblages	chl + ab ± epi ± act chl + prh + ab ± epi ± act	hbd + chl + epi + plag
Vesicle fill assemblages	chl ± epi ± act ± qtz ± and ± pyr prh + chl ± qtz ± epi	None. Vesicles absent.
Fracture fill assemblages	chl ± qtz; epi ± qtz ± act ± chl; prh ± chl ± qtz; zeolite and carbonate	chl ± qtz; epi ± qtz ± act ± chl; prh ± chl ± qtz; carbonate
Degree of alteration	Slight. Primary igneous features preserved. Alteration of primary igneous minerals is limited to grain boundaries and microfractures. Alteration minerals dominantly replace interstitial material and fill fractures and vesicles.	Pervasive. Primary igneous features obscured on all scales. Primary igneous minerals entirely replaced with the exception of occasional highly altered relic plagioclase grains. Some samples exhibit weak foliation of alteration minerals
Type of deformation at the Leech River Fault	Exclusively brittle fracture	Ductile folding and brittle fracture

Table 1: Summary of general alteration characteristics

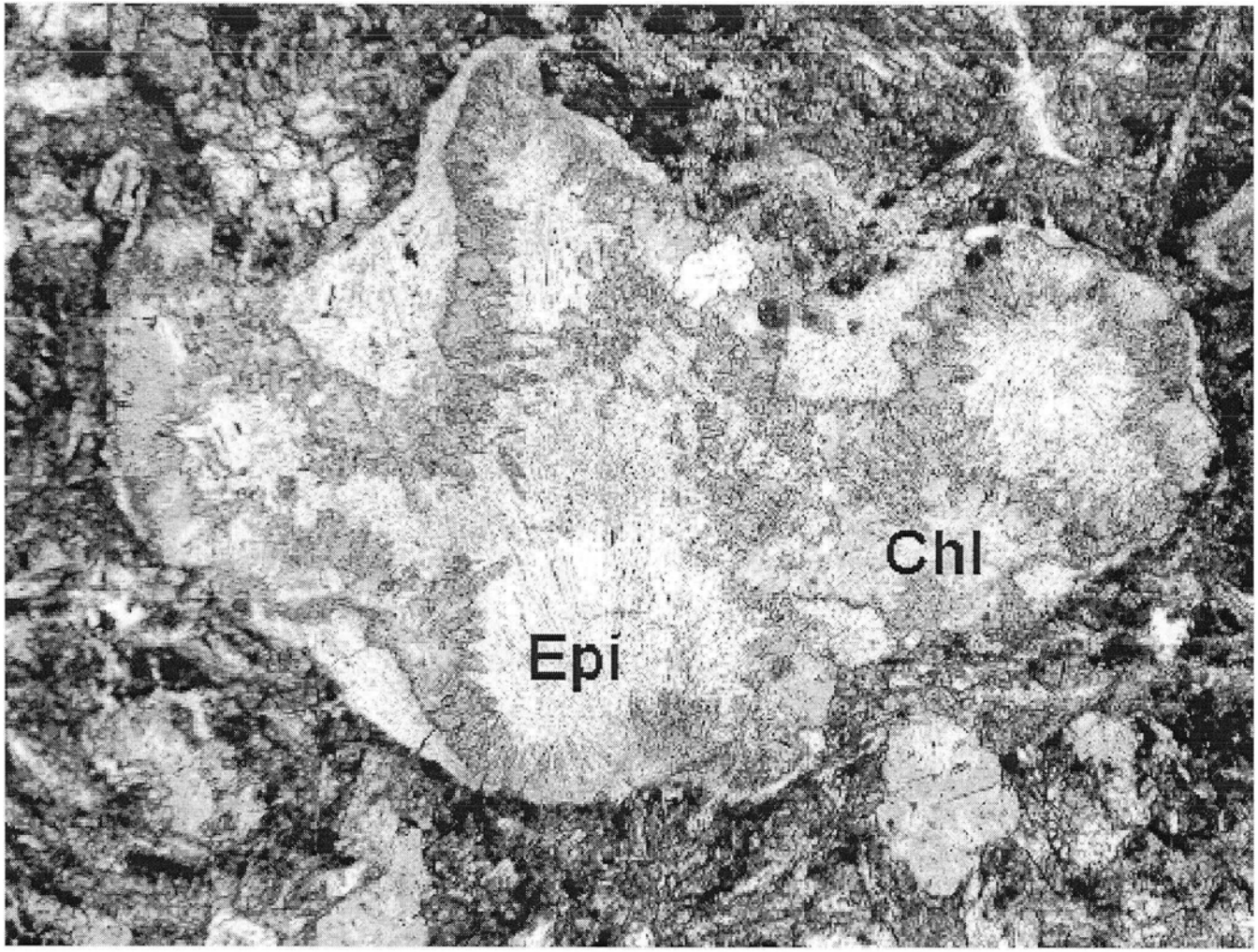

Figure 16: Photomicrograph of an amygdule filled with radial epidote (Epi) rimmed by chlorite characteristic of the eastern field area (field of view=3 mm).

epidote, and in one sample the andradite forms a shell within the epidote.

Vesicles with the chlorite + prehnite ± quartz ± epidote assemblage exhibit a wide range of mineral associations. Prehnite-dominated assemblages are the most common and occur in the sequence: cryptocrystalline intergrowths of prehnite + qtz → anhedral prehnite sheets → intergrown bundles of prehnite + chlorite (Figure 17) or prehnite → chlorite. Where present, epidote is the last mineral to have formed. None of the samples have both prehnite and amphibole in their vesicle filling assemblages.

Calcite and zeolites were also seen filling vesicles. In all instances where these minerals occur, the vesicles are connected by a network of fractures which contain calcite or zeolite, and other metamorphic minerals exhibit dissolution textures.

Brittle deformation in volcanic sequence in the east of the complex is limited to narrow cooling fractures (<1 mm wide). Fractures containing chlorite ± quartz are the oldest and are cross-cut by all other types of fractures. Fractures filled with epidote ± quartz ± actinolite ± chlorite or prehnite ± chlorite ± quartz are intermediate in age, cross-cutting fractures filled with chlorite ± quartz and are cross-cut by fractures filled with carbonate or zeolite. These intermediate aged fracture assemblages do not coexist, so no age relationship could be determined between them. Carbonate and zeolite veins commonly merge and appear to be coeval.

3.2.1.2. Western area

By contrast, in the west of the complex along the westernmost transect and three outcrops further to the west (Figure 2), the groundmass has been pervasively altered to amphibole + chlorite + epidote + plagioclase (Figure 18). Amphibole and epidote are dominant groundmass phases. Chlorite is less common than in the east but is still an

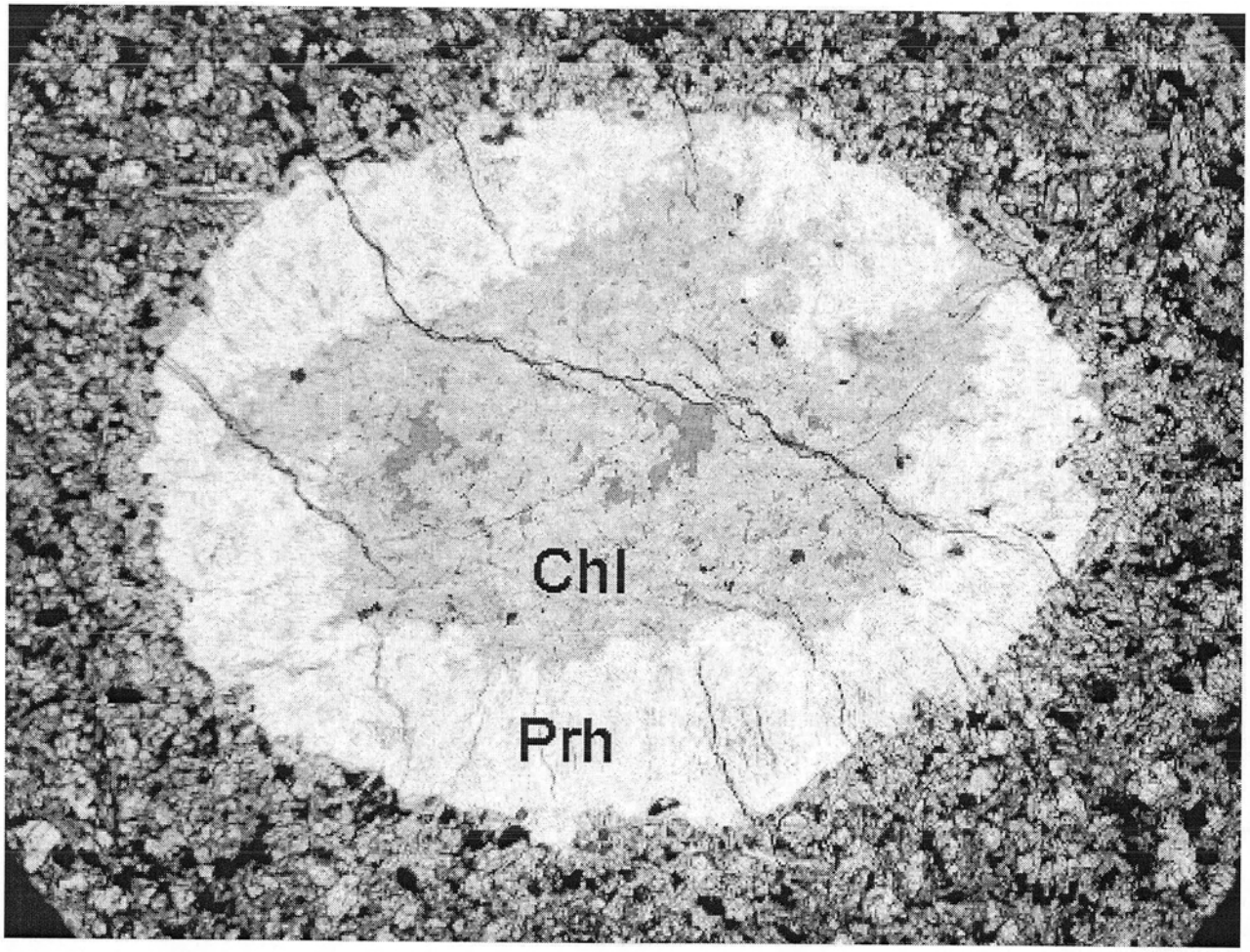

Figure 17: Photomicrograph of an amygdule filled with prehnite (Prh) surrounding chlorite (Chl) characteristic of the eastern field area (field of view=3 mm).

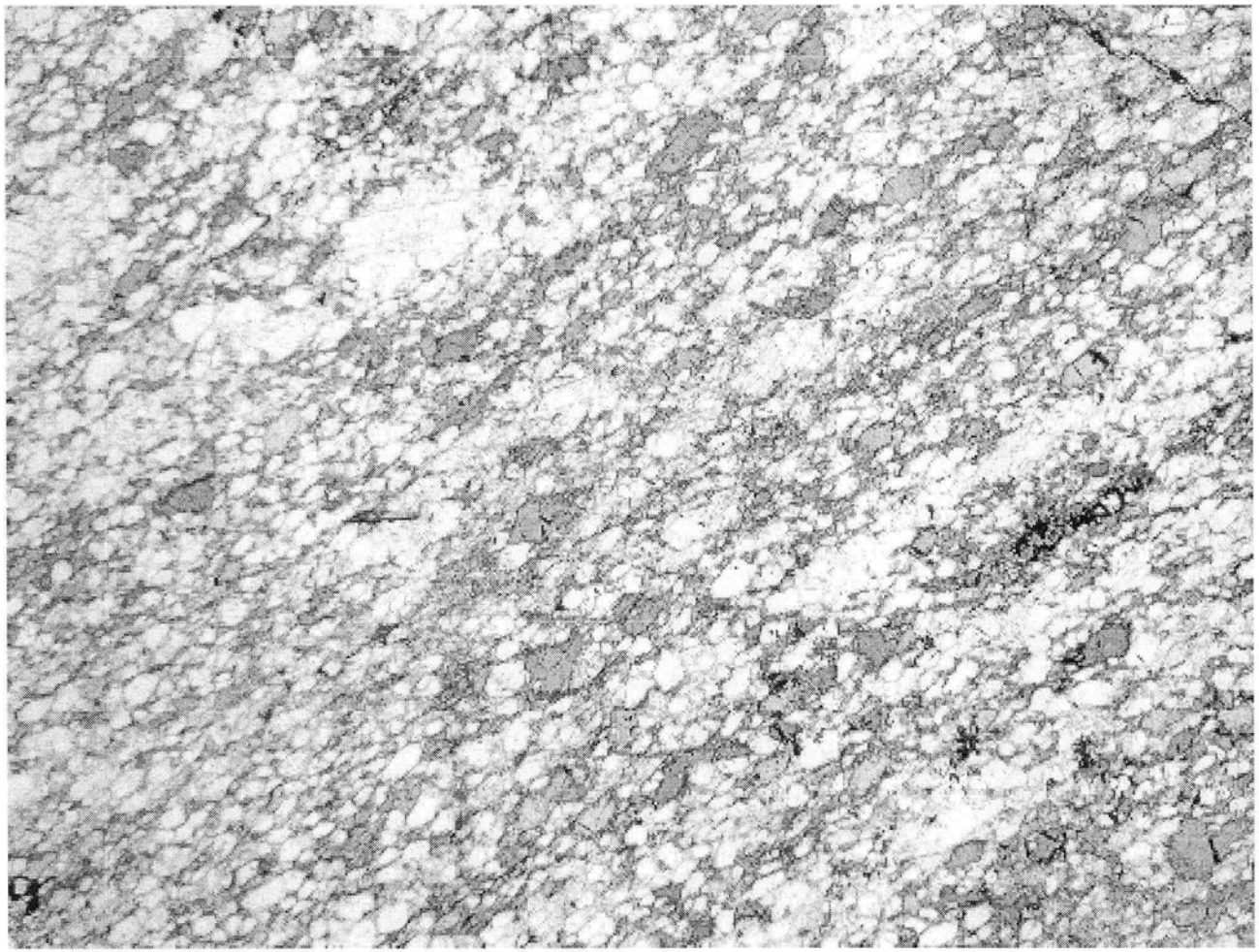

Figure 18: Photomicrograph of pervasively altered basalt showing slight foliation of magnesio-hornblende, characteristic of the western field area (field of view=1 mm).

abundant phase. Recrystallized plagioclase is intergrown with the other groundmass minerals and exhibits brittle deformation.

Fractures in the west of the complex are wider (up to 10 mm) than those in the east, and the veins exhibit ductile deformation. The fractures exhibit the same cross-cutting relationships as in the east, with the exception that zeolite is not observed in the west. Samples from near the Leech River Fault contain isoclinally folded epidote veins, demonstrating ductile deformation associated with the fault that is not observed in the east.

3.2.2. Mineral Compositions

3.2.2.1. Chlorite

Chlorite compositions are dominantly clinochlore with minor magnesian chamosite (Bailey, 1988). Chlorite in the groundmass, vesicles, and veins have Mg# (Mg/Mg+Fe) between 68 and 42. Compositions within individual samples are similar regardless of their mode of occurrence. No systematic variation between Mg# or minor element concentrations was noted with stratigraphy, associated metamorphic minerals, or geographic location. Mixed layer chlorite/smectite was identified in two samples on the basis of high CaO, Na_2O, and K_2O and octahedral silica contents. Both of these samples are coarse-grained and were sampled from flow centers, suggesting that the chlorite likely formed during cooling of the basalt rather than subsequent metamorphic events.

3.2.2.2. Amphibole

All amphiboles are calcic, ranging in composition from actinolite to magnesio-hornblende end members (nomenclature after Leake et al., 1997). Tetrahedral alumina is

positively correlated with Site A occupancy in all samples (Figure 19). Si shows a weak positive correlation with Mg# in samples from the west of the complex, but no correlation between Si and Mg# is observed in samples from the east of the complex. Fine grains nucleating in chlorite and acicular inclusions in epidote are actinolite but are too small to assess zoning. Larger grains filling vesicles, replacing the rims of clinopyroxene, and the groundmass of samples from the westernmost transect, exhibit zoning from actinolitic cores to magnesio-hornblende rims. Samples from further west contain unzoned magnesio-hornblende. Amphibole shows a broad trend of increasing Site A occupancy and increasing tetrahedral alumina from east to west (Figure 20).

3.2.2.3. Plagioclase

Primary plagioclase is preserved in the east of the complex but is completely recrystallized in the west. In the east, the degree of alteration of primary plagioclase (An_{73-43}) to albite (An_{0-9}) varies from zero to 100% (Figure 17). In the west, recrystallized plagioclase compositions range from An_{35} to An_{86} and are likely inherited from the basaltic protolith. A few compositions are more albite-rich An_{33} and An_{11} (Figure 21).

3.2.2.4. Epidote

Pistachite content ($Ps = Fe^{3+}/Fe^{3+}+^{VI}Al$) of epidote varies from Ps_{13} to Ps_{39}, similar to published values for epidote from other metabasalt suites (e.g. Hannington et al., 2003). Epidote in vesicles has iron-rich cores and aluminum-rich rims. Epidote in fractures may be unzoned or has either iron-rich or aluminum-rich cores. Groundmass epidote is too fine-grained to determine zoning in the east of the complex and is unzoned

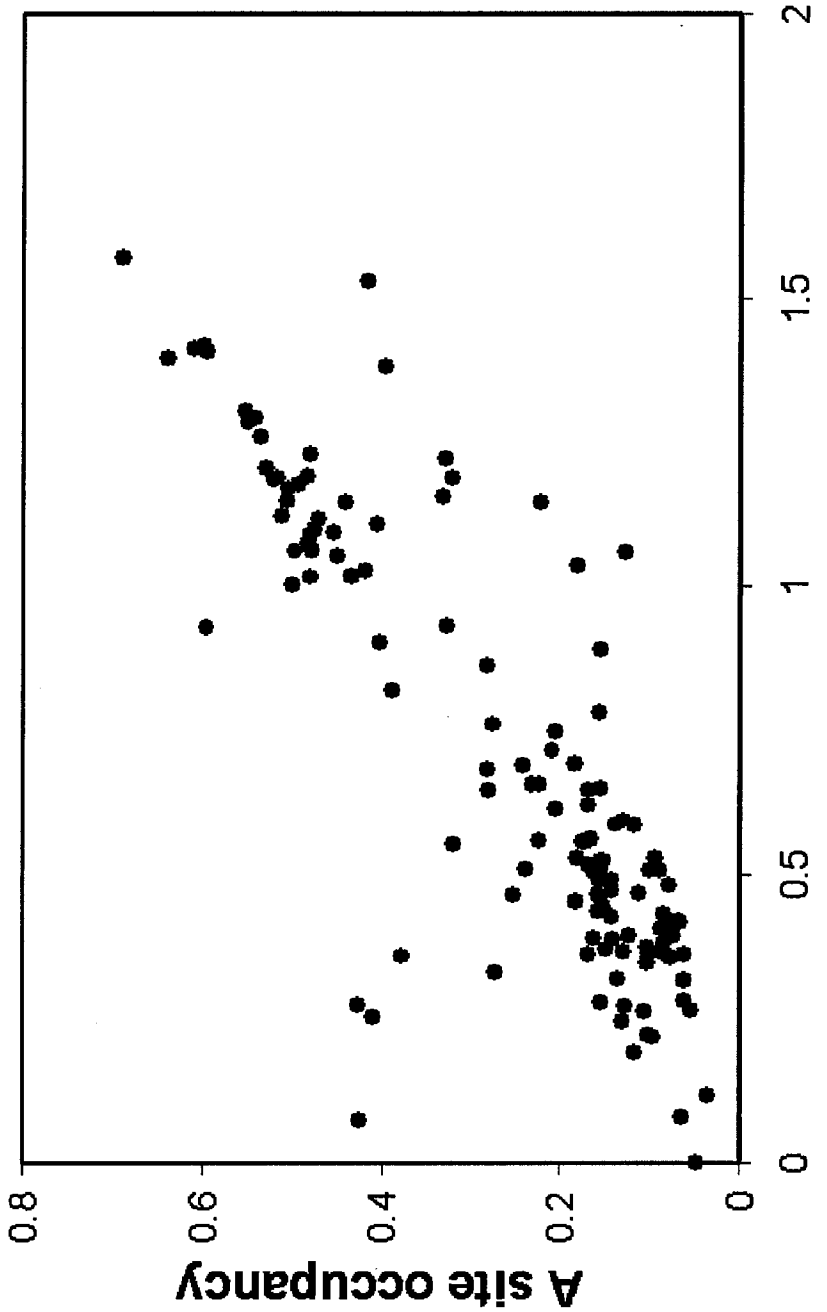

Figure 19: Amphibole compositions from volcanics in the Metchosin Igneous Complex. Mineral formulae were calculated on the basis of 15 cations, excluding Na and K (Robinson et al., 1982).

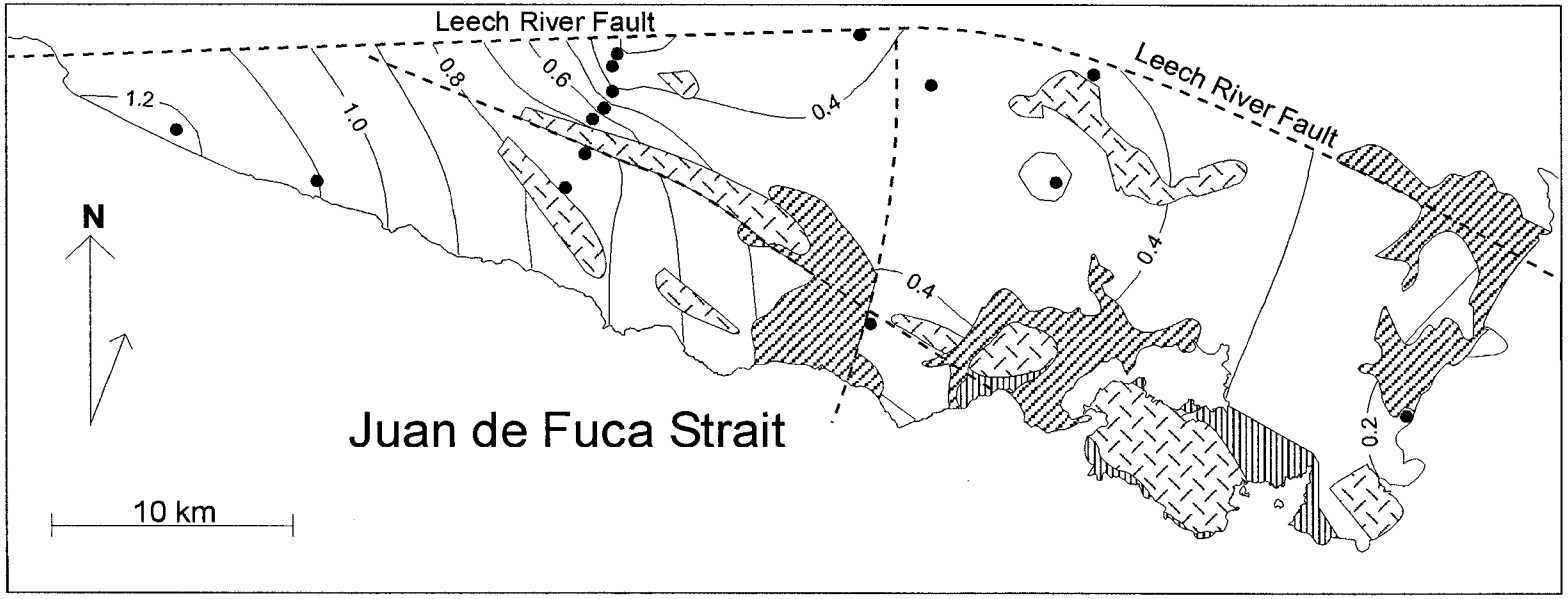

Figure 20: Tetrahedral aluminum in amphibole in the Metchosin Igneous Complex contoured over the field area. Points represent the mean of 2 to 25 analyses; standard deviations varied from 0.07 to 0.50.

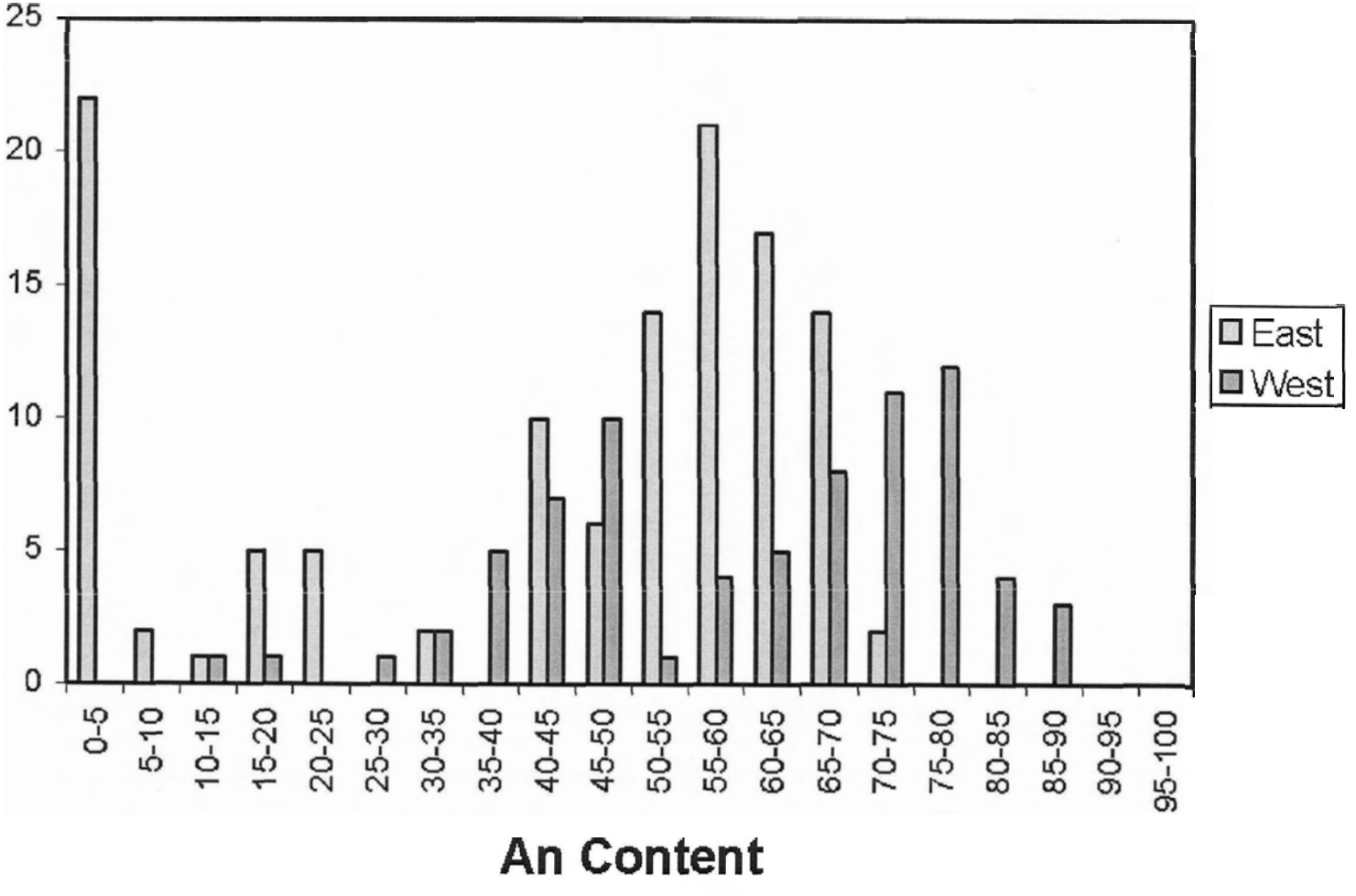

Figure 21: Regional variation in anorthite content (An) of plagioclase in the Metchosin Igneous Complex

in the west. There is no regional or stratigraphic variation in major or minor element compositions.

3.2.2.5. Prehnite

Compositions were determined in the groundmass, vesicles, and fracture fill of five basalt samples, and in the groundmass of one seafloor chert from the northeast of the complex. Prehnite exhibits a 1-15% substitution of Fe^{+3} for Al. Within samples there is even less variation. No systematic variation in the minor elements was observed.

3.2.2.6. Garnet

Garnet occurs as subhedral grains embedded in epidote in the vesicles of three samples. Garnet in the vesicles of two samples was analyzed. One sample contains unzoned andradite with less than 2% grossular. The other sample contains zoned garnets with alternating bands of nearly pure andradite (And_{100} to And_{93}) and moderately aluminous garnet ($Gross_{29}$ to $Gross_{47}$).

3.2.2.7. Zeolite

Zeolite occurs as fracture and vesicle fill in the east of the complex. All zeolites belong to calcic groups. Two samples contain laumontite, including the vesicle fill, two contain chabazite, and one contains barrerite. One sample contains both laumontite and barrerite as fracture fill.

3.2.2.8. Carbonate

Most carbonates display very little compositional variation and contain greater than 97% calcite component. The single exception contains up to 3% magnesite and 14% rhodocrosite component.

3.2.3. Geothermometry

3.2.3.1. Mineral Composition

The tetrahedral Al content of chlorite has been shown to increase with temperature and can be used as an empirical geothermometer. This geothermometer has been calibrated by comparing the Al^{IV} content of chlorite formation temperatures in meta-andesites from the Los Azufres geothermal field (Cathelineau, 1988; Cathelineau and Nieva, 1985). It has been successfully applied to other metamorphic environments and protoliths, including metabasalts from regional (Bevins et al., 1991) and seafloor hydrothermal systems (Gillis et al., 2001). The cumulative error for the geothermometer is ± 50° C (Cathelineau and Nieva, 1985).

The chlorite geothermometer was used to examine if there are regional variations in metamorphic temperature within the volcanic sequence of the Metchosin Igneous Complex. Chlorite compositions were recalculated on the basis of 14 anhydrous cations, excluding the interlayer cations. Calculated temperatures range between 235° and 315° C. The lowest temperatures are restricted to the prehnite-actinolite facies assemblages northeast part of the complex (Figure 18). A regional trend of increasing temperature from east to west spans the entire complex (Figure 22), suggestive of an east-west temperature gradient that is consistent with the metamorphic assemblages (see next section).

Amphibole compositions can provide a qualitative measure of temperature, because Al^{IV} systematically increases with increasing temperature with a concomitant increase in Na and K in the A site to maintain charge balance (Spear, 1981). Tetrahedral aluminum and A-site occupancy in amphibole increase from east to west in the volcanic

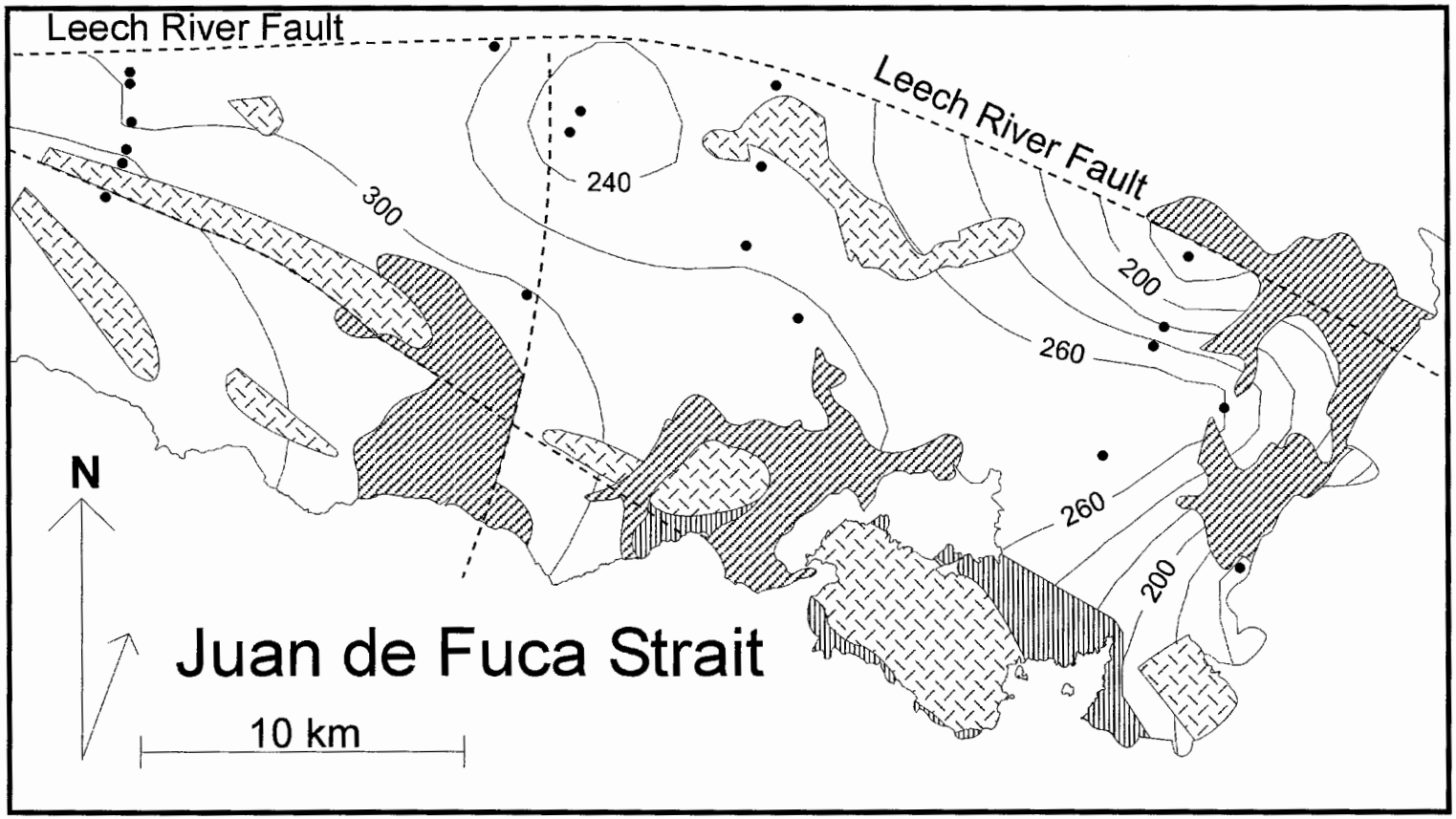

Figure 22: Temperatures (in °C) calculated by chlorite geothermometry in the volcanics of the Metchosin Igneous Complex contoured over the field area. Points indicate sample locations. Values for each point are the mean of 2 to 18 analyses, with a maximum relative standard deviation of 15%.

sequence (Figure 20), consistent with the temperature gradient inferred from chlorite geothermometry and mineral assemblages. The presence of actinolite in many of these assemblages shows that peak temperatures were greater than 300° C (Frey et al., 1991). The presence of magnesio-hornblende in the westernmost samples demonstrates that peak temperatures in the west exceeded 420° C (Maruyama et al., 1983).

3.2.3.2. Metamorphic Assemblages and Facies

Slow reaction rates, the effect of bulk composition and oxygen fugacity on mineral stability, and the overlapping stability of key indicator minerals make facies definitions within low P-T metabasaltic rocks difficult to establish precisely. For the purposes of this study, the prehnite–actinolite to greenschist facies transition is defined by the prehnite-out reaction: Prh + Chl + Ab → Act + Epi + H_2O (Beiersdorfer and Day, 1995; Digel and Gordon, 1995). This reaction occurs between 280° C and 340° C and up to 0.3 GPa for bulk compositions that are comparable to the Metchosin Igneous Complex (Digel and Gordon, 1995). This constrains the peak temperature in the northeast of the complex to <280° C.

The boundary between the greenschist and amphibolite facies is classically marked by the disappearance of chlorite, an increase in the anorthite content of plagioclase, and a change in the composition of amphibole from actinolite to hornblende (e.g. Maruyama et al., 1983). The greenschist to amphibolite transition is defined by the chlorite-out reaction: Ab + Act + Epi + Chl → Plag + Hbd + H_2O (Maruyama et al., 1983). The temperature of this reaction is highly dependant on P, P_{fluid}/P_{total}, f_{O2}, and bulk composition, among other factors. Experimental studies place this boundary at 420° C to 500° C and <0.2 to 1 GPa for redox conditions in the vicinity of the quartz-fayalite-

magnetite and nickel-nickel-oxide buffers (Liou et al., 1974; Moody et al., 1983). This constrains the peak temperatures in the west of the complex to >420° C.

3.2.3.3. Fluid Inclusions

Fluid inclusions for three samples from the east of the complex provide additional temperature constraints. Secondary fluid inclusions hosted in quartz associated with epidote + chlorite ± actinolite yield uncorrected homogenization temperatures between 145° and 301° C, with an average of 193° C (Rucks, 2002). If lithostatic conditions are assumed, a thickness of 3-5 km of overlying strata yields pressure-corrected homogenization temperatures between 191° C and 368° C. If hydrostatic conditions are assumed, (2.5 km depth of water overlying 3-5 km of lavas), pressure-corrected homogenization temperatures would be lower (175°-342° C). These temperatures and pressures are low relative to those inferred from metamorphic assemblages and mineral compositions which likely reflects entrapment after peak metamorphic conditions were achieved.

3.3. Discussion

3.3.1 Metamorphic Evolution of the Lavas

The volcanic sequence of the Metchosin Igneous Complex is dominated by greenschist facies assemblages, except for the northeast section of the upper volcanics, which exhibits prehnite-actinolite facies assemblages, and the west of the complex, which is dominated by upper greenschist and amphibolite facies assemblages. Two isograds have been identified: the greenschist facies isograd falls between the two easternmost transects and at the transition between the upper and lower volcanics, and the amphibolite

isograd is located west of the westernmost transect (Figure 23). Samples from the westernmost transect contain chlorite, although in smaller quantities than is observed in the east of the complex, actinolite and minor albite. These samples also contain magnesio-hornblende and metamorphic plagioclase, which indicate transition from greenschist to amphibolite facies (Maruyama et al., 1983). Samples from the western edge of the field area contain magnesio-hornblende and metamorphic plagioclase and lack chlorite or albite, indicating amphibolite grade metamorphism. Hence the amphibolite isograd is placed just west of the westernmost transect (Figure 23).

The changes in metamorphic assemblages are indicative of a regional temperature increase from east to west, from less than 280° to greater than 420°C. This thermal gradient of ~5°C/km is parallel, rather than perpendicular, to the strike of the volcanic stratigraphy. Subsequent to peak metamorphic conditions, zeolite and carbonate were deposited in fractures at temperatures less than 200° C. In the northeast of the Metchosin Igneous Complex, the presence of prehnite and absence of pumpellyite constrain pressures to less than 0.3 GPa, which is consistent with fluid inclusion data that place pressure at < 0.4 GPa. Pressure in the west of the complex is not well constrained and may be significantly higher than in the east.

3.3.2. Regional Versus. Seafloor Hydrothermal Metamorphism

The distribution of metamorphic facies in the Metchosin Igneous Complex may be the result of seafloor hydrothermal alteration, regional metamorphism related to the process of accretion, or a combination of the two processes. These two different styles of alteration may be distinguished on the basis of the spatial distribution of metamorphic

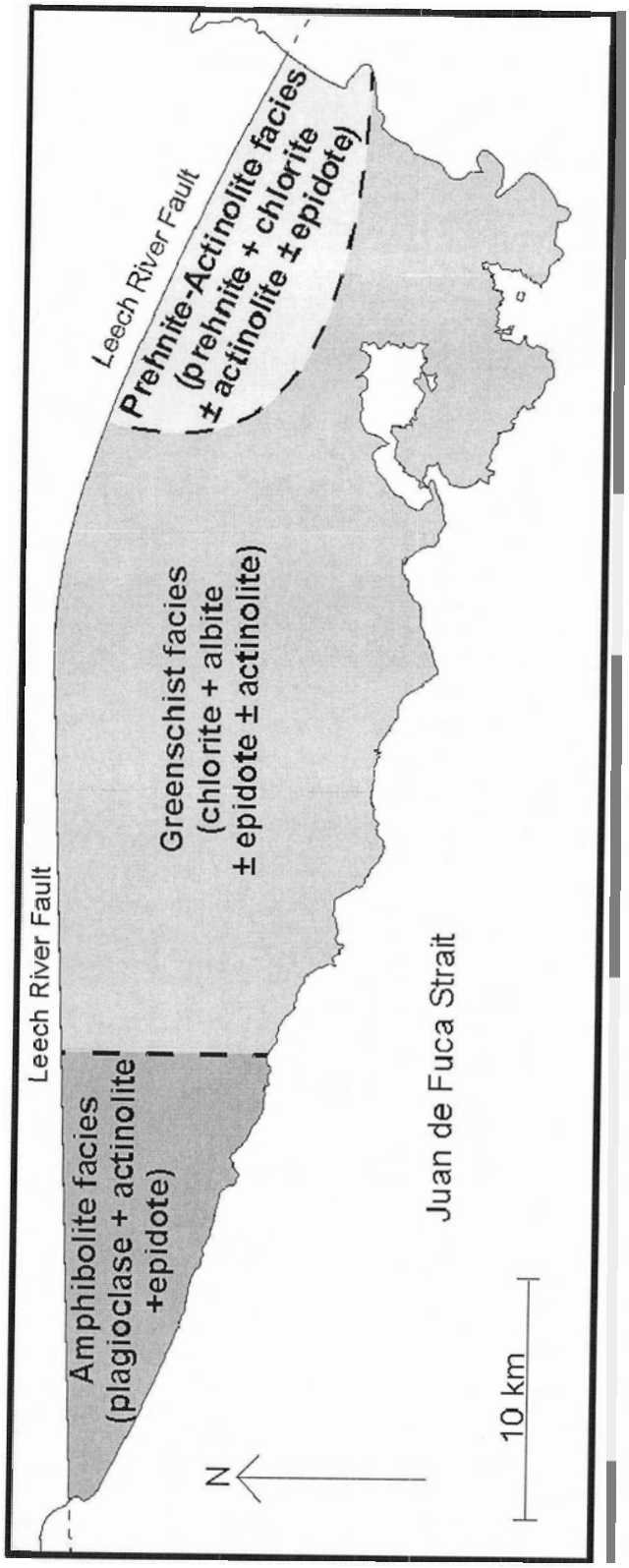

Figure 23: Distribution of metamorphic facies in the Metchosin Igneous Complex

facies relative to the stratigraphy of the volcanic sequence and paleo-geothermal gradients.

Away from ore deposits, alteration of submarine volcanics associated with *in situ* oceanic crust is dominated by palagonitization of glass, oxidative alteration, and formation of low-temperature phases such as saponite, celadonite, Fe-oxyhydroxides, and Na-K zeolites (Alt, 1995). Temperatures within porous volcanics are low (<50°C), because high permeability permits circulation of large volumes of cold seawater (Fisher, 1998). Temperature gradients inferred from secondary mineral assemblages within most volcanic sections drilled by DSDP and ODP are low, with only slight temperature increases with depth. For example, in situ measurements in 5.9 My old crust at ODP Hole 504 record temperatures below 50°C in the permeable upper volcanics, with increasing temperature with depth (Guerin et al., 1996). Greenschist conditions are not achieved until the sheeted dike complex is reached (Alt, 1995). Higher temperatures can be achieved where volcanic sequences are buried at a young age by sediments, as exemplified at the eastern flank of the Juan de Fuca ridge, which was buried by glacial turbidites within 1.5 million years of formation (Davis et al., 1992). In this case, the sedimentary cover limited convective cooling by seawater, causing a progressive increase in temperature due to the conductive cooling of the lithosphere. Calculated temperatures for the sediment–volcanic interface in 1 to 3.5 My crust range from 40 to 60°C, respectively, with higher temperatures predicted in older crust (>100°C in 4.5 My crust) (Davis et al., 1999). Mineral assemblages in the upper volcanics recovered by drilling from this area record temperatures below 60°C with no evidence for increasing temperatures with crustal age (Hunter et al., 1999). As the heat transfer is largely

conductive with localized advection, it is probable that basement temperatures increase with depth. It is not possible to evaluate directly the effect of sedimentary cover on the thermal gradient within the volcanic section of the Metchosin Igneous Complex, because no sedimentary cover is exposed in the complex. By analogy with *in situ* ocean crust, however, it is unlikely that the high temperatures inferred for the Metchosin Igneous Complex volcanics are a product of seafloor hydrothermal processes.

Iceland may be a more appropriate analogy for the Metchosin Igneous Complex, because lava thicknesses are more comparable, and the geochemistry of the lavas in the complex suggests a plume component. Metamorphic facies boundaries in drill cores from the Icelandic geothermal fields are oriented subparallel to stratigraphy and exhibit increasing temperature with increasing depth (Kristmannsdottir, 1982). Alteration minerals progress from low-temperature zeolites, such as chabazite and thomsonite near the surface, to laumontite, which is in turn followed by epidote, chlorite and quartz assemblages at depth. The sequence of alteration minerals is similar in different areas and is primarily affected by variations in the geothermal gradient (Kristmannsdottir, 1982). In contrast, the metamorphic facies in the Metchosin Igneous Complex cross-cut stratigraphy and show no correlation to depth, except in the easternmost transect. Drill cores from Icelandic geothermal fields contain epidote below 2.5 km to 3.5 km, depending on the local geothermal gradient. The geothermal gradient varies laterally from 68° C/km to 90° C/km due to differences in the number of dikes which had intruded the volcanic sequence (e.g. Franzson, 2000). Measured geothermal gradients vary spatially from less than 50° to greater than 200° C/km due to differences in the intensity of dike intrusion into the volcanic sequence (Kristmannsdottir, 1982).

If a typical Icelandic thermal gradient is applied to the Metchosin Igneous Complex, 2 to 4 km of additional stratigraphy would be required to achieve the observed temperatures in the upper volcanic unit. This would imply the subsequent removal of this extra thickness of volcanics during accretion or exhumation in order for hydrothermal processes to account for metamorphic temperatures recorded in the volcanics. This extra crust would produce higher pressures, and pumpellyite would be expected under these conditions (Beiersdorfer and Day, 1995), yet is not observed. In addition, the pressure-corrected homogenization temperatures for fluid inclusions in prehnite-actinolite and greenschist facies rocks would be much higher than the observed assemblages indicate. Although a small thermal gradient occurs in the upper volcanic sequence of the easternmost transect, it is too slight to have been produced by a hydrothermal system.

Lava sequences associated with most ophiolites exhibit higher temperature metamorphic assemblages than those found in *in situ* oceanic crust (Gillis and Banerjee, 2000). Typically, the uppermost lavas are altered to zeolite, prehnite-pumpellyite, or greenschist facies assemblages, and lava sequences are vertically zoned with metamorphic grade increasing with depth. These metamorphic assemblages are interpreted to have formed as a result of hydrothermal alteration rather than obduction-related metamorphism (e.g., Josephine ophiolite, Harper et al., 1988).

Metamorphism in the Metchosin Igneous Complex differs from most other ophiolites in two ways: (1) metamorphic zonations are oblique to the stratigraphy and (2) a higher metamorphic grade is locally recorded. These factors indicate that the metamorphism recorded in the complex is not typical of hydrothermal metamorphism. In the west of the complex, the ductile deformation along the Leech River Fault, the

destruction of large scale igneous textures by deformation and pervasive alteration, the greater degree of alteration, and geothermometric constraints suggest a higher P-T environment than in the east. This implies that the Metchosin Igneous Complex has been more deeply eroded and exhumed to the west (Figure 24). Alternatively, the west of the complex could be at a deeper stratigraphic level and the higher temperatures observed could be attributed to sampling the sheeted dike complex, where temperatures are higher. Although stratigraphy is poorly constrained in the west, the occurrence of volcaniclastic material in the lower portion of the westernmost transect and the occurrence of an ocean floor chert in one of the westernmost roadside outcrops demonstrates that samples from the west of the complex came from the volcanic sequence, not the sheeted dikes.

Assuming a 25°C/km temperature gradient, which is typical for stable continental crust, implies that crust in the west was buried by about 6 to 9 km deeper than in the east. Temperature gradients are higher in convergent margin settings than in stable crust, suggesting that a smaller amount of difference in burial may have been required. This difference in depth from east to west could be caused by tilting of the complex, either during or after accretion. Alternatively, an orographic effect (Hoffman and Grotzinger, 1993) produced by higher precipitation and higher erosion in the west, may have more deeply exhumed the western part of the complex. The Jurassic arc plutonic rocks within the Wrangellia Terrane to the north of the complex on Vancouver Island also exhibit greater depths of exhumation in the west that have been attributed to orographic effects (DeBari et al., 1999).

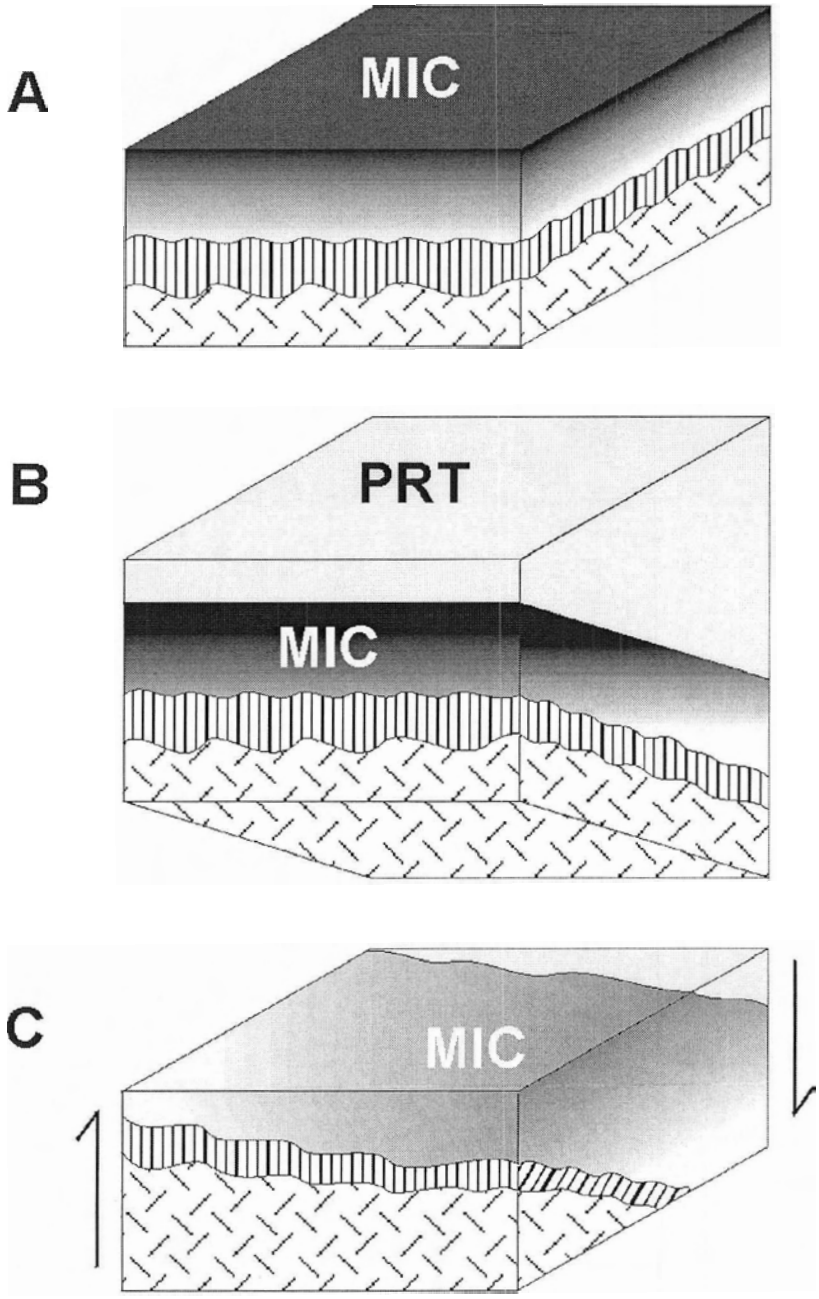

Figure 24: Block diagram representing the tectonic and thermal history of the Metchosin Igneous Complex. (A) Seafloor hydrothermal alteration produces metamorphic facies boundaries (shading) that are subparallel to stratigraphy. The volcanic sequence overlies a sheeted dike complex (striped) and gabbroic sequence (hatched). (B) Accretion of the complex beneath the Pacific Rim Terrane (PRT) along the Leech River Fault (LRF) causes regional metamorphism with facies boundaries that do not parallel the igneous stratigraphy. (C) Tilting and exhumation of the complex result in an east–west metamorphic gradient.

Chapter 4: Conclusions

4.1. Conclusions

Basalt from the Metchosin Igneous Complex is enriched in rare earth and high field strength elements and is transitional between E-MORB and N-MORB end-members. Variations in enrichment between samples correlate poorly with magma evolution and suggest heterogeneities in the mantle source. The similarity between the REE patterns of basalt from the Metchosin Igneous Complex and the Tofino Basin demonstrates that the Metchosin Igneous Complex extends as basement north along the west coast of Vancouver Island. Geochemically the basalt of the Metchosin Igneous Complex most closely resembles the lower member of the Crescent Formation, although no stratigraphic variation is observed within the complex.

The transitional geochemistry of the basalts does not provide a good basis for identifying their formative tectonic setting, but the presence of positive Nb and Ta anomalies in these lavas suggests that they did not form in a marginal basin overlying the subducting Kula or Farallon plates. An off-axis plume-ridge interaction between the Yellowstone hot spot and the Kula-Farallon spreading center is a tectonic setting that best satisfies all the geological and geochemical data for the Metchosin Igneous Complex and the Crescent Terrane as a whole.

Metamorphism in the volcanic sequence of the Metchosin Igneous Complex varies from prehnite-actinolite facies assemblages in the northeast through greenschist to amphibolite facies assemblages in the west. This pattern of metamorphism represents a regional east-west thermal gradient of ~5°C/km that is perpendicular to the volcanic

stratigraphy, implying progressively deeper levels of exhumation to the west due either to orographic effects or tectonic tilting.

Alteration of the Metchosin Igneous Complex is a result of emplacement-related regional metamorphism superimposed on seafloor hydrothermal alteration. The complex does not exhibit a gradient of temperature or metamorphic mineralogy which is expected for sea-floor hydrothermal systems. A small gradient observed along one transect is interpreted to have a tectonic origin on the basis of the occurrence of prehnite and fluid inclusion data. These results suggest that future research on ophiolites should examine with care the assumption that the observed mineralogy is the result of seafloor hydrothermal alteration.

4.2. Future Work

Although the positive Nb and Ta anomalies in the basalt of the Metchosin Igneous Complex demonstrates that it did not form in a subduction zone setting, the geochemistry of the REE and HFSE in the complex does not reveal the environment in which it did form. Arguments about the tectonic setting in which the complex formed are based on plate motion models proposed by other authors and are unfortunately speculative. A rigorous test which can distinguish between basalt formed with small degrees of plume enrichment and basalt formed at a rifted margin is required to determine the tectonic setting in which the complex formed. The lead isotopic composition of the basalts might be useful for distinguishing between these two possibilities. On the other hand, it may be more effective to investigate one of the other members of the Crescent Terrane in which the plume component is less diluted.

As this is the first study of the metamorphism of the Metchosin Igneous Complex there remains abundant work to be done on this aspect of the complex. The amphibolite facies rocks which occur west of Jordan River remain poorly characterized. This area is rugged and relatively inaccessible, but a combined study of the metamorphism and structural geology of this area could provide valuable information about the accretion and exhumation of the complex. An investigation examining the relationships between the metamorphic facies in the Metchosin Igneous Complex with the overlying Pacific Rim Terrane would also likely yield interesting results.

Bibliography:

Albarede, F. (1998) The growth of continental crust. Tectonophysics, **296**(1-2), 1-14.

Alt, J.C. (1995) Subseafloor processes in mid-ocean ridge hydrothermal systems. In S.E. Humphris, R.A. Zirenberg, L. Mullineaux, and T. R.E., Eds. Seafloor hydrothermal systems, **91**, p. 85-114. American Geophysical Union, Washington, D.C.

Babcock, R.S., Burmester, R.F., Engebretson, D.C., Warnock, A., and Clark, K.P. (1992) A rifted margin origin for the Crescent Basalts and related rocks in the northern coast range volcanic province, Washington and British Columbia. Journal of Geophysical Research, **97**(B5), 6799-6821.

Bailey, S.W. (1988) Chlorites: Structures and crystal chemistry. In S.W. Bailey, Ed. Hydrous Phyllosilicates (exclusive of micas), **19**, p. 347-403. Mineralogical Society of America, Washington, DC.

Beiersdorfer, R.E., and Day, H.W. (1995) Mineral paragenesis of pumpellyite in low-grade mafic rocks. In P. Schiffman, and H.W. Day, Eds. Low Grade Metamorphism, **296**, p. 5-28. Geological Society of America, Boulder, Co.

Bevins, R.E., Robinson, D., and Rowbotham, G. (1991) Compositional variations in mafic phyllosilicates from regional low-grade matabasites and application of the chlorite geothermometer. Journal of Metamorphic Geology, **9**, 711-721.

Cann, J.R. (1970) Rb, Sr, Y, Zr and Nb in some ocean floor basaltic rocks. Earth and Planetary Science Letters, **10**, 7-11.

Carmichael, I.S.E. (1991) The redox states of basic and silicic magmas: a reflection of their source regions? Contributions to Mineralogy and Petrology, **106**, 129-141.

Cathelineau, M. (1988) Cation site occupancy in chlorites and illites as a function of temperature. Clay Minerals, **23**, 471-485.

Cathelineau, M., and Nieva, D. (1985) A chlorite solid solution geothermometer: The Los Azufres (Mexico) geothermal system. Contributions to Mineralogy and Petrology, **91**, 235-244.

Clapp, C.H., and Cooke, H.C. (1917) Sooke and Duncan map areas, Vancouver Island, p. 455. Geological Survey of Canada.

Clowes, R.M., Brandon, M.T., Green, A.G., Yorath, C.J., Sutherland Brown, A., Kanasewich, E.R., and Spencer, C. (1987) Lithoprobe - southern Vancouver Island: Cenozoic subduction complex imaged by seismic reflections. Canadian Journal of Earth Sciences, **24**, 31-51.

Condie, K.C., and Abbott, D.H. (1999) Oceanic plateaus and hotspot islands: Identification and role in continental growth. Lithos, **46**(1), 1-4.

Cousens, B.L., Allan, J.F., Leybourne, M.I., Chase, R.L., and Vanwagoner, N. (1995) Mixing of Magmas from Enriched and Depleted Mantle Sources the Northeast Pacific - West-Valley Segment, Juan-De-Fuca Ridge. Contributions to Mineralogy and Petrology, **120**(3-4), 337-357.

Davis, E.E., Chapman, D.S., Mottl, M.J., Bentkowski, W.J., Dadey, K., Forster, C., Harris, R., Nagihara, S., Rohr, K., Wheat, G., and Whiticar, M. (1992) Flank Flux: an experiment to study the nature of hydrothermal circulation in young oceanic crust. Canadian Journal of Earth Sciences, **29**, 925-952.

Davis, E.E., Chapman, D.S., Wang, K., Villinger, H., Fisheer, A.T., Robinson, S.W., Grigel, J., Pribnow, D., Stein, J., and Becker, K. (1999) Regional heat flow variations across the sedimented Juan de Fuca Ridge eastern flank: constraints on lithospheric cooling and lateral hydrothermal heat transport. Journal of Geophysical Research, **104**, 17,675-17,688.

DeBari, S.M., Anderson, R.G., and Mortensen, J.K. (1999) Correlation among lower to upper crustal components in an island arc: the Jurassic Bonanza arc, Vancouver Island, Canada. Canadian Journal of Earth Sciences, **36**(8), 1371-1413.

Dick, H.J.B., and Johnson, K.T.M. (1995) REE and trace element composition of clinopyroxene megacrysts, xenocrysts, and phenocrysts in two diabase dikes from leg 140, hole 504B. Proceedings of the Ocean Drilling Program, Scientific Results, **137/140**, 121-130.

Digel, S.G., and Gordon, T.M. (1995) Phase relations in metabasites and pressure-temperature conditions at the prehnite-pumpellyite to greenschist facies transition, Flin Flon, Manitoba Canada. In P. Schiffman, Ed. Low-Grade Metamorphism of Mafic Rocks, **296**, p. 67-80. Geological Society of America, Boulder, Colorado.

Duncan, R.A. (1982) A captured island chain in the coast range of Oregon and Washington. Journal of Geophysical Research, **87**(B13), 10827-10837.

Engebretson, D.C., Cox, A., and Gordon, R.G. (1985) Relative motions between oceanic and continental plates in the Pacific basin. Geological Society of America Special Paper, **206**, 1-59.

Fisher, A.T. (1998) Permeability within basaltic oceanic crust. Reviews of Geophysics, **36**(2), 143-182.

Fitton, J.G., Saunders, A.D., Norry, M.J., Hardarson, B.S., and Taylor, R.N. (1997) Thermal and chemical structure of the Iceland plume. Earth and Planetary Science Letters, **153**(3-4), 197-208.

Franzson, H. (2000) Hydrothermal evolution of the Nesjavellir high temperature system, Iceland. World Geothermal Congress, p. 2075-2080.

Frey, M., de Capitani, C., and Liou, J.G. (1991) A new petrogenetic grid for low-grade metabasites. Journal of Metamorphic Geology, **9**, 497-509.

Gillis, K.M., and Banerjee, N.R. (2000) Hydrothermal alteration patterns in supra-subduction zone ophiolites. In Y. Dilek, E. Moores, D. Elthon, and A. Nicolas, Eds. Ophiolites and Oceanic Crust: New Insights from Field Studies and Ocean Drilling Program, **349**, p. 283-297. Geological Society of America, Boulder, CO.

Gillis, K.M., Muehlenbachs, K., Stewart, M., Karson, J., and Gleeson, T. (2001) Fluid flow patterns in fast-spreading East Pacific Rise crust exposed at Hess Deep. Journal of Geophysical Research, **106**, 26,311-26,329.

Glassley, W. (1974) Geochemistry and tectonics of Crescent volcanic rocks, Olympic Peninsula, Washington. Geological Society of America Bulletin, **85**(5), 785-794.

Guerin, G., Becker, K., Gable, R., and Pezaed, P. (1996) Temperature measurements and heat-flow analysis in Hole 504B. In J.C. Alt, H. Kinoshita, L.B. Stoking, and P.J. Michael, Eds. Proceedings of ODP Scientific Results, **168**, p. 291-296. Ocean Drilling Program, College Stn., Tex.

Hannington, M.D., Santaguida, F., Kjarsgaard, I.M., and Cathles, L.M. (2003) Regional-scale hydrothermal alteration in the Central Blake River Group, western Abitibi subprovince, Canada: implications for VMS prospectivity. Mineralium Deposita, **38**(4), 393-422.

Harper, G.D., Bowman, J.R., and Kuhns, R. (1988) A field, chemical, and stable isotope study of subseafloor metamorphism of the Josephine ophiolite, California-Oregon. Journal of Geophysical Research, **93**, 4625-4656.

Hoffman, P.F., and Grotzinger, J.P. (1993) Orographic precipitation, erosional unloading, and tectonic style. Geology, **21**(3), 195-198.

Hunter, A.G., Kempton, P.D., and Greenwood, P. (1999) Low-temperature fluid-rock interaction - an isotopic and mineralogical perspective of upper crustal evolution, eastern flank of the Juan de Fuca Ridge (JdFR), ODP Leg 168. Chemical Geology, **155**, 3-28.

Jenner, G.A., Longerich, H.P., Jackson, S.E., and Fryer, B.J. (1990) ICP-MS - a Powerful Tool for High-Precision Trace-Element Analysis in Earth Sciences - Evidence from Analysis of Selected USGS Reference Samples. Chemical Geology, **83**(1-2), 133-148.

Johnston, S.T., and Acton, S. (2003) The Eocene Southern Vancouver Island Orocline - a response to seamount accretion and the cause of fold-and-thrust belt and extensional basin formation. Tectonophysics, **365**(1-4), 165-183.

Kincaid, C., Schilling, J.G., and Gable, C. (1996) The dynamics of off-axis plume-ridge interaction in the uppermost mantle. Earth and Planetary Science Letters, **137**(1-4), 29-43.

Kingsley, R.H., and Schilling, J.G. (1998) Plume-ridge interaction in the Easter Salas y Gomez seamount chain Easter Microplate system: Pb isotope evidence. Journal of Geophysical Research-Solid Earth, **103**(B10), 24159-24177.

Klein, E.M., Langmuir, C.H., and Staudigel, H. (1991) Geochemistry of Basalts from the Southeast Indian Ridge, 115-Degrees-E-138-Degrees-E. Journal of Geophysical Research-Solid Earth and Planets, **96**(B2), 2089-2107.

Kristmannsdottir, H. (1982) Alteration in the IRDP Drill Hole compared with other drill holes in Iceland. Journal of Geophysical Research, **87**, 6525-6531.

Lapierre, H., Bosch, D., Tardy, M., and Struik, L.C. (2003) Late Paleozoic and Triassic plume-derived magmas in the Canadian Cordillera played a key role in continental growth. Chemical Geology, **201**, 55-89.

Leake, B.E., Woolley, A.R., Arps, C.E.S., Birch, W.D., Gilbert, M.C., Grice, J.D., Hawthorne, F.C., Kato, A., Kirsch, H.J., Krivovichev, V.G., Linthout, K., Laird, J., Mandarino, J.A., Maresh, W.V., Nickel, E.H., Rock, N.M.S., Schumacher, J.C., Smith, D.C., Stephenson, N.C.K., Ungaretti, L., Whittaker, E.J.W., and Youzhi, G. (1997) Nomenclature of amphiboles: Report of the Subcommittee on Amphiboles of the International Mineralogical Association, Commission on New Minerals and Mineral Names. American Mineralogist, **82**, 1019-1037.

Liou, J.G., Kuniyoshi, S., and Ito, K. (1974) Experimental studies of the phase relations between greenschist and amphibolite in a basaltic system. American Journal of Science, **274**, 613-632.

Maruyama, S., Suzuki, K., and Liou, J.G. (1983) Greenschist--amphibolite transition equilibria at low pressures. Journal of Petrology, **24, Pt. 4**, 583-694.

Massey, N.W.D. (1986) Metchosin Igneous Complex, southern Vancouver Island: Ophiolite stratigraphy developed in an emergent island setting. Geology, **14**, 602-605.

McDonough, W.F., and Sun, S.S. (1995) The Composition of the Earth. Chemical Geology, **120**(3-4), 223-253.

McKenzie, D., and O'Nions, R.K. (1991) Partial melt distributions from inversion of rare Earth element concentrations. Journal of Petrology, **32**, 1,021-1,091.

Meibom, A., and Anderson, D.L. (2003) The statistical upper mantle assemblage. Earth and Planetary Science Letters, **217**, 123-139.

Monger, J.W.H., Price, R.A., and Tempelman-Kluit, D.J. (1982) Tectonic accretion and the origin of two major metamorphic and plutonic welts in the Canadian Cordillera. Geology, **10**, 70-75.

Moody, J.B., Meyer, D., and Jenkins, J.E. (1983) Experimental characterization of the Greenschist/Amphibolite boundary in mafic systems. American Journal of Science, **283**, 48-92.

Muller, J.E. (1977) Metchosin volcanics and Sooke Intrusions of southern Vancouver Island, p. 287-294. Geological Survey of Canada.

Muller, J.E. (1980) Chemistry and origin of the Eocene Metchosin Volcanics, Vancouver Island, British Columbia. Canadian Journal of Earth Sciences, **17**, 199-209.

Muller, J.E. (1983) Geology of Victoria, British Columbia. Geological Survey of Canada.

Murphy, J.B., Hynes, A.J., Johnston, S.T., and Keppie, J.D. (2003) Reconstructing the ancestral Yellowstone plume from accreted seamounts and its relationship to flat-slab subduction. Tectonophysics, **365**(1-4), 185-194.

Pearce, J.A. (1996) A user's guide to basalt discrimination diagrams. In D.A. Wyman, Ed. Trace Element Geochemistry of Volcanic Rocks: Applications for Massive Sulphide Exploration, **12**, p. 79-113. Geological Association of Canada.

Pearce, T.H. (1968) A contribution to the theory of variation diagrams. Contributions to Mineralogy and Petrology, **19**, 142-157.

Putchel, L.S., Hoffman, A.W., Mezger, K., Jochum, K.P., Schipansky, A.A., and Samsonov, A.V. (1998) Oceanic plateau model for continental growth in the Archean: a case from the Kostomuksha greenstone belt, N. W. Baltic Shield. Earth and Planetary Science Letters, **155**, 57-74.

Pyle, D.G. (1988) Geochemical evolution of the Roseburg Formation basaltic rocks, southern Oregon coast range. Geology, p. 125. Oregon State University.

Ramachandran, K. (2001) Velocity structure of southwest British Columbia and northwest Washington, from 3-D non-linear seismic tomography. SEOS, p. 198. University of Victoria, Victoria.

Rhodes, J.M., Morgan, C., and Liias, R.A. (1990) Geochemistry of Axial Seamount Lavas - Magmatic Relationship between the Cobb Hotspot and the Juan-De-Fuca Ridge. Journal of Geophysical Research-Solid Earth and Planets, **95**(B8), 12713-12733.

Robillard, I., Francis, D., and Ludden, J.N. (1992) The Relationship between E-Type and N-Type Magmas in the Baffin-Bay Lavas. Contributions to Mineralogy and Petrology, **112**(2-3), 230-241.

Robinson, P., Spear, F.S., Schumacher, J.C., Laird, J., Klein, C., Evans, B.W., and Doolan, B.L. (1982) Phase relations of metamorphic amphiboles: Natural occurrence and theory. In P.H. Ribbe, Ed. Amphiboles: Petrology and Experimental Phase Relations, p. 1-211. Mineralogical Society of America, Blacksburg, Virginia.

Roeder, P.L., and Emslie, R.F. (1970) Olivine-liquid equilibrium. Contributions to Mineralogy and Petrology, **29**, 275-289.

Rucks, T. (2002) Hydrothermal and emplacement metamorphism within a Vancouver Island ophiolite: A fluid inclusion study of the Metchosin Igneous Complex. SEOS, p. 109. University of Victoria, Victoria.

Schilling, J.G. (1991) Fluxes and Excess Temperatures of Mantle Plumes Inferred from Their Interaction with Migrating Midocean Ridges. Nature, **352**(6334), 397-403.

Schubert, G., and Sandwell, D. (1989) Crustal volumes of the continent and of oceanic and continental submarine plateaus. Earth and Planetary Science Letters, **92**, 234-246.

Snavely, P.D., Macleod, N.S., and Wagner, H.C. (1968) Tholeiitic and Alkalic Basalts of Eocene Siletz River Volcanics Oregon Coast Range. American Journal of Science, **266**(6), 454-&.

Spear, F.S. (1981) An experimental study of hornblende stability and compositional variability in amphibolite. American Journal of Science, **281**, 697-734.

Stanley, C.R., and Madeisky, H.E. (1996) Lithogeochemical exploration for metasomatic zones associated with hydrothermal mineral deposits using Pearce element ratio analysis, p. 209. Mineral Deposit Research Unit, Lithogeochemical Exploration Research Project.

Sun, S.-S., and McDonough, W.F. (1989) Chemical and isotopic systematics of oceanic basalts: Implications for mantle composition and processes. In A.D. Saunders, and M.J. Norry, Eds. Magmatism in the Ocean Basins, **42**, p. 313-345. Geological Society Special Publication, London.

Wells, R.E., Engebretson, D.C., Snavely, P.D.J., and Coe, R.S. (1984) Cenozoic plate motions and the volcano-tectonic evolution of western Oregon and Washington. Tectonics, **3**(2), 275-294.

Yorath, C.J., Sutherland Brown, A., and Massey, N.W.D. (1999) Lithoprobe, southern Vancouver Island, British Columbia: Geology, p. 109-133. Geological Survey of Canada.

Appendix 1: Analyses of Major Element Weight Percent Oxides by XRF

Sample	SiO_2 (wt%)	TiO_2 (wt%)	Al_2O_3 (wt%)	FeO (wt%)	Fe_2O_3 (wt%)	MnO (wt%)	MgO (wt%)	CaO (wt%)	Na_2O (wt%)	K_2O (wt%)	P_2O_5 (wt%)	Total (wt%)	LOI wt %	Mg#	$Acc_{Mg\#}$	$Prec_{Mg\#}$
ST-8	52.1	1.29	13.8	10.17	1.99	0.24	6.25	10.27	3.66	0.07	0.14	100	3.10	0.52	1.24%	0.13%
ST-9	50.1	1.54	14.0	10.86	2.13	0.22	6.67	11.79	2.32	0.14	0.16	100	0.92	0.52	1.24%	0.13%
ST-15	49.7	1.86	13.9	12.46	2.44	0.25	5.88	10.58	2.51	0.13	0.24	100	1.16	0.46	1.25%	0.14%
ST-20	51.7	1.06	15.0	8.88	1.74	0.19	5.93	10.89	4.36	0.06	0.10	100	1.66	0.54	1.23%	0.12%
ST-23	50.3	2.20	13.2	13.01	2.55	0.26	5.34	10.10	2.71	0.13	0.27	100	1.13	0.42	1.26%	0.14%
ST-25	49.7	1.15	14.6	10.16	1.99	0.19	7.70	12.26	2.02	0.09	0.10	100	2.02	0.57	1.23%	0.12%
ST-35	49.8	1.53	13.3	11.36	2.23	0.26	6.87	11.56	2.81	0.12	0.16	100	1.61	0.52	1.24%	0.13%
ST-42	49.8	1.14	15.2	9.92	1.95	0.21	7.17	11.85	2.59	0.10	0.10	100	0.79	0.56	1.23%	0.12%
ST-43	49.5	1.06	14.6	9.43	1.85	0.20	7.68	12.83	2.65	0.10	0.11	100	2.08	0.59	1.23%	0.11%
ST-47	52.8	1.21	12.3	9.68	1.90	0.24	6.90	11.33	3.41	0.10	0.12	100	1.74	0.56	1.23%	0.12%
ST-51	50.5	1.73	14.3	11.54	2.26	0.20	7.23	8.13	3.94	0.05	0.18	100	2.99	0.53	1.24%	0.12%
ST-54	49.3	1.48	14.0	11.26	2.21	0.22	7.46	10.78	3.15	0.07	0.13	100	1.24	0.54	1.23%	0.12%
ST-55	49.4	1.16	14.5	9.99	1.96	0.21	8.04	11.62	2.88	0.11	0.11	100	1.75	0.59	1.23%	0.11%
ST-57	51.1	1.50	13.3	11.29	2.21	0.21	7.06	8.62	4.53	0.07	0.14	100	1.99	0.53	1.24%	0.12%
ST-59	51.6	1.54	13.1	10.74	2.11	0.21	6.50	10.50	3.50	0.04	0.16	100	2.06	0.52	1.24%	0.13%
ST-62	49.5	1.67	13.5	12.42	2.44	0.22	6.57	10.74	2.62	0.11	0.17	100	1.66	0.49	1.24%	0.13%
ST-65	50.0	1.16	14.2	9.96	1.95	0.18	8.91	9.42	3.95	0.07	0.11	100	2.55	0.61	1.23%	0.11%
MIC99-3	50.8	1.06	14.9	8.48	1.66	0.19	7.86	11.84	2.96	0.15	0.09	100	1.64	0.62	1.23%	0.11%
MIC99-5	51.0	0.80	16.8	6.48	1.27	0.18	6.68	14.17	2.34	0.24	0.07	100	1.23	0.65	1.22%	0.10%
MIC99-8	49.2	1.09	15.5	8.52	1.67	0.19	8.41	12.84	2.45	0.02	0.07	100	2.01	0.64	1.22%	0.10%
MIC99-9	49.6	1.13	15.5	8.81	1.73	0.16	7.62	13.33	2.06	0.02	0.09	100	1.37	0.61	1.23%	0.11%
MIC99-12	52.2	1.41	13.5	9.97	1.96	0.21	7.02	10.30	3.28	0.05	0.12	100	2.03	0.56	1.23%	0.12%
MIC99-13	50.1	1.29	14.4	9.63	1.89	0.18	7.91	12.54	1.95	0.05	0.11	100	2.13	0.59	1.23%	0.11%
MIC99-15	49.7	1.55	14.2	10.58	2.08	0.21	7.65	11.11	2.71	0.10	0.11	100	1.13	0.56	1.23%	0.12%
MIC99-16	52.0	1.43	13.7	9.74	1.91	0.19	6.25	10.93	3.73	0.03	0.12	100	2.47	0.53	1.23%	0.12%
MIC99-17	51.7	1.33	14.4	8.98	1.76	0.22	5.87	12.26	3.32	0.07	0.10	100	1.36	0.54	1.23%	0.12%
Accuracy:	0.5%	1.0%	1.0%	1.0%	1.0%	1.0%	1.0%	1.0%	1.0%	1.0%	1.0%					
Precision:	0.05%	0.43%	0.03%	0.20%	0.20%	0.80%	0.01%	0.03%	0.08%	7.36%	0.61%					

Appendix 1: Analyses of Trace Elements by XRF

Sample	Ni (ppm)	Sc (ppm)	V (ppm)	Ga (ppm)	Nb (ppm)	Pb (ppm)	Rb (ppm)	Sr (ppm)	Th (ppm)	U (ppm)	Y (ppm)	Zr (ppm)
ST-8	55	45	335	16	6.0	3.3	2.5	59	3.6	3.2	33	91
ST-9	57	44	344	18	6.5	3.4	3.2	134	2.9	1.4	34	96
ST-15	40	43	388	21	9.2	4.4	3.7	106	4.0	2.8	48	163
ST-20	77	35	297	15	4.4	3.2	1.9	172	2.7	2.4	24	51
ST-23	50	48	464	23	8.6	4.6	3.5	128	4.8	2.7	53	169
ST-25	74	52	323	18	5.4	2.9	3.5	110	2.3	2.1	29	67
ST-35	54	43	355	17	7.7	2.8	3.0	122	2.4	1.5	31	85
ST-42	68	50	311	17	4.5	3.3	2.7	106	2.0	0.2	28	59
ST-43	102	44	268	15	5.5	2.9	2.6	156	1.3	-0.2	24	56
ST-47	66	43	299	15	5.0	4.1	2.4	137	4.1	3.5	28	69
ST-51	65	52	417	17	7.0	2.7	2.3	102	2.1	1.2	44	117
ST-54	74	48	378	18	5.1	3.5	2.9	171	2.6	1.0	36	85
ST-55	77	44	308	16	5.3	1.9	2.3	111	1.5	0.6	28	67
ST-57	58	41	376	16	6.0	4.1	2.3	115	1.4	0.2	36	93
ST-59	58	42	376	17	6.0	3.5	2.0	93	4.9	4.5	38	109
ST-62	54	48	379	18	6.6	3.3	3.4	150	3.0	2.0	38	104
ST-65	88	45	268	14	5.7	1.6	2.0	138	0.7	-1.1	27	64
Accuracy	5%	5%	5%	5%	5%	5%	5%	5%	5%	5%	5%	5%
Precision	0.0%	14.1%	0.8%	5.1%	2.5%	10.5%	0.0%	0.9%	14.6%	282.8%	2.9%	1.6%
Detection Limits (ppm)	3	10	10	1	1	1	1	1	1	1	1	1

Appendix 1: Uncertainties in XRF Analyses

	SiO_2	TiO_2	Al_2O_3	FeO	Fe_2O_3	MnO	MgO	CaO	Na_2O	K_2O	P_2O_5
	(wt%)	*(wt%)*	*(wt%)*	*(wt%)*	*(wt%)*	*(wt%)*	*(wt%)*	*(wt%)*	*(wt%)*	*(wt%)*	*(wt%)*
ST-43 replicate A	49.48	1.07	14.58	9.46	1.86	0.20	7.68	12.82	2.65	0.09	0.10
ST-43 replicate B	49.52	1.06	14.57	9.43	1.85	0.20	7.68	12.83	2.65	0.10	0.11
Precision	**0.05%**	**0.43%**	**0.03%**	**0.20%**	**0.20%**	**0.80%**	**0.01%**	**0.03%**	**0.08%**	**7.4%**	**0.61%**

	Ni	Sc	V	Ga	Nb	Pb	Rb	Sr	Th	U	Y	Zr
	(ppm)	*(ppm)*	*(ppm)*	*(ppm)*	*(ppm)*	*(ppm)*	*(ppm)*	*(ppm)*	*(ppm)*	*(ppm)*	*(ppm)*	*(ppm)*
ST-43 replicate A	101	36	270	16	5.7	2.5	2.60	157	1.6	0.6	25.2	56.8
ST-43 replicate B	101	44	267	15	5.5	2.9	2.60	155	1.3	-0.2	24.2	55.5
Precision	**0.00%**	**14.1%**	**0.79%**	**5.07%**	**2.53%**	**10.5%**	**0.00%**	**0.86%**	**14.6%**	**283%**	**2.86%**	**1.64%**

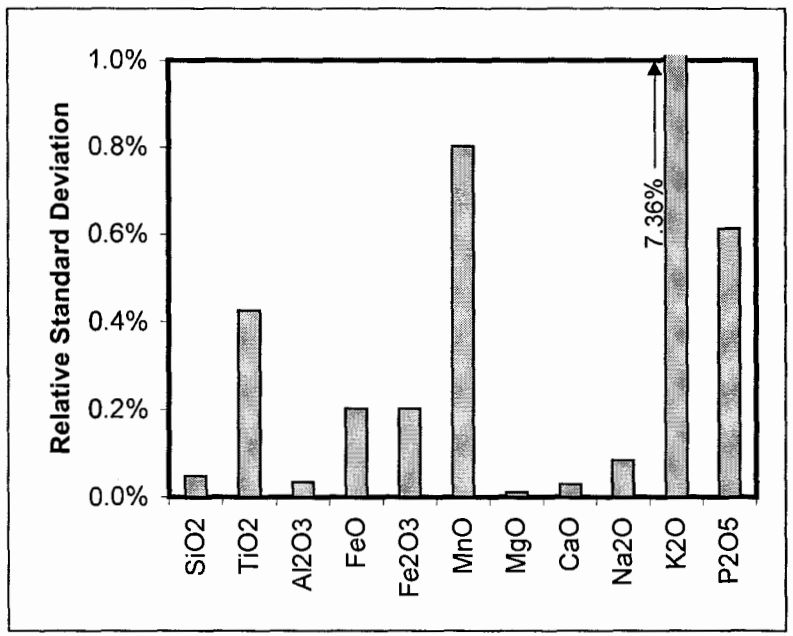

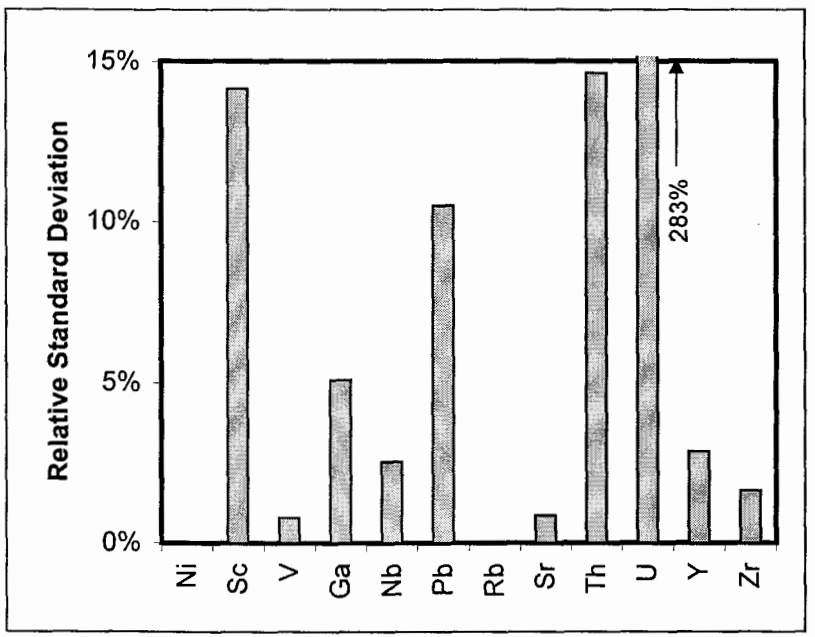

Appendix 1: Sample Characterization and Data Manipulations

Sample	Lithology	Glomerocryst (%)	Vessicles (%)	Stratigraphic Location (m)
ST-8	Pillow Basalt	-	20	3000
ST-9	Sheet Flow	-	-	3000
ST-15	Massive Flow	2	-	3500
ST-20	Pillow Basalt	-	15	2700
ST-23	Pillow Basalt	-	-	2300
ST-25	Pillow Basalt	-	10	2000
ST-35	Pillow Basalt	10	10	500
ST-42	Massive Flow	-	2	3700
ST-43	Pillow Basalt	10	15	500
ST-47	Pillow Basalt	15	10	1000
ST-51	Pillow Basalt	-	10	1500
ST-54	Massive Flow	-	12	3400
ST-55	Massive Flow	-	15	3200
ST-57	Massive Flow	-	5	3100
ST-59	Pillow Basalt	-	12	2900
ST-62	Pillow Basalt	-	4	2500
ST-65	Pillow Basalt	-	12	1500

Sample	Lithology	Glomerocryst (%)	Vessicles (%)	Stratigraphic Location (m)
MIC99-3	Pillow Basalt	-	15	3000
MIC99-5	Pillow Basalt	12	-	2500
MIC99-8	Pillow Basalt	-	5	1500
MIC99-9	Pillow Basalt	1	1	1000
MIC99-12	Pillow Basalt	-	15	1700
MIC99-13	Pillow Basalt	-	-	2000
MIC99-15	Massive Flow	10	-	6000
MIC99-16	Pillow Basalt	-	10	5000
MIC99-17	Pillow Basalt	Unknown - Slide Missing		4000

Analyses were performed by McGill University's Geochemical Laboratories with a Philips PW2400 XRF spectrometer.
Analyses were performed on 32 mm diameter beads prepared by lithium tetraborate fusion.
FeO was calculated from $Fe_2O_3^T$ as wt% $Fe_2O_3^T$ × 0.8998 g FeO/g Fe_2O_3 × 85% (Carmichael, 1991).
Fe_2O_3 was calculated from $Fe_2O_3^T$ as wt% $Fe_2O_3^T$ × 15% (Carmichael, 1991).
All weight percent oxides were recalculated to an anhydrous 100% total.
Stratigraphic height of samples is calculated based on their distance from the top of the sheeted dike complex and assuming a 30 degree dip. Where the sheeted dike complex is not exposed, it's top is assumed to be 3 km below the contact between the upper and lower units of the volcanic sequence.

Appendix 2: Analyses of Trace Elements Performed by ICP-MS

Sample	Sc (ppm)	V (ppm)	Sr (ppm)	Y (ppm)	Zr (ppm)	Nb (ppm)	Ba (ppm)	Hf (ppm)	Ta (ppm)	ΔNb	$(La/Sm)_N$	$(La/Yb)_N$	Eu/Eu*
ST-08	42	368	57	29	95	5.9	13.5	2.5	0.27	0.06	0.93	1.00	0.78
ST-09	52	409	130	31	113	8.7	40.6	3.0	0.34	0.11	0.91	1.06	0.83
ST-15	46	428	106	44	175	12.0	35.2	4.5	0.57	0.02	1.08	1.24	0.80
ST-20	36	350	195	21	56	4.0	17.3	1.6	0.19	0.19	0.81	0.91	1.06
ST-23	46	489	120	46	168	12.7	34.7	4.1	0.58	0.10	1.06	1.22	0.84
ST-25	51	394	107	25	69	6.0	16.4	2.0	0.20	0.27	0.87	0.79	0.89
ST-35	45	416	132	30	108	8.9	37.5	2.9	0.40	0.14	1.13	1.37	0.83
ST-42	49	389	107	25	83	4.7	15.7	2.4	0.18	0.01	0.70	0.67	0.97
ST-43	43	339	168	22	72	5.2	18.1	1.9	0.22	0.13	0.95	0.89	0.91
ST-47	43	352	146	25	82	5.2	22.9	2.4	0.24	0.07	0.85	0.85	1.06
ST-51	54	456	100	38	115	7.0	11.4	3.1	0.36	0.08	0.92	1.00	0.86
ST-54	52	409	168	31	73	5.7	20.1	2.0	0.24	0.29	0.74	0.79	0.82
ST-55	49	350	112	24	83	5.3	33.5	2.4	0.22	0.05	0.87	0.86	0.91
ST-57	46	414	117	33	117	6.0	15.9	3.1	0.29	-0.06	0.88	0.91	0.86
ST-59	48	404	97	34	112	7.4	2.8	2.9	0.34	0.08	0.95	0.96	0.82
ST-62	51	420	149	35	108	7.2	25.7	3.2	0.34	0.11	0.94	0.93	0.85
ST-65	52	322	144	23	76	4.8	13.5	2.2	0.22	0.07	0.74	0.94	0.74
MIC99-3	46	327	138	23	67	5.7	37.6	2.0	0.19	0.23	0.74	0.73	0.89
MIC99-5	38	260	145	18	74	6.1	44.6	2.1	0.19	0.10	0.88	0.95	0.88
MIC99-8	42	309	180	20	50	5.1	7.1	1.7	0.14	0.39	0.66	0.67	1.00
MIC99-9	50	340	111	25	73	5.2	11.2	2.0	0.22	0.16	0.82	0.82	0.86
MIC99-12	50	384	123	31	88	5.8	32.2	2.7	0.24	0.14	0.72	0.69	0.84
MIC99-13	52	418	123	27	98	7.6	25.1	2.3	0.22	0.12	0.78	0.80	0.96
MIC99-15	52	412	130	32	90	5.0	25.0	2.5	0.22	0.07	0.71	0.71	0.85
MIC99-16	46	413	54	33	105	6.7	14.8	2.8	0.33	0.08	0.91	0.94	0.82
MIC99-17	46	377	145	29	89	7.2	15.5	2.6	0.25	0.20	0.90	0.84	0.92
Accuracy	3.2%	4.5%	0.6%	-8.0%	8.7%	17.8%	4.9%	17.8%	-7.0%	13.0%	3.4%	3.0%	6.6%
Precision	0.9%	0.7%	0.5%	0.01%	0.5%	1.6%	2.2%	1.1%	3.3%	0.8%	1.3%	0.7%	2.3%
LOD (ppm)	0.224	0.718	1.667	0.112	0.338	0.242	1.884	0.130	0.003				

Appendix 2: Analyses of Trace Elements Performed by ICP-MS

Sample	La (ppm)	Ce (ppm)	Pr (ppm)	Nd (ppm)	Sm (ppm)	Eu (ppm)	Gd (ppm)	Tb (ppm)	Dy (ppm)	Ho (ppm)	Er (ppm)	Tm (ppm)	Yb (ppm)	Lu (ppm)
ST-08	4.7	12.2	2.04	9.4	3.20	0.94	4.24	0.77	5.0	1.09	3.5	0.58	3.24	0.44
ST-09	5.3	14.4	2.34	11.2	3.62	1.13	4.81	0.81	5.6	1.15	3.7	0.60	3.38	0.44
ST-15	8.9	23.1	3.54	17.0	5.12	1.58	7.03	1.21	7.7	1.67	5.0	0.78	4.85	0.69
ST-20	3.0	8.0	1.39	6.8	2.32	0.94	3.20	0.55	3.9	0.80	2.6	0.41	2.26	0.29
ST-23	8.9	23.2	3.64	17.9	5.26	1.68	7.02	1.22	8.1	1.68	5.3	0.79	4.95	0.71
ST-25	3.2	9.2	1.38	7.5	2.27	0.83	3.56	0.64	4.5	0.90	2.8	0.39	2.73	0.38
ST-35	6.4	15.7	2.43	11.4	3.55	1.12	4.78	0.83	5.3	1.09	3.5	0.60	3.19	0.45
ST-42	2.8	8.1	1.39	7.3	2.48	0.97	3.75	0.69	4.3	0.96	2.9	0.43	2.83	0.44
ST-43	3.2	8.8	1.35	6.8	2.12	0.79	3.27	0.57	3.9	0.82	2.6	0.41	2.46	0.32
ST-47	3.6	10.1	1.61	8.4	2.66	1.12	3.85	0.71	4.5	1.00	3.0	0.43	2.89	0.48
ST-51	6.0	16.0	2.49	12.5	4.06	1.35	5.65	1.05	6.9	1.42	4.6	0.72	4.05	0.60
ST-54	3.9	11.0	1.85	9.1	3.26	1.04	4.55	0.79	5.4	1.12	3.6	0.58	3.35	0.46
ST-55	3.4	9.6	1.52	7.4	2.45	0.91	3.79	0.66	4.4	0.93	2.8	0.36	2.68	0.40
ST-57	4.7	12.5	1.96	9.9	3.29	1.11	4.75	0.83	5.7	1.19	3.7	0.56	3.48	0.50
ST-59	5.3	13.9	2.21	11.0	3.49	1.11	4.90	0.87	5.9	1.21	4.0	0.66	3.77	0.51
ST-62	5.4	15.0	2.36	12.1	3.60	1.22	5.28	0.95	6.4	1.35	4.0	0.58	3.95	0.57
ST-65	3.4	8.9	1.68	7.8	2.85	0.76	3.43	0.60	4.3	0.87	3.0	0.61	2.45	0.36
MIC99-3	2.8	8.1	1.28	7.1	2.33	0.80	3.25	0.58	4.3	0.89	2.7	0.33	2.59	0.33
MIC99-5	2.7	7.3	1.16	6.2	1.92	0.65	2.65	0.49	3.2	0.69	2.1	0.27	1.94	0.26
MIC99-8	2.2	6.6	1.13	6.1	2.09	0.82	3.02	0.56	3.7	0.80	2.3	0.34	2.25	0.33
MIC99-9	3.3	8.9	1.52	7.5	2.54	0.85	3.63	0.65	4.4	0.95	3.0	0.52	2.79	0.40
MIC99-12	3.4	10.0	1.69	9.1	2.98	1.02	4.51	0.82	5.5	1.16	3.7	0.58	3.41	0.50
MIC99-13	3.4	9.7	1.58	8.1	2.74	1.06	4.12	0.74	4.8	1.05	3.1	0.45	2.91	0.47
MIC99-15	3.9	10.9	1.92	10.2	3.38	1.13	4.80	0.86	5.9	1.26	4.0	0.63	3.68	0.50
MIC99-16	5.1	13.7	2.16	10.6	3.53	1.09	4.69	0.87	5.7	1.22	3.9	0.61	3.72	0.51
MIC99-17	4.2	11.7	1.81	9.4	2.89	1.08	4.42	0.76	5.3	1.13	3.4	0.44	3.34	0.41
Accuracy	3.0%	3.4%	3.4%	4.2%	-1.6%	4.9%	8.6%	4.9%	6.3%	-1.4%	-3.1%	-4.7%	0.4%	15.9%
Precision	0.6%	0.1%	0.5%	0.1%	1.1%	2.2%	0.8%	1.0%	1.3%	1.9%	3.1%	3.6%	0.2%	5.2%
LOD *(ppm)*	0.161	0.229	0.156	0.397	0.427	0.263	0.322	0.115	0.091	0.096	0.175	0.160	0.124	0.151

Appendix 2: Analyses of Trace Elements Performed by ICP-MS
Tofino Basin Samples

Sample	Sc (ppm)	V (ppm)	Sr (ppm)	Y (ppm)	Zr (ppm)	Nb (ppm)	Ba (ppm)	Hf (ppm)	Ta (ppm)	ΔNb	$(La/Sm)_N$	$(La/Yb)_N$	Eu/Eu*
H-68 B	41.9	383	122	33	76	4.9	339	2.13	0.31	0.23	1.27	1.19	0.92
H-68 M	46.1	396	183	36	78	5.6	697	2.21	0.33	0.28	0.84	0.67	0.95
H-68 T	43.8	430	104	31	80	5.6	460	2.29	0.35	0.21	0.84	0.77	0.93
D-14	41.5	409	135	50	182	10.6	140	3.67	0.56	-0.01	0.89	1.03	0.97
Accuracy	-1.3%	9.1%	5.5%	-5.1%	2.6%	-2.1%	-0.8%	-1.8%	-0.3%	5.4%	6.4%	2.3%	3.6%
Precision	1.9%	0.0%	2.1%	4.0%	6.5%	8.3%	0.6%	2.0%	2.5%	7.5%	4.0%	4.2%	4.9%
LOD (ppm)	0.077	0.008	0.256	0.002	0.022	0.034	0.125	0.006	0.001				

Sample	La (ppm)	Ce (ppm)	Pr (ppm)	Nd (ppm)	Sm (ppm)	Eu (ppm)	Gd (ppm)	Tb (ppm)	Dy (ppm)	Ho (ppm)	Er (ppm)	Tm (ppm)	Yb (ppm)	Lu (ppm)
H-68 B	7.25	16.9	2.58	11.1	3.57	1.27	4.98	0.92	6.07	1.33	4.03	0.69	4.15	0.62
H-68 M	4.31	11.7	1.87	9.4	3.19	1.27	5.17	0.96	6.22	1.42	4.10	0.63	4.40	0.64
H-68 T	4.60	12.7	2.05	10.5	3.44	1.29	5.16	0.95	5.69	1.29	3.61	0.58	4.08	0.59
D-14	7.64	20.8	3.26	16.6	5.36	1.98	7.27	1.35	8.14	1.72	4.78	0.72	5.06	0.70
Accuracy	2.0%	2.6%	2.5%	4.1%	-6.1%	-1.9%	-0.1%	1.6%	-1.9%	-5.3%	-8.0%	-4.2%	1.2%	0.7%
Precision	0.9%	0.6%	1.1%	4.5%	3.9%	4.4%	1.8%	3.8%	4.1%	4.0%	1.2%	1.6%	4.1%	2.9%
LOD (ppm)	0.002	0.001	0.002	0.003	0.004	0.009	0.094	0.002	0.004	0.001	0.004	0.001	0.006	0.001

Appendix 2: Uncertainties in Analyses of Trace Elements Performed by ICP-MS

Metchosin Igneous Complex Analyses

	Sc	V	Sr	Y	Zr	Nb	Ba	Hf	Ta
BCR-2 replicate A	34.06	434.52	348.22	34.05	204.35	16.49	716.27	5.65	0.79
BCR-2 replicate B	33.64	430.39	345.89	34.04	202.82	16.12	694.19	5.57	0.75
BCR-2 accepted value	33	416	346	37	188	*14*	683	4.8	*0.81*
Accuracy:	3.2%	4.5%	0.6%	-8.0%	8.7%	17.8%	4.9%	17.8%	-7.0%
Precision:	0.9%	0.7%	0.5%	0.01%	0.5%	1.6%	2.2%	1.1%	3.3%

	La	Ce	Pr	Nd	Sm	Eu	Gd	Tb	Dy	Ho	Er	Tm	Yb	Lu
BCR-2 replicate A	25.76	54.80	7.03	29.18	6.70	2.10	7.30	1.11	6.70	1.35	3.85	0.51	3.50	0.55
BCR-2 replicate B	25.53	54.72	6.98	29.14	6.59	2.03	7.38	1.12	6.58	1.31	3.68	0.54	3.51	0.59
BCR-2 accepted value	25	53	6.8	28	6.7	*2*	6.8	1.07	*6.3*	1.33	*3.8*	0.54	3.5	0.51
Accuracy:	3.0%	3.4%	3.4%	4.2%	-1.6%	4.9%	8.6%	4.9%	6.3%	-1.4%	-3.1%	-4.7%	0.4%	15.9%
Precision:	0.6%	0.1%	0.5%	0.1%	1.1%	2.2%	0.8%	1.0%	1.3%	1.9%	3.1%	3.6%	0.2%	5.2%

Tofino Basin Analyses

	Sc	V	Sr	Y	Zr	Nb	Ba	Hf	Ta
D-14 replicate A	40.90	409.25	137.30	51.31	190.67	11.19	139.31	3.62	0.55
D-14 replicate B	42.03	408.97	133.20	48.46	173.92	9.95	140.56	3.72	0.57
BCR-2 this analysis	32.56	453.69	365.01	35.10	192.97	13.71	677.37	4.71	0.81
BCR-2 accepted value	33	416	346	37	188	*14*	683	4.8	*0.81*
Accuracy:	-1.3%	9.1%	5.5%	-5.1%	2.6%	-2.1%	-0.8%		
Precision:	1.9%	0.0%	2.1%	4.0%	6.5%	8.3%	0.6%	-1.8%	-0.3%

	La	Ce	Pr	Nd	Sm	Eu	Gd	Tb	Dy	Ho	Er	Tm	Yb	Lu
D-14 replicate A	7.59	20.74	3.29	16.07	5.22	1.92	7.17	1.31	7.90	1.67	4.74	0.71	4.91	0.68
D-14 replicate B	7.69	20.92	3.24	17.12	5.51	2.04	7.36	1.38	8.37	1.77	4.82	0.73	5.20	0.71
BCR-2 this analysis	25.49	54.37	6.97	29.15	6.29	1.96	6.79	1.09	6.18	1.26	3.49	0.52	3.54	0.51
BCR-2 accepted value	25	53	6.8	28	6.7	2	6.8	1.07	*6.3*	1.33	*3.8*	0.54	3.5	0.51
Accuracy:	2.0%	2.6%	2.5%	4.1%	-6.1%	-1.9%	-0.1%	1.6%	-1.9%	-5.3%	-8.0%	-4.2%	1.2%	0.7%
Precision:	0.9%	0.6%	1.1%	4.5%	3.9%	4.4%	1.8%	3.8%	4.1%	4.0%	1.2%	1.6%	4.1%	2.9%

Appendix 2: Uncertainties in Analyses of Trace Elements Performed by ICP-MS

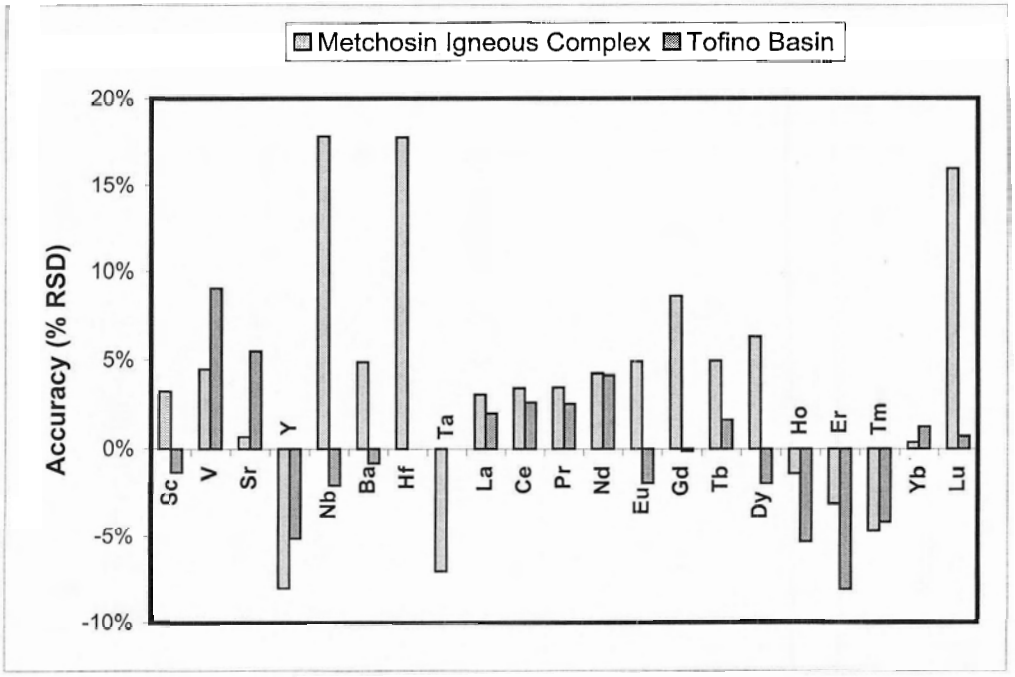

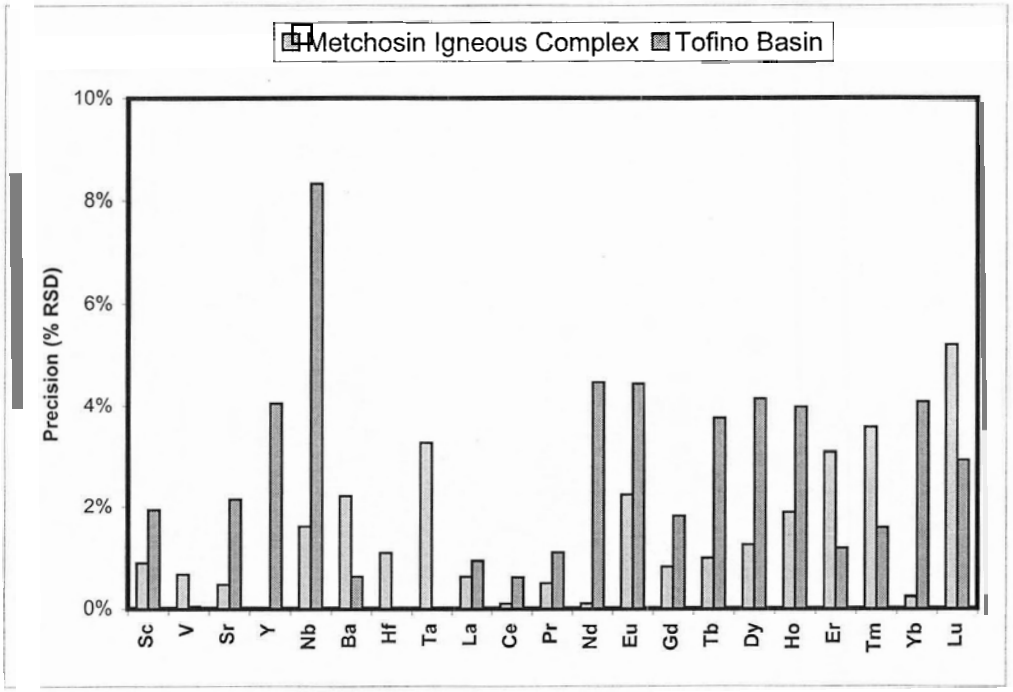

Appendix 3: Petrography

Both Alison Hartley and Glen Nevokshonoff used MIC-99-## as the numbering convention for their samples and consequently some sample numbers were duplicated in both collections. To avoid confusion they are referred to using the numbering conventions AH-## for Alison Hartley's samples and GN-## for Glen Nevokshonoff's samples. Only Alison Hartley's basaltic samples are described herein.

Sample: ST-08 **Lithology:** Pillow basalt
Igneous Mineralogy: 20% plag, 10% cpx, 65% interstitial material, 5% opaque minerals
Igneous Textures: 20% vesicles.
Groundmass Alteration: Interstitial material altered to chlorite + prehnite + quartz, 100% albitization of plagioclase.
Vesicle Assemblage: Prehnite + chlorite + quartz + actinolite + carbonate

Sample: ST-09 **Lithology:** Massive flow
Igneous Mineralogy: 50% plag, 40% cpx, 5% interstitial material, 5% opaque minerals
Igneous Textures: subophitic clinopyroxene
Groundmass Alteration: Interstitial material altered to chlorite + prehnite + quartz + actinolite; 5% albitization of plagioclase.

Sample: ST-11 **Lithology:** Pervasively altered basalt
Igneous Mineralogy: Indeterminate
Igneous Textures: None
Groundmass Alteration: Epidote + chlorite + actinolite + quartz.
Vein Assemblage: Epidote + quartz + chlorite + actinolite.

Sample: ST-15 **Lithology:** Massive flow
Igneous Mineralogy: 40% plag, 50% cpx, 5% interstitial material, 5% opaque minerals
Igneous Textures: Plagioclase is taxitic; 2% glomerocrysts, 100% of which are plagioclase, showing dissolution rims and extensive fracturing.
Groundmass Alteration: Interstitial material altered to chlorite; ~20% albitization of plagioclase.
Vein Assemblages: 1) Chlorite + quartz + epidote + actinolite cross-cut by 2) carbonate

Sample: ST-20 **Lithology:** Pillow basalt
Igneous Mineralogy: 50% plag, 15% cpx, 30% interstitial material, 5% opaque minerals
Igneous Textures: 15% vesicles.
Groundmass Alteration: Interstitial material altered to chlorite + epidote + quartz; 100% albitization of plagioclase.
Vesicle Assemblage: Epidote + chlorite + andradite + quartz + pyrite + magnetite + actinolite.

Sample: ST-23 **Lithology:** Pillow basalt
Igneous Mineralogy: 45% plag, 40% cpx, 5% interstitial material, 15% opaque minerals
Groundmass Alteration: Interstitial material altered to chlorite + epidote + quartz; ~10% albitization of plagioclase.

Sample: ST-25 **Lithology:** Pillow basalt
Igneous Mineralogy: 40% plag, 40% cpx, 10% interstitial material, 10% opaque minerals
Igneous Textures: 10% vesicles; subophitic clinopyroxene.
Groundmass Alteration: Interstitial material altered to chlorite + epidote + quartz + carbonate + actinolite; ~40% albitization of plagioclase.
Vesicle Assemblage: Chlorite + quartz + carbonate.

Appendix 3: Petrography

Sample: ST-35 **Lithology:** Pillow basalt
Igneous Mineralogy: 10% plag, 5% cpx, 1% olivine, 80% interstitial material, 4% opaque minerals
Igneous Textures: 10% vesicles; 10% glomerocrysts, 100% of which are plagioclase, showing dissolution rims and extensive fracturing.
Groundmass Alteration: Interstitial material altered to chlorite + epidote + quartz + prehnite; ~80% albitization of plagioclase.
Vesicle Assemblage: Chlorite + quartz + epidote + prehnite.
Vein Assemblages: 1) Chlorite + epidote + quartz cross-cut by 2) chlorite + quartz + prehnite cross-cut by 3) quartz + carbonate + zeolite.

Sample: ST-42 **Lithology:** Massive flow
Igneous Mineralogy: 45% plag, 40% cpx, 10% interstitial material, 5% opaque minerals
Igneous Textures: 2% vesicles.
Groundmass Alteration: Interstitial material altered to chlorite; ~40% albitization of plagioclase.
Vesicle Assemblage: Chlorite.

Sample: ST-43 **Lithology:** Pillow basalt
Igneous Mineralogy: 25% plag, 5% cpx, 1% olivine, 65% interstitial material, 4% opaque minerals
Igneous Textures: 10% vesicles; plagioclase is taxitic;15% glomerocrysts, 100% of which are plagioclase, showing dissolution rims and extensive fracturing.
Groundmass Alteration: Interstitial material altered to chlorite; ~80% albitization of plagioclase.
Vesicle Assemblage: Chlorite + quartz + carbonate + prehnite + zeolite.
Vein Assemblages: 1) Quartz cross-cut by 2) carbonate + zeolite.

Sample: ST-47 **Lithology:** Pillow basalt
Igneous Mineralogy: 10% plag, 10% cpx, 1% olivine, 75% interstitial material, 4% opaque minerals
Igneous Textures: 10% vesicles; 15% glomerocrysts, 50% of which are plagioclase and 50% of which are clinopyroxene, showing dissolution rims and extensive fracturing.
Groundmass Alteration: Interstitial material altered to chlorite + epidote + quartz; ~80% albitization of plagioclase.
Vesicle Assemblage: Chlorite + quartz + epidote + prehnite.
Vein Assemblages: 1) Epidote + chlorite + quartz cross-cut by 2) prehnite + quartz + chlorite.

Sample: ST-48 **Lithology:** Inter-flow sediment
Igneous Mineralogy: ~2% relic clinopyroxene
Groundmass Assemblage: Quartz + chlorite + albite + prehnite + carbonate.

Sample: ST-51 **Lithology:** Pillow basalt
Igneous Mineralogy: 50% plag, 35% cpx, 10% interstitial material, 5% opaque minerals
Igneous Textures: 10% vesicles.
Groundmass Alteration: Interstitial material altered to chlorite + prehnite + quartz; 100% albitization of plagioclase.
Vesicle Assemblage: Chlorite + carbonate + epidote + quartz.

Sample: ST-54 **Lithology:** Massive flow
Igneous Mineralogy: 45% plag, 40% cpx, 10% interstitial material, 10% opaque minerals
Igneous Textures: 12% vesicles.
Groundmass Alteration: Interstitial material altered to chlorite + prehnite + epidote + quartz; 100% albitization of plagioclase.
Vesicle Assemblage: Chlorite + quartz + epidote + prehnite.

Appendix 3: Petrography

Sample: ST-55 **Lithology:** Massive flow
Igneous Mineralogy: 40% plag, 45% cpx, 10% interstitial material, 5% opaque minerals
Igneous Textures: 15% vesicles.
Groundmass Alteration: Interstitial material altered to chlorite + quartz; ~60% albitization of plagioclase.
Vesicle Assemblage: Prehnite + chlorite + quartz.
Vein Assemblage: Prehnite + chlorite + quartz.

Sample: ST-57 **Lithology:** Massive flow
Igneous Mineralogy: 20% plag, 20% cpx, 50% interstitial material, 10% opaque minerals
Igneous Textures: 5% vesicles.
Groundmass Alteration: Interstitial material altered to chlorite + quartz + prehnite; ~90% albitization of plagioclase.
Vesicle Assemblage: Chlorite + prehnite + quartz + epidote + carbonate + magnetite.
Vein Assemblages: 1) Epidote + quartz + chlorite cross-cut by 2) prehnite + quartz + chlorite.

Sample: ST-59 **Lithology:** Pillow basalt
Igneous Mineralogy: 50% plag, 25% cpx, 20% interstitial material, 5% opaque minerals
Igneous Textures: 12% vesicles; plagioclase is taxitic; vesicles have rapidly quenched rims indicating vesicle rupture during cooling.
Groundmass Alteration: Interstitial material altered to chlorite + epidote + quartz; 100% albitization of plagioclase.
Vesicle Assemblage: Epidote + chlorite + quartz + pyrite + magnetite.
Vein Assemblages: 1) Epidote + quartz + chlorite.

Sample: ST-62 **Lithology:** Pillow basalt
Igneous Mineralogy: 45% plag, 40% cpx, 10% interstitial material, 5% opaque minerals
Igneous Textures: 4% vesicles.
Groundmass Alteration: Interstitial material altered to chlorite + prehnite + epidote + quartz + carbonate; ~10% albitization of plagioclase.
Vesicle Assemblage: Chlorite + quartz + prehnite + epidote.
Vein Assemblage: Quartz + chlorite.

Sample: ST-64 **Lithology:** Inter-flow sediment
Igneous Mineralogy: >1% relic clinopyroxene
Groundmass Assemblage: Quartz + chlorite + albite + prehnite + carbonate.

Sample: ST-65 **Lithology:** Pillow basalt
Igneous Mineralogy: 40% plag, 35% cpx, 20% interstitial material, 5% opaque minerals
Igneous Textures: 12% vesicles; plagioclase is taxitic; vesicles have rapidly quenched rims indicating vesicle rupture during cooling.
Groundmass Alteration: Interstitial material altered to chlorite + quartz + epidote; 100% albitization of plagioclase.
Vesicle Assemblage: Chlorite + epidote + quartz + actinolite + prehnite + pyrite + chalcopyrite.
Vein Assemblages: 1) Epidote + quartz + chlorite cross-cut by 2) carbonate + zeolite.

Sample: ST-66 **Lithology:** Massive flow
Igneous Mineralogy: 50% plag, 30% cpx, 5% interstitial material, 15% opaque minerals
Groundmass Alteration: Interstitial material altered to chlorite + quartz + epidote; 100% albitization of plagioclase; heavily fractured.
Vesicle Assemblage: Chlorite + epidote + quartz.
Vein Assemblages: 1) Epidote + quartz + chlorite cross-cut by 2) carbonate + chlorite.

Appendix 3: Petrography

Sample: ST-69 **Lithology:** Pervasively altered, possibly gabbro
Igneous Mineralogy: Relic medium grained plagioclase and clinopyroxene
Igneous Textures: None
Groundmass Alteration: Actinolite + epidote + chlorite + quartz + prehnite.
Vein Assemblage: Epidote + quartz + chlorite + actinolite + prehnite.

Sample: ST-70 **Lithology:** Greenschist
Metamorphic Textures: Unfoliated; veins exhibit ductile deformation.
Groundmass Assemblage: Epidote + chlorite + actinolite + plagioclase + quartz + magnetite.
Vein Assemblage: Epidote + quartz + chlorite.

Sample: ST-72 **Lithology:** Greenschist
Metamorphic Textures: Weakly foliated.
Groundmass Assemblage: Actinolite + epidote + quartz + plagioclase + chlorite + magnetite.

Sample: ST-75 **Lithology:** Greenschist
Metamorphic Textures: Weakly foliated.
Groundmass Assemblage: Actinolite + epidote + quartz + plagioclase + chlorite + magnetite.
Vein Assemblage: Epidote + actinolite + quartz + chlorite.

Sample: ST-77 **Lithology:** Greenschist
Metamorphic Textures: Weakly foliated.
Groundmass Assemblage: Actinolite + epidote + quartz + plagioclase + chlorite + magnetite.
Vein Assemblage: Epidote + quartz + actinolite + chlorite.

Sample: ST-78 **Lithology:** Greenschist
Metamorphic Textures: Unfoliated.
Groundmass Assemblage: Actinolite + chlorite + plagioclase + epidote + quartz.
Vesicle Assemblage: Epidote + quartz + chlorite + actinolite + pyrite.

Sample: ST-79 **Lithology:** Pervasively altered volcaniclastic
Metamorphic Textures: Pseudomorphs of original volcanic clasts.
Groundmass Assemblage: Epidote + chlorite + quartz + actinolite + plagioclase.

Sample: ST-80 **Lithology:** Massive flow
Igneous Mineralogy: 60% plag, 10% cpx, 20% interstitial material, 10% opaque minerals
Groundmass Alteration: Interstitial material altered to chlorite + epidote + quartz + actinolite; ~60% albitization of plagioclase.
Vesicle Assemblage: Chlorite + epidote + quartz + actinolite.

Sample: ST-83 **Lithology:** Greenschist
Metamorphic Textures: Unfoliated.
Groundmass Assemblage: Actinolite + plagioclase + epidote + quartz + chlorite + pyrite.
Vein Assemblage: Epidote + quartz + actinolite.

Sample: ST-87 **Lithology:** Greenschist
Metamorphic Textures: Unfoliated; Epidote-actinolite veins exhibit ductile deformation.
Groundmass Assemblage: Chlorite + epidote + quartz + plagioclase + actinolite + pyrite.
Vein Assemblages: 1) Epidote + actinolite + quartz + chlorite cross-cut by 2) quartz + chlorite.

Appendix 3: Petrography

Sample: ST-88 **Lithology:** Pervasively altered volcaniclastic
Metamorphic Textures: Pseudomorphs of original volcanic clasts; relic plagioclase preserved in some clasts.
Groundmass Assemblage: Actinolite + quartz + epidote + chlorite + plagioclase + prehnite + magnetite + pyrite + chalcopyrite.

Sample: ST-89 **Lithology:** Massive flow
Igneous Mineralogy: 40% plag, 40% cpx, 10% interstitial material, 10% opaque minerals.
Igneous Textures: Subophitic clinopyroxene
Groundmass Alteration: Interstitial material altered to chlorite + actinolite + epidote + quartz + prehnite; 0% albitization of plagioclase.

Sample: ST-90 **Lithology:** Greenschist
Metamorphic Textures: Unfoliated; Epidote-actinolite veins exhibit ductile deformation.
Groundmass Assemblage: Actinolite + epidote + quartz + plagioclase + chlorite + pyrite.
Vein Assemblages: 1) Actinolite + quartz cross-cut by 2) Epidote + quartz cross-cut by 3) chlorite cross-cut by 4) carbonate.

Sample: ST-92 **Lithology:** Greenschist
Metamorphic Textures: Unfoliated.
Groundmass Assemblage: Actinolite + epidote + quartz + plagioclase + chlorite + magnetite.
Vein Assemblages: 1) Actinolite + quartz + epidote + chlorite cross-cut by 2) Chlorite + quartz.

Sample: ST-94 **Lithology:** Greenschist
Metamorphic Textures: Unfoliated.
Groundmass Assemblage: Quartz + chlorite + epidote + plagioclase + pyrite.
Vein Assemblages: 1) Actinolite + quartz + epidote + chlorite cross-cut by 2) Chlorite + quartz.

Sample: ST-95 **Lithology:** Massive flow
Igneous Mineralogy: 40% plag, 35% cpx, 15% interstitial material, 10% opaque minerals.
Igneous Textures: 10% vesicles.
Groundmass Alteration: Interstitial material altered to chlorite + epidote + quartz + carbonate + actinolite; ~20% albitization of plagioclase.
Vesicle Assemblage: Chlorite + carbonate + quartz + actinolite.

Sample: ST-96 **Lithology:** Pillow basalt
Igneous Mineralogy: 10% plag, 15% cpx, 70% interstitial material, 5% opaque minerals.
Igneous Textures: 15% vesicles.
Groundmass Alteration: Interstitial material altered to chlorite + epidote + quartz + actinolite; ~50% albitization of plagioclase.
Vesicle Assemblage: Chlorite + prehnite + zeolite + carbonate + quartz + actinolite.
Vein Assemblage: Zeolite + carbonate.

Sample: ST-97 **Lithology:** Pillow basalt
Igneous Mineralogy: 50% plag, 35% cpx, 10% interstitial material, 5% opaque minerals.
Groundmass Alteration: Interstitial material altered to chlorite + epidote + quartz; ~60% albitization of plagioclase.
Vein Assemblage: Prehnite + chlorite + quartz.

Appendix 3: Petrography

Sample: ST-98 **Lithology:** Massive flow
Igneous Mineralogy: 10% plag, 10% cpx, 70% interstitial material, 10% opaque minerals.
Igneous Textures: 2% glomerocrysts, 100% of which are clinopyroxene, showing dissolution rims and extensive fracturing.
Groundmass Alteration: Interstitial material altered to chlorite + epidote + quartz; 100% albitization of plagioclase.
Vein Assemblages: 1) Epidote + quartz + chlorite cross-cut by 2) chlorite + quartz.

Sample: ST-99 **Lithology:** Gabbro
Igneous Mineralogy: 25% plag, 60% cpx, 5% opaque minerals.
Igneous Textures: Ophitic to subophitic clinopyroxene.
Groundmass Alteration: Groundmass altered to chlorite + epidote + actinolite + quartz + prehnite; ~40% albitization of plagioclase.
Vein Assemblage: Epidote + quartz + chlorite.

Sample: ST-101 **Lithology:** Pillow basalt
Igneous Mineralogy: 35% plag, 50% cpx, 10% interstitial material, 5% opaque minerals.
Igneous Textures: Subophitic clinopyroxene.
Groundmass Alteration: Interstitial material altered to chlorite + actinolite + epidote + quartz; ~30% albitization of plagioclase.

Sample: ST-103 **Lithology:** Pillow basalt
Igneous Mineralogy: 45% plag, 30% cpx, 20% interstitial material, 5% opaque minerals.
Igneous Textures: 5% vesicles.
Groundmass Alteration: Interstitial material altered to chlorite + epidote + quartz; 100% albitization of plagioclase.
Vesicle Assemblage: Chlorite
Vein Assemblages: 1) Epidote + quartz + chlorite cross-cut by 2) chlorite + quartz.

Sample: ST-107 **Lithology:** Fault gouge
Groundmass Assemblage: Chlorite + epidote + quartz + actinolite + plagioclase.
Vein Assemblages: 1) Epidote + quartz + chlorite + actinolite cross-cut by 2) Quartz + chlorite.

Sample: ST-109 **Lithology:** Fault gouge
Groundmass Assemblage: Epidote + quartz + chlorite + plagioclase + actinolite + magnetite.
Vein Assemblage: Epidote + quartz + chlorite.

Sample: ST-110 **Lithology:** Pillow basalt
Igneous Mineralogy: 30% plag, 10% cpx, 50% interstitial material, 10% opaque minerals.
Igneous Textures: 10% vesicles.
Groundmass Alteration: Interstitial material altered to chlorite + epidote + quartz; 100% albitization of plagioclase.
Vesicle Assemblage: Chlorite + epidote + quartz
Vein Assemblage: Chlorite + epidote + quartz.

Sample: ST-111 **Lithology:** Pillow basalt
Igneous Mineralogy: 50% plag, 35% cpx, 5% interstitial material, 10% opaque minerals.
Igneous Textures: 2% glomerocrysts, 100% of which are plagioclase, showing dissolution rims and extensive fracturing.
Groundmass Alteration: Interstitial material altered to chlorite + epidote + quartz; 100% albitization of plagioclase.
Vein Assemblage: Chlorite + epidote + quartz overlain by bands of hematite staining.

Appendix 3: Petrography

Sample: ST-112 **Lithology:** Pillow basalt
Igneous Mineralogy: 45% plag, 30% cpx, 20% interstitial material, 5% opaque minerals.
Igneous Textures: 10% vesicles.
Groundmass Alteration: Interstitial material altered to chlorite + epidote + quartz; 100% albitization of plagioclase.
Vesicle Assemblage: Epidote + carbonate + andradite-grossular + chlorite + quartz.

Sample: ST-115 **Lithology:** Amphibolite
Metamorphic Textures: Strongly foliated.
Groundmass Assemblage: Hornblende + plagioclase + quartz + epidote.
Vein Assemblages: 1) Quartz + epidote + chlorite cross-cut by 2) Chlorite + quartz.

Sample: ST-118 **Lithology:** Amphibolite
Metamorphic Textures: Weakly foliated.
Groundmass Assemblage: Hornblende + plagioclase + quartz + epidote + magnetite.

Sample: GN-03 **Lithology:** Pillow basalt
Igneous Mineralogy: 10% plag, 5% cpx, 1% olivine, 80% interstitial material, 4% opaque minerals
Igneous Textures: 15% vesicles.
Groundmass Alteration: Interstitial material altered to chlorite; 100% albitization of plagioclase.
Vesicle Assemblage: Prehnite + quartz + chlorite + epidote + carbonate + magnetite.
Vein Assemblage: Prehnite + quartz + chlorite.

Sample: GN-05 **Lithology:** Pillow basalt
Igneous Mineralogy: 20% plag, 5% cpx, 1% olivine, 70% interstitial material, 4% opaque minerals
Igneous Textures: 12% glomerocrysts, 100% of which are plagioclase, showing dissolution rims and extensive fracturing.
Groundmass Alteration: Interstitial material altered to chlorite actinolite; ~80% albitization of plagioclase.
Vein Assemblage: Chlorite + epidote + quartz.

Sample: GN-08 **Lithology:** Pillow basalt
Igneous Mineralogy: 50% plag, 40% cpx, 1% olivine, 5% interstitial material, 4% opaque minerals
Igneous Textures: 5% vesicles; vesicles have rapidly quenched rims indicating rupture during cooling.
Groundmass Alteration: Interstitial material altered to chlorite + actinolite + epidote + quartz; 100% albitization of plagioclase.
Vesicle Assemblage: Chlorite + quartz + carbonate + epidote + actinolite.
Vein Assemblage: Chlorite + quartz + carbonate.

Sample: GN-09 **Lithology:** Pillow basalt
Igneous Mineralogy: 50% plag, 35% cpx, 10% interstitial material, 5% opaque minerals
Igneous Textures: 1% vesicles; 1% glomerocrysts, 100% of which are plagioclase, showing dissolution rims and extensive fracturing.
Groundmass Alteration: Interstitial material altered to chlorite; ~10% albitization of plagioclase.
Vesicle Assemblage: Chlorite + prehnite + magnetite.

Sample: GN-12 **Lithology:** Pillow basalt
Igneous Mineralogy: 50% plag, 40% cpx, 5% interstitial material, 5% opaque minerals
Igneous Textures: 15% vesicles.
Groundmass Alteration: Interstitial material altered to chlorite + epidote + quartz + actinolite; 100% albitization of plagioclase.
Vesicle Assemblage: Chlorite + quartz + epidote + actinolite + garnet + pyrite.
Vein Assemblages: 1) Chlorite + epidote + quartz.

Appendix 3: Petrography

Sample: GN-13 **Lithology:** Pillow basalt
Igneous Mineralogy: 40% plag, 35% cpx, 10% interstitial material, 5% opaque minerals
Igneous Textures: Subophitic clinopyroxene.
Groundmass Alteration: Interstitial material altered to chlorite + carbonate + epidote + quartz; ~30% albitization of plagioclase.

Sample: GN-15 **Lithology:** Massive flow
Igneous Mineralogy: 40% plag, 40% cpx, 10% interstitial material, 10% opaque minerals
Igneous Textures: 10% glomerocrysts, 100% of which are plagioclase, showing dissolution rims and extensive fracturing.
Groundmass Alteration: Interstitial material altered to chlorite + prehnite + quartz; 100% albitization of plagioclase.
Vein Assemblages: 1) Prehnite + chlorite + quartz.

Sample: GN-16 **Lithology:** Pillow basalt
Igneous Mineralogy: 10% plag, 5% cpx, 1% olivine, 80% interstitial material, 4% opaque minerals
Igneous Textures: 10% vesicles; vesicles have rapidly quenched rims indicating vesicle rupture during cooling.
Groundmass Alteration: Interstitial material altered to chlorite + prehnite + quartz; 100% albitization of plagioclase.
Vesicle Assemblage: Prehnite + quartz + chlorite + carbonate + magnetite.
Vein Assemblage: prehnite + quartz + chlorite.

Sample: AH-04 **Lithology:** Pillow basalt
Igneous Mineralogy: 10% plag, 5% cpx, 1% olivine, 80% interstitial material, 4% opaque minerals
Igneous Textures: 10% vesicles; vesicles have rapidly quenched rims indicating vesicle rupture during cooling ; 10% glomerocrysts, 50% of which are clinopyroxene and 50% of which are plagioclase, showing dissolution rims and extensive fracturing.
Groundmass Alteration: Interstitial material altered to chlorite; 0% albitization of plagioclase.
Vesicle Assemblage: Chlorite.
Vein Assemblages: 1) Chlorite + epidote + quartz cross-cut by 2) carbonate + zeolite.

Sample: AH-16 **Lithology:** Pillow basalt
Igneous Mineralogy: 45% plag, 40% cpx, 10% interstitial material, 5% opaque minerals
Igneous Textures: 10% vesicles; 5% glomerocrysts, 70% of which are clinopyroxene and 30% of which are plagioclase, showing dissolution rims and extensive fracturing.
Groundmass Alteration: Interstitial material altered to chlorite + epidote + actinolite + quartz; 100% albitization of plagioclase.
Vesicle Assemblage: Actinolite + chlorite + epidote + quartz.
Vein Assemblage: Chlorite + epidote + quartz.

Sample: AH-31 **Lithology:** Pillow basalt
Igneous Mineralogy: 30% plag, 35% cpx, 30% interstitial material, 5% opaque minerals
Igneous Textures: 5% glomerocrysts, 20% of which are clinopyroxene and 80% of which are plagioclase, showing dissolution rims and extensive fracturing.
Groundmass Alteration: Interstitial material altered to chlorite + epidote + quartz+ prehnite; ~80% albitization of plagioclase.
Vein Assemblages: 1) Chlorite + prehnite + quartz.

Appendix 3: Petrography

Sample: AH-34 **Lithology:** Pillow basalt
Igneous Mineralogy: 10% plag, 10% cpx, 1% olivine, 75% interstitial material, 4% opaque minerals
Igneous Textures: 10% vesicles; 5% glomerocrysts, 50% of which are clinopyroxene and 50% of which are plagioclase, showing dissolution rims and extensive fracturing.
Groundmass Alteration: Interstitial material altered to chlorite + epidote + quartz; 100% albitization of plagioclase.
Vesicle Assemblage: Chlorite + epidote + quartz.
Vein Assemblage: Chlorite + quartz + carbonate.

Appendix 4: Chlorite Compositions

Sample	Lithology	Occurence	SiO2 (wt%)	TiO2 (wt%)	Al2O3 (wt%)	FeO (wt%)	MnO (wt%)	MgO (wt%)	CaO (wt%)	Na2O (wt%)	K2O (wt%)	Total (wt%)	SiIV	AlIV	AlVI	Fe	Mn	Mg	Mg#	T (°C)
ST-64	Sediment	Groundmass	27.12	N/A	17.88	29.38	0.55	12.56	0.18	0.03	0.03	87.75	2.93	1.07	1.21	2.65	0.051	2.02	43	283
ST-64	Sediment	Groundmass	27.03	N/A	17.63	29.56	0.55	12.15	0.14	0.00	0.05	87.13	2.94	1.06	1.21	2.69	0.051	1.97	42	278
ST-65	Pillow Basalt	Amygdule	28.68	0.00	17.60	24.66	0.33	16.96	0.17	0.00	0.00	88.41	2.98	1.02	1.14	2.14	0.029	2.63	55	266
ST-65	Pillow Basalt	Amygdule	27.65	0.00	18.60	24.70	0.24	17.12	0.11	0.00	0.01	88.45	2.88	1.12	1.16	2.15	0.021	2.66	55	300
ST-65	Pillow Basalt	Amygdule	27.41	N/A	18.08	24.29	0.30	17.19	0.09	0.00	0.01	87.38	2.89	1.11	1.13	2.14	0.027	2.70	55	297
ST-65	Pillow Basalt	Amygdule	27.07	N/A	18.90	24.50	0.29	16.93	0.11	0.00	0.00	87.82	2.84	1.16	1.17	2.15	0.026	2.65	55	312
ST-65	Pillow Basalt	Amygdule	28.28	N/A	17.80	24.17	0.28	17.30	0.19	0.00	0.00	88.05	2.95	1.05	1.14	2.11	0.025	2.69	56	277
ST-65	Pillow Basalt	Amygdule	28.73	0.00	17.52	24.12	0.25	17.42	0.15	0.00	0.00	88.30	2.98	1.02	1.13	2.09	0.022	2.70	56	265
ST-65	Pillow Basalt	Amygdule	29.10	0.02	16.85	24.34	0.30	17.80	0.10	0.00	0.00	88.52	3.01	0.99	1.07	2.11	0.026	2.75	56	255
ST-65	Pillow Basalt	Amygdule	27.62	0.00	18.49	25.14	0.28	16.95	0.10	0.00	0.00	88.63	2.88	1.12	1.15	2.19	0.025	2.63	54	300
ST-65	Pillow Basalt	Amygdule	27.20	0.00	19.06	26.15	0.34	16.18	0.05	0.01	0.00	88.99	2.83	1.17	1.17	2.28	0.030	2.51	52	313
ST-65	Pillow Basalt	Amygdule	29.26	0.00	16.48	23.43	0.25	18.52	0.12	0.00	0.00	88.08	3.03	0.97	1.05	2.03	0.022	2.86	58	249
ST-65	Pillow Basalt	Vein	28.21	0.01	17.92	24.54	0.29	17.49	0.10	0.01	0.00	88.62	2.93	1.07	1.12	2.13	0.025	2.70	56	284
G-16	Pillow Basalt	Amygdule	27.85	N/A	17.22	28.34	0.42	14.21	0.17	0.03	0.05	88.30	2.97	1.03	1.13	2.53	0.038	2.26	47	270
G-16	Pillow Basalt	Amygdule	27.86	N/A	17.85	28.66	0.37	14.76	0.05	0.01	0.06	89.61	2.92	1.08	1.13	2.51	0.033	2.31	48	286
G-16	Pillow Basalt	Groundmass	27.45	N/A	17.88	29.85	0.48	12.31	0.19	0.05	0.07	88.31	2.95	1.05	1.22	2.68	0.044	1.97	42	276
G-16	Pillow Basalt	Amygdule	26.86	N/A	18.08	28.83	0.43	13.35	0.28	0.08	0.05	87.96	2.89	1.11	1.18	2.59	0.039	2.14	45	295
G-16	Pillow Basalt	Amygdule	28.70	N/A	17.36	28.08	0.35	13.36	0.30	0.07	0.05	88.32	3.05	0.95	1.22	2.49	0.031	2.12	46	244
ST-55	Pillow Basalt	Amygdule	28.81	N/A	16.55	25.84	0.40	16.44	0.11	0.03	0.02	88.20	3.03	0.97	1.07	2.27	0.036	2.57	53	252
ST-55	Pillow Basalt	Amygdule	29.05	N/A	16.30	26.19	0.33	16.79	0.14	0.00	0.01	88.82	3.03	0.97	1.04	2.29	0.029	2.61	53	250
ST-55	Pillow Basalt	Groundmass	29.15	N/A	17.29	25.29	0.39	15.92	0.40	0.00	0.00	88.44	3.04	0.96	1.17	2.21	0.034	2.48	52	246
ST-55	Pillow Basalt	Amygdule	28.57	N/A	16.52	26.46	0.37	16.47	0.13	0.00	0.02	88.56	3.00	1.00	1.04	2.32	0.033	2.58	52	260
ST-96	Pillow Basalt	Amygdule	29.79	N/A	16.97	22.95	0.28	18.91	0.22	0.00	0.02	89.19	3.04	0.96	1.08	1.96	0.024	2.88	59	247
ST-96	Pillow Basalt	Amygdule	28.30	N/A	17.66	26.09	0.27	16.60	0.04	0.00	0.01	88.96	2.94	1.06	1.11	2.27	0.024	2.57	53	278
ST-96	Pillow Basalt	Amygdule	28.44	N/A	17.98	23.81	0.30	17.39	0.15	0.01	0.00	88.09	2.95	1.05	1.16	2.07	0.026	2.69	56	275
ST-96	Pillow Basalt	Amygdule	27.53	N/A	18.60	25.52	0.32	16.04	0.12	0.01	0.00	88.19	2.89	1.11	1.19	2.24	0.028	2.51	53	296
ST-96	Pillow Basalt	Amygdule	26.65	N/A	18.73	26.26	0.32	15.12	0.16	0.00	0.02	87.30	2.84	1.16	1.20	2.34	0.029	2.41	50	310
ST-96	Pillow Basalt	Amygdule	27.12	N/A	19.15	26.83	0.32	14.99	0.12	0.00	0.00	88.54	2.85	1.15	1.22	2.36	0.029	2.35	50	308
ST-20	Pillow Basalt	Amygdule	28.70	N/A	17.41	23.58	0.27	18.45	0.08	0.01	0.01	88.54	2.96	1.04	1.08	2.04	0.024	2.84	58	272
ST-20	Pillow Basalt	Amygdule	28.81	N/A	17.52	23.49	0.28	18.72	0.13	0.01	0.03	88.98	2.96	1.04	1.08	2.02	0.024	2.86	58	274
ST-20	Pillow Basalt	Vein	27.15	N/A	17.51	23.04	0.29	17.30	0.14	0.03	0.01	85.57	2.91	1.09	1.12	2.07	0.027	2.76	57	288
ST-20	Pillow Basalt	Vein	28.38	N/A	17.77	23.80	0.31	18.19	0.05	0.00	0.01	88.51	2.93	1.07	1.10	2.06	0.027	2.80	57	281
ST-20	Pillow Basalt	Amygdule	28.42	N/A	17.48	23.53	0.28	18.15	0.09	0.03	0.01	87.98	2.95	1.05	1.09	2.04	0.024	2.81	58	275
ST-20	Pillow Basalt	Amygdule	28.76	N/A	17.50	23.34	0.30	18.61	0.08	0.01	0.01	88.65	2.96	1.04	1.08	2.01	0.027	2.86	58	273
ST-20	Pillow Basalt	Amygdule	28.40	N/A	17.67	23.73	0.32	18.37	0.10	0.01	0.00	88.58	2.93	1.07	1.08	2.05	0.028	2.83	58	281
ST-25	Pillow Basalt	Groundmass	27.31	N/A	18.28	27.89	0.35	13.93	0.21	0.01	0.00	87.98	2.91	1.09	1.21	2.49	0.032	2.21	47	288
ST-25	Pillow Basalt	Groundmass	27.41	N/A	18.56	28.01	0.32	14.14	0.22	0.00	0.02	88.67	2.90	1.10	1.21	2.48	0.029	2.23	47	293
ST-25	Pillow Basalt	Groundmass	28.81	N/A	16.54	27.86	0.30	15.31	0.16	0.01	0.02	89.01	3.03	0.97	1.08	2.45	0.027	2.40	49	251
ST-25	Pillow Basalt	Groundmass	28.09	N/A	17.96	27.99	0.32	14.57	0.19	0.03	0.03	89.18	2.95	1.05	1.17	2.48	0.029	2.28	48	276
ST-25	Pillow Basalt	Groundmass	27.11	N/A	19.00	27.93	0.39	13.62	0.22	0.02	0.00	88.31	2.88	1.12	1.26	2.48	0.035	2.16	46	299
ST-25	Pillow Basalt	Groundmass	26.93	N/A	18.40	27.99	0.36	13.68	0.17	0.01	0.03	87.57	2.89	1.11	1.22	2.51	0.033	2.19	46	296
ST-66	Fault Gouge	Groundmass	28.21	0.00	18.80	21.98	0.46	18.97	0.09	0.00	0.00	88.51	2.89	1.11	1.16	1.88	0.040	2.90	60	296
ST-66	Fault Gouge	Vein	28.80	0.03	19.28	22.17	0.41	18.88	0.13	0.00	0.02	89.52	2.89	1.11	1.19	1.86	0.035	2.85	60	294
ST-66	Fault Gouge	Vein	28.06	0.02	18.78	22.59	0.38	18.75	0.05	0.00	0.00	88.65	2.88	1.12	1.15	1.94	0.033	2.87	59	299
ST-66	Fault Gouge	Vein	28.79	0.00	18.13	21.58	0.36	19.27	0.08	0.01	0.03	88.25	2.95	1.05	1.14	1.85	0.031	2.94	61	277
ST-66	Fault Gouge	Vein	29.05	0.01	17.27	23.36	0.42	18.20	0.30	0.00	0.03	88.66	3.00	1.00	1.10	2.02	0.037	2.80	58	261

Appendix 4: Chlorite Compositions

Sample	Lithology	Occurence	SiO2 (wt%)	TiO2 (wt%)	Al2O3 (wt%)	FeO (wt%)	MnO (wt%)	MgO (wt%)	CaO (wt%)	Na2O (wt%)	K2O (wt%)	Total (wt%)	SiIV	AlIV	AlVI	Fe	Mn	Mg	Mg#	T (°C)
ST-66	Fault Gouge	Vein	28.42	0.00	18.66	22.43	0.40	18.71	0.20	0.01	0.00	88.83	2.91	1.09	1.16	1.92	0.035	2.85	59	290
ST-66	Fault Gouge	Vein	28.83	0.00	18.56	21.73	0.35	18.99	0.04	0.02	0.00	88.53	2.94	1.06	1.17	1.85	0.030	2.89	61	279
ST-90	Fault Gouge	Groundmass	29.02	N/A	18.39	17.65	0.28	21.44	0.12	0.00	0.01	86.93	2.95	1.05	1.16	1.50	0.024	3.25	68	275
ST-90	Fault Gouge	Groundmass	28.44	N/A	19.85	17.98	0.28	20.08	0.09	0.00	0.00	86.73	2.90	1.10	1.29	1.53	0.024	3.05	66	291
ST-90	Fault Gouge	Groundmass	27.75	N/A	19.69	17.75	0.31	19.76	0.12	0.00	0.02	85.40	2.88	1.12	1.29	1.54	0.027	3.06	66	298
ST-90	Fault Gouge	Vein	28.12	N/A	19.86	17.88	0.31	20.15	0.07	0.02	0.02	86.50	2.88	1.12	1.28	1.53	0.027	3.08	66	298
ST-90	Fault Gouge	Vein	28.32	N/A	19.48	17.89	0.28	20.11	0.10	0.00	0.01	86.21	2.91	1.09	1.27	1.54	0.024	3.08	66	289
ST-90	Fault Gouge	Vein	29.05	N/A	19.61	18.10	0.27	20.60	0.12	0.00	0.01	87.84	2.93	1.07	1.26	1.53	0.023	3.10	67	283
ST-90	Fault Gouge	Vein	28.79	N/A	19.63	17.71	0.28	20.29	0.16	0.00	0.00	86.87	2.93	1.07	1.28	1.51	0.024	3.08	67	283
ST-90	Fault Gouge	Vein	29.02	N/A	18.95	17.74	0.31	20.46	0.18	0.00	0.01	86.67	2.96	1.04	1.24	1.51	0.027	3.11	67	272
ST-94	Massive Flow	Groundmass	29.16	0.02	16.15	25.63	0.23	17.51	0.09	0.03	0.02	88.83	3.03	0.97	1.01	2.23	0.020	2.71	55	249
ST-94	Massive Flow	Groundmass	29.38	0.01	16.01	25.57	0.26	18.03	0.11	0.00	0.03	89.39	3.03	0.97	0.98	2.21	0.023	2.78	55	249
ST-94	Massive Flow	Groundmass	29.40	0.00	15.82	26.09	0.23	17.47	0.10	0.00	0.06	89.16	3.05	0.95	0.99	2.27	0.020	2.70	54	243
ST-94	Massive Flow	Groundmass	29.62	0.02	15.73	25.55	0.23	17.34	0.23	0.00	0.13	88.85	3.08	0.92	1.01	2.22	0.020	2.69	55	233
ST-94	Massive Flow	Groundmass	29.31	0.00	16.27	25.59	0.21	17.71	0.07	0.02	0.02	89.19	3.03	0.97	1.01	2.21	0.018	2.73	55	250
ST-94	Massive Flow	Groundmass	29.59	0.05	16.60	25.86	0.27	16.42	0.08	0.05	0.57	89.48	3.07	0.93	1.10	2.25	0.024	2.54	53	237
ST-94	Massive Flow	Groundmass	29.70	0.03	15.96	26.19	0.25	17.09	0.06	0.00	0.04	89.34	3.08	0.92	1.02	2.27	0.022	2.64	54	236
ST-94	Massive Flow	Groundmass	28.85	0.00	15.48	25.77	0.26	17.75	0.05	0.01	0.02	88.19	3.03	0.97	0.95	2.26	0.023	2.78	55	250
ST-94	Massive Flow	Groundmass	29.70	0.00	14.87	25.37	0.28	17.73	0.11	0.01	0.02	88.10	3.11	0.89	0.95	2.22	0.025	2.77	55	224
ST-94	Massive Flow	Groundmass	29.22	0.00	15.73	25.41	0.25	17.36	0.09	0.01	0.03	88.12	3.06	0.94	1.01	2.23	0.022	2.71	55	240
ST-103	Pillow Basalt	Phenocryst	26.86	0.00	19.39	25.04	0.24	16.21	0.09	0.02	0.02	87.88	2.82	1.18	1.22	2.20	0.021	2.54	53	318
ST-103	Pillow Basalt	Phenocryst	27.07	0.00	19.81	25.17	0.33	16.01	0.03	0.01	0.03	88.46	2.82	1.18	1.25	2.19	0.029	2.49	53	318
ST-103	Pillow Basalt	Phenocryst	27.31	0.00	19.57	24.77	0.30	16.32	0.03	0.00	0.01	88.31	2.84	1.16	1.24	2.16	0.026	2.53	54	311
ST-103	Pillow Basalt	Phenocryst	27.46	0.00	19.63	25.17	0.25	15.89	0.04	0.00	0.02	88.50	2.86	1.14	1.26	2.19	0.022	2.46	53	306
ST-103	Pillow Basalt	Amygdule	28.37	0.00	17.94	25.69	0.27	16.03	0.07	0.00	0.00	88.37	2.96	1.04	1.17	2.24	0.024	2.50	52	272
ST-103	Pillow Basalt	Amygdule	27.60	0.00	17.52	26.17	0.23	16.03	0.04	0.00	0.01	87.61	2.92	1.08	1.11	2.32	0.021	2.53	52	285
ST-103	Pillow Basalt	Amygdule	28.61	0.00	17.27	25.53	0.28	16.86	0.03	0.00	0.00	88.58	2.98	1.02	1.10	2.22	0.024	2.62	54	267
ST-103	Pillow Basalt	Amygdule	26.17	0.00	19.10	27.30	0.25	15.01	0.05	0.01	0.01	87.91	2.79	1.21	1.18	2.43	0.023	2.38	49	329
ST-103	Pillow Basalt	Amygdule	28.36	0.00	17.73	26.61	0.23	15.97	0.00	0.00	0.01	88.97	2.96	1.04	1.13	2.32	0.020	2.48	51	274
ST-103	Pillow Basalt	Amygdule	27.03	0.00	17.56	25.67	0.29	16.65	0.05	0.04	0.01	87.29	2.87	1.13	1.08	2.28	0.026	2.64	53	300
ST-103	Pillow Basalt	Amygdule	27.20	0.00	17.38	25.91	0.27	16.57	0.10	0.00	0.00	87.42	2.89	1.11	1.07	2.30	0.024	2.63	53	295
ST-103	Pillow Basalt	Amygdule	28.08	0.00	18.03	26.61	0.26	15.78	0.07	0.01	0.00	88.84	2.93	1.07	1.15	2.32	0.023	2.46	51	281
ST-103	Pillow Basalt	Amygdule	27.02	0.00	18.63	26.01	0.27	16.02	0.12	0.00	0.01	88.13	2.85	1.15	1.16	2.29	0.024	2.52	52	309
ST-103	Pillow Basalt	Amygdule	27.27	0.01	17.42	26.50	0.30	15.61	0.12	0.00	0.01	87.23	2.91	1.09	1.11	2.37	0.027	2.49	51	288
ST-103	Pillow Basalt	Groundmass	27.00	0.01	18.97	26.66	0.25	15.60	0.23	0.04	0.01	88.78	2.84	1.16	1.18	2.34	0.022	2.44	51	313
ST-103	Pillow Basalt	Groundmass	24.48	0.01	18.94	25.94	0.28	15.88	0.38	0.00	0.01	85.94	2.68	1.32	1.12	2.37	0.026	2.59	52	364
ST-103	Pillow Basalt	Amygdule	27.28	0.00	19.07	25.92	0.37	15.73	0.12	0.00	0.02	88.51	2.86	1.14	1.21	2.27	0.033	2.46	52	306
ST-103	Pillow Basalt	Amygdule	26.85	0.00	19.34	25.97	0.32	15.41	0.09	0.02	0.02	88.00	2.83	1.17	1.23	2.29	0.029	2.42	51	315
ST-103	Pillow Basalt	Amygdule	25.92	0.02	19.32	25.54	0.31	15.53	0.12	0.01	0.04	86.80	2.77	1.23	1.21	2.29	0.028	2.48	52	333
ST-103	Pillow Basalt	Vein	27.59	0.03	17.65	25.98	0.25	16.32	0.09	0.00	0.01	87.92	2.91	1.09	1.11	2.29	0.023	2.57	53	289
ST-103	Pillow Basalt	Vein	27.95	0.00	18.18	25.88	0.27	16.53	0.03	0.00	0.01	88.85	2.91	1.09	1.14	2.25	0.023	2.56	53	290
ST-103	Pillow Basalt	Vein	26.64	0.00	18.79	25.25	0.25	16.42	0.30	0.01	0.00	87.67	2.82	1.18	1.16	2.23	0.022	2.59	53	318
ST-103	Pillow Basalt	Vein	27.34	0.00	19.17	25.53	0.28	16.56	0.09	0.03	0.00	88.99	2.84	1.16	1.18	2.22	0.024	2.56	53	312
ST-109	Fault Gouge	Vein	27.63	N/A	19.43	23.45	0.51	16.60	0.09	0.01	0.02	87.79	2.88	1.12	1.26	2.04	0.045	2.58	55	299
ST-109	Fault Gouge	Groundmass	26.84	N/A	19.89	25.38	0.54	15.31	0.08	0.00	0.01	88.07	2.82	1.18	1.28	2.23	0.048	2.40	51	319
ST-109	Fault Gouge	Vein	31.55	N/A	19.65	12.26	1.47	0.04	19.86	0.00	0.00	84.83	4.04	-0.04	3.00	1.31	0.159	0.01	1	-74

Appendix 4: Chlorite Compositions

Sample	Lithology	Occurence	SiO2 (wt%)	TiO2 (wt%)	Al2O3 (wt%)	FeO (wt%)	MnO (wt%)	MgO (wt%)	CaO (wt%)	Na2O (wt%)	K2O (wt%)	Total (wt%)	SiIV	AlIV	AlVI	Fe	Mn	Mg	Mg#	T (°C)
ST-109	Fault Gouge	Vein	32.10	N/A	21.39	9.46	0.24	0.05	21.72	0.01	0.00	85.07	4.08	-0.08	3.28	1.00	0.026	0.01	1	-87
ST-109	Fault Gouge	Groundmass	27.75	N/A	19.18	25.08	0.47	15.76	0.13	0.02	0.09	88.54	2.89	1.11	1.25	2.19	0.041	2.45	52	294
ST-109	Fault Gouge	Vein	27.87	N/A	19.80	24.37	0.49	16.12	0.08	0.03	0.04	88.81	2.88	1.12	1.29	2.10	0.043	2.48	54	299
ST-109	Fault Gouge	Groundmass	28.18	N/A	18.47	23.15	0.52	16.00	0.14	0.08	0.14	86.70	2.97	1.03	1.27	2.04	0.046	2.52	55	269
ST-109	Fault Gouge	Amygdule	26.48	N/A	18.82	25.16	0.56	15.34	0.05	0.01	0.00	86.61	2.84	1.16	1.22	2.26	0.051	2.45	52	312
ST-109	Fault Gouge	Vein	27.26	N/A	20.24	24.76	0.53	16.34	0.06	0.00	0.06	89.24	2.81	1.19	1.27	2.13	0.046	2.51	54	321
ST-109	Fault Gouge	Groundmass	28.51	N/A	19.75	24.57	0.49	14.26	0.20	0.02	0.14	87.98	2.97	1.03	1.40	2.14	0.043	2.22	50	268
ST-109	Fault Gouge	Groundmass	29.78	N/A	18.38	23.66	0.48	14.12	0.13	0.05	1.58	88.23	3.13	0.87	1.40	2.08	0.043	2.21	51	219
ST-109	Fault Gouge	Amygdule	27.60	N/A	19.24	24.64	0.49	16.28	0.03	0.00	0.02	88.31	2.87	1.13	1.23	2.14	0.043	2.53	54	301
ST-112	Massive Flow	Amygdule	27.95	N/A	19.12	22.82	0.31	16.78	0.22	0.01	0.03	87.23	2.92	1.08	1.27	1.99	0.028	2.61	56	286
ST-112	Massive Flow	Groundmass	28.46	N/A	18.45	22.94	0.31	18.00	0.05	0.00	0.00	88.20	2.93	1.07	1.17	1.98	0.027	2.77	58	281
ST-112	Massive Flow	Groundmass	28.31	N/A	18.78	22.40	0.30	17.28	0.15	0.00	0.01	87.24	2.95	1.05	1.25	1.95	0.027	2.68	58	278
ST-112	Massive Flow	Amygdule	27.50	N/A	19.68	24.39	0.33	16.56	0.02	0.00	0.00	88.48	2.85	1.15	1.25	2.11	0.029	2.56	54	309
ST-112	Massive Flow	Amygdule	27.81	N/A	19.98	23.04	0.23	16.72	0.16	0.00	0.00	87.94	2.88	1.12	1.31	1.99	0.021	2.58	56	300
ST-70	Fault Gouge	Vein	27.33	N/A	19.75	26.29	0.40	15.79	0.05	0.00	0.01	89.60	2.83	1.17	1.23	2.27	0.035	2.43	51	316
ST-70	Fault Gouge	Vein	27.01	N/A	19.72	24.68	0.45	16.26	0.09	0.02	0.01	88.24	2.82	1.18	1.24	2.15	0.039	2.53	54	318
ST-70	Fault Gouge	Vein	29.20	N/A	16.39	25.99	0.31	15.99	0.21	0.00	0.01	88.14	3.07	0.93	1.10	2.28	0.028	2.51	52	238
ST-70	Fault Gouge	Amygdule	27.33	N/A	19.24	24.51	0.40	16.49	0.08	0.00	0.01	88.07	2.85	1.15	1.22	2.14	0.035	2.57	54	307
ST-70	Fault Gouge	Vein	27.87	N/A	19.79	24.95	0.43	16.62	0.02	0.01	0.14	89.84	2.85	1.15	1.24	2.14	0.037	2.54	54	307
ST-70	Fault Gouge	Vein	27.19	N/A	20.05	24.27	0.41	16.62	0.08	0.00	0.04	88.68	2.81	1.19	1.26	2.10	0.036	2.57	55	320
ST-70	Fault Gouge	Vein	27.41	N/A	19.87	24.62	0.38	17.18	0.03	0.01	0.02	88.79	2.84	1.16	1.17	2.13	0.033	2.66	55	311
ST-70	Fault Gouge	Amygdule	27.22	N/A	19.36	24.59	0.35	16.04	0.15	0.02	0.01	87.76	2.86	1.14	1.25	2.16	0.031	2.51	53	306
ST-70	Fault Gouge	Vein	29.65	N/A	17.07	24.28	0.35	17.21	0.36	0.03	0.20	89.14	3.06	0.94	1.13	2.09	0.030	2.65	55	241
ST-71	Fault Gouge	Groundmass	27.64	0.00	15.85	23.87	0.31	18.05	0.16	0.04	0.03	85.98	2.97	1.03	0.97	2.14	0.028	2.89	57	271
ST-71	Fault Gouge	Groundmass	29.70	0.00	16.34	23.96	0.30	17.37	0.30	0.03	0.04	88.04	3.09	0.91	1.10	2.09	0.027	2.70	56	230
ST-71	Fault Gouge	Void	26.92	0.00	17.72	24.36	0.27	17.93	0.07	0.00	0.02	87.29	2.84	1.16	1.05	2.15	0.024	2.82	56	310
ST-71	Fault Gouge	Void	25.69	0.00	20.72	25.76	0.35	15.33	0.06	0.00	0.53	88.45	2.71	1.29	1.29	2.27	0.031	2.41	51	353
ST-71	Fault Gouge	Void	28.71	0.01	15.15	22.98	0.24	19.96	0.06	0.00	0.00	87.11	3.01	0.99	0.89	2.02	0.022	3.12	61	256
ST-71	Fault Gouge	Vein	26.97	0.01	19.67	25.45	0.35	16.28	0.04	0.00	0.00	88.77	2.81	1.19	1.22	2.21	0.031	2.53	53	322
ST-71	Fault Gouge	Vein	26.88	0.02	19.82	25.32	0.34	16.22	0.12	0.01	0.02	88.75	2.80	1.20	1.23	2.21	0.030	2.52	53	325
ST-71	Fault Gouge	Void	25.21	0.00	20.36	26.20	0.35	15.70	0.10	0.00	0.03	87.95	2.67	1.33	1.22	2.32	0.031	2.48	51	365
ST-71	Fault Gouge	Void	27.36	0.00	17.02	24.53	0.29	17.78	0.05	0.00	0.03	87.06	2.90	1.10	1.03	2.17	0.026	2.81	56	292
ST-71	Fault Gouge	Void	26.13	0.01	18.67	25.04	0.34	17.30	0.06	0.04	0.00	87.62	2.76	1.24	1.09	2.22	0.031	2.73	55	336
ST-71	Fault Gouge	Void	27.07	0.03	19.15	25.23	0.36	16.38	0.08	0.00	0.01	88.29	2.83	1.17	1.19	2.21	0.032	2.55	53	314
ST-71	Fault Gouge	Vein	27.09	0.02	19.27	24.85	0.35	17.10	0.05	0.01	0.00	88.72	2.81	1.19	1.17	2.16	0.031	2.65	55	320
ST-71	Fault Gouge	Vein	25.42	0.01	19.41	24.68	0.30	16.48	0.05	0.00	0.02	86.46	2.72	1.28	1.18	2.21	0.027	2.63	54	349
ST-71	Fault Gouge	Vein	25.84	0.02	20.03	25.23	0.26	16.09	0.17	0.02	0.03	87.74	2.73	1.27	1.23	2.23	0.023	2.54	53	346
ST-71	Fault Gouge	Vein	24.51	0.00	20.25	25.44	0.39	15.74	0.12	0.02	0.03	86.49	2.64	1.36	1.21	2.29	0.035	2.53	52	375
ST-71	Fault Gouge	Vein	26.51	0.01	20.45	25.73	0.33	15.62	0.06	0.00	0.05	88.76	2.76	1.24	1.28	2.24	0.029	2.43	52	336
ST-71	Fault Gouge	Vein	27.68	0.02	18.70	24.73	0.41	16.94	0.05	0.00	0.00	88.52	2.88	1.12	1.17	2.15	0.036	2.62	55	300
ST-71	Fault Gouge	Vein	26.44	0.01	19.21	24.91	0.35	17.01	0.03	0.00	0.00	87.96	2.78	1.22	1.15	2.19	0.031	2.66	55	332
ST-71	Fault Gouge	Vein	27.56	0.02	19.02	25.35	0.35	17.06	0.00	0.03	0.01	89.39	2.84	1.16	1.16	2.19	0.030	2.62	54	310
ST-71	Fault Gouge	Groundmass	29.68	0.00	15.53	23.44	0.27	18.84	0.12	0.01	0.05	87.96	3.08	0.92	0.99	2.04	0.024	2.92	59	233
ST-71	Fault Gouge	Groundmass	29.92	0.00	15.33	23.24	0.24	18.99	0.13	0.03	0.05	87.97	3.11	0.89	0.98	2.02	0.021	2.94	59	226
ST-78	Massive Flow	Amygdule	26.95	N/A	21.03	23.76	0.38	16.51	0.02	0.00	0.01	88.75	2.78	1.22	1.33	2.05	0.033	2.54	55	332
ST-78	Massive Flow	Groundmass	27.19	N/A	20.31	23.90	0.39	17.08	0.03	0.03	0.01	88.95	2.80	1.20	1.26	2.06	0.034	2.62	56	325

Appendix 4: Chlorite Compositions

Sample	Lithology	Occurence	SiO2 (wt%)	TiO2 (wt%)	Al2O3 (wt%)	FeO (wt%)	MnO (wt%)	MgO (wt%)	CaO (wt%)	Na2O (wt%)	K2O (wt%)	Total (wt%)	SiIV	AlIV	AlVI	Fe	Mn	Mg	Mg#	T (°C)
ST-78	Massive Flow	Groundmass	26.96	N/A	20.42	24.15	0.38	16.67	0.04	0.06	0.01	88.71	2.79	1.21	1.28	2.09	0.034	2.57	55	328
ST-78	Massive Flow	Amygdule	26.54	N/A	20.33	24.27	0.42	16.41	0.01	0.00	0.01	88.04	2.77	1.23	1.27	2.12	0.037	2.55	54	334
ST-78	Massive Flow	Amygdule	26.44	N/A	19.89	24.86	0.38	16.15	0.19	0.00	0.01	87.93	2.78	1.22	1.24	2.18	0.034	2.53	53	331
ST-88	Volcaniclastic	Groundmass	26.89	N/A	20.01	23.01	0.50	17.70	0.13	0.01	0.01	88.30	2.78	1.22	1.23	1.99	0.044	2.73	57	329
ST-88	Volcaniclastic	Groundmass	26.73	N/A	20.20	22.70	0.50	17.94	0.01	0.02	0.01	88.18	2.77	1.23	1.23	1.96	0.044	2.77	58	336
ST-88	Volcaniclastic	Groundmass	26.33	N/A	20.11	23.62	0.54	16.99	0.06	0.02	0.01	87.67	2.76	1.24	1.24	2.07	0.047	2.65	56	339
ST-95	Massive Flow	Amygdule	28.54	0.00	16.72	21.23	0.30	19.43	0.08	0.00	0.00	86.29	2.99	1.01	1.06	1.86	0.026	3.04	62	263
ST-95	Massive Flow	Amygdule	29.15	0.01	16.28	20.97	0.25	19.66	0.05	0.00	0.00	86.37	3.04	0.96	1.05	1.83	0.022	3.06	62	246
ST-95	Massive Flow	Amygdule	29.17	0.00	16.80	21.61	0.25	19.61	0.05	0.00	0.00	87.49	3.01	0.99	1.06	1.87	0.021	3.02	62	256
ST-95	Massive Flow	Amygdule	28.76	0.00	16.90	21.85	0.30	18.87	0.07	0.00	0.00	86.74	3.00	1.00	1.08	1.91	0.026	2.94	60	259
ST-95	Massive Flow	Amygdule	29.59	0.00	16.13	22.19	0.25	19.47	0.07	0.00	0.00	87.69	3.06	0.94	1.02	1.92	0.022	3.00	61	242
ST-95	Massive Flow	Amygdule	29.63	0.00	16.11	20.87	0.21	18.78	0.10	0.00	0.00	85.71	3.11	0.89	1.10	1.83	0.019	2.94	61	225
ST-95	Massive Flow	Amygdule	29.48	0.00	16.02	21.65	0.24	19.05	0.10	0.01	0.00	86.56	3.08	0.92	1.05	1.89	0.022	2.97	61	234
ST-95	Massive Flow	Amygdule	29.34	0.00	16.52	21.90	0.28	18.45	0.13	0.00	0.00	86.62	3.07	0.93	1.10	1.91	0.025	2.88	60	239
ST-95	Massive Flow	Amygdule	28.94	0.00	16.69	21.40	0.31	18.70	0.11	0.00	0.00	86.15	3.04	0.96	1.10	1.88	0.028	2.93	61	248
ST-95	Massive Flow	Amygdule	29.91	0.00	16.00	20.34	0.22	18.88	0.09	0.00	0.00	85.44	3.14	0.86	1.12	1.78	0.019	2.95	62	216
ST-95	Massive Flow	Amygdule	30.00	0.00	16.55	21.05	0.25	19.08	0.12	0.01	0.00	87.06	3.10	0.90	1.11	1.82	0.022	2.94	61	228
ST-95	Massive Flow	Amygdule	29.90	0.00	16.24	21.00	0.16	19.34	0.14	0.00	0.00	86.79	3.10	0.90	1.08	1.82	0.014	2.99	62	228
ST-95	Massive Flow	Amygdule	27.14	0.01	18.91	22.50	0.41	16.83	0.20	0.00	0.00	85.99	2.88	1.12	1.24	2.00	0.037	2.66	57	299
ST-95	Massive Flow	Amygdule	28.92	0.03	16.46	21.89	0.31	18.29	0.17	0.00	0.00	86.06	3.05	0.95	1.10	1.93	0.027	2.87	59	244
ST-95	Massive Flow	Amygdule	28.12	0.00	18.02	20.73	0.31	18.03	0.07	0.00	0.00	85.28	2.97	1.03	1.21	1.83	0.028	2.84	60	270
ST-95	Massive Flow	Amygdule	29.18	0.00	16.61	21.60	0.22	18.84	0.11	0.00	0.00	86.55	3.05	0.95	1.09	1.89	0.019	2.93	61	245
ST-95	Massive Flow	Amygdule	29.95	0.00	16.17	21.24	0.27	19.17	0.10	0.01	0.00	86.91	3.10	0.90	1.08	1.84	0.023	2.96	61	226
ST-95	Massive Flow	Amygdule	29.22	0.01	17.24	21.64	0.20	18.00	0.09	0.01	0.00	86.42	3.05	0.95	1.17	1.89	0.018	2.80	59	243
ST-95	Massive Flow	Amygdule	30.11	0.00	15.57	20.98	0.20	19.60	0.04	0.00	0.00	86.51	3.13	0.87	1.04	1.82	0.018	3.04	62	218
ST-95	Massive Flow	Amygdule	30.04	0.00	16.02	20.79	0.20	18.78	0.07	0.00	0.00	85.90	3.14	0.86	1.11	1.82	0.018	2.93	61	215
ST-15	Massive Flow	Vein	29.25	0.04	16.07	31.74	0.41	10.80	0.34	0.02	0.01	88.68	3.15	0.85	1.19	2.86	0.038	1.74	37	211
ST-15	Massive Flow	Vein	27.75	0.02	16.22	31.87	0.38	10.49	0.24	0.01	0.02	87.00	3.06	0.94	1.17	2.94	0.036	1.73	37	239
ST-15	Massive Flow	Vein	27.31	0.02	16.72	32.21	0.46	10.34	0.43	0.00	0.04	87.54	3.01	0.99	1.19	2.97	0.043	1.70	36	256
ST-15	Massive Flow	Vein	27.41	0.01	16.72	32.81	0.42	10.63	0.22	0.01	0.08	88.32	3.00	1.00	1.15	3.00	0.039	1.73	36	261
ST-15	Massive Flow	Groundmass	27.34	0.02	16.62	31.75	0.49	10.29	0.48	0.01	0.00	87.01	3.03	0.97	1.20	2.94	0.046	1.70	36	251
ST-15	Massive Flow	Groundmass	27.95	0.00	16.75	31.84	0.47	10.28	0.49	0.02	0.01	87.81	3.06	0.94	1.22	2.92	0.043	1.68	36	241
ST-15	Massive Flow	Groundmass	27.86	0.02	17.16	31.91	0.45	10.30	0.49	0.03	0.01	88.24	3.04	0.96	1.24	2.91	0.042	1.67	36	249
ST-15	Massive Flow	Groundmass	27.67	0.02	16.82	32.24	0.46	10.37	0.44	0.01	0.01	88.04	3.03	0.97	1.20	2.95	0.042	1.69	36	251
ST-15	Massive Flow	Groundmass	27.00	0.02	16.87	32.10	0.41	10.08	0.45	0.01	0.01	86.95	3.00	1.00	1.21	2.98	0.038	1.67	36	260
ST-15	Massive Flow	Groundmass	27.60	0.01	16.85	32.18	0.36	10.45	0.47	0.01	0.01	87.95	3.02	0.98	1.20	2.95	0.034	1.71	36	252
ST-15	Massive Flow	Groundmass	27.38	0.01	16.62	31.13	0.51	10.24	0.46	0.01	0.02	86.38	3.05	0.95	1.22	2.90	0.048	1.70	37	246
ST-15	Massive Flow	Groundmass	27.70	0.02	16.91	32.11	0.50	10.41	0.48	0.02	0.01	88.14	3.03	0.97	1.21	2.94	0.046	1.70	36	251
ST-15	Massive Flow	Groundmass	27.18	0.03	16.84	31.69	0.41	10.38	0.53	0.01	0.02	87.09	3.01	0.99	1.21	2.93	0.039	1.71	37	257
ST-15	Massive Flow	Groundmass	27.29	0.07	17.52	31.23	0.40	10.57	0.64	0.04	0.02	87.77	2.99	1.01	1.25	2.86	0.037	1.73	37	263
ST-15	Massive Flow	Groundmass	27.78	0.05	17.12	31.76	0.41	10.53	0.49	0.00	0.01	88.15	3.03	0.97	1.23	2.89	0.038	1.71	37	251
ST-15	Massive Flow	Groundmass	28.05	0.09	16.80	32.21	0.43	10.30	0.64	0.03	0.06	88.59	3.06	0.94	1.21	2.94	0.039	1.67	36	242
ST-15	Massive Flow	Vein	26.18	0.01	16.96	33.24	0.49	9.83	0.05	0.00	0.00	86.75	2.93	1.07	1.16	3.11	0.046	1.64	34	283
ST-15	Massive Flow	Vein	26.14	0.02	16.87	33.74	0.48	9.67	0.07	0.00	0.03	87.02	2.92	1.08	1.15	3.16	0.045	1.61	34	284
ST-15	Massive Flow	Vein	26.08	0.01	16.88	33.61	0.48	9.99	0.04	0.01	0.00	87.30	2.91	1.09	1.13	3.15	0.046	1.66	34	290
ST-15	Massive Flow	Vein	26.37	0.02	16.74	34.11	0.46	9.70	0.07	0.00	0.02	87.49	2.94	1.06	1.13	3.18	0.043	1.61	33	280

Appendix 4: Chlorite Compositions

Sample	Lithology	Occurence	SiO2 (wt%)	TiO2 (wt%)	Al2O3 (wt%)	FeO (wt%)	MnO (wt%)	MgO (wt%)	CaO (wt%)	Na2O (wt%)	K2O (wt%)	Total (wt%)	SiIV	AlIV	AlVI	Fe	Mn	Mg	Mg#	T (°C)
ST-15	Massive Flow	Amygdule	27.65	0.01	16.93	32.49	0.51	10.52	0.45	0.01	0.01	88.56	3.01	0.99	1.19	2.96	0.047	1.71	36	256
ST-15	Massive Flow	Amygdule	27.71	0.01	16.88	31.64	0.50	10.39	0.40	0.01	0.03	87.58	3.04	0.96	1.22	2.90	0.047	1.70	37	247
ST-15	Massive Flow	Amygdule	27.41	0.04	16.85	32.41	0.48	10.25	0.53	0.01	0.02	88.00	3.01	0.99	1.19	2.98	0.045	1.68	36	256
ST-15	Massive Flow	Amygdule	27.50	0.03	17.12	31.73	0.48	10.57	0.38	0.01	0.02	87.84	3.01	0.99	1.22	2.90	0.045	1.72	37	257
ST-15	Massive Flow	Groundmass	26.36	0.05	17.11	31.43	0.47	9.74	0.50	0.01	0.00	85.67	2.97	1.03	1.25	2.96	0.045	1.64	35	269
ST-15	Massive Flow	Groundmass	27.65	0.05	16.97	31.48	0.42	10.36	0.62	0.01	0.03	87.59	3.04	0.96	1.24	2.89	0.039	1.70	37	248
ST-15	Massive Flow	Groundmass	26.96	0.24	17.07	31.61	0.45	10.20	0.64	0.02	0.04	87.23	2.99	1.01	1.23	2.93	0.042	1.69	36	262
ST-15	Massive Flow	Groundmass	27.36	0.10	18.08	31.63	0.51	10.17	0.65	0.01	0.01	88.52	2.98	1.02	1.29	2.88	0.047	1.65	36	268
ST-101	Pillow Basalt	Groundmass	30.01	0.00	16.19	23.39	0.21	17.06	0.34	0.03	0.00	87.24	3.14	0.86	1.14	2.05	0.019	2.66	56	215
ST-101	Pillow Basalt	Groundmass	29.82	0.00	14.60	23.62	0.28	18.25	0.20	0.02	0.00	86.78	3.15	0.85	0.96	2.08	0.025	2.87	58	213
ST-101	Pillow Basalt	Groundmass	29.97	0.00	16.36	24.20	0.27	16.98	0.35	0.03	0.00	88.16	3.12	0.88	1.12	2.10	0.023	2.63	55	223
ST-101	Pillow Basalt	Groundmass	29.41	0.00	16.81	23.47	0.22	15.42	0.43	0.03	0.03	85.82	3.14	0.86	1.25	2.09	0.020	2.45	54	216
ST-101	Pillow Basalt	Groundmass	31.40	0.01	17.01	23.53	0.26	15.93	0.61	0.04	0.02	88.81	3.22	0.78	1.28	2.02	0.023	2.44	54	189
ST-101	Pillow Basalt	Groundmass	30.22	0.00	16.33	23.33	0.28	16.03	0.48	0.02	0.01	86.71	3.18	0.82	1.21	2.05	0.025	2.52	55	202
ST-101	Pillow Basalt	Groundmass	30.35	0.01	16.43	23.08	0.19	16.64	0.42	0.01	0.00	87.13	3.17	0.83	1.19	2.02	0.017	2.59	56	205
ST-101	Pillow Basalt	Groundmass	30.25	0.00	15.87	23.23	0.23	16.51	0.39	0.03	0.00	86.52	3.19	0.81	1.16	2.05	0.021	2.60	56	199
ST-101	Pillow Basalt	Groundmass	29.93	0.00	15.68	23.56	0.27	16.84	0.35	0.02	0.00	86.65	3.16	0.84	1.11	2.08	0.024	2.65	56	209
ST-101	Pillow Basalt	Groundmass	29.33	0.00	15.79	23.58	0.21	16.24	0.38	0.01	0.00	85.55	3.14	0.86	1.14	2.11	0.019	2.59	55	214
ST-101	Pillow Basalt	Groundmass	29.34	0.01	16.70	24.09	0.25	15.36	0.50	0.02	0.04	86.30	3.12	0.88	1.22	2.15	0.023	2.44	53	220
ST-101	Pillow Basalt	Groundmass	29.20	0.00	16.47	23.71	0.28	15.56	0.45	0.02	0.01	85.71	3.13	0.87	1.20	2.12	0.025	2.48	54	219
ST-101	Pillow Basalt	Groundmass	29.83	0.00	16.18	23.78	0.24	17.02	0.31	0.01	0.01	87.39	3.12	0.88	1.12	2.08	0.022	2.66	56	220
ST-101	Pillow Basalt	Groundmass	30.12	0.00	15.99	23.22	0.18	16.63	0.40	0.03	0.01	86.59	3.17	0.83	1.16	2.05	0.016	2.61	56	204
ST-101	Pillow Basalt	Groundmass	28.96	0.01	16.79	24.10	0.29	15.98	0.38	0.02	0.01	86.53	3.08	0.92	1.18	2.14	0.026	2.53	54	236
ST-101	Pillow Basalt	Groundmass	29.01	0.01	16.37	23.70	0.26	16.48	0.46	0.02	0.00	86.31	3.09	0.91	1.14	2.11	0.024	2.61	55	232
ST-101	Pillow Basalt	Groundmass	29.46	0.02	17.42	24.39	0.29	15.70	0.41	0.03	0.05	87.77	3.08	0.92	1.23	2.13	0.026	2.45	53	233
ST-101	Pillow Basalt	Groundmass	28.74	0.01	16.05	23.64	0.26	15.81	0.43	0.01	0.06	85.00	3.11	0.89	1.16	2.14	0.024	2.55	54	225
ST-101	Pillow Basalt	Groundmass	29.37	0.02	16.80	24.16	0.28	15.76	0.31	0.00	0.05	86.74	3.11	0.89	1.20	2.14	0.025	2.49	53	226
ST-101	Pillow Basalt	Groundmass	29.40	0.04	15.94	23.55	0.22	16.68	0.31	0.02	0.06	86.23	3.13	0.87	1.12	2.09	0.020	2.64	56	220
ST-77	Mafic Schist	Groundmass	26.40	0.01	20.80	21.92	0.34	17.47	0.26	0.00	0.00	87.21	2.75	1.25	1.31	1.91	0.030	2.72	58	339
ST-77	Mafic Schist	Groundmass	27.05	0.01	19.78	20.18	0.34	17.59	0.14	0.00	0.00	85.09	2.86	1.14	1.32	1.78	0.031	2.77	60	306
ST-77	Mafic Schist	Groundmass	29.32	0.03	20.66	19.98	0.42	16.45	0.41	0.37	0.00	87.64	3.00	1.00	1.49	1.71	0.036	2.51	59	259
ST-77	Mafic Schist	Groundmass	27.22	0.00	20.16	21.34	0.48	17.59	0.05	0.00	0.00	86.84	2.83	1.17	1.30	1.86	0.043	2.73	59	314
ST-77	Mafic Schist	Groundmass	27.66	0.08	19.79	21.29	0.34	16.30	0.25	0.05	0.00	85.76	2.92	1.08	1.38	1.88	0.031	2.56	57	286
ST-75	Mafic Schist	Groundmass	27.65	0.01	19.39	19.57	0.41	18.65	0.02	0.00	0.00	85.69	2.89	1.11	1.27	1.71	0.036	2.90	62	296
ST-75	Mafic Schist	Groundmass	28.83	0.02	19.77	18.66	0.18	18.95	0.41	0.04	0.00	86.87	2.95	1.05	1.34	1.60	0.016	2.90	64	275
ST-75	Mafic Schist	Groundmass	27.71	0.03	20.24	18.56	0.19	18.79	0.09	0.01	0.00	85.62	2.88	1.12	1.35	1.61	0.017	2.91	64	300
ST-75	Mafic Schist	Groundmass	27.69	0.03	20.07	19.26	0.21	18.89	0.06	0.00	0.00	86.21	2.87	1.13	1.31	1.67	0.018	2.91	63	303
ST-75	Mafic Schist	Groundmass	27.44	0.03	20.33	18.52	0.21	18.89	0.12	0.01	0.00	85.54	2.85	1.15	1.34	1.61	0.018	2.93	64	307
ST-42	Massive Flow	Groundmass	30.82	0.01	13.70	25.09	0.23	15.65	0.22	0.01	0.00	85.72	3.31	0.69	1.04	2.25	0.021	2.51	52	160
ST-42	Massive Flow	Amygdule	30.64	0.01	13.81	25.08	0.25	15.43	0.19	0.01	0.00	85.42	3.30	0.70	1.06	2.26	0.022	2.48	52	163
ST-42	Massive Flow	Amygdule	30.72	0.01	13.80	24.89	0.11	15.21	0.27	0.00	0.00	85.01	3.32	0.68	1.08	2.26	0.010	2.45	52	156
ST-42	Massive Flow	Amygdule	30.94	0.00	13.41	24.63	0.19	15.76	0.10	0.00	0.00	85.03	3.34	0.66	1.04	2.22	0.017	2.53	53	152
ST-42	Massive Flow	Amygdule	31.60	0.02	13.62	25.30	0.22	16.57	0.10	0.00	0.00	87.44	3.32	0.68	1.00	2.22	0.019	2.59	54	158
ST-42	Massive Flow	Amygdule	30.82	0.01	13.21	25.10	0.22	15.90	0.13	0.00	0.00	85.38	3.32	0.68	1.00	2.26	0.020	2.56	53	156
ST-42	Massive Flow	Amygdule	31.24	0.00	13.06	25.46	0.27	16.31	0.08	0.01	0.00	86.44	3.33	0.67	0.97	2.27	0.024	2.59	53	154
ST-42	Massive Flow	Amygdule	29.89	0.02	13.66	25.53	0.30	15.73	0.14	0.01	0.00	85.28	3.24	0.76	0.99	2.32	0.027	2.55	52	181

Appendix 4: Chlorite Compositions

Sample	Lithology	Occurence	SiO2 (wt%)	TiO2 (wt%)	Al2O3 (wt%)	FeO (wt%)	MnO (wt%)	MgO (wt%)	CaO (wt%)	Na2O (wt%)	K2O (wt%)	Total (wt%)	SiIV	AlIV	AlVI	Fe	Mn	Mg	Mg#	T (°C)
ST-42	Massive Flow	Amygdule	29.62	0.01	14.83	25.55	0.28	14.65	0.19	0.00	0.00	85.14	3.22	0.78	1.12	2.32	0.026	2.37	50	190
ST-42	Massive Flow	Groundmass	31.27	0.03	13.35	24.49	0.22	15.91	0.18	0.01	0.00	85.46	3.35	0.65	1.04	2.20	0.020	2.54	53	146
ST-42	Massive Flow	Groundmass	30.47	0.01	14.14	25.20	0.22	15.01	0.17	0.00	0.00	85.22	3.29	0.71	1.09	2.28	0.020	2.42	51	166
ST-42	Massive Flow	Groundmass	30.85	0.00	13.43	24.69	0.30	15.83	0.14	0.00	0.00	85.24	3.32	0.68	1.03	2.22	0.027	2.54	53	156
ST-54	Massive Flow	Amygdule	28.48	0.05	17.15	23.88	0.16	16.01	0.11	0.02	0.00	85.85	3.04	0.96	1.19	2.13	0.014	2.55	54	248
ST-54	Massive Flow	Amygdule	29.36	0.03	15.87	25.23	0.12	15.70	0.10	0.00	0.00	86.42	3.13	0.87	1.12	2.25	0.011	2.49	52	219
ST-54	Massive Flow	Amygdule	28.99	0.03	16.52	24.25	0.13	15.54	0.12	0.00	0.00	85.58	3.10	0.90	1.19	2.17	0.012	2.48	53	226
ST-54	Massive Flow	Amygdule	29.71	0.02	16.42	24.70	0.14	14.63	0.20	0.00	0.00	85.82	3.17	0.83	1.24	2.21	0.013	2.33	51	204
ST-54	Massive Flow	Amygdule	28.66	0.04	16.54	25.76	0.21	14.33	0.23	0.00	0.00	85.77	3.09	0.91	1.20	2.33	0.019	2.31	50	229
ST-54	Massive Flow	Amygdule	29.05	0.05	16.25	26.11	0.24	14.26	0.44	0.02	0.00	86.41	3.13	0.87	1.19	2.35	0.022	2.29	49	219
ST-54	Massive Flow	Amygdule	28.26	0.01	16.96	25.09	0.17	15.07	0.16	0.00	0.00	85.71	3.04	0.96	1.19	2.26	0.015	2.42	52	247
ST-54	Massive Flow	Amygdule	29.42	0.04	15.67	25.81	0.16	14.64	0.21	0.01	0.00	85.95	3.17	0.83	1.15	2.32	0.015	2.35	50	206
ST-54	Massive Flow	Amygdule	29.13	0.02	15.64	25.92	0.16	14.62	0.20	0.00	0.00	85.69	3.15	0.85	1.14	2.34	0.015	2.36	50	212
ST-54	Massive Flow	Groundmass	29.76	0.09	14.73	24.93	0.16	15.43	0.15	0.00	0.00	85.25	3.22	0.78	1.09	2.25	0.015	2.49	52	190
ST-54	Massive Flow	Amygdule	29.92	0.05	14.62	25.35	0.18	15.60	0.10	0.01	0.00	85.84	3.22	0.78	1.07	2.28	0.016	2.50	52	191
ST-54	Massive Flow	Groundmass	29.78	0.04	15.53	25.27	0.14	14.48	0.32	0.04	0.00	85.60	3.21	0.79	1.18	2.28	0.013	2.33	50	192
ST-54	Massive Flow	Groundmass	29.30	0.00	15.92	25.77	0.31	14.53	0.25	0.03	0.00	86.11	3.15	0.85	1.17	2.32	0.028	2.33	50	212
ST-54	Massive Flow	Groundmass	29.75	0.00	15.41	25.67	0.29	15.30	0.16	0.02	0.00	86.59	3.17	0.83	1.11	2.29	0.026	2.43	51	204
ST-89	Pillow Basalt	Groundmass	31.31	0.00	14.43	25.60	0.28	13.58	0.64	0.03	0.00	85.86	3.37	0.63	1.20	2.31	0.026	2.18	48	140
ST-89	Pillow Basalt	Groundmass	31.37	0.00	13.44	26.21	0.28	13.39	0.49	0.05	0.00	85.22	3.41	0.59	1.14	2.39	0.025	2.17	47	127
ST-89	Pillow Basalt	Groundmass	29.83	0.00	14.26	27.19	0.26	13.12	0.53	0.02	0.00	85.21	3.28	0.72	1.13	2.50	0.024	2.15	46	170
ST-89	Pillow Basalt	Groundmass	31.28	0.00	13.65	26.75	0.34	13.58	0.58	0.04	0.00	86.23	3.38	0.62	1.12	2.42	0.031	2.19	47	138
ST-89	Pillow Basalt	Groundmass	30.89	0.00	14.06	25.66	0.24	13.94	0.50	0.03	0.00	85.32	3.35	0.65	1.15	2.33	0.022	2.25	49	147
ST-89	Pillow Basalt	Groundmass	31.97	0.00	13.75	27.21	0.27	14.17	0.48	0.03	0.00	87.88	3.38	0.62	1.10	2.41	0.024	2.23	48	137
ST-89	Pillow Basalt	Groundmass	31.69	0.00	14.11	26.61	0.34	13.77	0.60	0.01	0.00	87.13	3.38	0.62	1.15	2.37	0.031	2.19	48	139
ST-89	Pillow Basalt	Groundmass	31.80	0.00	14.74	26.02	0.23	13.16	0.64	0.03	0.00	86.63	3.39	0.61	1.25	2.32	0.021	2.09	47	134
ST-89	Pillow Basalt	Groundmass	31.12	0.00	15.42	26.22	0.31	13.48	0.80	0.04	0.00	87.38	3.31	0.69	1.24	2.33	0.028	2.13	48	161
ST-89	Pillow Basalt	Groundmass	30.99	0.00	15.56	26.51	0.26	13.47	0.70	0.03	0.00	87.52	3.29	0.71	1.23	2.35	0.024	2.13	47	167
ST-89	Pillow Basalt	Groundmass	32.23	0.03	15.38	26.17	0.33	13.29	1.13	0.17	0.00	88.73	3.38	0.62	1.28	2.29	0.029	2.08	47	139
ST-89	Pillow Basalt	Groundmass	30.72	0.00	14.08	26.52	0.36	12.89	0.75	0.03	0.00	85.35	3.36	0.64	1.17	2.43	0.033	2.10	46	144
ST-113	Undiff Basalt	Vein	30.74	0.00	17.08	22.39	0.20	16.22	0.27	0.19	0.01	87.10	3.19	0.81	1.29	1.95	0.017	2.51	56	198
ST-113	Undiff Basalt	Vein	29.25	0.00	18.28	23.35	0.22	16.25	0.11	0.03	0.00	87.50	3.04	0.96	1.28	2.03	0.019	2.52	55	248
ST-113	Undiff Basalt	Vein	27.22	0.02	19.63	24.97	0.23	15.84	0.12	0.05	0.00	88.09	2.85	1.15	1.27	2.18	0.021	2.47	53	309
ST-113	Undiff Basalt	Vein	26.26	0.01	17.70	26.10	0.23	14.82	0.11	0.01	0.00	85.24	2.87	1.13	1.16	2.39	0.022	2.42	50	301
ST-113	Undiff Basalt	Vein	28.15	0.01	18.16	24.10	0.22	16.39	0.02	0.00	0.00	87.06	2.96	1.04	1.21	2.12	0.020	2.57	55	273
ST-113	Undiff Basalt	Groundmass	27.55	0.03	18.79	23.09	0.16	15.40	0.32	0.12	0.00	85.47	2.95	1.05	1.32	2.07	0.014	2.46	54	276
ST-113	Undiff Basalt	Vein	27.99	0.02	18.64	22.81	0.26	15.87	0.08	0.03	0.24	85.93	2.97	1.03	1.30	2.02	0.023	2.51	55	269
ST-115	Mafic Schist	Groundmass	27.67	0.08	18.57	22.13	0.36	18.41	0.05	0.00	0.00	87.27	2.88	1.12	1.16	1.93	0.032	2.86	59	298
ST-115	Mafic Schist	Groundmass	27.95	0.06	18.38	21.02	0.35	18.74	0.09	0.00	0.01	86.61	2.92	1.08	1.18	1.83	0.031	2.91	61	287
ST-115	Mafic Schist	Groundmass	28.14	0.09	18.66	22.08	0.29	18.67	0.07	0.00	0.01	88.02	2.90	1.10	1.17	1.90	0.025	2.87	60	292
ST-115	Mafic Schist	Groundmass	28.09	0.07	19.90	20.34	0.37	18.14	0.08	0.00	0.01	87.01	2.90	1.10	1.32	1.75	0.032	2.79	61	293
ST-115	Mafic Schist	Groundmass	27.09	0.07	19.86	23.24	0.34	15.03	0.24	0.00	0.00	85.88	2.89	1.11	1.38	2.07	0.031	2.39	53	297
ST-115	Mafic Schist	Groundmass	27.49	0.09	19.46	22.62	0.36	15.55	0.19	0.00	0.00	85.76	2.92	1.08	1.36	2.01	0.032	2.46	55	286
ST-115	Mafic Schist	Groundmass	27.60	0.06	19.42	21.23	0.34	17.18	0.18	0.00	0.00	86.02	2.90	1.10	1.31	1.87	0.031	2.69	59	292
ST-115	Mafic Schist	Groundmass	26.95	0.05	19.36	24.11	0.43	14.54	0.22	0.00	0.01	85.67	2.89	1.11	1.35	2.17	0.039	2.33	51	294
ST-115	Mafic Schist	Groundmass	27.39	0.07	19.53	22.95	0.37	16.56	0.07	0.01	0.00	86.95	2.87	1.13	1.29	2.01	0.033	2.59	56	301

Appendix 4: Chlorite Compositions

Sample	Lithology	Occurence	SiO2 (wt%)	TiO2 (wt%)	Al2O3 (wt%)	FeO (wt%)	MnO (wt%)	MgO (wt%)	CaO (wt%)	Na2O (wt%)	K2O (wt%)	Total (wt%)	SiIV	AlIV	AlVI	Fe	Mn	Mg	Mg#	T (°C)
ST-115	Mafic Schist	Groundmass	27.61	0.06	19.82	23.28	0.27	15.77	0.07	0.01	0.01	86.91	2.90	1.10	1.35	2.04	0.024	2.47	54	294
ST-115	Mafic Schist	Groundmass	27.81	0.04	19.60	22.75	0.35	16.65	0.11	0.01	0.00	87.31	2.90	1.10	1.30	1.98	0.030	2.58	56	293
ST-115	Mafic Schist	Groundmass	28.15	0.08	19.27	22.41	0.36	16.97	0.08	0.00	0.02	87.33	2.93	1.07	1.29	1.95	0.032	2.63	57	284
ST-115	Mafic Schist	Groundmass	27.76	0.03	18.86	23.48	0.41	14.57	0.21	0.00	0.03	85.35	2.98	1.02	1.36	2.11	0.037	2.33	52	268
ST-115	Mafic Schist	Groundmass	27.11	0.07	19.74	21.78	0.38	16.56	0.21	0.01	0.00	85.87	2.87	1.13	1.33	1.93	0.034	2.61	57	303
ST-115	Mafic Schist	Groundmass	27.02	0.05	19.36	22.57	0.43	16.21	0.24	0.00	0.02	85.89	2.87	1.13	1.30	2.01	0.039	2.57	56	301
ST-115	Mafic Schist	Groundmass	27.20	0.06	19.20	24.85	0.39	14.50	0.12	0.00	0.02	86.34	2.91	1.09	1.32	2.22	0.035	2.31	51	290
ST-115	Mafic Schist	Groundmass	27.23	0.06	19.14	25.31	0.39	14.38	0.10	0.00	0.01	86.61	2.91	1.09	1.31	2.26	0.035	2.29	50	291
ST-115	Mafic Schist	Groundmass	27.13	0.03	19.22	25.77	0.45	14.08	0.16	0.00	0.01	86.83	2.90	1.10	1.31	2.30	0.041	2.24	49	293
ST-115	Mafic Schist	Groundmass	27.27	0.04	19.14	25.80	0.42	14.36	0.17	0.02	0.00	87.21	2.90	1.10	1.30	2.29	0.038	2.28	49	293

Appendix 4: Mean Chlorite Compositions

Sample	Lithology	n	SiO2 (wt%)	TiO2 (wt%)	Al2O3 (wt%)	FeO (wt%)	MnO (wt%)	MgO (wt%)	CaO (wt%)	Na2O (wt%)	K2O (wt%)	Total (wt%)	SiIV	AlIV	AlVI	Fe	Mn	Mg	Mg#	T (°C)
Means																				
ST-64	Sediment	2	27.08		17.76	29.47	0.55	12.35	0.16	0.01	0.04	87.44	2.94	1.06	1.21	2.67	0.051	2.00	42	280
ST-65	Pillow Basalt	11	28.11	0.00	17.94	24.55	0.29	17.26	0.12	0.00	0.00	88.30	2.93	1.07	1.13	2.14	0.025	2.68	55	283
G-16	Pillow Basalt	5	27.74		17.68	28.75	0.41	13.60	0.20	0.05	0.06	88.50	2.96	1.04	1.18	2.56	0.037	2.16	45	274
ST-55	Pillow Basalt	4	28.90		16.66	25.94	0.37	16.41	0.20	0.01	0.01	88.51	3.03	0.97	1.08	2.27	0.033	2.56	53	252
ST-96	Pillow Basalt	6	27.97		18.18	25.24	0.30	16.51	0.14	0.00	0.01	88.38	2.92	1.08	1.16	2.21	0.027	2.57	53	286
ST-20	Pillow Basalt	7	28.38		17.55	23.50	0.29	18.26	0.09	0.01	0.01	88.12	2.94	1.06	1.09	2.04	0.026	2.82	58	278
ST-25	Pillow Basalt	5	27.61		18.12	27.94	0.34	14.21	0.19	0.01	0.01	88.45	2.93	1.07	1.19	2.48	0.031	2.24	47	284
ST-66	Fault Gouge	7	28.57	0.01	18.50	22.26	0.40	18.82	0.13	0.01	0.01	88.71	2.92	1.08	1.15	1.90	0.034	2.87	60	285
ST-90	Fault Gouge	8	28.56		19.43	17.84	0.29	20.36	0.12	0.00	0.01	86.64	2.92	1.08	1.26	1.52	0.025	3.10	67	286
ST-94	Massive Flow	10	29.39	0.01	15.86	25.70	0.25	17.44	0.10	0.01	0.09	88.86	3.06	0.94	1.00	2.24	0.022	2.71	54	241
ST-103	Pillow Basalt	23	27.19	0.00	18.54	25.86	0.28	16.04	0.10	0.01	0.01	88.04	2.86	1.14	1.16	2.28	0.025	2.52	52	304
ST-112	Massive Flow	5	28.01		19.20	23.12	0.30	17.07	0.12	0.00	0.01	87.82	2.90	1.10	1.25	2.00	0.026	2.64	57	291
ST-70	Fault Gouge	8	27.80		18.94	24.91	0.39	16.47	0.12	0.01	0.05	88.69	2.89	1.11	1.21	2.16	0.034	2.55	54	296
ST-71	Fault Gouge	21	27.09	0.01	18.46	24.78	0.32	17.06	0.09	0.01	0.05	87.87	2.85	1.15	1.13	2.18	0.028	2.67	55	310
ST-78	Massive Flow	5	26.82		20.40	24.19	0.39	16.56	0.06	0.02	0.01	88.48	2.78	1.22	1.28	2.10	0.034	2.56	55	330
ST-88	Volcaniclastic	3	26.65		20.10	23.11	0.51	17.54	0.07	0.02	0.01	88.05	2.77	1.23	1.23	2.01	0.045	2.72	57	335
ST-95	Massive Flow	20	29.25	0.00	16.60	21.37	0.26	18.84	0.10	0.00	0.00	86.43	3.06	0.94	1.10	1.87	0.023	2.93	61	242
ST-15	Massive Flow	28	27.35	0.04	16.90	32.15	0.45	10.28	0.42	0.01	0.02	87.61	3.01	0.99	1.20	2.96	0.042	1.69	36	257
ST-101	Pillow Basalt	20	29.71	0.01	16.29	23.67	0.25	16.34	0.39	0.02	0.02	86.70	3.14	0.86	1.16	2.09	0.022	2.57	55	216
ST-77	Mafic Schist	5	27.53	0.03	20.24	20.94	0.38	17.08	0.22	0.08	0.00	86.51	2.87	1.13	1.36	1.83	0.034	2.66	59	301
ST-75	Mafic Schist	5	27.86	0.02	19.96	18.91	0.24	18.83	0.14	0.01	0.00	85.98	2.89	1.11	1.32	1.64	0.021	2.91	64	296
ST-42	Massive Flow	12	30.74	0.01	13.67	25.08	0.23	15.66	0.16	0.00	0.00	85.56	3.31	0.69	1.04	2.26	0.021	2.51	52	162
ST-54	Massive Flow	14	29.25	0.03	15.94	25.27	0.18	15.01	0.20	0.01	0.00	85.90	3.14	0.86	1.16	2.27	0.017	2.40	51	214
ST-89	Pillow Basalt	12	31.27	0.00	14.41	26.39	0.29	13.49	0.65	0.04	0.00	86.54	3.36	0.64	1.18	2.37	0.026	2.16	47	145
ST-113	Undiff Basalt	7	28.17	0.01	18.33	23.83	0.22	15.83	0.15	0.06	0.04	86.63	2.98	1.02	1.26	2.11	0.019	2.49	54	268
ST-115	Mafic Schist	19	27.51	0.06	19.29	23.04	0.37	16.15	0.14	0.00	0.01	86.57	2.90	1.10	1.30	2.03	0.033	2.54	55	292
Standard Deviations																				
ST-64	Sediment	2	0.07		0.17	0.12	0.00	0.29	0.03	0.02	0.01	0.44	0.01	0.01	0.00	0.03	0.00	0.04	0.68	3.38
ST-65	Pillow Basalt	11	0.77	0.01	0.81	0.68	0.03	0.59	0.04	0.00	0.00	0.44	0.07	0.07	0.04	0.06	0.00	0.09	1.49	22.58
G-16	Pillow Basalt	5	0.67		0.37	0.68	0.05	0.94	0.10	0.03	0.01	0.64	0.06	0.06	0.05	0.08	0.01	0.13	2.16	19.24
ST-55	Pillow Basalt	4	0.26		0.43	0.51	0.03	0.36	0.14	0.01	0.01	0.26	0.02	0.02	0.06	0.05	0.00	0.06	0.33	5.98
ST-96	Pillow Basalt	6	1.12		0.80	1.53	0.02	1.48	0.06	0.01	0.01	0.68	0.07	0.07	0.06	0.16	0.00	0.19	3.65	23.94
ST-20	Pillow Basalt	7	0.57		0.12	0.25	0.02	0.47	0.03	0.01	0.01	1.16	0.02	0.02	0.02	0.02	0.00	0.03	0.54	6.12
ST-25	Pillow Basalt	5	0.71		0.84	0.06	0.03	0.64	0.03	0.01	0.01	0.62	0.06	0.06	0.06	0.02	0.00	0.09	1.16	17.82
ST-66	Fault Gouge	7	0.36	0.01	0.64	0.60	0.04	0.33	0.09	0.01	0.01	0.40	0.04	0.04	0.03	0.06	0.00	0.04	1.07	13.62
ST-90	Fault Gouge	8	0.48		0.51	0.15	0.02	0.50	0.04	0.01	0.01	0.69	0.03	0.03	0.04	0.01	0.00	0.06	0.62	9.84
ST-94	Massive Flow	10	0.27	0.02	0.47	0.27	0.02	0.44	0.05	0.02	0.17	0.55	0.03	0.03	0.04	0.02	0.00	0.07	0.79	8.92
ST-103	Pillow Basalt	23	0.88	0.01	0.84	0.60	0.03	0.45	0.09	0.01	0.01	0.76	0.07	0.07	0.06	0.07	0.00	0.07	1.13	22.32
ST-112	Massive Flow	5	0.39		0.63	0.75	0.04	0.59	0.08	0.00	0.01	0.57	0.04	0.04	0.05	0.06	0.00	0.08	1.40	13.10
ST-70	Fault Gouge	8	0.96		1.30	0.73	0.04	0.50	0.11	0.01	0.07	0.72	0.10	0.10	0.06	0.07	0.00	0.07	1.35	32.48
ST-71	Fault Gouge	21	1.47	0.01	1.84	0.87	0.05	1.21	0.07	0.01	0.11	0.88	0.14	0.14	0.11	0.08	0.00	0.19	2.58	43.87
ST-78	Massive Flow	5	0.32		0.41	0.43	0.01	0.35	0.07	0.03	0.00	0.46	0.01	0.01	0.03	0.06	0.00	0.04	0.88	3.52
ST-88	Volcaniclastic	3	0.29		0.10	0.47	0.02	0.49	0.06	0.01	0.00	0.33	0.01	0.01	0.01	0.05	0.00	0.06	1.20	4.63
ST-95	Massive Flow	20	0.74	0.01	0.76	0.54	0.06	0.69	0.04	0.00	0.00	0.61	0.06	0.06	0.06	0.05	0.01	0.09	1.30	20.50
ST-15	Massive Flow	28	0.68	0.05	0.36	0.76	0.04	0.28	0.18	0.01	0.02	0.72	0.05	0.05	0.04	0.09	0.00	0.03	1.03	15.99
ST-101	Pillow Basalt	20	0.61	0.01	0.60	0.36	0.03	0.71	0.09	0.01	0.02	0.90	0.04	0.04	0.07	0.04	0.00	0.11	1.22	12.04
ST-77	Mafic Schist	5	1.10	0.03	0.48	0.83	0.06	0.65	0.13	0.16	0.00	1.06	0.09	0.09	0.08	0.08	0.01	0.11	1.14	30.06
ST-75	Mafic Schist	5	0.55	0.01	0.39	0.47	0.09	0.12	0.16	0.02	0.00	0.56	0.04	0.04	0.03	0.05	0.01	0.01	0.77	12.71
ST-42	Massive Flow	12	0.55	0.01	0.47	0.35	0.05	0.53	0.05	0.01	0.00	0.70	0.04	0.04	0.04	0.04	0.00	0.07	0.97	12.50
ST-54	Massive Flow	14	0.52	0.02	0.75	0.65	0.06	0.58	0.09	0.01	0.00	0.37	0.06	0.06	0.05	0.06	0.01	0.09	1.50	18.55
ST-89	Pillow Basalt	12	0.64	0.01	0.72	0.52	0.04	0.36	0.18	0.04	0.00	1.19	0.04	0.04	0.06	0.06	0.00	0.06	0.83	13.82
ST-113	Undiff Basalt	7	1.46	0.01	0.81	1.32	0.03	0.55	0.11	0.07	0.09	1.09	0.11	0.11	0.06	0.14	0.00	0.05	2.00	36.97
ST-115	Mafic Schist	19	0.40	0.02	0.43	1.56	0.05	1.58	0.07	0.01	0.01	0.72	0.02	0.02	0.06	0.16	0.00	0.22	3.92	7.73

Appendix 4: Mean Chlorite Compositions

Sample	Lithology	n	SiO2 (wt%)	TiO2 (wt%)	Al2O3 (wt%)	FeO (wt%)	MnO (wt%)	MgO (wt%)	CaO (wt%)	Na2O (wt%)	K2O (wt%)	Total (wt%)	SiIV	AlIV	AlVI	Fe	Mn	Mg	Mg#	T (°C)
Relative Standard Deviations																				
ST-64	Sediment	2	0.2%		1.0%	0.4%	0.6%	2.4%	16.7%	141.4%	32.6%	0.5%	0.4%	1.0%	0.2%	1.0%	0.0%	1.8%	1.6%	1.2%
ST-65	Pillow Basalt	11	2.7%	193.7%	4.5%	2.8%	11.1%	3.4%	33.7%	211.0%	134.3%	0.5%	2.4%	6.5%	3.5%	2.9%	11.2%	3.2%	2.7%	8.0%
G-16	Pillow Basalt	5	2.4%		2.1%	2.4%	12.7%	6.9%	50.8%	64.7%	17.4%	0.7%	2.0%	5.7%	3.9%	3.0%	13.5%	6.1%	4.8%	7.0%
ST-55	Pillow Basalt	4	0.9%		2.6%	1.9%	9.0%	2.2%	70.5%	200.0%	80.6%	0.3%	0.6%	1.9%	5.7%	2.1%	9.2%	2.3%	0.6%	2.4%
ST-96	Pillow Basalt	6	4.0%		4.4%	6.1%	7.1%	9.0%	44.5%	155.2%	123.4%	0.8%	2.5%	6.9%	4.8%	7.2%	8.3%	7.6%	6.8%	6.4%
ST-20	Pillow Basalt	7	2.0%		0.7%	1.1%	5.9%	2.6%	31.6%	87.7%	92.0%	1.3%	0.6%	1.8%	1.5%	1.0%	6.1%	1.2%	0.9%	2.2%
ST-25	Pillow Basalt	5	2.6%		4.7%	0.2%	9.7%	4.5%	13.7%	67.8%	87.5%	0.7%	1.9%	5.2%	5.2%	0.9%	10.3%	3.8%	2.5%	6.3%
ST-66	Fault Gouge	7	1.2%	152.8%	3.5%	2.7%	9.5%	1.8%	72.1%	127.7%	124.2%	0.4%	1.4%	3.9%	2.6%	3.1%	9.7%	1.5%	1.8%	4.8%
ST-90	Fault Gouge	8	1.7%		2.6%	0.9%	5.5%	2.5%	29.5%	229.8%	71.5%	0.8%	1.0%	2.8%	3.4%	1.0%	6.1%	2.1%	0.9%	3.4%
ST-94	Massive Flow	10	0.9%	127.7%	3.0%	1.1%	9.0%	2.5%	50.2%	118.5%	183.5%	0.6%	0.9%	2.9%	4.4%	1.0%	9.2%	2.7%	1.4%	3.7%
ST-103	Pillow Basalt	23	3.3%	215.6%	4.6%	2.3%	12.6%	2.8%	90.4%	148.0%	91.8%	0.9%	2.4%	6.1%	4.9%	2.9%	12.7%	2.7%	2.2%	7.3%
ST-112	Massive Flow	5	1.4%		3.3%	3.3%	12.3%	3.4%	70.6%	223.6%	159.9%	0.6%	1.4%	3.7%	4.0%	3.1%	12.4%	3.2%	2.5%	4.5%
ST-70	Fault Gouge	8	3.4%		6.9%	2.9%	10.8%	3.1%	91.9%	110.1%	147.1%	0.8%	3.5%	9.1%	4.8%	3.2%	10.5%	2.7%	2.5%	11.0%
ST-71	Fault Gouge	21	5.4%	104.9%	10.0%	3.5%	14.2%	7.1%	74.2%	127.1%	249.3%	1.0%	4.8%	11.8%	9.8%	3.8%	14.2%	7.0%	4.7%	14.2%
ST-78	Massive Flow	5	1.2%		2.0%	1.8%	3.8%	2.1%	123.6%	149.1%	33.4%	0.5%	0.4%	0.9%	2.6%	2.6%	4.2%	1.4%	1.6%	1.1%
ST-88	Volcaniclastic	3	1.1%		0.5%	2.0%	4.0%	2.8%	85.9%	35.9%	25.0%	0.4%	0.5%	1.2%	0.5%	2.7%	4.7%	2.2%	2.1%	1.4%
ST-95	Massive Flow	20	2.5%	256.8%	4.6%	2.5%	21.7%	3.6%	39.8%	165.4%		0.7%	2.1%	6.7%	5.1%	2.7%	22.3%	3.1%	2.1%	8.5%
ST-15	Massive Flow	28	2.5%	125.1%	2.1%	2.4%	9.1%	2.8%	43.9%	77.8%	93.5%	0.8%	1.6%	5.0%	3.1%	2.9%	9.3%	2.0%	2.9%	6.2%
ST-101	Pillow Basalt	20	2.1%	164.7%	3.7%	1.5%	13.3%	4.3%	21.7%	45.9%	108.7%	1.0%	1.2%	4.3%	5.7%	2.0%	13.3%	4.1%	2.2%	5.6%
ST-77	Mafic Schist	5	4.0%	127.4%	2.4%	4.0%	16.6%	3.8%	60.7%	194.5%		1.2%	3.2%	8.3%	5.8%	4.4%	15.9%	4.3%	1.9%	10.0%
ST-75	Mafic Schist	5	2.0%	42.6%	1.9%	2.5%	39.2%	0.6%	111.2%	124.4%		0.6%	1.4%	3.5%	2.5%	2.9%	39.8%	0.4%	1.2%	4.3%
ST-42	Massive Flow	12	1.8%	67.9%	3.4%	1.4%	22.3%	3.4%	33.6%	102.1%		0.8%	1.2%	5.6%	4.2%	1.7%	22.5%	2.7%	1.8%	7.7%
ST-54	Massive Flow	14	1.8%	66.0%	4.7%	2.6%	31.2%	3.9%	48.5%	105.5%		0.4%	1.8%	6.7%	4.2%	2.9%	31.2%	3.6%	2.9%	8.7%
ST-89	Pillow Basalt	12	2.0%	319.4%	5.0%	2.0%	14.7%	2.7%	27.9%	96.9%		1.4%	1.3%	6.7%	5.0%	2.5%	14.8%	2.6%	1.8%	9.5%
ST-113	Undiff Basalt	7	5.2%	87.0%	4.4%	5.5%	14.8%	3.5%	72.0%	111.5%	247.3%	1.3%	3.9%	11.2%	4.6%	6.9%	15.1%	1.9%	3.7%	13.8%
ST-115	Mafic Schist	19	1.4%	30.7%	2.2%	6.8%	12.2%	9.8%	46.8%	164.7%	93.2%	0.8%	0.8%	2.2%	4.9%	7.7%	13.1%	8.6%	7.1%	2.6%

Appendix 4: Amphibole Compositions

Sample	Lithology	Occurence	SiO2 (wt%)	TiO2 (wt%)	Al2O3 (wt%)	FeO (wt%)	MnO (wt%)	MgO (wt%)	CaO (wt%)	Na2O (wt%)	K2O (wt%)	Total (wt%)	T Si	T Al	TFe3	Sum T	C Al	CFe3	C Ti	C Mg	CFe2	C Mn	C Ca	BFe2	B Mn	B Ca	A Na	A K	Sum A
ST-20	Pillow Basalt	Amygdule	52.27	N/A	1.01	24.73	0.50	8.78	11.03	0.12	0.00	98.50	7.88	0.12	0.00	8.00	0.06	0.02	0.00	1.97	2.95	0.00	0.00	0.15	0.06	1.78	0.04	0.00	0.04
ST-20	Pillow Basalt	Groundmass	51.46	N/A	4.58	15.33	0.28	14.44	11.47	0.60	0.04	98.32	7.44	0.56	0.00	8.00	0.22	0.16	0.00	3.11	1.50	0.00	0.00	0.19	0.04	1.78	0.17	0.01	0.18
ST-20	Pillow Basalt	Amygdule	51.79	N/A	3.57	16.17	0.31	13.30	11.30	0.40	0.29	97.14	7.64	0.36	0.00	8.00	0.26	0.00	0.00	2.92	1.82	0.00	0.00	0.18	0.04	1.79	0.11	0.05	0.17
ST-20	Pillow Basalt	Amygdule	47.76	N/A	9.99	16.03	0.22	11.23	12.49	0.44	0.02	98.18	6.94	1.06	0.00	8.00	0.65	0.28	0.00	2.43	1.64	0.00	0.00	0.03	0.03	1.95	0.12	0.00	0.13
ST-66	Fault Gouge	Groundmass	50.46	0.26	5.35	16.08	0.53	13.52	11.49	0.65	0.06	98.44	7.33	0.67	0.00	8.00	0.24	0.18	0.03	2.93	1.62	0.00	0.00	0.15	0.07	1.79	0.18	0.01	0.19
ST-66	Fault Gouge	Groundmass	53.48	0.27	1.99	14.40	0.46	15.42	11.26	0.29	0.01	97.66	7.75	0.25	0.00	8.00	0.09	0.02	0.03	3.33	1.53	0.00	0.00	0.20	0.06	1.75	0.08	0.00	0.08
ST-66	Fault Gouge	Groundmass	53.75	0.11	1.36	17.13	0.70	15.76	8.79	0.31	0.00	97.97	7.81	0.19	0.00	8.00	0.04	0.04	0.01	3.41	1.49	0.00	0.00	0.55	0.09	1.37	0.09	0.00	0.09
ST-66	Fault Gouge	Groundmass	53.62	0.25	2.13	12.93	0.33	16.68	11.27	0.29	0.02	97.55	7.71	0.29	0.00	8.00	0.07	0.09	0.03	3.58	1.24	0.00	0.00	0.22	0.04	1.74	0.08	0.00	0.08
ST-66	Fault Gouge	Vein	52.46	0.52	5.18	8.11	0.23	19.20	11.48	0.65	0.04	97.91	7.36	0.64	0.00	8.00	0.22	0.12	0.06	4.02	0.59	0.00	0.00	0.25	0.03	1.73	0.18	0.01	0.19
ST-90	Fault Gouge	Groundmass	54.34	N/A	2.92	10.63	0.17	17.23	12.54	0.33	0.06	98.26	7.69	0.31	0.00	8.00	0.18	0.02	0.00	3.64	1.16	0.00	0.00	0.08	0.02	1.90	0.09	0.01	0.10
ST-90	Fault Gouge	Groundmass	52.37	N/A	4.80	11.34	0.15	15.55	13.01	0.69	0.11	98.02	7.50	0.50	0.00	8.00	0.31	0.00	0.00	3.32	1.36	0.02	0.00	0.00	0.00	2.00	0.19	0.02	0.21
ST-90	Fault Gouge	Vein	54.80	N/A	2.35	10.48	0.15	17.33	12.67	0.27	0.05	98.23	7.77	0.24	0.00	8.00	0.16	0.00	0.00	3.66	1.18	0.00	0.00	0.06	0.02	1.92	0.08	0.01	0.08
ST-90	Fault Gouge	Vein	54.74	N/A	2.51	10.49	0.22	17.45	12.41	0.22	0.05	98.18	7.75	0.25	0.00	8.00	0.17	0.02	0.00	3.68	1.14	0.00	0.00	0.09	0.03	1.88	0.06	0.01	0.07
ST-90	Fault Gouge	Vein	55.16	N/A	2.11	10.72	0.20	17.31	12.53	0.22	0.05	98.29	7.81	0.20	0.00	8.00	0.16	0.00	0.00	3.65	1.19	0.00	0.00	0.08	0.02	1.90	0.06	0.01	0.07
ST-90	Fault Gouge	Vein	54.58	N/A	2.05	11.98	0.28	16.28	12.45	0.24	0.06	97.92	7.81	0.19	0.00	8.00	0.15	0.00	0.00	3.47	1.38	0.00	0.00	0.06	0.03	1.91	0.07	0.01	0.08
ST-90	Fault Gouge	Vein	52.86	N/A	4.83	10.95	0.19	15.04	13.51	0.31	0.06	97.74	7.57	0.43	0.00	8.00	0.38	0.00	0.00	3.21	1.31	0.02	0.07	0.00	0.00	2.00	0.09	0.01	0.10
ST-90	Fault Gouge	Groundmass	53.61	N/A	3.02	14.66	0.38	13.88	13.21	0.14	0.03	99.17	7.70	0.30	0.00	8.00	0.21	0.04	0.00	2.96	1.71	0.05	0.03	0.00	0.00	2.00	0.04	0.01	0.04
ST-90	Fault Gouge	Vein	51.88	N/A	5.58	12.18	0.19	15.79	12.39	0.71	0.11	98.84	7.37	0.63	0.00	8.00	0.30	0.12	0.00	3.34	1.24	0.00	0.00	0.09	0.02	1.89	0.20	0.02	0.22
ST-90	Fault Gouge	Vein	52.48	N/A	4.86	11.66	0.15	16.27	12.42	0.72	0.09	98.66	7.45	0.55	0.00	8.00	0.26	0.07	0.00	3.44	1.22	0.00	0.00	0.09	0.02	1.89	0.20	0.02	0.21
ST-112	Sheet Flow	Amygdule	52.98	N/A	3.51	16.47	0.25	13.31	12.26	0.33	0.05	99.18	7.64	0.36	0.00	8.00	0.23	0.03	0.00	2.86	1.88	0.00	0.00	0.08	0.03	1.89	0.09	0.01	0.10
ST-112	Sheet Flow	Amygdule	50.86	N/A	2.68	15.87	0.23	12.34	13.08	0.26	0.05	95.36	7.64	0.36	0.00	8.00	0.11	0.17	0.00	2.76	1.83	0.03	0.11	0.00	0.00	2.00	0.08	0.01	0.08
ST-70	Fault Gouge	Vein	54.92	N/A	0.80	13.64	0.36	15.48	12.37	0.12	0.04	97.77	7.93	0.07	0.00	8.00	0.07	0.00	0.00	3.33	1.60	0.00	0.00	0.04	0.04	1.91	0.03	0.01	0.04
ST-70	Fault Gouge	Vein	53.62	N/A	2.24	17.37	0.47	12.96	12.35	0.22	0.15	99.36	7.75	0.25	0.00	8.00	0.14	0.02	0.00	2.79	2.05	0.00	0.00	0.03	0.06	1.91	0.06	0.03	0.09
ST-70	Fault Gouge	Vein	52.53	N/A	2.88	16.52	0.35	13.43	11.35	0.28	0.35	97.71	7.71	0.29	0.00	8.00	0.21	0.00	0.00	2.94	1.86	0.00	0.00	0.17	0.04	1.79	0.08	0.07	0.15
ST-70	Fault Gouge	Amygdule	51.18	N/A	4.65	17.72	0.31	12.19	12.12	0.63	0.26	99.05	7.46	0.54	0.00	8.00	0.26	0.06	0.00	2.65	2.04	0.00	0.00	0.07	0.04	1.89	0.18	0.05	0.23
ST-70	Fault Gouge	Vein	53.46	N/A	2.12	16.03	0.45	13.39	12.07	0.28	0.10	97.88	7.81	0.19	0.00	8.00	0.18	0.00	0.00	2.92	1.90	0.00	0.00	0.06	0.06	1.89	0.08	0.02	0.10
ST-71	Fault Gouge	Groundmass	52.32	0.00	2.77	16.45	0.27	13.66	12.56	0.27	0.08	98.38	7.59	0.41	0.00	8.00	0.06	0.26	0.00	2.96	1.73	0.00	0.00	0.02	0.03	1.95	0.08	0.02	0.09
ST-71	Fault Gouge	Groundmass	49.99	0.00	1.98	15.74	0.33	13.92	12.68	0.22	0.07	94.91	7.49	0.35	0.16	8.00	0.00	0.43	0.00	3.11	1.38	0.04	0.04	0.00	0.00	2.00	0.06	0.01	0.08
ST-71	Fault Gouge	Groundmass	48.38	0.03	4.33	17.12	0.24	12.76	12.40	0.39	0.17	95.85	7.23	0.76	0.00	8.00	0.00	0.62	0.00	2.84	1.52	0.02	0.00	0.00	0.01	1.99	0.11	0.03	0.15
ST-78	Sheet Flow	Amygdule	51.60	N/A	4.81	15.04	0.36	13.41	12.35	0.47	0.12	98.16	7.49	0.51	0.00	8.00	0.31	0.05	0.00	2.90	1.74	0.00	0.00	0.04	0.04	1.92	0.13	0.02	0.15
ST-78	Sheet Flow	Amygdule	50.28	N/A	5.58	17.55	0.33	11.99	12.16	0.68	0.17	98.85	7.34	0.66	0.00	8.00	0.30	0.13	0.00	2.61	1.96	0.00	0.00	0.06	0.04	1.90	0.19	0.03	0.22
ST-78	Sheet Flow	Groundmass	50.83	N/A	4.11	16.95	0.22	12.64	12.25	0.45	0.12	97.62	7.47	0.53	0.00	8.00	0.19	0.19	0.00	2.77	1.86	0.00	0.00	0.04	0.03	1.93	0.13	0.02	0.15
ST-78	Sheet Flow	Groundmass	49.23	N/A	7.69	17.01	0.38	11.76	12.26	0.86	0.22	99.52	7.14	0.87	0.00	8.00	0.45	0.14	0.00	2.54	1.88	0.00	0.00	0.05	0.05	1.90	0.24	0.04	0.28
ST-83	Sheet Flow	Groundmass	52.00	0.16	4.01	15.08	0.28	14.24	12.09	0.46	0.07	98.41	7.51	0.49	0.00	8.00	0.19	0.12	0.02	3.07	1.60	0.00	0.00	0.10	0.03	1.87	0.13	0.01	0.14
ST-83	Sheet Flow	Groundmass	46.00	0.39	10.21	18.23	0.25	10.25	11.90	1.05	0.16	98.43	6.78	1.22	0.00	8.00	0.55	0.26	0.04	2.25	1.90	0.00	0.00	0.09	0.03	1.88	0.30	0.03	0.33
ST-83	Sheet Flow	Groundmass	49.46	0.21	6.18	16.56	0.30	12.42	11.99	0.63	0.14	97.91	7.25	0.75	0.00	8.00	0.32	0.19	0.02	2.71	1.76	0.00	0.00	0.08	0.04	1.88	0.18	0.03	0.21
ST-83	Sheet Flow	Groundmass	50.15	0.21	5.71	16.09	0.26	12.71	11.84	0.50	0.07	97.56	7.35	0.65	0.00	8.00	0.34	0.11	0.02	2.78	1.75	0.00	0.00	0.11	0.03	1.86	0.14	0.01	0.16
ST-83	Sheet Flow	Vein	52.32	0.42	2.90	15.51	0.26	14.04	12.33	0.23	0.07	98.08	7.59	0.41	0.00	8.00	0.09	0.15	0.05	3.04	1.68	0.00	0.00	0.05	0.03	1.92	0.07	0.01	0.08
ST-83	Sheet Flow	Vein	46.20	0.32	9.50	18.54	0.24	10.28	11.74	1.02	0.21	98.10	6.85	1.16	0.00	8.00	0.50	0.25	0.04	2.27	1.94	0.00	0.00	0.11	0.03	1.86	0.29	0.04	0.33
ST-83	Sheet Flow	Vein	44.52	0.28	11.13	19.34	0.31	9.29	11.96	1.16	0.33	98.39	6.62	1.38	0.00	8.00	0.57	0.36	0.03	2.06	1.99	0.00	0.00	0.06	0.04	1.90	0.34	0.06	0.40
ST-83	Sheet Flow	Vein	50.31	0.21	5.38	16.11	0.28	12.89	12.05	0.53	0.09	97.91	7.35	0.65	0.00	8.00	0.28	0.16	0.02	2.81	1.73	0.00	0.00	0.08	0.03	1.89	0.15	0.02	0.17
ST-88	Volcaniclastic	Groundmass	48.70	N/A	7.24	17.83	0.40	12.31	11.97	1.02	0.26	99.73	7.05	0.95	0.00	8.00	0.28	0.34	0.00	2.66	1.72	0.00	0.00	0.10	0.05	1.86	0.29	0.05	0.33
ST-88	Volcaniclastic	Groundmass	52.23	N/A	4.16	15.48	0.45	13.77	12.12	0.65	0.13	99.09	7.54	0.47	0.00	8.00	0.24	0.02	0.00	2.96	1.78	0.00	0.00	0.07	0.06	1.87	0.18	0.02	0.21
ST-88	Volcaniclastic	Groundmass	49.40	N/A	6.68	16.49	0.38	12.56	11.96	0.88	0.25	98.69	7.20	0.80	0.00	8.00	0.35	0.16	0.00	2.73	1.77	0.00	0.00	0.09	0.05	1.87	0.25	0.05	0.30
ST-95	Sheet Flow	Groundmass	52.52	0.24	1.31	18.20	0.62	13.43	10.06	0.50	0.04	96.91	7.82	0.18	0.00	8.00	0.05	0.00	0.03	2.98	1.95	0.00	0.00	0.32	0.08	1.60	0.14	0.01	0.15
ST-95	Sheet Flow	Amygdule	42.56	3.81	9.46	12.14	0.28	14.86	10.67	3.12	0.29	97.18	6.35	1.65	0.00	8.00	0.01	0.00	0.43	3.31	1.26	0.00	0.00	0.26	0.04	1.71	0.90	0.06	0.96

Appendix 4: Amphibole Compositions

Sample	Lithology	Occurence	SiO2 (wt%)	TiO2 (wt%)	Al2O3 (wt%)	FeO (wt%)	MnO (wt%)	MgO (wt%)	CaO (wt%)	Na2O (wt%)	K2O (wt%)	Total (wt%)	T Si	T Al	TFe3	Sum T	C Al	CFe3	C Ti	C Mg	CFe2	C Mn	C Ca	BFe2	B Mn	B Ca	A Na	A K	Sum A
ST-95	Sheet Flow	Groundmass	52.00	0.17	1.93	15.60	0.32	13.87	12.19	0.22	0.01	96.32	7.69	0.31	0.00	8.00	0.02	0.19	0.02	3.06	1.72	0.00	0.00	0.03	0.04	1.93	0.06	0.00	0.07
ST-95	Sheet Flow	Groundmass	54.42		2.40	13.91	0.27	14.86	12.66	0.24	0.02	98.77	7.79	0.21	0.00	8.00	0.19	0.00	0.00	3.17	1.64	0.00	0.00	0.03	0.03	1.94	0.07	0.00	0.07
ST-95	Sheet Flow	Groundmass	54.12	0.00	2.57	13.65	0.32	14.73	12.94	0.27	0.01	98.61	7.76	0.24	0.00	8.00	0.19	0.00	0.00	3.15	1.64	0.03	0.00	0.00	0.01	1.99	0.08	0.00	0.08
ST-95	Sheet Flow	Groundmass	52.02	0.03	4.35	16.31	0.30	12.96	12.70	0.47	0.11	99.25	7.50	0.50	0.00	8.00	0.24	0.10	0.00	2.79	1.87	0.00	0.00	0.00	0.04	1.96	0.13	0.02	0.15
ST-95	Sheet Flow	Groundmass	52.62	0.13	1.92	17.80	0.50	10.86	12.69	0.24	0.05	96.81	7.89	0.11	0.00	8.00	0.23	0.00	0.02	2.43	2.23	0.06	0.04	0.00	0.00	2.00	0.07	0.01	0.08
ST-95	Sheet Flow	Groundmass	52.69	0.07	2.24	17.03	0.40	12.40	12.55	0.22	0.06	97.65	7.76	0.24	0.00	8.00	0.15	0.01	0.01	2.72	2.09	0.03	0.00	0.00	0.02	1.98	0.06	0.01	0.07
ST-95	Sheet Flow	Groundmass	52.92	0.07	2.14	19.04	0.53	11.13	12.80	0.26	0.03	98.93	7.77	0.23	0.00	8.00	0.14	0.00	0.01	2.44	2.34	0.07	0.01	0.00	0.00	2.00	0.07	0.01	0.08
ST-95	Sheet Flow	Groundmass	52.39	0.11	2.23	19.04	0.63	10.96	12.53	0.21	0.04	98.15	7.76	0.24	0.00	8.00	0.15	0.01	0.01	2.42	2.35	0.07	0.00	0.00	0.01	1.99	0.06	0.01	0.07
ST-95	Sheet Flow	Amygdule	48.25	1.58	6.66	12.79	0.45	15.05	10.18	2.61	0.35	97.92	7.12	0.88	0.00	8.00	0.27	0.00	0.18	3.31	1.24	0.00	0.00	0.34	0.06	1.61	0.75	0.07	0.81
ST-95	Sheet Flow	Amygdule	45.07	3.74	8.61	10.75	0.40	15.37	10.51	3.00	0.24	97.67	6.66	1.34	0.00	8.00	0.16	0.00	0.42	3.39	1.04	0.00	0.00	0.29	0.05	1.66	0.86	0.05	0.91
ST-95	Sheet Flow	Groundmass	53.22	0.32	1.33	20.92	0.55	11.07	10.15	0.53	0.03	98.13	7.95	0.05	0.00	8.00	0.19	0.00	0.04	2.47	2.31	0.00	0.00	0.31	0.07	1.63	0.15	0.01	0.16
ST-77	Mafic Schist	Groundmass	47.64	0.05	8.21	15.22	0.38	13.11	11.83	0.57	0.10	97.11	6.96	1.04	0.00	8.00	0.38	0.47	0.01	2.86	1.29	0.00	0.00	0.10	0.05	1.85	0.16	0.02	0.18
ST-77	Mafic Schist	Groundmass	48.37	0.10	7.25	13.87	0.34	13.74	11.87	0.48	0.09	96.10	7.11	0.89	0.00	8.00	0.36	0.35	0.01	3.01	1.26	0.00	0.00	0.09	0.04	1.87	0.14	0.02	0.15
ST-77	Mafic Schist	Groundmass	51.04	0.04	4.79	15.69	0.41	12.98	12.84	0.44	0.07	98.29	7.41	0.59	0.00	8.00	0.23	0.21	0.00	2.81	1.70	0.05	0.00	0.00	0.00	2.00	0.12	0.01	0.14
ST-77	Mafic Schist	Groundmass	46.74	0.08	9.20	15.79	0.30	12.84	11.25	0.71	0.11	97.02	6.85	1.15	0.00	8.00	0.44	0.46	0.01	2.81	1.28	0.00	0.00	0.20	0.04	1.77	0.20	0.02	0.22
ST-77	Mafic Schist	Groundmass	50.77	0.17	6.45	15.50	0.75	13.03	10.13	0.75	0.06	97.60	7.44	0.56	0.00	8.00	0.55	0.00	0.02	2.85	1.58	0.00	0.00	0.32	0.09	1.59	0.21	0.01	0.22
ST-77	Mafic Schist	Groundmass	46.37	0.07	9.95	15.89	0.32	12.66	10.77	1.06	0.10	97.19	6.81	1.19	0.00	8.00	0.53	0.32	0.01	2.77	1.37	0.00	0.00	0.27	0.04	1.70	0.30	0.02	0.32
ST-77	Mafic Schist	Groundmass	49.30	0.07	6.49	13.83	0.35	13.84	12.13	0.51	0.06	96.57	7.22	0.78	0.00	8.00	0.33	0.28	0.01	3.02	1.36	0.00	0.00	0.05	0.04	1.90	0.15	0.01	0.16
ST-77	Mafic Schist	Groundmass	43.26	0.07	12.70	18.16	0.28	9.66	11.40	1.25	0.28	97.05	6.47	1.53	0.00	8.00	0.71	0.39	0.01	2.15	1.74	0.00	0.00	0.14	0.04	1.83	0.36	0.05	0.42
ST-77	Mafic Schist	Groundmass	50.72	0.21	6.12	13.30	0.36	13.46	12.63	0.53	0.10	97.44	7.38	0.62	0.00	8.00	0.43	0.00	0.02	2.92	1.62	0.01	0.00	0.00	0.03	1.97	0.15	0.02	0.17
ST-77	Mafic Schist	Groundmass	53.71	0.08	8.38	11.71	0.30	12.03	11.81	1.51	0.03	99.56	7.73	0.27	0.00	8.00	1.15	0.00	0.01	2.58	1.27	0.00	0.00	0.14	0.04	1.82	0.42	0.01	0.43
ST-77	Mafic Schist	Groundmass	52.81	0.06	4.09	13.38	0.34	14.08	12.81	0.35	0.02	97.94	7.63	0.37	0.00	8.00	0.32	0.00	0.01	3.03	1.62	0.02	0.00	0.00	0.02	1.98	0.10	0.00	0.10
ST-77	Mafic Schist	Groundmass	51.99	0.08	6.98	12.93	0.30	12.85	12.16	0.85	0.07	98.20	7.53	0.47	0.00	8.00	0.73	0.00	0.01	2.78	1.49	0.00	0.00	0.08	0.04	1.89	0.24	0.01	0.25
ST-77	Mafic Schist	Groundmass	51.91	0.06	7.58	11.91	0.38	11.67	12.10	0.89	0.09	96.59	7.67	0.33	0.00	8.00	0.99	0.00	0.01	2.57	1.44	0.00	0.00	0.04	0.05	1.92	0.26	0.02	0.27
ST-77	Mafic Schist	Groundmass	48.65	0.10	12.85	14.36	0.33	9.97	11.40	1.97	0.22	99.84	7.07	0.93	0.00	8.00	1.27	0.00	0.01	2.16	1.56	0.00	0.00	0.18	0.04	1.78	0.56	0.04	0.60
ST-77	Mafic Schist	Groundmass	50.37	0.07	7.59	14.48	0.33	12.28	12.43	0.80	0.09	98.44	7.31	0.69	0.00	8.00	0.61	0.00	0.01	2.66	1.73	0.00	0.00	0.03	0.04	1.93	0.23	0.02	0.24
ST-77	Mafic Schist	Groundmass	50.65	0.07	8.59	14.16	0.36	12.73	11.57	0.69	0.09	98.91	7.28	0.72	0.00	8.00	0.74	0.00	0.01	2.73	1.53	0.00	0.00	0.17	0.04	1.78	0.19	0.02	0.21
ST-77	Mafic Schist	Groundmass	50.71	0.08	9.20	12.98	0.26	11.53	11.45	1.09	0.05	97.33	7.45	0.55	0.00	8.00	1.04	0.00	0.01	2.52	1.43	0.00	0.00	0.17	0.03	1.80	0.31	0.01	0.32
ST-77	Mafic Schist	Groundmass	51.20	0.09	5.97	14.39	0.41	12.74	12.69	0.54	0.07	98.10	7.44	0.56	0.00	8.00	0.46	0.00	0.01	2.76	1.75	0.03	0.00	0.00	0.03	1.98	0.15	0.01	0.17
ST-77	Mafic Schist	Groundmass	50.47	0.07	8.32	13.79	0.35	12.86	10.89	0.90	0.14	97.81	7.35	0.65	0.00	8.00	0.78	0.00	0.01	2.79	1.42	0.00	0.00	0.26	0.04	1.70	0.25	0.03	0.28
ST-77	Mafic Schist	Groundmass	52.09	0.04	4.86	14.57	0.25	12.83	12.89	0.47	0.05	98.05	7.57	0.43	0.00	8.00	0.41	0.00	0.00	2.78	1.77	0.03	0.01	0.00	0.00	2.00	0.13	0.01	0.14
ST-77	Mafic Schist	Groundmass	51.55	0.56	5.31	13.86	0.36	12.95	12.99	0.55	0.07	98.19	7.48	0.52	0.00	8.00	0.39	0.00	0.06	2.80	1.68	0.04	0.02	0.00	0.00	2.00	0.16	0.01	0.17
ST-77	Mafic Schist	Groundmass	49.85	0.06	6.82	14.04	0.29	12.91	12.29	0.59	0.08	96.94	7.31	0.69	0.00	8.00	0.49	0.01	0.01	2.82	1.68	0.00	0.00	0.03	0.04	1.93	0.17	0.02	0.18
ST-77	Mafic Schist	Groundmass	52.35	0.09	8.47	13.39	0.36	10.90	11.77	1.27	0.10	98.69	7.64	0.36	0.00	8.00	1.10	0.00	0.01	2.37	1.52	0.00	0.00	0.12	0.05	1.84	0.36	0.02	0.38
ST-77	Mafic Schist	Groundmass	50.74	0.09	5.97	14.83	0.29	12.13	12.77	0.56	0.07	97.44	7.44	0.56	0.00	8.00	0.48	0.00	0.01	2.65	1.82	0.04	0.01	0.00	0.00	2.00	0.16	0.01	0.17
ST-77	Mafic Schist	Groundmass	51.62	0.14	5.59	13.70	0.34	13.07	12.68	0.52	0.05	97.71	7.51	0.49	0.00	8.00	0.47	0.00	0.02	2.83	1.67	0.02	0.00	0.00	0.02	1.98	0.15	0.01	0.16
ST-77	Mafic Schist	Groundmass	51.97	0.06	5.85	13.46	0.24	13.01	12.65	0.60	0.07	97.90	7.55	0.45	0.00	8.00	0.55	0.00	0.01	2.82	1.63	0.00	0.00	0.00	0.03	1.97	0.17	0.01	0.18
ST-77	Mafic Schist	Groundmass	51.98	0.12	8.44	11.86	0.38	10.69	11.63	1.36	0.09	96.55	7.75	0.25	0.00	8.00	1.23	0.00	0.01	2.38	1.38	0.00	0.00	0.10	0.05	1.86	0.39	0.02	0.41
ST-77	Mafic Schist	Groundmass	49.54	0.14	8.06	14.62	0.31	11.78	12.60	0.89	0.13	98.06	7.24	0.76	0.00	8.00	0.62	0.00	0.02	2.57	1.79	0.01	0.00	0.00	0.03	1.97	0.25	0.02	0.28
ST-75	Mafic Schist	Groundmass	52.87	0.26	5.83	11.04	0.13	15.05	13.19	0.57	0.03	98.97	7.49	0.51	0.00	8.00	0.47	0.00	0.03	3.18	1.31	0.02	0.00	0.00	0.00	2.00	0.16	0.01	0.16
ST-75	Mafic Schist	Groundmass	51.08	0.16	6.70	12.47	0.17	13.74	12.70	0.64	0.14	97.81	7.39	0.62	0.00	8.00	0.53	0.00	0.02	2.96	1.50	0.00	0.00	0.01	0.02	1.97	0.18	0.03	0.21
ST-75	**Mafic Schist**	**Groundmass**	**53.64**	**0.17**	**4.58**	**11.01**	**0.14**	**15.51**	**13.15**	**0.48**	**0.05**	**98.72**	**7.61**	**0.39**	**0.00**	**8.00**	**0.38**	**0.00**	**0.02**	**3.28**	**1.31**	**0.02**	**0.00**	**0.00**	**0.00**	**2.00**	**0.13**	**0.01**	**0.14**
ST-75	Mafic Schist	Groundmass	52.89	0.22	5.21	10.93	0.25	15.33	13.08	0.48	0.05	98.45	7.53	0.47	0.00	8.00	0.40	0.00	0.02	3.25	1.30	0.02	0.00	0.00	0.01	1.99	0.13	0.01	0.14
ST-75	Mafic Schist	Groundmass	50.83	0.15	8.69	11.23	0.15	13.15	12.99	0.95	0.09	98.23	7.32	0.68	0.00	8.00	0.79	0.00	0.02	2.82	1.35	0.02	0.00	0.00	0.00	2.00	0.27	0.02	0.28
ST-75	Mafic Schist	Groundmass	53.93	0.44	4.07	10.33	0.17	15.82	13.34	0.36	0.02	98.48	7.65	0.35	0.00	8.00	0.33	0.00	0.05	3.35	1.23	0.02	0.03	0.00	0.00	2.00	0.10	0.00	0.10
ST-75	Mafic Schist	Groundmass	53.10	0.22	4.95	10.31	0.09	15.23	12.93	0.45	0.02	97.29	7.63	0.37	0.00	8.00	0.47	0.00	0.02	3.26	1.24	0.00	0.00	0.00	0.01	1.99	0.13	0.00	0.13

Appendix 4: Amphibole Compositions

Sample	Lithology	Occurence	SiO2 (wt%)	TiO2 (wt%)	Al2O3 (wt%)	FeO (wt%)	MnO (wt%)	MgO (wt%)	CaO (wt%)	Na2O (wt%)	K2O (wt%)	Total (wt%)	T Si	T Al	TFe3	Sum T	C Al	CFe3	C Ti	C Mg	CFe2	C Mn	C Ca	BFe2	B Mn	B Ca	A Na	A K	Sum A
ST-75	Mafic Schist	Groundmass	53.55	0.12	4.74	10.24	0.16	15.20	13.07	0.47	0.02	97.57	7.68	0.32	0.00	8.00	0.48	0.00	0.01	3.25	1.23	0.02	0.01	0.00	0.00	2.00	0.13	0.00	0.13
ST-75	Mafic Schist	Groundmass	54.59	0.36	3.36	10.64	0.22	15.62	13.15	0.36	0.01	98.30	7.78	0.22	0.00	8.00	0.34	0.00	0.04	3.32	1.27	0.03	0.01	0.00	0.00	2.00	0.10	0.00	0.10
ST-75	Mafic Schist	Groundmass	50.89	0.19	7.30	12.36	0.23	13.57	12.66	0.73	0.15	98.08	7.34	0.66	0.00	8.00	0.58	0.00	0.02	2.92	1.48	0.00	0.00	0.02	0.03	1.96	0.20	0.03	0.23
ST-75	Mafic Schist	Groundmass	52.24	0.20	5.65	13.11	0.41	13.49	12.59	0.48	0.11	98.28	7.54	0.46	0.00	8.00	0.50	0.00	0.02	2.90	1.58	0.00	0.00	0.00	0.05	1.95	0.13	0.02	0.16
ST-75	Mafic Schist	Groundmass	52.50	0.20	5.49	11.88	0.23	14.05	13.09	0.50	0.07	98.00	7.56	0.44	0.00	8.00	0.49	0.00	0.02	3.02	1.43	0.03	0.02	0.00	0.00	2.00	0.14	0.01	0.15
ST-75	Mafic Schist	Groundmass	52.54	0.14	5.45	12.48	0.29	14.09	12.92	0.52	0.07	98.49	7.54	0.47	0.00	8.00	0.46	0.00	0.02	3.01	1.50	0.02	0.00	0.00	0.02	1.99	0.15	0.01	0.16
ST-75	Mafic Schist	Groundmass	52.18	0.14	6.08	12.35	0.24	13.96	13.05	0.59	0.09	98.69	7.47	0.53	0.00	8.00	0.50	0.00	0.02	2.98	1.48	0.03	0.00	0.00	0.00	2.00	0.16	0.02	0.18
ST-75	Mafic Schist	Groundmass	51.97	0.18	5.71	11.98	0.27	14.36	12.88	0.53	0.04	97.92	7.48	0.53	0.00	8.00	0.44	0.00	0.02	3.08	1.44	0.02	0.00	0.00	0.02	1.99	0.15	0.01	0.16
ST-75	Mafic Schist	Groundmass	52.39	0.18	5.41	11.69	0.22	14.21	12.94	0.52	0.06	97.62	7.56	0.44	0.00	8.00	0.48	0.00	0.02	3.06	1.41	0.03	0.00	0.00	0.00	2.00	0.15	0.01	0.16
ST-75	Mafic Schist	Groundmass	53.99	0.40	4.26	11.12	0.23	14.61	12.94	0.42	0.07	98.03	7.75	0.25	0.00	8.00	0.47	0.00	0.04	3.13	1.34	0.02	0.00	0.00	0.01	1.99	0.12	0.01	0.13
ST-75	Mafic Schist	Groundmass	51.58	0.19	7.00	12.17	0.22	13.04	12.62	0.75	0.15	97.73	7.49	0.51	0.00	8.00	0.69	0.00	0.02	2.82	1.47	0.00	0.00	0.01	0.03	1.96	0.21	0.03	0.24
ST-75	Mafic Schist	Groundmass	54.05	0.08	9.11	9.58	0.16	11.24	11.71	1.43	0.10	97.46	7.93	0.07	0.00	8.00	1.50	0.00	0.01	2.46	1.04	0.00	0.00	0.14	0.02	1.84	0.41	0.02	0.43
ST-75	Mafic Schist	Groundmass	53.74	0.18	4.58	10.76	0.22	14.81	12.85	0.43	0.04	97.61	7.73	0.27	0.00	8.00	0.50	0.00	0.02	3.18	1.29	0.01	0.00	0.00	0.02	1.98	0.12	0.01	0.13
ST-75	Mafic Schist	Groundmass	53.54	0.18	5.39	11.89	0.25	13.64	12.60	0.51	0.07	98.07	7.72	0.28	0.00	8.00	0.64	0.00	0.02	2.93	1.41	0.00	0.00	0.02	0.03	1.95	0.14	0.01	0.16
ST-75	Mafic Schist	Groundmass	54.04	0.12	4.16	10.90	0.22	14.98	13.17	0.37	0.01	97.97	7.74	0.26	0.00	8.00	0.44	0.00	0.01	3.20	1.31	0.03	0.02	0.00	0.00	2.00	0.10	0.00	0.11
ST-75	Mafic Schist	Groundmass	52.54	0.15	5.65	11.95	0.20	13.69	12.77	0.53	0.07	97.53	7.61	0.39	0.00	8.00	0.57	0.00	0.02	2.96	1.45	0.01	0.00	0.00	0.02	1.98	0.15	0.01	0.16
ST-75	Mafic Schist	Groundmass	53.05	0.14	5.34	12.07	0.21	13.98	12.83	0.49	0.06	98.17	7.63	0.37	0.00	8.00	0.53	0.00	0.02	3.00	1.45	0.00	0.00	0.00	0.02	1.98	0.14	0.01	0.15
ST-75	Mafic Schist	Groundmass	54.49	0.15	7.22	11.33	0.26	11.82	13.30	0.39	0.04	98.99	7.81	0.19	0.00	8.00	1.03	0.00	0.02	2.53	1.36	0.03	0.04	0.00	0.00	2.00	0.11	0.01	0.12
ST-89	Pillow Basalt	Groundmass	52.36	0.04	2.47	21.88	0.39	7.47	12.28	0.16	-	97.08	8.00	0.00	0.00	8.00	0.44	0.00	0.01	1.70	2.79	0.05	0.01	0.00	0.00	2.00	0.05	0.00	0.05
ST-89	Pillow Basalt	Groundmass	52.34	0.02	2.84	21.97	0.42	7.70	12.34	0.21	0.02	97.86	7.92	0.08	0.00	8.00	0.43	0.00	0.00	1.74	2.78	0.05	0.00	0.00	0.00	2.00	0.06	0.00	0.07
ST-89	Pillow Basalt	Groundmass	49.95	0.03	4.84	22.07	0.37	7.26	12.36	0.31	0.16	97.35	7.61	0.39	0.00	8.00	0.47	0.00	0.00	1.65	2.81	0.05	0.02	0.00	0.00	2.00	0.09	0.03	0.12
ST-89	Pillow Basalt	Groundmass	50.50	0.06	3.95	22.45	0.40	6.71	12.16	0.26	0.10	96.59	7.78	0.22	0.00	8.00	0.50	0.00	0.01	1.54	2.89	0.05	0.01	0.00	0.00	2.00	0.08	0.02	0.10
ST-115	Mafic Schist	Groundmass	45.86	1.48	8.56	16.17	0.30	11.10	12.47	1.54	0.32	97.81	6.83	1.17	0.00	8.00	0.33	0.01	0.17	2.46	2.01	0.03	0.00	0.00	0.01	1.99	0.45	0.06	0.51
ST-115	Mafic Schist	Groundmass	47.04	1.21	7.77	15.16	0.29	11.82	12.52	1.33	0.27	97.39	6.98	1.02	0.00	8.00	0.34	0.00	0.14	2.62	1.88	0.03	0.00	0.00	0.01	1.99	0.38	0.05	0.43
ST-115	Mafic Schist	Groundmass	44.72	1.10	9.28	17.30	0.25	10.56	12.41	1.69	0.32	97.63	6.70	1.31	0.00	8.00	0.33	0.18	0.12	2.36	1.99	0.02	0.00	0.00	0.01	1.99	0.49	0.06	0.55
ST-115	Mafic Schist	Groundmass	43.67	1.39	10.39	17.50	0.25	9.63	12.19	1.90	0.42	97.35	6.60	1.40	0.00	8.00	0.45	0.00	0.16	2.17	2.21	0.01	0.00	0.00	0.03	1.98	0.56	0.08	0.64
ST-115	Mafic Schist	Groundmass	43.86	1.42	10.03	16.18	0.30	10.90	12.34	1.80	0.39	97.25	6.58	1.42	0.00	8.00	0.35	0.15	0.16	2.44	1.88	0.02	0.00	0.00	0.02	1.98	0.52	0.08	0.60
ST-115	Mafic Schist	Groundmass	44.08	1.47	9.82	16.10	0.23	11.13	12.41	1.79	0.40	97.42	6.59	1.41	0.00	8.00	0.32	0.16	0.17	2.48	1.85	0.02	0.00	0.00	0.01	1.99	0.52	0.08	0.60
ST-115	Mafic Schist	Groundmass	45.58	1.58	8.82	15.39	0.27	11.56	12.26	1.63	0.31	97.39	6.80	1.21	0.00	8.00	0.34	0.00	0.18	2.57	1.91	0.00	0.00	0.01	0.03	1.96	0.47	0.06	0.53
ST-115	Mafic Schist	Groundmass	42.68	1.35	11.43	17.25	0.31	9.78	12.30	2.06	0.45	97.61	6.43	1.57	0.00	8.00	0.46	0.12	0.15	2.20	2.05	0.02	0.00	0.00	0.02	1.99	0.60	0.09	0.69
ST-115	Mafic Schist	Groundmass	48.87	0.57	7.11	13.67	0.33	12.94	12.56	1.23	0.20	97.50	7.18	0.82	0.00	8.00	0.41	0.00	0.06	2.83	1.68	0.02	0.00	0.00	0.02	1.98	0.35	0.04	0.39
ST-115	Mafic Schist	Groundmass	46.45	1.07	8.68	14.66	0.27	11.93	12.59	1.46	0.28	97.38	6.88	1.12	0.00	8.00	0.40	0.01	0.12	2.64	1.81	0.03	0.00	0.00	0.00	2.00	0.42	0.05	0.47
ST-115	Mafic Schist	Groundmass	46.12	1.45	8.38	14.56	0.33	12.03	12.59	1.54	0.33	97.34	6.85	1.15	0.00	8.00	0.32	0.00	0.16	2.67	1.81	0.04	0.00	0.00	0.00	2.00	0.44	0.06	0.51
ST-115	Mafic Schist	Groundmass	46.08	1.57	8.65	14.63	0.27	11.96	12.64	1.51	0.32	97.62	6.82	1.18	0.00	8.00	0.33	0.00	0.18	2.64	1.81	0.03	0.01	0.00	0.00	2.00	0.43	0.06	0.49
ST-115	Mafic Schist	Groundmass	45.78	1.40	8.99	15.85	0.24	11.81	12.49	1.66	0.33	98.55	6.74	1.26	0.00	8.00	0.30	0.11	0.16	2.59	1.84	0.00	0.00	0.00	0.03	1.97	0.47	0.06	0.54
ST-115	Mafic Schist	Groundmass	43.64	1.37	10.12	15.89	0.38	10.63	12.45	1.81	0.41	96.69	6.59	1.41	0.00	8.00	0.39	0.11	0.16	2.39	1.90	0.05	0.01	0.00	0.00	2.00	0.53	0.08	0.61
ST-115	Mafic Schist	Groundmass	46.87	1.52	8.26	15.33	0.32	11.80	12.43	1.50	0.29	98.29	6.91	1.09	0.00	8.00	0.34	0.00	0.17	2.59	1.89	0.00	0.00	0.00	0.04	1.96	0.43	0.05	0.48
ST-115	Mafic Schist	Groundmass	46.76	1.59	8.45	14.88	0.32	11.66	12.22	1.52	0.32	97.70	6.94	1.06	0.00	8.00	0.41	0.00	0.18	2.58	1.83	0.00	0.00	0.02	0.04	1.94	0.44	0.06	0.50
ST-115	Mafic Schist	Groundmass	46.76	1.48	8.43	14.85	0.36	11.85	12.54	1.46	0.31	98.03	6.90	1.10	0.00	8.00	0.37	0.00	0.16	2.61	1.83	0.03	0.00	0.00	0.02	1.98	0.42	0.06	0.48
ST-118	Mafic Schist	Groundmass	45.33	1.16	7.90	15.47	0.33	12.52	12.16	1.50	0.24	96.60	6.77	1.23	0.00	8.00	0.16	0.33	0.13	2.79	1.59	0.00	0.00	0.01	0.04	1.95	0.43	0.05	0.48
ST-118	Mafic Schist	Groundmass	44.96	0.94	8.21	16.05	0.41	12.25	12.29	1.71	0.25	97.07	6.71	1.29	0.00	8.00	0.15	0.39	0.11	2.73	1.62	0.02	0.00	0.00	0.04	1.97	0.50	0.05	0.54
ST-118	Mafic Schist	Groundmass	46.30	1.34	7.25	15.04	0.26	13.18	11.84	1.67	0.17	97.05	6.88	1.12	0.00	8.00	0.15	0.16	0.15	2.92	1.62	0.00	0.00	0.08	0.03	1.88	0.48	0.03	0.51
ST-118	Mafic Schist	Groundmass	48.26	1.07	5.92	14.24	0.27	14.07	12.39	1.08	0.11	97.41	7.07	0.93	0.00	8.00	0.09	0.28	0.12	3.07	1.44	0.00	0.00	0.02	0.03	1.94	0.31	0.02	0.33
ST-118	Mafic Schist	Groundmass	45.56	1.14	7.60	15.28	0.27	12.74	12.13	1.54	0.20	96.45	6.81	1.19	0.00	8.00	0.15	0.30	0.13	2.84	1.58	0.00	0.00	0.02	0.03	1.94	0.45	0.04	0.48
ST-118	Mafic Schist	Groundmass	46.13	1.31	7.12	14.86	0.26	13.33	12.09	1.41	0.18	96.69	6.85	1.15	0.00	8.00	0.10	0.32	0.15	2.95	1.49	0.00	0.00	0.04	0.03	1.92	0.41	0.03	0.44
ST-118	Mafic Schist	Groundmass	46.24	1.40	7.14	14.05	0.30	13.28	12.24	1.30	0.16	96.10	6.89	1.11	0.00	8.00	0.15	0.24	0.16	2.95	1.51	0.00	0.00	0.01	0.04	1.96	0.38	0.03	0.41

Appendix 4: Amphibole Compositions

Sample	Lithology	Occurence	SiO2 (wt%)	TiO2 (wt%)	Al2O3 (wt%)	FeO (wt%)	MnO (wt%)	MgO (wt%)	CaO (wt%)	Na2O (wt%)	K2O (wt%)	Total (wt%)	T Si	T Al	TFe3	Sum T	C Al	CFe3	C Ti	C Mg	CFe2	C Mn	C Ca	BFe2	B Mn	B Ca	A Na	A K	Sum A
ST-118	Mafic Schist	Groundmass	45.13	1.34	8.02	15.74	0.28	12.86	11.83	1.77	0.21	97.17	6.71	1.29	0.00	8.00	0.12	0.32	0.15	2.85	1.56	0.00	0.00	0.08	0.04	1.89	0.51	0.04	0.55
ST-118	Mafic Schist	Groundmass	45.70	1.36	7.41	15.02	0.36	13.23	11.71	1.67	0.20	96.68	6.82	1.19	0.00	8.00	0.12	0.24	0.15	2.94	1.55	0.00	0.00	0.08	0.05	1.87	0.48	0.04	0.52
ST-118	Mafic Schist	Groundmass	45.74	1.31	7.58	15.45	0.23	13.07	11.65	1.66	0.20	96.88	6.81	1.19	0.00	8.00	0.14	0.24	0.15	2.90	1.57	0.00	0.00	0.11	0.03	1.86	0.48	0.04	0.52
ST-118	Mafic Schist	Groundmass	47.03	1.58	7.34	15.20	0.31	12.87	12.25	1.47	0.19	98.24	6.91	1.09	0.00	8.00	0.18	0.12	0.18	2.82	1.72	0.00	0.00	0.03	0.04	1.93	0.42	0.04	0.45
ST-118	Mafic Schist	Groundmass	47.00	1.34	7.39	14.56	0.32	12.47	12.46	1.33	0.20	97.09	6.97	1.03	0.00	8.00	0.27	0.04	0.15	2.76	1.76	0.02	0.00	0.00	0.02	1.98	0.38	0.04	0.42
ST-118	Mafic Schist	Groundmass	47.57	1.21	7.59	14.47	0.30	13.07	12.07	1.55	0.21	98.04	6.98	1.02	0.00	8.00	0.30	0.00	0.13	2.86	1.71	0.00	0.00	0.06	0.04	1.90	0.44	0.04	0.48
ST-118	Mafic Schist	Groundmass	47.41	1.11	7.35	15.18	0.37	12.88	11.71	1.62	0.20	97.82	7.00	1.00	0.00	8.00	0.27	0.00	0.12	2.83	1.77	0.00	0.00	0.10	0.05	1.85	0.46	0.04	0.50
ST-118	Mafic Schist	Groundmass	48.34	1.20	7.09	13.73	0.26	13.27	12.25	1.29	0.19	97.63	7.10	0.91	0.00	8.00	0.32	0.00	0.13	2.90	1.64	0.00	0.00	0.04	0.03	1.93	0.37	0.04	0.40
ST-118	Mafic Schist	Groundmass	47.47	1.26	7.91	15.02	0.27	12.82	12.01	1.46	0.19	98.42	6.95	1.05	0.00	8.00	0.31	0.02	0.14	2.80	1.74	0.00	0.00	0.08	0.03	1.88	0.41	0.04	0.45
ST-118	Mafic Schist	Groundmass	46.94	1.18	7.50	15.66	0.39	12.73	11.78	1.55	0.21	97.93	6.92	1.08	0.00	8.00	0.23	0.10	0.13	2.80	1.74	0.00	0.00	0.09	0.05	1.86	0.44	0.04	0.48
ST-118	Mafic Schist	Groundmass	46.97	1.28	7.59	14.95	0.27	12.90	11.89	1.54	0.20	97.60	6.94	1.06	0.00	8.00	0.26	0.04	0.14	2.84	1.72	0.00	0.00	0.09	0.03	1.88	0.44	0.04	0.48

Appendix 4: Mean Amphibole Compositions

Sample	Lithology	Occurence	SiO2 (wt%)	TiO2 (wt%)	Al2O3 (wt%)	FeO (wt%)	MnO (wt%)	MgO (wt%)	CaO (wt%)	Na2O (wt%)	K2O (wt%)	Total (wt%)	T Si	T Al	TFe3	Sum T	C Al	CFe3	C Ti	C Mg	CFe2	C Mn	C Ca	BFe2	B Mn	B Ca	A Na	A K	Sum A
Means																													
ST-20	Pillow Basalt	4	50.82		4.79	18.06	0.33	11.94	11.57	0.39	0.09	98.03	7.48	0.52	0.00	8.00	0.30	0.12	0.00	2.61	1.98	0.00	0.00	0.14	0.04	1.82	0.11	0.02	0.13
ST-66	Fault Gouge	5	52.75	0.28	3.20	13.73	0.45	16.12	10.86	0.44	0.03	97.91	7.59	0.41	0.00	8.00	0.13	0.09	0.03	3.45	1.29	0.00	0.00	0.27	0.06	1.67	0.12	0.00	0.13
ST-90	Fault Gouge	10	53.70		3.50	11.51	0.21	16.21	12.71	0.38	0.07	98.33	7.64	0.36	0.00	8.00	0.23	0.03	0.00	3.44	1.29	0.01	0.01	0.05	0.02	1.93	0.11	0.01	0.12
ST-112	Sheet Flow	2	51.92		3.09	16.17	0.24	12.82	12.67	0.30	0.05	97.27	7.64	0.36	0.00	8.00	0.17	0.10	0.00	2.81	1.85	0.01	0.05	0.04	0.02	1.95	0.08	0.01	0.09
ST-70	Fault Gouge	5	53.14		2.54	16.26	0.39	13.49	12.05	0.31	0.18	98.35	7.73	0.27	0.00	8.00	0.17	0.02	0.00	2.93	1.89	0.00	0.00	0.07	0.05	1.88	0.09	0.03	0.12
ST-71	Fault Gouge	3	50.23	0.01	3.03	16.43	0.28	13.45	12.55	0.29	0.11	96.38	7.44	0.51	0.05	8.00	0.02	0.43	0.00	2.97	1.54	0.02	0.01	0.01	0.02	1.98	0.08	0.02	0.10
ST-78	Sheet Flow	4	50.49		5.55	16.63	0.32	12.45	12.26	0.62	0.16	98.54	7.36	0.64	0.00	8.00	0.31	0.13	0.00	2.71	1.86	0.00	0.00	0.05	0.04	1.91	0.17	0.03	0.20
ST-83	Sheet Flow	8	48.87	0.27	6.88	16.93	0.27	12.02	11.99	0.70	0.14	98.10	7.16	0.84	0.00	8.00	0.35	0.20	0.03	2.62	1.79	0.00	0.00	0.08	0.03	1.88	0.20	0.03	0.23
ST-88	Volcaniclastic	8	50.11		6.03	16.60	0.41	12.88	12.02	0.85	0.21	99.17	7.26	0.74	0.00	8.00	0.29	0.17	0.00	2.78	1.76	0.00	0.00	0.08	0.05	1.87	0.24	0.04	0.28
ST-95	Sheet Flow	13	51.14	0.86	3.63	15.94	0.43	13.20	11.74	0.91	0.10	97.87	7.52	0.48	0.00	8.00	0.15	0.02	0.09	2.89	1.82	0.02	0.00	0.12	0.03	1.85	0.26	0.02	0.28
ST-77	Mafic Schist	28	50.30	0.11	7.50	14.13	0.34	12.44	12.02	0.81	0.09	97.74	7.34	0.66	0.00	8.00	0.63	0.09	0.01	2.71	1.55	0.01	0.00	0.09	0.03	1.88	0.23	0.02	0.25
ST-75	Mafic Schist	25	52.89	0.20	5.68	11.43	0.21	14.17	12.90	0.56	0.06	98.10	7.60	0.40	0.00	8.00	0.56	0.00	0.02	3.03	1.37	0.01	0.01	0.01	0.01	1.98	0.16	0.01	0.17
ST-89	Pillow Basalt	4	51.29	0.04	3.52	22.09	0.40	7.29	12.29	0.24	0.09	97.22	7.83	0.17	0.00	8.00	0.46	0.00	0.00	1.66	2.82	0.05	0.01	0.00	0.00	2.00	0.07	0.01	0.08
ST-115	Mafic Schist	17	45.58	1.35	9.01	15.61	0.30	11.36	12.44	1.61	0.33	97.59	6.78	1.22	0.00	8.00	0.36	0.05	0.15	2.52	1.89	0.02	0.00	0.00	0.02	1.98	0.47	0.06	0.53
ST-118	Mafic Schist	18	46.56	1.25	7.44	15.00	0.30	12.98	12.04	1.51	0.20	97.27	6.89	1.11	0.00	8.00	0.19	0.17	0.14	2.86	1.63	0.00	0.00	0.05	0.04	1.91	0.43	0.04	0.47
Standard Deviations																													
ST-20	Pillow Basalt	4	2.07		3.78	4.46	0.12	2.49	0.64	0.20	0.14	0.61	0.40	0.40	0.00	0.00	0.25	0.13	0.00	0.51	0.66	0.00	0.00	0.07	0.02	0.08	0.05	0.03	0.06
ST-66	Fault Gouge	5	1.38	0.15	1.91	3.53	0.18	2.07	1.16	0.19	0.02	0.35	0.23	0.23	0.00	0.00	0.09	0.06	0.02	0.40	0.42	0.00	0.00	0.16	0.02	0.17	0.05	0.00	0.06
ST-90	Fault Gouge	10	1.20		1.36	1.27	0.07	1.18	0.39	0.23	0.03	0.44	0.16	0.16	0.00	0.00	0.08	0.04	0.00	0.23	0.17	0.02	0.02	0.04	0.01	0.05	0.06	0.01	0.07
ST-112	Sheet Flow	2	1.50		0.59	0.43	0.01	0.68	0.58	0.05	0.00	2.70	0.00	0.00	0.00	0.00	0.09	0.10	0.00	0.07	0.04	0.02	0.07	0.05	0.02	0.08	0.01	0.00	0.01
ST-70	Fault Gouge	5	1.39		1.40	1.61	0.07	1.22	0.41	0.19	0.12	0.79	0.17	0.17	0.00	0.00	0.07	0.02	0.00	0.25	0.18	0.00	0.00	0.06	0.01	0.05	0.05	0.02	0.07
ST-71	Fault Gouge	3	1.98	0.02	1.19	0.69	0.04	0.61	0.14	0.09	0.05	1.80	0.18	0.22	0.09	0.00	0.04	0.18	0.00	0.13	0.17	0.02	0.02	0.01	0.02	0.02	0.03	0.01	0.04
ST-78	Sheet Flow	4	1.00		1.55	1.10	0.07	0.74	0.07	0.20	0.04	0.82	0.16	0.16	0.00	0.00	0.11	0.06	0.00	0.16	0.09	0.00	0.00	0.01	0.01	0.01	0.05	0.01	0.06
ST-83	Sheet Flow	8	2.93	0.09	3.03	1.56	0.02	1.86	0.18	0.33	0.09	0.31	0.36	0.36	0.00	0.00	0.17	0.08	0.01	0.38	0.13	0.00	0.00	0.02	0.00	0.02	0.10	0.02	0.11
ST-88	Volcaniclastic	8	1.87		1.64	1.18	0.04	0.78	0.09	0.19	0.07	0.53	0.25	0.25	0.00	0.00	0.05	0.16	0.00	0.16	0.03	0.00	0.00	0.01	0.00	0.01	0.05	0.01	0.07
ST-95	Sheet Flow	13	3.60	1.43	2.79	3.09	0.13	1.74	1.20	1.15	0.12	0.89	0.50	0.50	0.00	0.00	0.08	0.06	0.16	0.37	0.45	0.03	0.01	0.15	0.02	0.17	0.33	0.02	0.35
ST-77	Mafic Schist	28	2.24	0.10	2.10	1.36	0.09	1.09	0.73	0.38	0.05	0.88	0.30	0.30	0.00	0.00	0.30	0.16	0.01	0.23	0.17	0.02	0.00	0.09	0.02	0.11	0.11	0.01	0.11
ST-75	Mafic Schist	25	1.09	0.09	1.38	0.87	0.06	1.12	0.33	0.23	0.04	0.47	0.15	0.15	0.00	0.00	0.24	0.00	0.01	0.22	0.12	0.01	0.01	0.03	0.01	0.03	0.06	0.01	0.07
ST-89	Pillow Basalt	4	1.25	0.02	1.08	0.25	0.02	0.43	0.09	0.06	0.07	0.53	0.17	0.17	0.00	0.00	0.03	0.00	0.00	0.09	0.05	0.00	0.01	0.00	0.00	0.00	0.02	0.01	0.03
ST-115	Mafic Schist	17	1.59	0.25	1.06	1.07	0.04	0.85	0.14	0.21	0.06	0.42	0.19	0.19	0.00	0.00	0.05	0.07	0.03	0.17	0.12	0.01	0.00	0.00	0.01	0.02	0.06	0.01	0.08
ST-118	Mafic Schist	18	1.04	0.14	0.49	0.61	0.05	0.41	0.25	0.18	0.03	0.66	0.11	0.11	0.00	0.00	0.08	0.13	0.02	0.08	0.10	0.01	0.00	0.04	0.01	0.04	0.05	0.01	0.06

Appendix 4: Mean Amphibole Compositions

Sample	Lithology	Occurence	SiO2 (wt%)	TiO2 (wt%)	Al2O3 (wt%)	FeO (wt%)	MnO (wt%)	MgO (wt%)	CaO (wt%)	Na2O (wt%)	K2O (wt%)	Total (wt%)
Relative Standard Deviations												
ST-20	Pillow Basalt	4	4.1%		79.0%	24.7%	97.2%	20.9%	5.5%	50.7%	154.6%	0.6%
ST-66	Fault Gouge	5	2.6%	52.5%	59.6%	25.7%	40.4%	12.9%	10.7%	44.6%	97.8%	0.4%
ST-90	Fault Gouge	10	2.2%		38.7%	11.0%	34.8%	7.3%	3.1%	59.2%	39.1%	0.4%
ST-112	Sheet Flow	2	2.9%		19.0%	2.6%	4.7%	5.3%	4.6%	18.2%	6.0%	2.8%
ST-70	Fault Gouge	5	2.6%		55.2%	9.9%	17.1%	9.0%	3.4%	62.3%	68.8%	0.6%
ST-71	Fault Gouge	3	3.9%	173.2%	39.4%	4.2%	15.7%	4.5%	1.1%	30.2%	51.2%	1.9%
ST-78	Sheet Flow	4	2.0%		27.9%	6.6%	22.4%	5.9%	0.6%	31.7%	28.8%	0.8%
ST-83	Sheet Flow	8	6.0%	33.7%	44.0%	9.2%	9.0%	15.4%	1.5%	48.0%	63.7%	0.3%
ST-86	Volcaniclastic	8	3.7%		27.2%	7.1%	9.6%	6.1%	0.7%	22.1%	32.7%	0.5%
ST-95	Sheet Flow	13	7.0%	166.7%	77.0%	19.4%	30.2%	13.2%	10.2%	125.5%	118.1%	0.9%
ST-77	Mafic Schist	28	4.4%	92.9%	28.0%	9.7%	26.4%	8.7%	6.1%	46.9%	59.5%	0.9%
ST-75	Mafic Schist	25	2.1%	43.9%	24.3%	7.6%	29.5%	7.9%	2.5%	40.5%	64.7%	0.5%
ST-89	Pillow Basalt	4	2.4%	49.3%	30.6%	1.1%	4.3%	5.9%	0.7%	27.2%	73.8%	0.5%
ST-115	Mafic Schist	17	3.5%	18.7%	11.8%	6.9%	14.3%	7.5%	1.1%	13.0%	19.1%	0.4%
ST-118	Mafic Schist	18	2.2%	11.5%	6.6%	4.0%	16.4%	3.1%	2.1%	11.7%	15.2%	0.7%

Sample	Lithology	Occurence	T Si	T Al	TFe3	Sum T	C Al	CFe3	C Ti	C Mg	CFe2	C Mn	C Ca	BFe2	B Mn	B Ca	A Na	A K	Sum A
Relative Standard Deviations																			
ST-20	Pillow Basalt	4	5.4%	76.3%		0.0%	84.0%	114.4%		19.8%	33.4%			54.0%	39.1%	4.5%	49.7%	155.9%	50.5%
ST-66	Fault Gouge	5	3.0%	55.6%		0.0%	70.2%	72.0%	50.6%	11.5%	32.5%			58.2%	41.5%	10.3%	43.9%	94.8%	45.9%
ST-90	Fault Gouge	10	2.1%	44.0%		0.0%	35.6%	147.2%		6.8%	13.2%	184.6%	238.7%	72.6%	69.1%	2.6%	59.1%	41.7%	57.1%
ST-112	Sheet Flow	2	0.0%	0.2%		0.0%	49.9%	98.6%		2.4%	2.1%	141.4%	141.4%	141.4%	141.4%	3.9%	15.2%	8.3%	13.0%
ST-70	Fault Gouge	5	2.2%	64.9%		0.0%	43.5%	156.5%		8.7%	9.6%			76.9%	16.6%	2.8%	62.7%	66.7%	58.0%
ST-71	Fault Gouge	3	2.5%	43.9%	166.9%	0.0%	173.2%	41.5%	173.2%	4.5%	11.2%	108.5%	173.2%	173.2%	109.5%	1.3%	30.3%	49.8%	34.9%
ST-78	Sheet Flow	4	2.2%	25.6%		0.0%	34.3%	46.1%		6.0%	4.8%			19.1%	22.3%	0.7%	31.5%	28.9%	30.7%
ST-83	Sheet Flow	8	5.1%	43.5%		0.0%	49.1%	42.0%	34.3%	14.5%	7.5%			25.1%	8.8%	1.1%	48.8%	63.8%	49.8%
ST-86	Volcaniclastic	8	3.4%	33.8%		0.0%	18.5%	93.3%		5.8%	1.6%			14.4%	6.3%	0.5%	22.2%	33.9%	23.7%
ST-95	Sheet Flow	13	6.7%	105.1%		0.0%	53.7%	242.7%	175.8%	12.8%	24.5%	145.6%	276.6%	125.0%	72.7%	9.3%	126.0%	116.7%	125.0%
ST-77	Mafic Schist	28	4.1%	45.4%		0.0%	46.8%	182.3%	91.5%	8.4%	11.2%	168.7%	333.5%	107.0%	55.9%	5.8%	47.0%	58.4%	46.1%
ST-75	Mafic Schist	25	2.0%	37.1%		0.0%	43.6%		43.3%	7.4%	8.7%	79.4%	200.7%	347.8%	114.0%	1.7%	41.3%	63.5%	41.0%
ST-89	Pillow Basalt	4	2.2%	99.1%		0.0%	7.1%		52.2%	5.1%	1.8%	5.1%	72.2%			0.0%	28.0%	104.8%	40.7%
ST-115	Mafic Schist	17	2.7%	15.3%		0.0%	12.8%	139.2%	18.7%	6.7%	6.3%	71.8%	254.6%	302.3%	80.5%	0.8%	13.8%	19.8%	14.5%
ST-118	Mafic Schist	18	1.6%	9.9%		0.0%	40.2%	77.4%	11.7%	2.9%	6.2%	294.0%		69.7%	49.1%	2.1%	12.0%	15.7%	11.9%

Appendix 4: Plagioclase Compositions

Sample	Lithology	Occurence	SiO2 (wt%)	Al2O3 (wt%)	FeO (wt%)	MnO (wt%)	MgO (wt%)	CaO (wt%)	Na2O (wt%)	K2O (wt%)	Total (wt%)	An	Ab	Or
ST-66	Fault Gouge	Vein	64.97	21.79	0.28	0.01	0.00	1.92	10.77	0.07	99.93	9	91	0
ST-66	Fault Gouge	Vein	66.70	21.47	0.22	0.02	0.01	1.48	10.98	0.03	100.92	7	93	0
ST-66	Fault Gouge	Amygdule	67.51	20.98	0.36	0.03	0.00	1.10	11.10	0.09	101.15	5	94	0
ST-66	Fault Gouge	Amygdule	66.72	21.20	0.32	0.00	0.00	1.16	10.97	0.04	100.42	6	94	0
ST-66	Fault Gouge	Vein	66.11	21.90	0.18	0.00	0.01	2.08	10.35	0.05	100.69	10	90	0
ST-66	Fault Gouge	Vein	65.73	21.81	0.30	0.00	0.01	2.08	10.40	0.08	100.44	10	90	0
ST-90	Fault Gouge	Vein	67.86	20.93	0.16	0.00	0.00	1.09	11.13	0.08	101.38	5	94	0
ST-90	Fault Gouge	Vein	66.05	22.15	0.18	0.02	0.00	2.65	10.13	0.06	101.25	13	87	0
ST-90	Fault Gouge	Vein	66.63	20.83	0.28	0.02	0.02	1.43	10.83	0.09	100.14	7	93	1
ST-94	Massive Flow	Groundmass	66.46	20.58	0.04	0.00	0.00	0.90	11.07	0.06	99.13	4	95	0
ST-94	Massive Flow	Groundmass	67.49	20.04	0.09	0.00	0.04	0.60	11.42	0.07	99.80	3	97	0
ST-94	Massive Flow	Groundmass	66.88	20.46	0.40	0.01	0.00	0.89	11.13	0.07	100.05	4	95	0
ST-94	Massive Flow	Groundmass	67.27	20.51	0.20	0.00	0.00	0.92	11.10	0.08	100.11	4	95	0
ST-94	Massive Flow	Groundmass	67.83	20.45	0.07	0.00	0.00	0.95	11.07	0.09	100.47	5	95	1
ST-94	Massive Flow	Groundmass	64.98	20.54	0.08	0.00	0.00	0.90	11.34	0.05	99.15	4	96	0
ST-94	Massive Flow	Groundmass	67.16	20.29	0.18	0.00	0.02	0.69	11.36	0.09	99.95	3	96	1
ST-94	Massive Flow	Groundmass	62.44	23.58	0.20	0.01	0.00	4.81	8.92	0.48	99.98	20	77	3
ST-94	Massive Flow	Groundmass	62.82	22.41	0.15	0.00	0.01	3.46	9.29	0.73	98.87	16	80	4
ST-70	Fault Gouge	Vein	67.08	20.75	0.23	0.00	0.00	1.22	10.89	0.09	100.37	6	94	1
ST-70	Fault Gouge	Vein	67.79	21.06	0.19	0.02	0.01	1.35	10.82	0.10	101.35	6	93	1
ST-70	Fault Gouge	Vein	66.32	21.17	0.09	0.00	0.00	1.24	10.57	0.08	99.61	6	93	0
ST-71	Fault Gouge	Vein	59.83	25.71	0.00	0.00	0.00	6.81	7.88	0.08	100.58	32	67	0
ST-71	Fault Gouge	Vein	60.81	24.53	0.01	0.00	0.01	5.59	8.55	0.07	99.75	26	73	0
ST-71	Fault Gouge	Vein	60.19	25.71	0.02	0.02	0.00	6.63	7.90	0.06	100.57	32	68	0
ST-71	Fault Gouge	Vein	60.25	25.79	0.03	0.00	0.00	6.89	7.88	0.04	100.91	33	67	0
ST-71	Fault Gouge	Vein	61.99	24.22	0.02	0.00	0.00	5.19	8.73	0.06	100.29	25	75	0
ST-71	Fault Gouge	Vein	61.24	24.80	0.00	0.00	0.02	5.79	8.27	0.09	100.26	28	72	0
ST-71	Fault Gouge	Vein	62.52	23.84	0.04	0.00	0.00	4.69	8.93	0.06	100.12	22	77	0
ST-71	Fault Gouge	Vein	63.02	23.34	0.01	0.02	0.01	4.03	9.44	0.10	99.98	19	80	1
ST-83	Massive Flow	Phenocryst	64.90	22.18	0.11	0.00	0.01	2.38	10.27	0.06	100.00	11	88	0
ST-83	Massive Flow	Phenocryst	59.11	26.71	0.12	0.00	0.00	7.16	7.55	0.05	100.71	34	65	0
ST-83	Massive Flow	Vein	54.36	30.50	0.23	0.00	0.00	11.73	4.96	0.03	101.86	57	43	0
ST-83	Massive Flow	Vein	58.13	27.02	0.07	0.06	0.00	7.85	7.09	0.04	100.27	38	62	0
ST-83	Massive Flow	Vein	60.31	24.90	0.08	0.00	0.03	5.45	8.54	0.05	99.42	26	74	0
ST-88	Volcaniclastic	Groundmass	67.68	21.80	0.35	0.02	0.00	2.00	10.69	0.07	102.60	9	90	0
ST-88	Volcaniclastic	Groundmass	68.50	21.04	0.13	0.00	0.00	1.18	11.00	0.08	101.91	6	94	0
ST-88	Volcaniclastic	Groundmass	69.10	20.86	0.05	0.01	0.00	0.60	11.56	0.07	102.26	3	97	0
ST-88	Volcaniclastic	Groundmass	68.27	20.90	0.07	0.01	0.00	1.23	10.97	0.04	101.50	6	94	0
ST-88	Volcaniclastic	Groundmass	64.58	23.08	0.41	0.02	0.12	3.47	9.65	0.03	101.39	17	83	0
ST-88	Volcaniclastic	Groundmass	68.39	20.80	0.25	0.02	0.02	1.01	11.23	0.04	101.82	5	95	0
ST-88	Volcaniclastic	Groundmass	69.45	20.53	0.02	0.02	0.00	0.40	11.47	0.04	101.99	2	98	0
ST-88	Volcaniclastic	Groundmass	66.78	22.13	0.10	0.00	0.00	2.39	10.22	0.05	101.67	11	88	0
ST-88	Volcaniclastic	Groundmass	66.90	22.09	0.38	0.02	0.02	2.29	10.64	0.06	102.40	11	89	0
ST-96	Pillow Basalt	Groundmass	68.61	20.15	0.12	0.07	0.00	0.15	11.57	0.02	100.70	1	99	0
ST-96	Pillow Basalt	Groundmass	69.23	20.27	0.21	0.05	0.00	0.28	11.65	0.05	101.75	1	98	0
ST-96	Pillow Basalt	Groundmass	69.63	19.80	0.30	0.08	0.00	0.23	11.70	0.02	101.80	1	99	0

Appendix 4: Plagioclase Compositions

Sample	Lithology	Occurence	SiO2 (wt%)	Al2O3 (wt%)	FeO (wt%)	MnO (wt%)	MgO (wt%)	CaO (wt%)	Na2O (wt%)	K2O (wt%)	Total (wt%)	An	Ab	Or
ST-96	Pillow Basalt	Groundmass	69.62	19.80	0.27	0.02	0.00	0.19	12.01	0.02	101.93	1	99	0
ST-96	Pillow Basalt	Groundmass	68.68	20.04	0.29	0.01	0.01	0.15	11.74	0.01	100.93	1	99	0
ST-96	Pillow Basalt	Groundmass	68.34	19.80	0.39	0.07	0.00	0.19	11.62	0.03	100.43	1	99	0
ST-96	Pillow Basalt	Groundmass	68.62	20.47	0.28	0.05	0.00	0.24	11.77	0.03	101.47	1	99	0
ST-96	Pillow Basalt	Groundmass	67.84	19.80	0.32	0.09	0.01	0.35	11.02	0.03	99.47	2	98	0
ST-96	Pillow Basalt	Groundmass	69.79	19.73	0.21	0.05	0.00	0.27	11.64	0.04	101.75	1	99	0
ST-96	Pillow Basalt	Groundmass	69.05	19.97	0.27	0.06	0.00	0.54	11.55	0.03	101.49	3	97	0
ST-96	Pillow Basalt	Groundmass	69.08	20.34	0.25	0.11	0.00	0.77	11.36	0.03	101.96	4	96	0
ST-95	Massive Flow	Groundmass	50.44	30.31	0.67	0.00	0.15	13.83	3.88	0.03	99.36	66	34	0
ST-95	Massive Flow	Groundmass	63.30	22.73	0.11	0.00	0.00	3.99	9.76	0.02	99.91	18	81	0
ST-95	Massive Flow	Groundmass	50.85	29.26	0.79	0.00	0.23	12.92	4.15	0.12	98.38	63	37	1
ST-95	Massive Flow	Groundmass	61.51	23.58	0.61	0.00	0.25	4.69	9.06	0.02	99.72	22	78	0
ST-95	Massive Flow	Groundmass	57.66	26.10	0.65	0.00	0.05	8.84	6.68	0.14	100.15	42	57	1
ST-95	Massive Flow	Groundmass	56.02	26.95	0.65	0.00	0.07	10.02	5.93	0.12	99.81	48	51	1
ST-95	Massive Flow	Groundmass	65.55	22.22	0.32	0.00	0.00	2.98	10.31	0.06	101.43	14	86	0
ST-95	Massive Flow	Groundmass	56.64	26.50	0.66	0.00	0.06	9.28	6.23	0.13	99.54	45	54	1
ST-95	Massive Flow	Groundmass	52.85	29.37	0.87	0.00	0.12	13.17	4.20	0.04	100.67	63	37	0
ST-95	Massive Flow	Groundmass	63.36	23.13	0.58	0.00	0.01	4.72	8.88	0.33	101.05	22	76	2
ST-95	Massive Flow	Groundmass	58.07	26.10	0.84	0.00	0.07	9.20	6.58	0.11	101.02	43	56	1
ST-95	Massive Flow	Groundmass	65.03	23.12	0.49	0.00	0.03	3.52	8.80	0.05	101.05	18	82	0
ST-95	Massive Flow	Groundmass	52.70	29.07	0.87	0.00	0.13	12.92	4.32	0.06	100.11	62	38	0
ST-95	Massive Flow	Groundmass	57.34	26.48	0.74	0.00	0.05	9.17	6.45	0.11	100.38	44	56	1
ST-95	Massive Flow	Groundmass	52.78	29.12	0.91	0.00	0.16	12.94	4.31	0.05	100.31	62	38	0
ST-95	Massive Flow	Groundmass	54.79	28.19	0.80	0.00	0.08	11.53	5.27	0.09	100.83	54	45	1
ST-95	Massive Flow	Groundmass	52.68	29.08	0.81	0.00	0.13	13.39	4.06	0.05	100.23	64	35	0
ST-95	Massive Flow	Groundmass	64.17	22.91	0.16	0.00	0.00	4.59	9.30	0.01	101.15	21	79	0
ST-95	Massive Flow	Groundmass	52.99	28.13	1.15	0.00	0.22	12.86	4.17	0.04	99.60	63	37	0
ST-95	Massive Flow	Groundmass	63.94	23.23	0.21	0.00	0.00	4.61	9.18	0.01	101.18	22	78	0
ST-15	Massive Flow	Groundmass	54.93	27.88	1.12	0.00	0.15	12.05	4.92	0.03	101.16	57	42	0
ST-15	Massive Flow	Groundmass	57.31	25.90	1.16	0.00	0.20	10.11	5.95	0.08	100.77	48	51	0
ST-15	Massive Flow	Groundmass	56.18	26.75	1.06	0.00	0.10	10.74	5.60	0.06	100.57	51	48	0
ST-15	Massive Flow	Groundmass	58.46	25.38	1.05	0.00	0.07	9.21	6.42	0.11	100.77	44	55	1
ST-15	Massive Flow	Groundmass	54.30	27.44	1.25	0.01	0.29	12.25	4.81	0.04	100.49	58	41	0
ST-15	Massive Flow	Groundmass	53.25	28.45	1.16	0.00	0.18	12.52	4.57	0.03	100.18	60	40	0
ST-15	Massive Flow	Groundmass	53.79	28.25	1.11	0.00	0.17	12.46	4.68	0.04	100.51	59	40	0
ST-15	Massive Flow	Groundmass	54.93	27.30	1.04	0.05	0.14	11.28	5.31	0.03	100.13	54	46	0
ST-15	Massive Flow	Groundmass	53.20	28.02	1.10	0.00	0.20	12.16	4.80	0.03	99.57	58	42	0
ST-15	Massive Flow	Groundmass	53.39	28.58	1.18	0.00	0.14	12.33	4.92	0.03	100.60	58	42	0
ST-15	Massive Flow	Groundmass	55.54	26.93	1.30	0.02	0.10	10.54	5.71	0.06	100.24	50	49	0
ST-15	Massive Flow	Groundmass	53.66	28.01	1.17	0.03	0.23	12.28	4.87	0.03	100.34	58	42	0
ST-15	Massive Flow	Groundmass	55.86	26.39	1.21	0.00	0.10	10.06	6.11	0.09	99.86	47	52	1
ST-15	Massive Flow	Groundmass	59.84	24.34	1.89	0.00	0.27	6.18	6.93	0.14	99.61	33	66	1
ST-15	Massive Flow	Groundmass	54.87	27.02	1.15	0.00	0.13	11.00	5.67	0.05	99.99	52	48	0
ST-15	Massive Flow	Groundmass	53.88	28.52	1.24	0.00	0.13	11.93	5.08	0.04	100.89	56	43	0
ST-15	Massive Flow	Groundmass	54.08	27.22	1.52	0.03	0.24	10.79	5.49	0.06	99.50	52	48	0
ST-15	Massive Flow	Groundmass	54.44	27.38	1.24	0.00	0.15	10.76	5.61	0.05	99.72	51	48	0

Appendix 4: Plagioclase Compositions

Sample	Lithology	Occurence	SiO2 (wt%)	Al2O3 (wt%)	FeO (wt%)	MnO (wt%)	MgO (wt%)	CaO (wt%)	Na2O (wt%)	K2O (wt%)	Total (wt%)	An	Ab	Or
ST-15	Massive Flow	Groundmass	54.15	26.80	1.12	0.03	0.11	10.61	5.59	0.04	98.50	51	49	0
ST-15	Massive Flow	Groundmass	54.93	26.96	1.06	0.03	0.09	10.70	5.54	0.07	99.41	51	48	0
ST-101	Pillow Basalt	Groundmass	54.06	27.83	1.06	0.00	0.14	11.61	5.12	0.01	99.86	56	44	0
ST-101	Pillow Basalt	Groundmass	54.29	27.86	0.98	0.01	0.13	12.10	4.91	0.00	100.31	58	42	0
ST-101	Pillow Basalt	Groundmass	54.67	27.67	0.81	0.00	0.14	12.13	4.90	0.00	100.34	58	42	0
ST-101	Pillow Basalt	Groundmass	53.69	28.10	0.96	0.02	0.12	12.10	4.95	0.01	99.97	57	42	0
ST-101	Pillow Basalt	Groundmass	52.30	28.93	0.99	0.02	0.19	13.06	4.39	0.00	99.90	62	38	0
ST-101	Pillow Basalt	Groundmass	51.87	29.58	0.79	0.08	0.20	14.37	3.57	0.00	100.46	69	31	0
ST-101	Pillow Basalt	Groundmass	51.15	29.40	1.18	0.06	0.49	14.34	3.44	0.00	100.06	70	30	0
ST-101	Pillow Basalt	Groundmass	49.86	30.87	0.86	0.01	0.22	15.38	3.11	0.00	100.31	73	27	0
ST-101	Pillow Basalt	Groundmass	57.95	25.84	0.80	0.00	0.06	9.04	6.73	0.03	100.45	43	57	0
ST-101	Pillow Basalt	Groundmass	57.31	25.88	0.69	0.00	0.07	9.07	6.64	0.04	99.72	43	57	0
ST-101	Pillow Basalt	Groundmass	51.60	29.30	0.81	0.00	0.19	13.76	3.93	0.00	99.60	66	34	0
ST-101	Pillow Basalt	Groundmass	50.15	29.24	1.11	0.02	0.40	13.29	3.93	0.00	98.16	65	35	0
ST-101	Pillow Basalt	Groundmass	54.72	27.11	1.02	0.00	0.27	10.01	5.48	0.02	98.65	50	50	0
ST-101	Pillow Basalt	Groundmass	50.69	29.93	0.94	0.03	0.18	14.10	3.82	0.00	99.68	67	33	0
ST-101	Pillow Basalt	Groundmass	50.45	30.00	0.71	0.00	0.19	14.18	3.77	0.00	99.30	67	33	0
ST-101	Pillow Basalt	Groundmass	54.42	27.43	1.12	0.00	0.12	11.45	5.24	0.04	99.88	55	45	0
ST-101	Pillow Basalt	Groundmass	53.93	27.85	1.11	0.00	0.14	11.94	5.04	0.03	100.09	57	43	0
ST-101	Pillow Basalt	Groundmass	51.44	29.60	1.00	0.00	0.17	14.10	3.81	0.02	100.17	67	33	0
ST-101	Pillow Basalt	Groundmass	50.94	24.12	1.16	0.00	0.09	7.11	7.51	0.14	101.13	34	65	1
ST-77	Mafic Schist	Groundmass	51.06	29.38	1.25	0.07	0.65	14.45	3.62	0.00	100.48	69	31	0
ST-77	Mafic Schist	Groundmass	51.79	29.92	0.69	0.06	0.21	14.19	3.61	0.00	100.47	69	31	0
ST-77	Mafic Schist	Groundmass	51.25	29.91	0.92	0.01	0.34	15.17	3.26	0.00	100.87	72	28	0
ST-77	Mafic Schist	Groundmass	61.73	24.03	0.43	0.04	0.10	6.56	8.08	0.00	100.98	31	69	0
ST-77	Mafic Schist	Groundmass	60.29	24.04	0.59	0.00	0.36	7.65	7.32	0.00	100.24	37	63	0
ST-77	Mafic Schist	Groundmass	53.40	27.01	1.64	0.00	0.76	12.11	4.35	0.00	99.26	61	39	0
ST-77	Mafic Schist	Groundmass	51.45	29.70	0.69	0.06	0.25	15.12	3.21	0.00	100.49	72	28	0
ST-77	Mafic Schist	Groundmass	59.11	25.15	0.77	0.03	0.29	8.44	6.48	0.00	100.26	42	58	0
ST-77	Mafic Schist	Groundmass	54.13	27.68	1.12	0.05	0.33	12.83	4.39	0.00	100.53	62	38	0
ST-77	Mafic Schist	Groundmass	53.85	28.19	0.56	0.05	0.15	12.93	4.48	0.00	100.21	61	39	0
ST-77	Mafic Schist	Groundmass	65.96	22.26	0.40	0.01	0.29	3.46	9.21	0.01	101.60	17	83	0
ST-77	Mafic Schist	Groundmass	59.13	26.26	0.58	0.00	0.15	9.21	6.49	0.01	101.84	44	56	0
ST-77	Mafic Schist	Groundmass	56.07	27.21	0.51	0.04	0.23	11.01	5.47	0.00	100.52	53	47	0
ST-77	Mafic Schist	Groundmass	54.62	25.74	1.41	0.05	1.05	11.51	4.87	0.01	99.43	57	43	0
ST-77	Mafic Schist	Groundmass	67.73	20.99	0.55	0.06	0.37	2.40	10.42	0.00	102.53	11	89	0
ST-77	Mafic Schist	Groundmass	51.55	27.53	1.28	0.02	0.69	14.10	3.47	0.00	98.65	69	31	0
ST-77	Mafic Schist	Groundmass	60.70	25.12	0.40	0.07	0.28	7.47	6.91	0.02	100.96	37	63	0
ST-77	Mafic Schist	Groundmass	59.60	23.11	1.22	0.06	1.30	5.68	7.79	0.00	98.75	29	71	0
ST-77	Mafic Schist	Groundmass	53.80	26.90	1.29	0.04	0.96	12.09	4.37	0.00	99.45	60	40	0
ST-75	Mafic Schist	Groundmass	49.78	30.67	0.70	0.00	0.03	16.46	2.36	0.00	100.03	79	21	0
ST-75	Mafic Schist	Groundmass	60.80	24.66	0.24	0.00	0.00	7.58	7.51	0.00	100.79	36	64	0
ST-75	Mafic Schist	Groundmass	48.57	31.72	0.76	0.00	0.08	17.31	1.84	0.00	100.28	84	16	0
ST-75	Mafic Schist	Groundmass	59.53	23.82	0.27	0.00	0.00	9.23	7.30	0.00	100.15	41	59	0
ST-75	Mafic Schist	Groundmass	50.21	29.81	1.13	0.02	0.94	15.02	2.76	0.00	99.89	75	25	0
ST-75	Mafic Schist	Groundmass	61.80	24.40	0.30	0.05	0.02	6.92	7.79	0.00	101.28	33	67	0

Appendix 4: Plagioclase Compositions

Sample	Lithology	Occurence	SiO2 (wt%)	Al2O3 (wt%)	FeO (wt%)	MnO (wt%)	MgO (wt%)	CaO (wt%)	Na2O (wt%)	K2O (wt%)	Total (wt%)	An	Ab	Or
ST-75	Mafic Schist	Groundmass	49.90	31.47	0.42	0.00	0.01	16.45	2.29	0.00	100.55	80	20	0
ST-75	Mafic Schist	Groundmass	60.32	24.87	0.24	0.00	0.07	7.97	7.20	0.00	100.68	38	62	0
ST-75	Mafic Schist	Groundmass	50.13	31.07	0.75	0.03	0.09	16.76	2.31	0.00	101.16	80	20	0
ST-75	Mafic Schist	Groundmass	49.22	30.85	0.73	0.00	0.11	16.61	2.26	0.00	99.79	80	20	0
ST-75	Mafic Schist	Groundmass	48.33	31.47	0.38	0.00	0.05	17.58	1.71	0.00	99.52	85	15	0
ST-75	Mafic Schist	Groundmass	51.86	28.26	1.07	0.00	1.29	12.57	3.67	0.00	98.73	65	35	0
ST-75	Mafic Schist	Groundmass	48.78	32.06	0.27	0.00	0.02	17.37	1.84	0.00	100.34	84	16	0
ST-75	Mafic Schist	Groundmass	47.84	31.77	0.17	0.00	0.08	18.11	1.64	0.00	99.62	86	14	0
ST-75	Mafic Schist	Groundmass	48.20	31.62	0.74	0.00	0.57	17.40	1.57	0.00	100.10	86	14	0
ST-75	Mafic Schist	Groundmass	51.59	29.97	0.53	0.00	0.03	15.10	3.16	0.00	100.43	73	27	0
ST-42	Massive Flow	Groundmass	55.11	25.74	1.03	0.00	0.08	11.88	4.88	0.04	98.61	58	42	0
ST-42	Massive Flow	Groundmass	55.92	25.57	1.10	0.00	0.17	11.30	4.91	0.05	99.07	56	44	0
ST-42	Massive Flow	Groundmass	54.92	26.92	1.01	0.00	0.14	12.54	4.28	0.02	99.85	62	38	0
ST-42	Massive Flow	Groundmass	56.13	25.78	0.95	0.00	0.09	11.40	4.92	0.06	99.37	56	44	0
ST-42	Massive Flow	Groundmass	52.48	28.18	0.93	0.00	0.07	14.23	3.50	0.00	99.41	69	31	0
ST-42	Massive Flow	Groundmass	53.53	27.00	1.44	0.00	0.11	12.97	3.91	0.05	99.04	65	35	0
ST-42	Massive Flow	Groundmass	54.02	26.73	1.12	0.02	0.06	12.79	4.12	0.01	98.89	63	37	0
ST-42	Massive Flow	Groundmass	57.91	24.64	0.95	0.00	0.07	9.58	5.76	0.14	99.12	47	52	1
ST-42	Massive Flow	Groundmass	55.26	27.10	1.09	0.03	0.07	12.08	4.57	0.05	100.30	59	41	0
ST-54	Massive Flow	Groundmass	70.00	20.00	0.23	0.00	0.01	0.43	10.80	0.00	101.47	2	98	0
ST-54	Massive Flow	Groundmass	69.36	19.57	0.32	0.00	0.02	0.67	10.78	0.00	100.71	3	97	0
ST-54	Massive Flow	Groundmass	70.20	19.56	0.23	0.00	0.00	0.40	10.99	0.00	101.38	2	98	0
ST-54	Massive Flow	Groundmass	54.08	27.44	1.06	0.02	0.08	12.74	4.27	0.00	99.73	62	38	0
ST-54	Massive Flow	Groundmass	59.62	24.95	0.76	0.00	0.08	9.03	6.18	0.00	100.65	45	55	0
ST-54	Massive Flow	Groundmass	54.84	26.25	1.04	0.02	0.13	11.52	4.78	0.00	98.64	57	43	0
ST-54	Massive Flow	Groundmass	69.89	19.42	0.37	0.00	0.00	1.15	10.41	0.00	101.24	6	94	0
ST-54	Massive Flow	Groundmass	70.70	18.94	0.27	0.03	0.00	0.48	10.88	0.00	101.31	2	98	0
ST-54	Massive Flow	Groundmass	67.78	19.73	0.32	0.01	0.00	1.93	10.39	0.00	100.15	9	91	0
ST-54	Massive Flow	Groundmass	53.68	27.26	0.90	0.00	0.08	13.18	3.98	0.00	99.13	65	35	0
ST-54	Massive Flow	Groundmass	56.13	25.73	1.04	0.04	0.09	10.77	5.22	0.00	99.06	53	47	0
ST-54	Massive Flow	Groundmass	57.34	25.12	1.87	0.05	0.77	8.66	6.13	0.00	99.95	44	56	0
ST-54	Massive Flow	Groundmass	57.30	24.84	1.82	0.00	0.23	9.05	5.16	0.11	98.56	49	50	1
ST-54	Massive Flow	Groundmass	55.90	25.57	1.25	0.00	0.14	11.24	5.11	0.00	99.25	55	45	0
ST-54	Massive Flow	Groundmass	54.09	24.93	1.88	0.03	0.76	11.08	4.23	0.00	97.04	59	41	0
ST-54	Massive Flow	Groundmass	54.55	26.36	1.05	0.00	0.13	12.23	4.35	0.00	98.72	61	39	0
ST-89	Pillow Basalt	Groundmass	59.23	23.85	0.56	0.04	0.05	8.70	6.32	0.00	98.74	43	57	0
ST-89	Pillow Basalt	Groundmass	57.88	24.56	0.81	0.05	0.10	9.91	5.74	0.00	99.06	49	51	0
ST-89	Pillow Basalt	Groundmass	52.66	27.85	0.69	0.08	0.23	13.82	3.62	0.00	98.96	68	32	0
ST-89	Pillow Basalt	Groundmass	53.15	27.47	0.79	0.09	0.20	13.53	3.75	0.00	98.97	67	33	0
ST-89	Pillow Basalt	Groundmass	52.22	28.31	0.71	0.03	0.21	14.42	3.38	0.00	99.28	70	30	0
ST-89	Pillow Basalt	Groundmass	52.63	27.65	0.70	0.01	0.21	13.83	3.62	0.00	98.64	68	32	0
ST-89	Pillow Basalt	Groundmass	54.06	27.27	0.88	0.07	0.19	12.99	4.26	0.00	99.72	63	37	0
ST-89	Pillow Basalt	Groundmass	54.34	26.80	1.01	0.10	0.15	12.17	4.49	0.00	99.06	60	40	0
ST-89	Pillow Basalt	Groundmass	52.46	28.11	0.82	0.10	0.21	14.04	3.47	0.00	99.20	69	31	0
ST-89	Pillow Basalt	Groundmass	55.50	25.98	0.86	0.05	0.14	11.76	4.74	0.00	99.04	58	42	0
ST-89	Pillow Basalt	Groundmass	54.86	26.19	0.80	0.06	0.15	12.02	4.39	0.00	98.48	60	40	0

Appendix 4: Plagioclase Compositions

Sample	Lithology	Occurence	SiO2 (wt%)	Al2O3 (wt%)	FeO (wt%)	MnO (wt%)	MgO (wt%)	CaO (wt%)	Na2O (wt%)	K2O (wt%)	Total (wt%)	An	Ab	Or
ST-89	Pillow Basalt	Groundmass	56.00	25.25	0.97	0.04	0.13	11.02	5.25	0.00	98.65	54	46	0
ST-89	Pillow Basalt	Groundmass	54.70	25.93	1.06	0.06	0.14	12.10	4.46	0.00	98.47	60	40	0
ST-89	Pillow Basalt	Groundmass	53.80	26.43	0.71	0.07	0.15	12.98	4.01	0.00	98.14	64	36	0
ST-89	Pillow Basalt	Groundmass	52.26	27.63	0.64	0.04	0.20	14.14	3.43	0.00	98.35	69	31	0
ST-113	Undiff Basalt	Groundmass	52.89	28.28	0.98	0.00	0.53	13.77	3.79	0.00	100.26	67	33	0
ST-113	Undiff Basalt	Groundmass	52.39	29.54	0.76	0.00	0.35	14.61	3.41	0.00	101.07	70	30	0
ST-113	Undiff Basalt	Groundmass	52.44	29.18	0.71	0.00	0.30	13.46	3.74	0.00	99.84	67	33	0
ST-113	Undiff Basalt	Groundmass	53.36	28.16	1.24	0.00	0.48	13.33	3.87	0.00	100.46	66	34	0
ST-113	Undiff Basalt	Groundmass	50.74	30.73	0.53	0.00	0.27	15.52	2.95	0.00	100.74	74	26	0
ST-113	Undiff Basalt	Groundmass	50.47	30.47	0.56	0.00	0.27	15.26	2.99	0.00	100.04	74	26	0
ST-113	Undiff Basalt	Groundmass	50.34	30.51	0.63	0.00	0.27	15.38	3.06	0.00	100.20	74	26	0
ST-113	Undiff Basalt	Groundmass	50.18	30.98	0.62	0.00	0.27	15.48	2.93	0.00	100.44	75	25	0
ST-113	Undiff Basalt	Groundmass	51.22	29.22	0.94	0.00	0.44	14.50	3.45	0.00	99.78	70	30	0
ST-113	Undiff Basalt	Groundmass	51.30	29.01	1.13	0.00	0.43	14.63	3.46	0.00	99.98	70	30	0
ST-113	Undiff Basalt	Groundmass	51.80	28.87	1.18	0.00	0.45	14.23	3.65	0.00	100.21	68	32	0
ST-113	Undiff Basalt	Groundmass	52.83	28.98	0.88	0.00	0.41	13.56	3.98	0.00	100.64	65	35	0
ST-113	Undiff Basalt	Groundmass	50.99	29.21	1.40	0.00	0.73	13.76	3.48	0.00	99.61	69	31	0
ST-113	Undiff Basalt	Groundmass	49.59	31.36	0.70	0.00	0.25	15.78	2.85	0.00	100.54	75	25	0
ST-113	Undiff Basalt	Groundmass	49.85	30.86	0.70	0.00	0.29	15.33	3.00	0.00	100.05	74	26	0
ST-113	Undiff Basalt	Groundmass	49.64	31.23	0.54	0.00	0.26	15.78	2.86	0.00	100.32	75	25	0
ST-115	Mafic Schist	Groundmass	50.52	31.06	0.13	0.06	0.01	15.08	3.27	0.01	100.18	72	28	0
ST-115	Mafic Schist	Groundmass	50.00	31.44	0.11	0.06	0.01	15.50	3.02	0.01	100.16	74	26	0
ST-115	Mafic Schist	Groundmass	50.95	30.96	0.21	0.10	0.00	14.70	3.54	0.01	100.53	70	30	0
ST-115	Mafic Schist	Groundmass	51.90	30.05	0.10	0.06	0.01	13.60	4.02	0.02	99.80	65	35	0
ST-115	Mafic Schist	Groundmass	50.71	31.30	0.26	0.03	0.01	15.11	3.29	0.02	100.74	72	28	0
ST-115	Mafic Schist	Groundmass	49.90	31.91	0.29	0.12	0.00	15.73	3.01	0.02	101.03	74	26	0
ST-115	Mafic Schist	Groundmass	49.75	31.80	0.23	0.07	0.00	15.85	2.80	0.00	100.52	76	24	0
ST-115	Mafic Schist	Groundmass	50.61	31.28	0.14	0.09	0.00	15.25	3.24	0.01	100.64	72	28	0
ST-115	Mafic Schist	Groundmass	50.12	31.57	0.19	0.09	0.01	15.94	2.71	0.00	100.68	76	24	0
ST-115	Mafic Schist	Groundmass	49.44	31.74	0.30	0.10	0.01	16.10	2.52	0.02	100.23	78	22	0
ST-115	Mafic Schist	Groundmass	49.72	31.65	0.23	0.06	0.01	16.23	2.58	0.00	100.48	78	22	0
ST-115	Mafic Schist	Groundmass	49.71	31.75	0.13	0.10	0.01	16.39	2.50	0.01	100.62	78	22	0
ST-115	Mafic Schist	Groundmass	49.88	31.51	0.11	0.10	0.01	15.71	2.97	0.00	100.30	74	25	0
ST-115	Mafic Schist	Groundmass	51.43	30.97	0.14	0.08	0.00	14.42	3.74	0.03	100.83	68	32	0
ST-115	Mafic Schist	Groundmass	49.05	32.12	0.30	0.12	0.02	16.22	2.68	0.00	100.56	77	23	0
ST-115	Mafic Schist	Groundmass	49.04	32.19	0.17	0.07	0.00	16.29	2.62	0.01	100.41	77	23	0
ST-115	Mafic Schist	Groundmass	49.98	31.44	0.22	0.08	0.01	15.79	2.79	0.02	100.37	76	24	0
ST-115	Mafic Schist	Groundmass	50.05	31.55	0.25	0.12	0.00	16.17	2.73	0.02	100.88	77	23	0
ST-115	Mafic Schist	Groundmass	50.35	30.96	0.13	0.08	0.01	15.42	3.12	0.01	100.11	73	27	0
ST-115	Mafic Schist	Groundmass	49.73	31.05	0.14	0.10	0.01	15.64	2.93	0.00	99.63	75	25	0
ST-118	Mafic Schist	Groundmass	56.01	27.53	0.16	0.00	0.01	9.64	6.52	0.00	99.87	45	55	0
ST-118	Mafic Schist	Groundmass	56.12	27.69	0.03	0.05	0.00	9.51	6.51	0.01	99.91	45	55	0
ST-118	Mafic Schist	Groundmass	55.60	27.85	0.15	0.00	0.00	10.18	6.20	0.00	99.97	48	52	0
ST-118	Mafic Schist	Groundmass	55.59	27.80	0.05	0.01	0.01	9.83	6.30	0.00	99.58	46	54	0
ST-118	Mafic Schist	Groundmass	51.26	29.98	0.18	0.04	0.00	12.38	4.93	0.00	98.80	58	42	0
ST-118	Mafic Schist	Groundmass	54.88	27.89	0.00	0.00	0.00	9.67	6.43	0.00	98.88	45	55	0

Appendix 4: Plagioclase Compositions

Sample	Lithology	Occurence	SiO2 (wt%)	Al2O3 (wt%)	FeO (wt%)	MnO (wt%)	MgO (wt%)	CaO (wt%)	Na2O (wt%)	K2O (wt%)	Total (wt%)	An	Ab	Or
ST-118	Mafic Schist	Groundmass	55.00	27.46	0.26	0.02	0.01	9.59	6.55	0.01	98.91	45	55	0
ST-118	Mafic Schist	Groundmass	55.04	27.63	0.23	0.04	0.00	9.47	6.66	0.01	99.08	44	56	0
ST-118	Mafic Schist	Groundmass	55.89	26.80	0.08	0.05	0.00	7.95	7.37	0.00	98.14	37	63	0
ST-118	Mafic Schist	Groundmass	53.93	28.28	0.00	0.00	0.00	9.84	6.40	0.00	98.44	46	54	0
ST-118	Mafic Schist	Groundmass	50.52	30.45	0.04	0.02	0.00	13.04	4.63	0.00	98.71	61	39	0
ST-118	Mafic Schist	Groundmass	50.57	29.77	1.70	0.00	0.03	12.11	4.94	0.01	99.20	57	42	0
ST-118	Mafic Schist	Groundmass	56.10	27.64	0.17	0.04	0.00	10.00	6.16	0.00	100.12	47	53	0
ST-118	Mafic Schist	Groundmass	56.24	27.84	0.25	0.02	0.00	10.37	6.08	0.00	100.80	48	51	0
ST-118	Mafic Schist	Groundmass	56.69	27.73	0.12	0.08	0.00	10.26	6.20	0.00	101.09	48	52	0
ST-118	Mafic Schist	Groundmass	56.35	28.04	0.19	0.04	0.00	10.58	5.95	0.00	101.16	50	50	0
ST-118	Mafic Schist	Groundmass	50.98	31.22	0.14	0.05	0.00	14.25	3.76	0.00	100.40	68	32	0
ST-118	Mafic Schist	Groundmass	55.52	28.31	0.05	0.08	0.00	10.39	5.91	0.00	100.26	49	51	0
ST-118	Mafic Schist	Groundmass	55.99	27.96	0.12	0.00	0.00	10.17	6.17	0.00	100.41	48	52	0
ST-118	Mafic Schist	Groundmass	54.06	29.15	0.11	0.00	0.00	11.73	5.28	0.00	100.34	55	45	0

Appendix 4: Mean Plagioclase Compositions

Sample	Lithology	n	SiO2 (wt%)	Al2O3 (wt%)	FeO (wt%)	MnO (wt%)	MgO (wt%)	CaO (wt%)	Na2O (wt%)	K2O (wt%)	Total (wt%)	An	Ab	Or
Means														
ST-66	Fault Gouge	6	66.29	21.52	0.28	0.01	0.00	1.64	10.76	0.06	100.59	7.74	91.93	0.33
ST-90	Fault Gouge	3	66.84	21.31	0.21	0.01	0.01	1.72	10.70	0.08	100.92	8.15	91.43	0.42
ST-94	Massive Flow	9	65.93	20.98	0.16	0.00	0.01	1.51	10.74	0.19	99.61	7.16	91.75	1.08
ST-70	Fault Gouge	3	67.07	20.99	0.17	0.01	0.00	1.27	10.76	0.09	100.44	6.09	93.41	0.50
ST-71	Fault Gouge	8	61.23	24.74	0.02	0.00	0.00	5.70	8.45	0.07	100.31	27.06	72.54	0.40
ST-83	Massive Flow	5	59.36	26.26	0.12	0.01	0.01	6.91	7.68	0.05	100.45	33.19	66.55	0.26
ST-88	Volcaniclastic	9	67.74	21.47	0.20	0.01	0.02	1.62	10.82	0.05	101.95	7.63	92.07	0.30
ST-96	Pillow Basalt	11	68.95	20.02	0.26	0.06	0.00	0.31	11.60	0.03	101.24	1.43	98.42	0.15
ST-95	Massive Flow	20	57.63	26.28	0.64	0.00	0.09	8.96	6.58	0.08	100.29	42.89	56.65	0.45
ST-15	Massive Flow	20	55.05	27.17	1.21	0.01	0.16	11.00	5.43	0.06	100.14	52.55	47.13	0.32
ST-101	Pillow Basalt	19	53.45	28.24	0.95	0.01	0.18	12.27	4.75	0.02	99.90	58.75	41.15	0.10
ST-77	Mafic Schist	19	56.70	26.32	0.86	0.04	0.46	10.34	5.67	0.00	100.40	50.12	49.86	0.01
ST-75	Mafic Schist	16	52.30	29.28	0.54	0.01	0.21	14.26	3.58	0.00	100.21	69.07	30.93	0.00
ST-42	Massive Flow	9	55.03	26.41	1.07	0.01	0.09	12.09	4.52	0.05	99.30	59.48	40.25	0.27
ST-54	Massive Flow	16	60.97	23.48	0.90	0.01	0.16	7.16	7.10	0.01	99.81	35.90	64.06	0.04
ST-89	Pillow Basalt	15	54.38	26.62	0.80	0.06	0.16	12.50	4.33	0.00	98.85	61.46	38.54	0.00
ST-113	Undiff Basalt	16	51.25	29.79	0.84	0.00	0.37	14.65	3.34	0.00	100.26	70.75	29.25	0.00
ST-115	Mafic Schist	20	50.14	31.41	0.19	0.08	0.01	15.56	3.00	0.01	100.44	74.07	25.87	0.06
ST-118	Mafic Schist	20	54.62	28.35	0.20	0.03	0.00	10.55	5.95	0.00	99.70	49.50	50.49	0.01
Standard Deviations														
ST-66	Fault Gouge	6	0.89	0.37	0.06	0.01	0.00	0.45	0.32	0.02	0.43	2.16	2.17	0.14
ST-90	Fault Gouge	3	0.92	0.74	0.07	0.01	0.01	0.82	0.51	0.01	0.68	3.94	3.87	0.08
ST-94	Massive Flow	9	2.04	1.19	0.11	0.00	0.01	1.36	0.95	0.24	0.74	6.49	7.76	1.37
ST-70	Fault Gouge	3	0.74	0.22	0.07	0.01	0.00	0.07	0.17	0.01	0.87	0.32	0.34	0.04
ST-71	Fault Gouge	8	1.17	0.93	0.01	0.01	0.01	1.04	0.57	0.02	0.37	4.92	4.88	0.10
ST-83	Massive Flow	5	3.81	3.05	0.07	0.02	0.01	3.42	1.95	0.01	0.91	16.56	16.50	0.07
ST-88	Volcaniclastic	9	1.49	0.85	0.15	0.01	0.04	0.99	0.61	0.02	0.41	4.72	4.69	0.09
ST-96	Pillow Basalt	11	0.60	0.26	0.07	0.03	0.00	0.19	0.25	0.01	0.78	0.89	0.92	0.06
ST-95	Massive Flow	20	5.16	2.74	0.27	0.00	0.08	3.94	2.27	0.07	0.77	19.13	19.11	0.40
ST-15	Massive Flow	20	1.76	1.09	0.19	0.02	0.06	1.48	0.62	0.03	0.63	6.47	6.30	0.18
ST-101	Pillow Basalt	19	2.92	1.69	0.15	0.02	0.11	2.19	1.21	0.03	0.66	10.50	10.36	0.18
ST-77	Mafic Schist	19	5.06	2.62	0.39	0.03	0.34	3.94	2.15	0.00	1.00	18.88	18.88	0.03
ST-75	Mafic Schist	16	5.10	3.04	0.30	0.01	0.38	4.03	2.38	0.00	0.64	19.93	19.93	0.00
ST-42	Massive Flow	9	1.59	1.06	0.16	0.01	0.04	1.30	0.66	0.04	0.51	6.21	6.00	0.25
ST-54	Massive Flow	16	7.13	3.25	0.59	0.02	0.25	5.21	2.95	0.03	1.27	26.07	26.10	0.17
ST-89	Pillow Basalt	15	2.09	1.33	0.14	0.03	0.05	1.65	0.88	0.00	0.41	7.97	7.97	0.00
ST-113	Undiff Basalt	16	1.23	1.07	0.27	0.00	0.13	0.87	0.39	0.00	0.38	3.63	3.63	0.00
ST-115	Mafic Schist	20	0.72	0.49	0.07	0.02	0.01	0.71	0.41	0.01	0.35	3.52	3.50	0.04
ST-118	Mafic Schist	20	2.07	1.15	0.36	0.03	0.01	1.46	0.84	0.00	0.89	7.00	6.99	0.02

Appendix 4: Mean Plagioclase Compositions

Sample	Lithology	n	SiO2 (wt%)	Al2O3 (wt%)	FeO (wt%)	MnO (wt%)	MgO (wt%)	CaO (wt%)	Na2O (wt%)	K2O (wt%)	Total (wt%)	An	Ab	Or
Relative Standard Deviations														
ST-66	Fault Gouge	6	1%	2%	23%	122%	126%	27%	3%	41%	0%	28%	2%	41%
ST-90	Fault Gouge	3	1%	3%	32%	87%	173%	48%	5%	19%	1%	48%	4%	19%
ST-94	Massive Flow	9	3%	6%	69%	170%	174%	90%	9%	126%	1%	91%	8%	126%
ST-70	Fault Gouge	3	1%	1%	42%	149%	173%	6%	2%	10%	1%	5%	0%	8%
ST-71	Fault Gouge	8	2%	4%	88%	185%	130%	18%	7%	25%	0%	18%	7%	25%
ST-83	Massive Flow	5	6%	12%	54%	201%	163%	49%	25%	25%	1%	50%	25%	25%
ST-88	Volcaniclastic	9	2%	4%	79%	72%	216%	61%	6%	30%	0%	62%	5%	29%
ST-96	Pillow Basalt	11	1%	1%	27%	46%	228%	62%	2%	44%	1%	62%	1%	44%
ST-95	Massive Flow	20	9%	10%	42%	447%	88%	44%	35%	90%	1%	45%	34%	89%
ST-15	Massive Flow	20	3%	4%	16%	152%	39%	13%	11%	54%	1%	12%	13%	57%
ST-101	Pillow Basalt	19	6%	6%	16%	175%	57%	18%	25%	184%	1%	18%	25%	184%
ST-77	Mafic Schist	19	9%	10%	46%	67%	74%	38%	38%	194%	1%	38%	38%	194%
ST-75	Mafic Schist	16	10%	10%	56%	215%	181%	28%	67%		1%	29%	64%	
ST-42	Massive Flow	9	3%	4%	15%	203%	41%	11%	15%	91%	1%	10%	15%	91%
ST-54	Massive Flow	16	12%	14%	65%	136%	156%	73%	42%	400%	1%	73%	41%	400%
ST-89	Pillow Basalt	15	4%	5%	17%	45%	31%	13%	20%		0%	13%	21%	
ST-113	Undiff Basalt	16	2%	4%	32%		35%	6%	12%		0%	5%	12%	
ST-115	Mafic Schist	20	1%	2%	36%	28%	79%	5%	14%	63%	0%	5%	14%	63%
ST-118	Mafic Schist	20	4%	4%	178%	97%	242%	14%	14%	159%	1%	14%	14%	159%

Appendix 4: Epidote Compositions

Sample	Lithology	Occurence	SiO2 (wt%)	Al2O3 (wt%)	FeO (wt%)	MnO (wt%)	MgO (wt%)	CaO (wt%)	Na2O (wt%)	K2O (wt%)	Total (wt%)	Si	AlIV	AlVI	Fe+3	Fe+2	Mn	Mg	Ca	Na	K	Ps
ST-77	Mafic Schist	Groundmass	40.40	22.36	9.77	0.13	1.28	23.30	0.05	0.00	97.32	3.25	0.00	2.12	0.66	0.00	0.01	0.15	2.01	0.01	0.00	24
ST-77	Mafic Schist	Groundmass	39.00	24.81	9.01	0.18	0.59	23.39	0.00	0.00	97.01	3.14	0.00	2.35	0.61	0.00	0.01	0.07	2.01	0.00	0.00	20
ST-77	Mafic Schist	Groundmass	38.51	23.56	10.20	0.14	0.03	24.57	0.00	0.00	97.07	3.13	0.00	2.26	0.69	0.00	0.01	0.00	2.14	0.00	0.00	23
ST-77	Mafic Schist	Groundmass	39.30	22.35	9.98	0.15	0.53	23.97	0.01	0.00	96.31	3.21	0.00	2.15	0.68	0.00	0.01	0.06	2.10	0.00	0.00	24
ST-77	Mafic Schist	Groundmass	38.78	23.01	10.64	0.12	0.05	24.01	0.00	0.00	96.66	3.17	0.00	2.21	0.73	0.00	0.01	0.01	2.10	0.00	0.00	25
ST-75	Mafic Schist	Groundmass	39.42	22.51	10.34	0.16	0.08	23.70	0.00	0.00	96.29	3.22	0.00	2.17	0.71	0.00	0.01	0.01	2.08	0.00	0.00	25
ST-75	Mafic Schist	Groundmass	39.56	24.39	8.45	0.04	0.02	24.31	0.01	0.00	96.84	3.18	0.00	2.31	0.57	0.00	0.00	0.00	2.09	0.00	0.00	20
ST-75	Mafic Schist	Groundmass	39.60	24.30	8.13	0.19	0.03	24.25	0.00	0.00	96.52	3.19	0.00	2.31	0.55	0.00	0.01	0.00	2.09	0.00	0.00	19
ST-75	Mafic Schist	Groundmass	39.88	22.62	9.45	0.19	0.36	23.60	0.01	0.00	96.25	3.24	0.00	2.17	0.64	0.00	0.01	0.04	2.06	0.00	0.00	23
ST-75	Mafic Schist	Groundmass	39.59	22.21	10.02	0.11	0.59	23.41	0.02	0.00	96.04	3.24	0.00	2.14	0.69	0.00	0.01	0.07	2.05	0.00	0.00	24
ST-77	Mafic Schist	Groundmass	38.03	25.30	8.90	0.15	0.14	24.03	0.00	0.00	96.56	3.08	0.00	2.42	0.58	0.02	0.01	0.02	2.09	0.00	0.00	19
ST-77	Mafic Schist	Groundmass	41.13	19.99	10.54	0.20	4.14	20.27	0.09	0.00	96.37	3.33	0.00	1.91	0.71	0.00	0.01	0.50	1.76	0.01	0.00	27
ST-77	Mafic Schist	Groundmass	41.78	19.27	10.27	0.28	4.90	21.07	0.13	0.00	97.71	3.34	0.00	1.81	0.69	0.00	0.02	0.58	1.80	0.02	0.00	27
ST-77	Mafic Schist	Groundmass	40.23	23.27	10.34	0.12	0.82	22.81	0.23	0.00	97.87	3.22	0.00	2.19	0.69	0.00	0.01	0.10	1.96	0.04	0.00	24
ST-77	Mafic Schist	Groundmass	39.91	23.22	9.61	0.16	1.70	23.39	0.05	0.00	98.09	3.18	0.00	2.18	0.64	0.00	0.01	0.20	2.00	0.01	0.00	23
ST-77	Mafic Schist	Groundmass	39.60	24.09	9.56	0.16	0.32	24.19	0.02	0.00	98.02	3.17	0.00	2.27	0.64	0.00	0.01	0.04	2.07	0.00	0.00	22
ST-65	Pillow Basalt	Vein	37.65	21.99	13.73	0.05	0.03	22.87	0.00	0.00	96.32	3.13	0.00	2.16	0.84	0.11	0.00	0.00	2.04	0.00	0.00	28
ST-65	Pillow Basalt	Amygdule	37.75	23.20	12.09	0.23	0.12	22.63	0.04	0.00	96.06	3.12	0.00	2.26	0.74	0.09	0.02	0.01	2.00	0.01	0.00	25
ST-65	Pillow Basalt	Amygdule	38.08	24.31	10.70	0.14	0.10	23.26	0.00	0.01	96.63	3.11	0.00	2.34	0.66	0.07	0.01	0.01	2.03	0.00	0.00	22
ST-65	Pillow Basalt	Amygdule	38.02	24.24	10.63	0.11	0.10	23.36	0.03	0.00	96.49	3.10	0.00	2.33	0.67	0.06	0.01	0.01	2.04	0.01	0.00	22
ST-65	Pillow Basalt	Amygdule	38.22	23.02	12.45	0.08	0.03	23.24	0.00	0.02	97.06	3.13	0.00	2.22	0.78	0.08	0.01	0.00	2.04	0.00	0.00	26
ST-65	Pillow Basalt	Amygdule	38.54	24.18	10.66	0.20	0.29	22.73	0.03	0.01	96.74	3.13	0.00	2.32	0.68	0.04	0.01	0.03	1.98	0.01	0.00	23
ST-65	Pillow Basalt	Amygdule	38.70	21.95	13.35	0.06	0.33	22.54	0.00	0.01	96.93	3.18	0.00	2.13	0.87	0.04	0.00	0.04	1.99	0.00	0.00	29
ST-65	Pillow Basalt	Amygdule	38.54	25.24	10.03	0.21	0.11	22.99	0.00	0.00	97.14	3.11	0.00	2.40	0.60	0.07	0.01	0.01	1.99	0.00	0.00	20
ST-65	Pillow Basalt	Amygdule	38.38	24.95	10.40	0.22	0.04	22.94	0.04	0.01	96.99	3.11	0.00	2.38	0.62	0.08	0.02	0.00	1.99	0.01	0.00	21
ST-65	Pillow Basalt	Vein	37.69	21.98	13.43	0.04	0.10	22.87	0.01	0.02	96.24	3.14	0.00	2.16	0.84	0.09	0.00	0.01	2.04	0.00	0.00	28
ST-65	Pillow Basalt	Vein	37.79	25.18	9.99	0.10	0.11	22.73	0.00	0.00	95.91	3.09	0.00	2.42	0.58	0.11	0.01	0.01	1.99	0.00	0.00	19
ST-20	Pillow Basalt	Amygdule	38.57	24.67	10.65	0.06	0.02	23.42	0.01	0.00	97.44	3.11	0.00	2.35	0.65	0.07	0.00	0.00	2.03	0.00	0.00	22
ST-20	Pillow Basalt	Amygdule	38.17	23.12	12.20	0.10	0.04	23.52	0.00	0.01	97.24	3.12	0.00	2.23	0.77	0.06	0.01	0.00	2.06	0.00	0.00	26
ST-20	Pillow Basalt	Amygdule	38.26	26.07	9.61	0.07	0.05	23.37	0.00	0.00	97.43	3.07	0.00	2.47	0.53	0.11	0.00	0.01	2.01	0.00	0.00	18
ST-20	Pillow Basalt	Amygdule	38.29	24.96	10.45	0.07	0.01	23.60	0.00	0.01	97.40	3.09	0.00	2.38	0.62	0.08	0.00	0.00	2.04	0.00	0.00	21
ST-20	Pillow Basalt	Amygdule	38.84	26.44	8.50	0.04	0.00	23.83	0.00	0.01	97.69	3.09	0.00	2.48	0.52	0.04	0.00	0.00	2.03	0.00	0.00	17
ST-20	Pillow Basalt	Amygdule	37.96	21.32	13.73	0.10	0.04	23.20	0.02	0.00	96.38	3.16	0.00	2.09	0.91	0.05	0.01	0.00	2.07	0.00	0.00	30
ST-20	Pillow Basalt	Amygdule	38.21	25.92	9.31	0.08	0.04	23.66	0.00	0.01	97.24	3.07	0.00	2.46	0.54	0.08	0.01	0.00	2.04	0.00	0.00	18
ST-20	Pillow Basalt	Groundmass	38.81	22.49	12.42	0.12	0.41	22.83	0.02	0.00	97.11	3.17	0.00	2.17	0.83	0.01	0.01	0.05	2.00	0.00	0.00	28
ST-20	Pillow Basalt	Groundmass	38.99	25.83	9.34	0.04	0.11	23.47	0.00	0.00	97.78	3.11	0.00	2.43	0.57	0.05	0.00	0.01	2.00	0.00	0.00	19
ST-20	Pillow Basalt	Groundmass	37.96	22.88	12.80	0.16	0.08	23.19	0.01	0.01	97.11	3.12	0.00	2.21	0.79	0.09	0.01	0.01	2.04	0.00	0.00	26
ST-20	Pillow Basalt	Groundmass	38.12	23.08	12.92	0.09	0.05	23.15	0.03	0.00	97.43	3.12	0.00	2.22	0.78	0.11	0.01	0.01	2.03	0.00	0.00	26
ST-20	Pillow Basalt	Groundmass	38.52	25.17	10.46	0.03	0.08	23.44	0.02	0.01	97.75	3.10	0.00	2.38	0.62	0.09	0.00	0.01	2.02	0.00	0.00	21
ST-20	Pillow Basalt	Groundmass	38.54	24.18	11.39	0.10	0.06	23.41	0.00	0.00	97.73	3.12	0.00	2.30	0.70	0.07	0.01	0.01	2.03	0.00	0.00	23
ST-20	Pillow Basalt	Amygdule	38.70	25.41	10.39	0.11	0.01	23.39	0.00	0.01	98.03	3.10	0.00	2.40	0.60	0.09	0.01	0.00	2.01	0.00	0.00	20
ST-20	Pillow Basalt	Amygdule	38.30	21.73	14.55	0.04	0.05	22.97	0.00	0.00	97.67	3.15	0.00	2.11	0.89	0.11	0.00	0.01	2.02	0.00	0.00	30
ST-20	Pillow Basalt	Amygdule	37.50	22.24	13.58	0.01	0.07	22.85	0.02	0.01	96.29	3.12	0.00	2.18	0.82	0.12	0.00	0.01	2.04	0.00	0.00	27
ST-20	Pillow Basalt	Amygdule	37.76	25.62	10.06	0.20	0.04	22.90	0.00	0.02	96.62	3.07	0.00	2.45	0.55	0.13	0.01	0.00	1.99	0.00	0.00	18
ST-20	Pillow Basalt	Amygdule	38.81	24.19	11.09	0.22	0.27	23.02	0.00	0.02	97.54	3.12	0.00	2.31	0.69	0.06	0.02	0.03	1.99	0.00	0.00	23
ST-20	Pillow Basalt	Amygdule	38.15	23.77	11.82	0.34	0.20	22.72	0.00	0.01	97.02	3.11	0.00	2.29	0.71	0.09	0.02	0.02	1.99	0.00	0.00	24

Appendix 4: Epidote Compositions

Sample	Lithology	Occurence	SiO2 (wt%)	Al2O3 (wt%)	FeO (wt%)	MnO (wt%)	MgO (wt%)	CaO (wt%)	Na2O (wt%)	K2O (wt%)	Total (wt%)	Si	AlIV	AlVI	Fe+3	Fe+2	Mn	Mg	Ca	Na	K	Ps
ST-20	Pillow Basalt	Amygdule	37.91	22.09	13.58	0.02	0.06	23.38	0.00	0.00	97.05	3.13	0.00	2.15	0.85	0.09	0.00	0.01	2.07	0.00	0.00	28
ST-20	Pillow Basalt	Amygdule	37.90	25.48	9.92	0.21	0.04	23.32	0.00	0.00	96.88	3.07	0.00	2.43	0.57	0.10	0.01	0.00	2.02	0.00	0.00	19
ST-66	Fault Gouge	Vein	38.36	26.53	8.97	0.09	0.05	23.94	0.00	0.00	97.97	3.06	0.00	2.49	0.51	0.09	0.01	0.01	2.04	0.00	0.00	17
ST-66	Fault Gouge	Vein	36.75	22.58	13.10	0.03	0.00	23.03	0.00	0.00	95.62	3.08	0.00	2.23	0.77	0.15	0.00	0.00	2.07	0.00	0.00	26
ST-66	Fault Gouge	Groundmass	38.29	27.57	8.23	0.06	0.02	23.54	0.02	0.00	97.79	3.04	0.00	2.68	0.42	0.12	0.00	0.00	2.00	0.00	0.00	14
ST-66	Fault Gouge	Groundmass	37.30	23.14	12.94	0.10	0.01	23.49	0.00	0.00	97.06	3.08	0.00	2.25	0.75	0.14	0.01	0.00	2.08	0.00	0.00	25
ST-66	Fault Gouge	Vein	38.01	27.19	8.61	0.07	0.03	23.28	0.01	0.01	97.21	3.04	0.00	2.56	0.44	0.14	0.00	0.00	1.99	0.00	0.00	15
ST-66	Fault Gouge	Vein	37.60	23.86	12.28	0.29	0.03	22.97	0.00	0.00	97.19	3.08	0.00	2.30	0.70	0.15	0.02	0.00	2.02	0.00	0.00	23
ST-90	Fault Gouge	Groundmass	38.39	23.84	11.93	0.12	0.01	23.07	0.05	0.00	97.41	3.12	0.00	2.28	0.72	0.10	0.01	0.00	2.01	0.01	0.00	24
ST-90	Fault Gouge	Groundmass	39.24	28.57	6.62	0.16	0.08	23.83	0.01	0.00	98.51	3.06	0.00	2.62	0.38	0.06	0.01	0.01	1.99	0.00	0.00	13
ST-90	Fault Gouge	Vein	38.50	23.89	11.56	0.03	0.06	23.16	0.01	0.00	97.40	3.13	0.00	2.29	0.71	0.07	0.00	0.01	2.02	0.00	0.00	24
ST-90	Fault Gouge	Vein	39.34	27.16	7.72	0.14	0.18	23.57	0.04	0.00	98.15	3.10	0.00	2.52	0.48	0.03	0.01	0.02	1.99	0.01	0.00	16
ST-90	Fault Gouge	Vein	39.07	25.07	9.57	0.10	0.26	23.32	0.01	0.00	97.51	3.13	0.00	2.37	0.63	0.01	0.01	0.03	2.00	0.00	0.00	21
ST-90	Fault Gouge	Groundmass	40.84	25.12	7.87	0.07	1.81	22.69	0.02	0.00	98.41	3.20	0.00	2.32	0.51	0.00	0.00	0.21	1.90	0.00	0.00	18
ST-90	Fault Gouge	Groundmass	38.14	21.36	14.48	0.09	0.07	22.94	0.00	0.00	97.08	3.16	0.00	2.08	0.92	0.09	0.01	0.01	2.04	0.00	0.00	31
ST-90	Fault Gouge	Vein	38.50	23.71	11.47	0.14	0.13	23.28	0.02	0.00	97.32	3.13	0.00	2.27	0.73	0.05	0.01	0.02	2.03	0.00	0.00	24
ST-90	Fault Gouge	Vein	38.72	24.59	11.05	0.21	0.04	22.72	0.01	0.00	97.45	3.13	0.00	2.34	0.66	0.09	0.01	0.01	1.97	0.00	0.00	22
ST-103	Pillow Basalt	Amygdule	37.69	23.55	12.85	0.09	0.03	23.62	0.00	0.00	98.03	3.08	0.00	2.26	0.74	0.14	0.01	0.00	2.07	0.00	0.00	25
ST-103	Pillow Basalt	Amygdule	34.63	21.74	14.87	0.15	0.01	23.53	0.00	0.00	95.09	2.98	0.02	2.18	0.82	0.25	0.01	0.00	2.17	0.00	0.00	27
ST-103	Pillow Basalt	Amygdule	37.40	23.30	12.88	0.06	0.01	23.74	0.00	0.00	97.50	3.07	0.00	2.25	0.75	0.14	0.00	0.00	2.09	0.00	0.00	25
ST-103	Pillow Basalt	Amygdule	37.26	21.08	13.02	0.07	0.08	23.45	0.02	0.00	96.75	3.15	0.00	2.10	0.90	0.02	0.00	0.01	2.12	0.00	0.00	30
ST-103	Pillow Basalt	Amygdule	36.55	18.21	18.97	0.01	0.00	22.93	0.04	0.00	96.71	3.13	0.00	1.84	1.16	0.20	0.00	0.00	2.11	0.01	0.00	39
ST-103	Pillow Basalt	Amygdule	36.80	18.66	18.58	0.02	0.00	23.13	0.00	0.00	97.25	3.13	0.00	1.87	1.13	0.19	0.00	0.00	2.11	0.00	0.00	38
ST-103	Pillow Basalt	Vein	38.09	23.87	11.93	0.07	0.05	23.85	0.00	0.00	98.24	3.09	0.00	2.28	0.72	0.09	0.00	0.01	2.07	0.00	0.00	24
ST-103	Pillow Basalt	Vein	38.08	24.75	11.25	0.11	0.05	23.44	0.01	0.00	98.13	3.08	0.00	2.36	0.64	0.12	0.01	0.01	2.03	0.00	0.00	21
ST-103	Pillow Basalt	Vein	38.29	26.32	9.36	0.15	0.03	23.79	0.03	0.00	98.09	3.06	0.00	2.48	0.52	0.10	0.01	0.00	2.03	0.00	0.00	17
ST-103	Pillow Basalt	Vein	38.29	24.78	11.57	0.09	0.06	23.74	0.00	0.00	99.06	3.07	0.00	2.35	0.65	0.12	0.01	0.01	2.04	0.00	0.00	22
ST-103	Pillow Basalt	Vein	37.93	26.28	9.49	0.09	0.00	23.82	0.00	0.01	97.77	3.04	0.00	2.48	0.52	0.12	0.01	0.00	2.05	0.00	0.00	17
ST-103	Pillow Basalt	Vein	37.62	24.07	11.99	0.11	0.03	23.49	0.00	0.00	97.58	3.07	0.00	2.32	0.68	0.13	0.01	0.00	2.05	0.00	0.00	23
ST-109	Fault Gouge	Vein	38.38	25.30	10.35	0.23	0.02	23.26	0.00	0.02	97.68	3.09	0.00	2.40	0.60	0.10	0.02	0.00	2.01	0.00	0.00	20
ST-109	Fault Gouge	Vein	38.07	23.01	12.81	0.66	0.02	22.73	0.00	0.00	97.29	3.12	0.00	2.22	0.78	0.10	0.05	0.00	2.00	0.00	0.00	26
ST-109	Fault Gouge	Vein	36.90	20.89	13.62	0.24	0.03	22.78	0.00	0.01	94.51	3.14	0.00	2.10	0.90	0.07	0.02	0.00	2.08	0.00	0.00	30
ST-109	Fault Gouge	Vein	37.75	24.30	10.44	0.22	0.01	23.22	0.04	0.00	96.01	3.10	0.00	2.35	0.65	0.07	0.02	0.00	2.04	0.01	0.00	22
ST-109	Fault Gouge	Vein	38.40	22.40	13.11	0.27	0.03	23.21	0.00	0.00	97.50	3.15	0.00	2.16	0.84	0.06	0.02	0.00	2.04	0.00	0.00	28
ST-109	Fault Gouge	Vein	38.74	25.19	10.44	0.26	0.02	22.99	0.00	0.00	97.65	3.11	0.00	2.38	0.62	0.09	0.02	0.00	1.98	0.00	0.00	21
ST-109	Fault Gouge	Vein	37.73	21.06	14.03	0.13	0.05	22.84	0.00	0.00	95.85	3.16	0.00	2.08	0.92	0.06	0.01	0.01	2.05	0.00	0.00	31
ST-109	Fault Gouge	Vein	38.73	23.63	11.77	0.12	0.01	23.06	0.01	0.00	97.46	3.15	0.00	2.26	0.74	0.06	0.01	0.00	2.01	0.00	0.00	25
ST-109	Fault Gouge	Vein	37.93	22.49	13.48	0.15	0.01	23.26	0.03	0.00	97.39	3.12	0.00	2.18	0.82	0.11	0.01	0.00	2.05	0.01	0.00	27
ST-109	Fault Gouge	Vein	38.07	25.20	9.74	0.27	0.01	23.43	0.00	0.00	96.74	3.09	0.00	2.41	0.59	0.07	0.02	0.00	2.04	0.00	0.00	20
ST-109	Fault Gouge	Amygdule	37.88	21.01	13.91	0.13	0.02	22.98	0.00	0.00	95.97	3.17	0.00	2.07	0.93	0.05	0.01	0.00	2.06	0.00	0.00	31
ST-109	Fault Gouge	Amygdule	38.42	25.53	9.64	0.24	0.03	23.28	0.02	0.00	97.15	3.09	0.00	2.42	0.58	0.07	0.02	0.00	2.01	0.00	0.00	19
ST-112	Massive Flow	Amygdule	39.18	23.00	12.52	0.09	0.51	22.88	0.02	0.00	98.21	3.16	0.00	2.19	0.81	0.03	0.01	0.06	1.98	0.00	0.00	27
ST-112	Massive Flow	Amygdule	38.78	20.34	15.02	0.07	0.59	22.85	0.00	0.00	97.66	3.20	0.00	1.98	1.02	0.01	0.00	0.07	2.02	0.00	0.00	34
ST-112	Massive Flow	Amygdule	38.45	22.51	13.22	0.15	0.22	23.14	0.00	0.01	97.70	3.14	0.00	2.17	0.83	0.07	0.01	0.03	2.03	0.00	0.00	28
ST-112	Massive Flow	Groundmass	38.26	23.00	12.82	0.09	0.07	22.96	0.01	0.01	97.21	3.13	0.00	2.22	0.78	0.10	0.01	0.01	2.01	0.00	0.00	26
ST-112	Massive Flow	Amygdule	38.18	22.28	12.33	0.07	0.00	23.35	0.00	0.01	96.31	3.16	0.00	2.17	0.83	0.02	0.00	0.00	2.07	0.00	0.00	28

Appendix 4: Epidote Compositions

Sample	Lithology	Occurence	SiO2 (wt%)	Al2O3 (wt%)	FeO (wt%)	MnO (wt%)	MgO (wt%)	CaO (wt%)	Na2O (wt%)	K2O (wt%)	Total (wt%)	Si	AlIV	AlVI	Fe+3	Fe+2	Mn	Mg	Ca	Na	K	Ps
ST-70	Fault Gouge	Vein	38.39	24.78	11.07	0.14	0.00	23.08	0.00	0.00	97.47	3.10	0.00	2.36	0.64	0.11	0.01	0.00	2.00	0.00	0.00	21
ST-70	Fault Gouge	Vein	38.17	21.54	13.79	0.04	0.05	23.28	0.00	0.00	96.96	3.16	0.00	2.10	0.90	0.06	0.00	0.01	2.06	0.00	0.00	30
ST-70	Fault Gouge	Vein	38.67	24.97	10.63	0.34	0.03	23.29	0.00	0.00	97.93	3.11	0.00	2.36	0.64	0.08	0.02	0.00	2.00	0.00	0.00	21
ST-70	Fault Gouge	Vein	38.02	20.87	15.21	0.09	0.02	23.12	0.00	0.00	97.35	3.16	0.00	2.04	0.96	0.10	0.01	0.00	2.06	0.00	0.00	32
ST-70	Fault Gouge	Vein	37.79	23.61	11.85	0.23	0.01	23.27	0.00	0.00	96.77	3.10	0.00	2.28	0.72	0.10	0.02	0.00	2.05	0.00	0.00	24
ST-70	Fault Gouge	Vein	37.69	21.93	13.59	0.10	0.00	23.24	0.00	0.00	96.55	3.13	0.00	2.15	0.85	0.09	0.01	0.00	2.07	0.00	0.00	28
ST-70	Fault Gouge	Vein	38.29	24.80	10.99	0.31	0.04	23.17	0.02	0.00	97.63	3.09	0.00	2.36	0.64	0.10	0.02	0.01	2.00	0.00	0.00	21
ST-70	Fault Gouge	Vein	38.16	21.47	14.34	0.07	0.03	23.83	0.00	0.01	97.96	3.14	0.00	2.08	0.92	0.07	0.00	0.00	2.10	0.00	0.00	31
ST-70	Fault Gouge	Amygdule	37.84	23.32	12.02	0.12	0.00	23.34	0.00	0.00	96.66	3.11	0.00	2.26	0.74	0.09	0.01	0.00	2.06	0.00	0.00	25
ST-70	Fault Gouge	Amygdule	39.33	26.06	9.38	0.12	0.02	23.71	0.03	0.00	98.66	3.11	0.00	2.43	0.57	0.05	0.01	0.00	2.01	0.00	0.00	19
ST-70	Fault Gouge	Amygdule	38.09	21.00	14.92	0.04	0.02	23.37	0.00	0.01	97.46	3.16	0.00	2.05	0.95	0.08	0.00	0.00	2.07	0.00	0.00	32
ST-70	Fault Gouge	Amygdule	38.90	26.01	9.34	0.10	0.00	23.59	0.03	0.00	98.00	3.10	0.00	2.44	0.56	0.06	0.01	0.00	2.01	0.00	0.00	19
ST-70	Fault Gouge	Amygdule	38.41	25.68	9.99	0.09	0.03	23.17	0.01	0.00	97.36	3.09	0.00	2.43	0.57	0.10	0.01	0.00	2.00	0.00	0.00	19
ST-70	Fault Gouge	Amygdule	38.27	23.08	12.74	0.08	0.04	23.06	0.01	0.01	97.31	3.13	0.00	2.22	0.78	0.10	0.01	0.01	2.02	0.00	0.00	26
ST-70	Fault Gouge	Amygdule	38.10	20.83	14.84	0.09	0.02	23.42	0.00	0.00	97.31	3.16	0.00	2.04	0.96	0.07	0.01	0.00	2.08	0.00	0.00	32
ST-70	Fault Gouge	Amygdule	38.43	25.90	9.52	0.14	0.02	23.73	0.01	0.00	97.76	3.08	0.00	2.44	0.56	0.08	0.01	0.00	2.03	0.00	0.00	19
ST-70	Fault Gouge	Vein	38.22	22.02	13.55	0.05	0.02	23.26	0.01	0.01	97.26	3.15	0.00	2.14	0.86	0.07	0.00	0.00	2.05	0.00	0.00	29
ST-70	Fault Gouge	Vein	38.30	23.90	12.01	0.06	0.04	23.41	0.00	0.00	97.72	3.11	0.00	2.29	0.71	0.10	0.00	0.00	2.03	0.00	0.00	24
ST-70	Fault Gouge	Vein	38.20	24.69	10.61	0.13	0.02	23.32	0.01	0.00	96.99	3.10	0.00	2.36	0.64	0.08	0.01	0.00	2.03	0.00	0.00	21
ST-70	Fault Gouge	Vein	38.23	21.71	14.07	0.12	0.02	23.38	0.01	0.00	97.54	3.15	0.00	2.11	0.89	0.08	0.01	0.00	2.06	0.00	0.00	30
ST-70	Fault Gouge	Vein	38.38	22.69	13.07	0.09	0.02	23.19	0.02	0.00	97.48	3.14	0.00	2.19	0.81	0.08	0.01	0.00	2.03	0.00	0.00	27
ST-70	Fault Gouge	Vein	38.42	23.09	13.01	0.19	0.03	23.29	0.02	0.00	98.05	3.12	0.00	2.21	0.79	0.10	0.01	0.00	2.03	0.00	0.00	26
ST-71	Fault Gouge	Vein	37.87	24.04	11.91	0.09	0.02	23.69	0.00	0.02	97.75	3.08	0.00	2.30	0.70	0.11	0.01	0.00	2.06	0.00	0.00	23
ST-71	Fault Gouge	Vein	38.22	23.68	12.30	0.19	0.00	23.38	0.01	0.00	97.78	3.11	0.00	2.27	0.73	0.10	0.01	0.00	2.04	0.00	0.00	24
ST-71	Fault Gouge	Vein	37.61	24.27	11.92	0.25	0.00	23.24	0.00	0.00	97.56	3.07	0.00	2.33	0.67	0.15	0.02	0.00	2.03	0.00	0.00	22
ST-71	Fault Gouge	Vein	37.89	23.98	11.81	0.25	0.04	23.13	0.00	0.00	97.25	3.09	0.00	2.31	0.69	0.11	0.02	0.01	2.02	0.00	0.00	23
ST-71	Fault Gouge	Vein	37.59	24.24	11.86	0.12	0.02	23.73	0.02	0.00	97.71	3.06	0.00	2.33	0.67	0.13	0.01	0.00	2.07	0.00	0.00	22
ST-71	Fault Gouge	Vein	37.50	23.13	13.51	0.27	0.01	23.28	0.00	0.00	97.74	3.08	0.00	2.24	0.76	0.16	0.02	0.00	2.05	0.00	0.00	25
ST-71	Fault Gouge	Vein	37.91	23.39	12.89	0.27	0.03	23.39	0.02	0.00	98.10	3.09	0.00	2.25	0.75	0.13	0.02	0.00	2.04	0.00	0.00	25
ST-71	Fault Gouge	Vein	38.02	23.79	12.54	0.20	0.03	23.07	0.00	0.00	97.90	3.10	0.00	2.28	0.72	0.14	0.01	0.00	2.01	0.00	0.00	24
ST-71	Fault Gouge	Vein	37.57	23.06	13.40	0.14	0.01	23.22	0.00	0.00	97.39	3.09	0.00	2.23	0.77	0.15	0.01	0.00	2.04	0.00	0.00	26
ST-71	Fault Gouge	Vein	37.76	22.83	13.35	0.14	0.08	23.40	0.00	0.00	97.73	3.10	0.00	2.21	0.79	0.12	0.01	0.01	2.06	0.00	0.00	26
ST-71	Fault Gouge	Vein	37.85	22.99	12.83	0.16	0.06	23.38	0.00	0.01	97.42	3.11	0.00	2.22	0.78	0.10	0.01	0.01	2.06	0.00	0.00	26
ST-71	Fault Gouge	Vein	36.49	24.13	12.01	0.19	0.04	23.56	0.02	0.00	96.49	3.02	0.00	2.35	0.65	0.18	0.01	0.00	2.09	0.00	0.00	22
ST-71	Fault Gouge	Vein	38.01	25.02	10.95	0.15	0.06	23.99	0.00	0.00	98.27	3.06	0.00	2.37	0.63	0.11	0.01	0.01	2.07	0.00	0.00	21
ST-71	Fault Gouge	Vein	37.78	23.36	13.00	0.19	0.00	23.28	0.01	0.01	97.64	3.09	0.00	2.25	0.75	0.14	0.01	0.00	2.04	0.00	0.00	25
ST-71	Fault Gouge	Vein	37.48	23.95	12.50	0.26	0.01	23.04	0.00	0.00	97.37	3.07	0.00	2.31	0.69	0.17	0.02	0.00	2.02	0.00	0.00	23
ST-78	Massive Flow	Amygdule	38.99	25.43	10.52	0.10	0.03	23.30	0.00	0.00	98.37	3.11	0.00	2.39	0.61	0.09	0.01	0.00	1.99	0.00	0.00	20
ST-78	Massive Flow	Amygdule	38.95	24.06	11.48	0.06	0.02	23.50	0.03	0.02	98.20	3.13	0.00	2.28	0.72	0.05	0.00	0.00	2.03	0.01	0.00	24
ST-78	Massive Flow	Amygdule	38.36	21.98	13.82	0.06	0.04	23.62	0.00	0.01	97.90	3.14	0.00	2.12	0.88	0.07	0.00	0.01	2.07	0.00	0.00	29
ST-78	Massive Flow	Groundmass	39.52	28.47	7.05	0.09	0.01	23.63	0.04	0.01	98.81	3.07	0.00	2.61	0.39	0.07	0.01	0.00	1.97	0.01	0.00	13
ST-78	Massive Flow	Groundmass	38.72	22.80	12.62	0.06	0.04	23.24	0.01	0.00	97.49	3.16	0.00	2.19	0.81	0.05	0.00	0.00	2.03	0.00	0.00	27
ST-78	Massive Flow	Amygdule	38.46	24.23	11.74	0.13	0.01	23.05	0.00	0.01	97.63	3.11	0.00	2.31	0.69	0.11	0.01	0.00	2.00	0.00	0.00	23
ST-78	Massive Flow	Amygdule	37.84	23.63	11.51	0.12	0.03	23.52	0.01	0.00	96.70	3.10	0.00	2.28	0.72	0.07	0.01	0.00	2.07	0.00	0.00	24
ST-83	Massive Flow	Vein	38.02	24.67	11.31	0.20	0.02	23.30	0.00	0.00	97.54	3.08	0.00	2.36	0.64	0.12	0.01	0.00	2.02	0.00	0.00	21
ST-83	Massive Flow	Vein	37.77	23.03	13.35	0.08	0.02	23.77	0.01	0.01	98.05	3.09	0.00	2.22	0.78	0.13	0.01	0.00	2.08	0.00	0.00	26

Appendix 4: Epidote Compositions

Sample	Lithology	Occurence	SiO2 (wt%)	Al2O3 (wt%)	FeO (wt%)	MnO (wt%)	MgO (wt%)	CaO (wt%)	Na2O (wt%)	K2O (wt%)	Total (wt%)	Si	AlIV	AlVI	Fe+3	Fe+2	Mn	Mg	Ca	Na	K	Ps
ST-88	Volcaniclastic	Groundmass	35.85	20.68	12.83	0.21	0.02	23.70	0.04	0.00	93.34	3.10	0.00	2.11	0.89	0.03	0.02	0.00	2.19	0.01	0.00	30
ST-88	Volcaniclastic	Groundmass	38.03	22.89	13.16	0.18	0.01	22.96	0.01	0.00	97.24	3.12	0.00	2.21	0.79	0.12	0.01	0.00	2.02	0.00	0.00	26
ST-88	Volcaniclastic	Groundmass	39.15	26.94	8.58	0.15	0.02	23.79	0.01	0.05	98.74	3.08	0.00	2.50	0.50	0.06	0.01	0.00	2.01	0.00	0.00	17
ST-88	Volcaniclastic	Groundmass	39.44	28.30	7.44	0.26	0.02	23.56	0.00	0.03	99.05	3.07	0.00	2.60	0.40	0.08	0.02	0.00	1.96	0.00	0.00	13
ST-88	Volcaniclastic	Groundmass	38.23	21.51	14.83	0.17	0.01	23.07	0.00	0.01	97.83	3.15	0.00	2.09	0.91	0.11	0.01	0.00	2.04	0.00	0.00	30
ST-88	Volcaniclastic	Groundmass	37.26	21.01	11.50	0.15	0.05	24.23	0.01	0.00	94.20	3.16	0.00	2.10	0.82	0.00	0.01	0.01	2.20	0.00	0.00	28
ST-77	Mafic Schist	Groundmass	38.03	25.30	8.90	0.15	0.14	24.03	0.00	0.00	96.56	3.08	0.00	2.42	0.58	0.02	0.01	0.02	2.09	0.00	0.00	19
ST-77	Mafic Schist	Groundmass	41.13	19.99	10.54	0.20	4.14	20.27	0.09	0.00	96.37	3.33	0.00	1.91	0.71	0.00	0.01	0.50	1.76	0.01	0.00	27
ST-77	Mafic Schist	Groundmass	41.78	19.27	10.27	0.28	4.90	21.07	0.13	0.00	97.71	3.34	0.00	1.81	0.69	0.00	0.02	0.58	1.80	0.02	0.00	27
ST-77	Mafic Schist	Groundmass	40.23	23.27	10.34	0.12	0.82	22.81	0.23	0.00	97.87	3.22	0.00	2.19	0.69	0.00	0.01	0.10	1.96	0.04	0.00	24
ST-77	Mafic Schist	Groundmass	39.91	23.22	9.61	0.16	1.70	23.39	0.05	0.00	98.09	3.18	0.00	2.18	0.64	0.00	0.01	0.20	2.00	0.01	0.00	23
ST-77	Mafic Schist	Groundmass	39.60	24.09	9.56	0.16	0.32	24.19	0.02	0.00	98.02	3.17	0.00	2.27	0.64	0.00	0.01	0.04	2.07	0.00	0.00	22

Appendix 4: Mean Epidote Compositions

Sample	Lithology	n	SiO2 (wt%)	Al2O3 (wt%)	FeO (wt%)	MnO (wt%)	MgO (wt%)	CaO (wt%)	Na2O (wt%)	K2O (wt%)	Total (wt%)	Si	AlIV	AlVI	Fe+3	Fe+2	Mn	Mg	Ca	Na	K	Ps
Means																						
ST-65	Pillow Basalt	11	38.12	23.66	11.59	0.13	0.12	22.92	0.01	0.01	96.59	3.12	0.00	2.28	0.72	0.08	0.01	0.01	2.01	0.00	0.00	24
ST-20	Pillow Basalt	21	38.29	24.13	11.37	0.11	0.08	23.27	0.01	0.01	97.28	3.11	0.00	2.31	0.69	0.08	0.01	0.01	2.03	0.00	0.00	23
ST-66	Fault Gouge	6	37.72	25.15	10.69	0.11	0.02	23.37	0.00	0.00	97.14	3.06	0.00	2.40	0.60	0.13	0.01	0.00	2.03	0.00	0.00	20
ST-90	Fault Gouge	9	38.97	24.81	10.25	0.12	0.29	23.18	0.02	0.00	97.69	3.13	0.00	2.34	0.64	0.05	0.01	0.03	1.99	0.00	0.00	21
ST-103	Pillow Basalt	12	37.38	23.05	13.06	0.09	0.03	23.55	0.01	0.00	97.52	3.08	0.00	2.23	0.77	0.14	0.01	0.00	2.08	0.00	0.00	26
ST-109	Fault Gouge	12	38.08	23.33	11.95	0.24	0.02	23.09	0.01	0.00	96.77	3.12	0.00	2.25	0.75	0.07	0.02	0.00	2.03	0.00	0.00	25
ST-112	Sheet Flow	5	38.57	22.23	13.18	0.09	0.28	23.03	0.01	0.01	97.42	3.16	0.00	2.14	0.86	0.05	0.01	0.03	2.02	0.00	0.00	29
ST-70	Fault Gouge	22	38.29	23.36	12.30	0.12	0.02	23.34	0.01	0.00	97.46	3.12	0.00	2.24	0.76	0.08	0.01	0.00	2.04	0.00	0.00	25
ST-71	Fault Gouge	15	37.70	23.72	12.45	0.19	0.03	23.39	0.00	0.00	97.61	3.08	0.00	2.28	0.72	0.13	0.01	0.00	2.05	0.00	0.00	24
ST-78	Sheet Flow	7	38.69	24.37	11.25	0.09	0.03	23.41	0.01	0.01	97.87	3.12	0.00	2.31	0.69	0.07	0.01	0.00	2.02	0.00	0.00	23
ST-83	Sheet Flow	2	37.89	23.85	12.33	0.14	0.02	23.53	0.01	0.01	97.80	3.08	0.00	2.29	0.71	0.13	0.01	0.00	2.05	0.00	0.00	24
ST-88	Volcaniclastic	6	38.00	23.55	11.39	0.19	0.02	23.55	0.01	0.01	96.73	3.11	0.00	2.27	0.72	0.07	0.01	0.00	2.07	0.00	0.00	24
ST-77	Mafic Schist	11	40.12	22.52	9.87	0.18	2.00	22.63	0.09	0.00	97.44	3.22	0.00	2.13	0.66	0.00	0.01	0.24	1.95	0.01	0.00	24
ST-75	Mafic Schist	5	39.61	23.21	9.28	0.14	0.21	23.85	0.01	0.00	96.39	3.22	0.00	2.22	0.63	0.00	0.01	0.03	2.07	0.00	0.00	22
Standard Deviations																						
ST-65	Pillow Basalt	11	0.38	1.29	1.45	0.07	0.10	0.27	0.02	0.01	0.42	0.03	0.00	0.10	0.10	0.02	0.00	0.01	0.03	0.00	0.00	3.5
ST-20	Pillow Basalt	21	0.39	1.59	1.71	0.08	0.10	0.30	0.01	0.01	0.46	0.03	0.00	0.13	0.13	0.03	0.01	0.01	0.02	0.00	0.00	4.2
ST-66	Fault Gouge	6	0.62	2.20	2.31	0.09	0.02	0.36	0.01	0.00	0.83	0.02	0.00	0.16	0.16	0.02	0.01	0.00	0.03	0.00	0.00	5.3
ST-90	Fault Gouge	9	0.81	2.08	2.51	0.05	0.57	0.37	0.02	0.00	0.52	0.04	0.00	0.15	0.16	0.04	0.00	0.07	0.04	0.00	0.00	5.3
ST-103	Pillow Basalt	12	1.03	2.65	3.06	0.04	0.03	0.28	0.01	0.00	1.01	0.05	0.01	0.21	0.21	0.06	0.00	0.00	0.04	0.00	0.00	6.9
ST-109	Fault Gouge	12	0.51	1.78	1.73	0.14	0.01	0.23	0.01	0.01	0.98	0.03	0.00	0.14	0.14	0.02	0.01	0.00	0.03	0.00	0.00	4.5
ST-112	Sheet Flow	5	0.41	1.10	1.08	0.03	0.26	0.21	0.01	0.01	0.71	0.03	0.00	0.10	0.10	0.03	0.00	0.03	0.03	0.00	0.00	3.2
ST-70	Fault Gouge	22	0.36	1.79	1.89	0.08	0.01	0.21	0.01	0.00	0.50	0.03	0.00	0.14	0.14	0.02	0.01	0.00	0.03	0.00	0.00	4.7
ST-71	Fault Gouge	15	0.40	0.60	0.72	0.06	0.02	0.26	0.01	0.01	0.41	0.02	0.00	0.05	0.05	0.02	0.00	0.00	0.02	0.00	0.00	1.7
ST-78	Sheet Flow	7	0.54	2.11	2.12	0.03	0.01	0.22	0.02	0.01	0.69	0.03	0.00	0.16	0.16	0.02	0.00	0.00	0.04	0.00	0.00	5.2
ST-83	Sheet Flow	2	0.18	1.16	1.44	0.08	0.00	0.34	0.01	0.01	0.36	0.00	0.00	0.10	0.10	0.01	0.01	0.00	0.04	0.00	0.00	3.3
ST-88	Volcaniclastic	6	1.31	3.27	2.85	0.04	0.01	0.47	0.01	0.02	2.40	0.04	0.00	0.22	0.21	0.04	0.00	0.00	0.10	0.00	0.00	7.2
ST-77	Mafic Schist	11	1.30	2.38	0.62	0.05	2.04	1.61	0.09	0.00	0.76	0.10	0.00	0.23	0.05	0.01	0.00	0.24	0.14	0.01	0.00	3.1
ST-75	Mafic Schist	5	0.17	1.05	0.96	0.07	0.25	0.40	0.01	0.00	0.30	0.03	0.00	0.08	0.07	0.00	0.00	0.03	0.02	0.00	0.00	2.5
Relative Standard Deviations																						
ST-65	Pillow Basalt	11	1.0%	5.5%	12.5%	54.5%	81.0%	1.2%	119.1%	101.9%	0.4%	0.8%		4.6%	14.6%	30.1%	54.1%	81.0%	1.3%	118.9%	102.3%	14.6%
ST-20	Pillow Basalt	21	1.0%	6.6%	15.1%	76.9%	119.6%	1.3%	147.6%	100.0%	0.5%	0.9%		5.4%	18.2%	35.4%	77.1%	119.7%	1.2%	147.6%	99.9%	18.2%
ST-66	Fault Gouge	6	1.7%	8.8%	21.6%	85.5%	79.9%	1.5%	195.6%	162.0%	0.9%	0.7%		6.6%	26.7%	17.5%	86.4%	79.3%	1.7%	195.4%	162.1%	26.7%
ST-90	Fault Gouge	9	2.1%	8.4%	24.5%	44.6%	194.5%	1.6%	94.5%	142.8%	0.5%	1.2%		6.6%	25.2%	64.7%	44.5%	192.7%	2.0%	95.0%	142.1%	24.7%
ST-103	Pillow Basalt	12	2.8%	11.5%	23.4%	51.5%	95.2%	1.2%	158.3%	230.1%	1.0%	1.5%		9.2%	26.8%	42.9%	51.8%	96.3%	2.0%	160.0%	228.6%	26.8%
ST-109	Fault Gouge	12	1.3%	7.6%	14.4%	59.4%	57.1%	1.0%	165.5%	253.4%	1.0%	0.9%		6.0%	18.1%	24.4%	59.3%	58.4%	1.5%	166.1%	251.1%	18.1%
ST-112	Sheet Flow	5	1.1%	4.9%	8.2%	34.2%	94.6%	0.9%	150.8%	95.0%	0.7%	0.8%		4.4%	11.2%	72.5%	33.9%	94.8%	1.6%	150.3%	94.9%	11.2%
ST-70	Fault Gouge	22	0.9%	7.7%	15.4%	63.7%	60.3%	0.9%	135.1%	216.7%	0.5%	0.8%		6.3%	18.6%	19.7%	63.0%	60.4%	1.4%	134.1%	216.6%	18.6%
ST-71	Fault Gouge	15	1.1%	2.5%	5.8%	31.1%	90.2%	1.1%	145.7%	197.3%	0.4%	0.7%		2.2%	7.0%	18.1%	31.2%	90.2%	1.0%	145.8%	197.1%	7.0%
ST-78	Sheet Flow	7	1.4%	8.7%	18.9%	33.6%	48.0%	0.9%	123.6%	125.3%	0.7%	0.9%		6.8%	22.7%	26.3%	33.8%	49.0%	1.9%	122.3%	125.4%	22.7%
ST-83	Sheet Flow	2	0.5%	4.9%	11.7%	57.6%	0.0%	1.4%	141.4%	141.4%	0.4%	0.1%		4.3%	13.7%	4.0%	57.1%	0.6%	2.0%	141.4%	141.4%	13.7%
ST-88	Volcaniclastic	6	3.5%	13.9%	25.0%	22.1%	67.7%	2.0%	117.4%	147.2%	2.5%	1.2%		9.9%	29.7%	66.7%	20.8%	70.3%	4.9%	120.6%	146.8%	29.9%
ST-77	Mafic Schist	11	3.2%	10.5%	6.3%	30.3%	101.8%	7.1%	97.6%		0.8%	3.1%		10.7%	7.1%	244.9%	30.2%	101.9%	7.1%	97.5%		13.0%
ST-75	Mafic Schist	5	0.4%	4.5%	10.4%	48.1%	117.4%	1.7%	70.2%		0.3%	0.9%		3.8%	11.1%		48.1%	117.7%	1.0%	70.6%		11.4%

Appendix 4: Prehnite Compositions

Sample	Lithology	Occurence	SiO2 (wt%)	Al2O3 (wt%)	Fe2O3 (wt%)	MnO (wt%)	MgO (wt%)	CaO (wt%)	Na2O (wt%)	K2O (wt%)	F (wt%)	Cl (wt%)	Total (wt%)	Si	AlIV	AlVI	Fe	Mn	Mg	Ca	Na	K
ST-64	Sediment	Groundmass	43.59	23.30	1.32	0.14	0.01	26.37	0.00	0.00	0.00	0.02	94.72	6.06	1.94	1.88	0.14	0.02	0.00	3.93	0.00	0.00
ST-64	Sediment	Groundmass	43.17	22.76	2.11	0.15	0.00	26.49	0.00	0.00	0.00	0.01	94.68	6.09	1.91	1.88	0.07	0.02	0.00	4.01	0.00	0.00
ST-64	Sediment	Groundmass	43.39	22.76	2.65	0.09	0.12	26.13	0.00	0.00	0.00	0.00	95.14	6.11	1.89	1.89	0.09	0.01	0.03	3.94	0.00	0.00
ST-64	Sediment	Groundmass	43.39	23.04	2.07	0.06	0.14	26.25	0.02	0.01	0.00	0.00	94.97	6.09	1.91	1.90	0.07	0.01	0.03	3.95	0.00	0.00
ST-64	Sediment	Groundmass	43.06	22.84	1.95	0.12	0.10	26.23	0.02	0.01	0.00	0.01	94.33	6.09	1.91	1.89	0.07	0.01	0.02	3.97	0.01	0.00
ST-64	Sediment	Groundmass	43.48	22.23	2.80	0.06	0.08	26.31	0.01	0.01	0.00	0.00	94.98	6.14	1.86	1.85	0.10	0.01	0.02	3.98	0.00	0.00
ST-64	Sediment	Groundmass	43.40	23.03	1.75	0.10	0.03	26.45	0.00	0.01	0.06	0.00	94.76	6.10	1.90	1.91	0.06	0.01	0.01	3.98	0.00	0.00
ST-64	Sediment	Groundmass	42.59	21.21	4.26	0.08	0.01	26.06	0.00	0.00	0.00	0.00	94.21	6.15	1.85	1.76	0.15	0.01	0.00	4.03	0.00	0.00
ST-64	Sediment	Groundmass	42.97	21.39	4.00	0.07	0.00	26.37	0.00	0.01	0.00	0.00	94.80	6.16	1.84	1.77	0.14	0.01	0.00	4.05	0.00	0.00
ST-64	Sediment	Groundmass	43.52	22.77	2.19	0.20	0.00	26.18	0.01	0.01	0.00	0.01	94.86	6.12	1.88	1.90	0.08	0.02	0.00	3.95	0.00	0.00
G-16	Pillow Basalt	Amygdule	43.83	21.67	3.38	0.05	0.01	25.73	0.09	0.01	0.18	0.00	94.76	6.22	1.78	1.85	0.12	0.01	0.00	3.91	0.02	0.00
G-16	Pillow Basalt	Amygdule	43.01	18.76	7.72	0.05	0.00	26.09	0.05	0.01	0.18	0.01	95.69	6.30	1.70	1.54	0.28	0.01	0.00	4.09	0.01	0.00
G-16	Pillow Basalt	Amygdule	43.25	21.60	3.66	0.08	0.00	26.08	0.04	0.00	0.01	0.00	94.71	6.17	1.83	1.81	0.13	0.01	0.00	3.99	0.01	0.00
G-16	Pillow Basalt	Groundmass	43.19	21.84	3.75	0.10	0.01	26.21	0.01	0.02	0.00	0.00	95.12	6.15	1.85	1.81	0.13	0.01	0.00	4.00	0.00	0.00
G-16	Pillow Basalt	Groundmass	43.17	19.36	7.42	0.05	0.01	26.03	0.02	0.00	0.13	0.01	96.06	6.26	1.72	1.59	0.27	0.01	0.00	4.05	0.01	0.00
G-16	Pillow Basalt	Groundmass	43.21	20.24	5.59	0.03	0.00	26.21	0.08	0.00	0.10	0.00	95.36	6.23	1.77	1.68	0.20	0.00	0.00	4.05	0.02	0.00
G-16	Pillow Basalt	Groundmass	43.70	21.60	3.31	0.05	0.00	25.60	0.16	0.02	0.02	0.02	94.44	6.22	1.78	1.85	0.12	0.01	0.00	3.91	0.04	0.00
G-16	Pillow Basalt	Groundmass	43.65	21.33	3.94	0.03	0.02	25.74	0.08	0.00	0.00	0.02	94.78	6.23	1.77	1.81	0.14	0.00	0.00	3.93	0.02	0.00
G-16	Pillow Basalt	Amygdule	43.73	21.70	2.77	0.04	0.00	26.44	0.09	0.00	0.00	0.00	93.77	6.24	1.76	1.88	0.10	0.00	0.00	3.89	0.03	0.00
G-16	Pillow Basalt	Amygdule	43.75	22.01	2.73	0.09	0.02	25.50	0.08	0.01	0.02	0.00	94.20	6.21	1.79	1.89	0.10	0.01	0.00	3.88	0.02	0.00
G-16	Pillow Basalt	Amygdule	43.35	21.74	2.89	0.06	0.00	25.78	0.12	0.01	0.15	0.00	93.95	6.19	1.81	1.85	0.10	0.01	0.00	3.95	0.03	0.00
G-16	Pillow Basalt	Amygdule	43.65	21.72	3.04	0.02	0.00	25.79	0.10	0.00	0.00	0.00	94.31	6.21	1.79	1.86	0.11	0.00	0.00	3.93	0.03	0.00
G-16	Pillow Basalt	Amygdule	44.06	24.09	0.43	0.00	0.01	26.56	0.05	0.01	0.00	0.00	95.22	6.08	1.92	2.00	0.02	0.00	0.00	3.93	0.01	0.00
G-16	Pillow Basalt	Amygdule	42.78	19.45	6.65	0.05	0.03	26.07	0.03	0.00	0.04	0.00	95.04	6.25	1.75	1.61	0.24	0.01	0.01	4.08	0.01	0.00
G-16	Pillow Basalt	Amygdule	42.50	19.45	6.98	0.02	0.00	25.92	0.00	0.01	0.06	0.00	94.88	6.24	1.76	1.61	0.26	0.00	0.00	4.08	0.00	0.00
G-16	Pillow Basalt	Amygdule	43.23	23.30	1.39	0.01	0.00	26.45	0.00	0.01	0.00	0.01	94.38	6.08	1.92	1.94	0.05	0.00	0.00	3.98	0.00	0.00
G-16	Pillow Basalt	Amygdule	43.23	23.09	1.90	0.09	0.00	26.55	0.01	0.00	0.00	0.01	94.87	6.08	1.92	1.90	0.07	0.01	0.00	4.00	0.00	0.00
G-16	Pillow Basalt	Amygdule	43.24	23.34	1.57	0.04	0.00	26.67	0.00	0.02	0.00	0.00	94.88	6.06	1.94	1.92	0.06	0.00	0.00	4.01	0.00	0.00
G-16	Pillow Basalt	Amygdule	43.23	22.46	2.78	0.08	0.00	26.30	0.03	0.01	0.21	0.01	94.88	6.12	1.88	1.86	0.10	0.01	0.00	3.99	0.01	0.00
G-16	Pillow Basalt	Amygdule	44.01	22.11	2.63	0.08	0.00	25.61	0.08	0.01	0.02	0.00	94.53	6.22	1.78	1.90	0.09	0.01	0.00	3.88	0.02	0.00
G-16	Pillow Basalt	Amygdule	43.63	21.53	3.21	0.01	0.00	25.90	0.12	0.02	0.08	0.02	94.42	6.22	1.78	1.83	0.11	0.00	0.00	3.95	0.03	0.00
G-16	Pillow Basalt	Amygdule	42.73	18.68	7.70	0.02	0.01	25.64	0.05	0.00	0.00	0.01	94.82	6.31	1.69	1.56	0.29	0.00	0.00	4.06	0.01	0.00
G-16	Pillow Basalt	Amygdule	43.20	21.57	3.69	0.13	0.00	26.23	0.02	0.00	0.08	0.00	94.84	6.17	1.83	1.79	0.13	0.02	0.00	4.01	0.01	0.00
ST-55	Pillow Basalt	Amygdule	42.53	22.59	3.43	0.06	0.84	25.20	0.00	0.00	0.00	0.01	94.64	6.05	1.95	1.84	0.12	0.01	0.18	3.84	0.00	0.00
ST-55	Pillow Basalt	Amygdule	43.13	23.36	1.86	0.00	0.44	25.99	0.01	0.00	0.00	0.01	94.78	6.05	1.95	1.92	0.07	0.00	0.09	3.91	0.00	0.00
ST-55	Pillow Basalt	Vein	43.19	21.61	3.85	0.22	0.01	26.03	0.01	0.00	0.26	0.00	94.91	6.16	1.84	1.80	0.14	0.03	0.00	3.98	0.00	0.00
ST-55	Pillow Basalt	Vein	43.01	20.85	5.41	0.13	0.03	26.00	0.02	0.00	0.00	0.01	95.45	6.19	1.81	1.72	0.20	0.02	0.01	4.01	0.00	0.00
ST-55	Pillow Basalt	Amygdule	43.80	23.75	0.73	0.16	0.03	26.41	0.02	0.00	0.00	0.00	94.89	6.09	1.91	1.97	0.03	0.02	0.01	3.93	0.01	0.00
ST-55	Pillow Basalt	Amygdule	43.49	23.10	2.22	0.06	0.38	25.76	0.00	0.00	0.00	0.00	95.00	6.10	1.90	1.92	0.08	0.01	0.08	3.87	0.00	0.00
ST-94	Massive Flow	Groundmass	42.55	20.48	6.19	0.06	0.04	26.23	0.05	0.01	0.43	0.00	95.61	6.16	1.84	1.66	0.23	0.01	0.01	4.07	0.01	0.00
ST-94	Massive Flow	Groundmass	41.89	20.21	6.78	0.04	0.33	25.54	0.00	0.02	0.00	0.00	94.81	6.15	1.85	1.64	0.25	0.01	0.07	4.01	0.00	0.00
ST-94	Massive Flow	Groundmass	41.33	20.95	5.14	0.00	0.04	26.16	0.07	0.03	0.00	0.00	93.71	6.07	1.93	1.70	0.19	0.00	0.01	4.12	0.02	0.01
ST-94	Massive Flow	Groundmass	42.72	21.04	5.44	0.05	0.11	26.04	0.05	0.01	0.00	0.00	95.45	6.15	1.85	1.72	0.20	0.01	0.02	4.01	0.01	0.00
ST-94	Massive Flow	Groundmass	43.00	20.66	6.11	0.04	0.02	26.37	0.02	0.04	0.00	0.01	96.26	6.18	1.82	1.67	0.22	0.00	0.00	4.06	0.01	0.01
ST-94	Massive Flow	Groundmass	43.02	20.36	6.22	0.05	0.03	26.30	0.02	0.00	0.00	0.00	96.00	6.20	1.80	1.66	0.22	0.01	0.01	4.06	0.01	0.00
ST-94	Massive Flow	Groundmass	42.53	19.87	6.86	0.04	0.10	25.92	0.01	0.04	0.00	0.00	95.36	6.21	1.79	1.62	0.25	0.00	0.02	4.05	0.00	0.01
ST-94	Massive Flow	Groundmass	43.69	20.74	5.36	0.07	0.15	25.61	0.00	0.02	0.00	0.00	95.65	6.25	1.75	1.75	0.19	0.01	0.03	3.92	0.00	0.00

Appendix 4: Mean Prehnite Compositions

Sample	Lithology	n	SiO2 (wt%)	Al2O3 (wt%)	Fe2O3 (wt%)	MnO (wt%)	MgO (wt%)	CaO (wt%)	Na2O (wt%)	K2O (wt%)	F (wt%)	Cl (wt%)	Total (wt%)	Si	AlIV	AlVI	Fe	Mn	Mg	Ca	Na	K
Means																						
ST-64	Sediment	10	43.26	22.53	2.51	0.11	0.05	26.28	0.01	0.00	0.01	0.01	94.75	6.11	1.89	1.86	0.10	0.01	0.01	3.98	0.00	0.00
G-16	Pillow Basalt	23	43.36	21.42	3.88	0.05	0.01	26.00	0.06	0.01	0.06	0.00	94.78	6.19	1.81	1.80	0.14	0.01	0.00	3.98	0.02	0.00
ST-55	Pillow Basalt	6	43.19	22.54	2.92	0.10	0.29	25.90	0.01	0.00	0.04	0.00	94.95	6.11	1.89	1.86	0.10	0.01	0.06	3.92	0.00	0.00
ST-94	Massive Flow	8	42.59	20.54	6.01	0.04	0.10	26.02	0.03	0.02	0.05	0.00	95.36	6.17	1.83	1.68	0.22	0.01	0.02	4.04	0.01	0.00
Standard Deviations																						
ST-64	Sediment	10	0.31	0.71	0.95	0.04	0.06	0.14	0.01	0.00	0.02	0.01	0.29	0.03	0.03	0.05	0.03	0.01	0.01	0.04	0.00	0.00
G-16	Pillow Basalt	23	0.40	1.47	2.10	0.03	0.01	0.35	0.04	0.01	0.07	0.01	0.52	0.07	0.07	0.13	0.08	0.00	0.00	0.07	0.01	0.00
ST-55	Pillow Basalt	6	0.43	1.11	1.66	0.08	0.33	0.40	0.01	0.00	0.11	0.01	0.28	0.06	0.06	0.09	0.06	0.01	0.07	0.06	0.00	0.00
ST-94	Massive Flow	8	0.72	0.39	0.64	0.02	0.10	0.31	0.03	0.01	0.15	0.00	0.79	0.05	0.05	0.04	0.02	0.00	0.02	0.06	0.01	0.00
Relative Standard Deviations																						
ST-64	Sediment	10	0.7%	3.1%	37.9%	42.4%	113.0%	0.5%	114.1%	80.8%	316.2%	122.6%	0.3%	0.5%	1.7%	2.9%	34.9%	42.0%	112.8%	1.0%	113.8%	81.2%
G-16	Pillow Basalt	23	0.9%	6.9%	54.3%	66.5%	147.0%	1.4%	79.1%	95.5%	125.3%	147.9%	0.5%	1.2%	4.0%	7.3%	55.9%	66.1%	147.4%	1.7%	78.8%	95.5%
ST-55	Pillow Basalt	6	1.0%	4.9%	56.9%	76.8%	114.5%	1.6%	87.0%	154.9%	244.9%	123.2%	0.3%	0.9%	3.0%	5.0%	57.9%	77.0%	115.0%	1.6%	86.6%	154.9%
ST-94	Massive Flow	8	1.7%	1.9%	10.7%	48.0%	101.5%	1.2%	94.5%	66.2%	282.8%	186.7%	0.8%	0.9%	2.9%	2.5%	11.1%	47.6%	102.4%	1.4%	95.0%	66.3%

Appendix 4: Garnet Compositions

Sample	Lithology	Occurence	SiO_2 (wt%)	TiO_2 (wt%)	Al_2O_3 (wt%)	Fe_2O_3 (wt%)	MnO (wt%)	CaO (wt%)	Total (wt%)	And	Gross
ST-20	Pillow Basalt	Amygdule	35.15	0.00	0.05	32.62	0.34	32.62	100.78	99.77	0.23
ST-20	Pillow Basalt	Amygdule	35.27	0.00	0.03	32.72	0.32	32.43	100.76	99.84	0.16
ST-20	Pillow Basalt	Amygdule	35.38	0.02	0.10	31.86	0.11	33.05	100.51	99.53	0.47
ST-20	Pillow Basalt	Amygdule	35.49	0.00	0.06	32.11	0.38	32.33	100.36	99.71	0.29
ST-20	Pillow Basalt	Amygdule	34.90	0.00	0.17	32.54	0.08	33.32	101.00	99.20	0.80
ST-20	Pillow Basalt	Amygdule	35.31	0.00	0.16	32.05	0.17	33.05	100.75	99.21	0.79
ST-20	Pillow Basalt	Amygdule	34.94	0.03	0.01	32.94	0.17	32.65	100.73	99.97	0.03
ST-20	Pillow Basalt	Amygdule	35.03	0.02	0.07	32.54	0.19	32.57	100.41	99.65	0.35
ST-20	Pillow Basalt	Amygdule	35.24	0.00	0.01	32.44	0.10	32.94	100.73	99.97	0.03
ST-20	Pillow Basalt	Amygdule	35.42	0.04	0.09	32.34	0.13	33.03	101.04	99.56	0.44
ST-20	Pillow Basalt	Amygdule	35.29	0.02	0.24	31.48	0.04	33.50	100.57	98.82	1.18
ST-20	Pillow Basalt	Amygdule	35.44	0.01	0.15	32.20	0.10	33.13	101.03	99.30	0.70
ST-20	Pillow Basalt	Amygdule	34.85	0.01	0.04	32.88	0.20	32.75	100.72	99.79	0.21
ST-20	Pillow Basalt	Amygdule	35.35	0.02	0.31	31.61	0.15	33.07	100.51	98.47	1.53
ST-20	Pillow Basalt	Amygdule	34.34	0.00	0.15	32.43	0.18	32.66	99.76	99.28	0.72
ST-20	Pillow Basalt	Amygdule	34.46	0.00	0.10	32.27	0.15	32.81	99.79	99.50	0.50
ST-112	Massive Flow	Amygdule	35.98	0.01	0.98	30.64	0.51	32.72	100.84	95.24	4.76
ST-112	Massive Flow	Amygdule	37.21	0.00	8.56	19.88	0.92	33.58	100.15	59.71	40.29
ST-112	Massive Flow	Amygdule	35.44	0.00	0.22	31.80	0.33	32.86	100.64	98.95	1.05
ST-112	Massive Flow	Amygdule	37.09	0.05	8.19	20.68	0.69	33.91	100.61	61.72	38.28
ST-112	Massive Flow	Amygdule	35.48	0.05	0.31	31.39	0.15	32.93	100.31	98.47	1.53
ST-112	Massive Flow	Amygdule	37.30	0.09	9.97	17.72	0.41	33.87	99.35	53.16	46.84
ST-112	Massive Flow	Amygdule	35.89	0.03	0.22	31.80	0.17	32.91	101.02	98.93	1.07
ST-112	Massive Flow	Amygdule	37.54	0.08	9.43	18.57	0.34	34.72	100.68	55.69	44.31
ST-112	Massive Flow	Amygdule	35.67	0.00	0.00	32.38	0.23	33.03	101.31	100.00	0.00
ST-112	Massive Flow	Amygdule	37.23	0.10	8.31	20.27	0.30	33.91	100.10	60.91	39.09
ST-112	Massive Flow	Amygdule	35.71	0.00	0.20	31.78	0.16	33.08	100.94	99.00	1.00
ST-112	Massive Flow	Amygdule	37.50	0.11	9.40	18.62	0.24	34.28	100.15	55.85	44.15
ST-112	Massive Flow	Amygdule	35.30	0.00	0.36	31.73	0.17	32.92	100.48	98.27	1.73
ST-112	Massive Flow	Amygdule	36.90	0.06	7.44	21.73	0.22	34.03	100.38	65.09	34.91
ST-112	Massive Flow	Amygdule	35.32	0.05	0.00	31.81	0.21	32.87	100.26	100.00	0.00
ST-112	Massive Flow	Amygdule	36.46	0.03	6.00	23.28	0.19	33.68	99.64	71.24	28.76
ST-112	Massive Flow	Amygdule	35.62	0.00	1.46	29.68	0.17	32.82	99.75	92.84	7.16
ST-112	Massive Flow	Amygdule	36.57	0.02	7.02	22.02	0.22	33.92	99.77	66.71	33.29

Appendix 4: Mean Garnet Compositions

Sample	Lithology	n	SiO_2 (wt%)	TiO_2 (wt%)	Al_2O_3 (wt%)	Fe_2O_3 (wt%)	MnO (wt%)	CaO (wt%)	Total (wt%)	And	Gross
Means											
ST-20	Pillow Basalt	16	35.11	0.01	0.11	32.31	0.18	32.87	100.59	99.47	0.53
ST-112	Massive Flow	18	36.34	0.04	4.34	25.88	0.31	33.45	100.35	79.54	20.46
Standard Deviations											
ST-20	Pillow Basalt	16	0.34	0.01	0.08	0.42	0.10	0.32	0.38	0.41	0.41
ST-112	Massive Flow	18	0.83	0.04	4.14	5.89	0.21	0.61	0.52	19.45	19.45
Relative Standard Deviations											
ST-20	Pillow Basalt	16	1.0%	110.6%	77.6%	1.3%	54.6%	1.0%	0.4%	0.4%	78.2%
ST-112	Massive Flow	18	2.3%	99.7%	95.5%	22.8%	66.2%	1.8%	0.5%	24.4%	95.1%

Appendix 4: Carbonate Compositions

Sample	Lithology	Occurence	CaO (wt%)	MgO (wt%)	FeO (wt%)	MnO (wt%)	CO2 (wt%)	Total (wt%)	Cct	Mag	Sid	Rod
ST-65	Pillow Basalt	Vein	55.82	0.72	1.54	1.86	40.07	100	93.8	1.7	2.0	2.5
ST-65	Pillow Basalt	Vein	57.28	0.59	0.99	1.69	39.46	100	95.1	1.4	1.3	2.2
ST-96	Pillow Basalt	Amygdule	54.34	0.19	0.22	0.00	45.25	100	99.2	0.5	0.3	0.0
ST-96	Pillow Basalt	Amygdule	54.24	0.00	0.12	0.04	45.60	100	99.8	0.0	0.2	0.1
ST-25	Pillow Basalt	Groundmass	53.39	0.08	0.23	1.64	44.66	100	97.1	0.2	0.3	2.4
ST-25	Pillow Basalt	Groundmass	54.64	0.00	0.17	0.08	45.11	100	99.6	0.0	0.2	0.1
ST-25	Pillow Basalt	Groundmass	54.52	0.05	0.08	1.14	44.22	100	98.2	0.1	0.1	1.6
ST-25	Pillow Basalt	Groundmass	55.11	0.00	0.21	0.06	44.62	100	99.6	0.0	0.3	0.1
ST-25	Pillow Basalt	Groundmass	54.06	0.08	0.25	1.53	44.09	100	97.3	0.2	0.3	2.2
ST-25	Pillow Basalt	Groundmass	54.24	0.18	0.44	0.04	45.11	100	98.9	0.5	0.6	0.1
ST-25	Pillow Basalt	Groundmass	54.39	0.04	0.13	1.12	44.32	100	98.1	0.1	0.2	1.6
ST-25	Pillow Basalt	Groundmass	54.71	0.01	0.15	0.06	45.08	100	99.7	0.0	0.2	0.1
ST-25	Pillow Basalt	Groundmass	53.83	0.04	0.15	0.88	45.10	100	98.4	0.1	0.2	1.3
ST-25	Pillow Basalt	Groundmass	54.39	0.03	0.19	0.04	45.35	100	99.6	0.1	0.3	0.1
ST-66	Fault Gouge	Vein	51.18	0.01	0.23	0.07	48.52	100	99.5	0.0	0.3	0.1
ST-66	Fault Gouge	Groundmass	54.26	0.00	0.00	0.02	45.72	100	100.0	0.0	0.0	0.0
ST-66	Fault Gouge	Groundmass	54.91	0.00	0.07	0.08	44.94	100	99.8	0.0	0.1	0.1
ST-66	Fault Gouge	Groundmass	55.12	0.00	0.10	0.07	44.72	100	99.8	0.0	0.1	0.1
ST-66	Fault Gouge	Groundmass	54.89	0.00	0.22	0.04	44.85	100	99.6	0.0	0.3	0.1
ST-94	Massive Flow	Amygdule	55.64	0.02	0.03	0.04	44.27	100	99.8	0.0	0.0	0.1
ST-94	Massive Flow	Amygdule	55.41	0.01	0.23	0.04	44.32	100	99.6	0.0	0.3	0.1
ST-94	Massive Flow	Groundmass	55.13	0.03	0.15	0.03	44.67	100	99.7	0.1	0.2	0.0
ST-94	Massive Flow	Groundmass	55.86	0.06	0.23	0.14	43.71	100	99.3	0.1	0.3	0.2
ST-94	Massive Flow	Amygdule	55.15	0.01	0.08	0.07	44.70	100	99.8	0.0	0.1	0.1
ST-94	Massive Flow	Amygdule	55.10	0.04	0.15	0.13	44.59	100	99.5	0.1	0.2	0.2
ST-103	Pillow Basalt	Groundmass	53.65	0.14	0.32	0.13	45.76	100	99.0	0.3	0.5	0.2
ST-103	Pillow Basalt	Vein	53.88	0.12	0.51	0.08	45.42	100	98.9	0.3	0.7	0.1
ST-112	Massive Flow	Amygdule	56.29	0.00	0.00	0.12	43.59	100	99.8	0.0	0.0	0.2
ST-112	Massive Flow	Amygdule	50.52	0.93	0.05	7.65	40.85	100	87.3	2.2	0.1	10.4
ST-112	Massive Flow	Amygdule	54.06	0.94	0.31	5.28	39.41	100	90.4	2.2	0.4	7.0
ST-112	Massive Flow	Amygdule	56.82	0.37	0.40	2.89	39.52	100	94.8	0.9	0.5	3.8
ST-112	Massive Flow	Amygdule	47.41	1.10	0.09	10.22	41.18	100	83.0	2.7	0.1	14.1
ST-112	Massive Flow	Amygdule	48.46	1.21	0.10	8.47	41.76	100	85.1	3.0	0.1	11.8
ST-112	Massive Flow	Amygdule	56.87	0.02	0.09	0.05	42.97	100	99.8	0.0	0.1	0.1
ST-112	Massive Flow	Amygdule	49.49	0.60	0.09	8.20	41.62	100	87.0	1.5	0.1	11.4
ST-112	Massive Flow	Amygdule	56.86	0.03	0.14	0.23	42.74	100	99.4	0.1	0.2	0.3
ST-112	Massive Flow	Amygdule	54.37	0.36	0.03	5.30	39.94	100	92.0	0.8	0.0	7.1

Appendix 4: Mean Carbonate Compositions

Sample	Lithology	n	CaO (wt%)	MgO (wt%)	FeO (wt%)	MnO (wt%)	CO2 (wt%)	Total (wt%)	Cct	Mag	Sid	Rod
Means												
ST-65	Pillow Basalt	2	56.55	0.65	1.26	1.77	39.77	100	94.5	1.5	1.6	2.3
ST-96	Pillow Basalt	2	54.29	0.10	0.17	0.02	45.42	100	99.5	0.2	0.2	0.0
ST-25	Pillow Basalt	10	54.33	0.05	0.20	0.66	44.77	100	98.6	0.1	0.3	0.9
ST-66	Fault Gouge	5	54.07	0.00	0.12	0.05	45.75	100	99.7	0.0	0.2	0.1
ST-94	Massive Flow	6	55.38	0.03	0.15	0.07	44.38	100	99.6	0.1	0.2	0.1
ST-103	Pillow Basalt	2	53.76	0.13	0.41	0.11	45.59	100	98.9	0.3	0.6	0.2
ST-112	Massive Flow	10	53.12	0.56	0.13	4.84	41.36	100	91.9	1.3	0.2	6.6
Standard Deviations												
ST-65	Pillow Basalt	2	1.03	0.09	0.39	0.12	0.43	0	0.9	0.2	0.5	0.2
ST-96	Pillow Basalt	2	0.07	0.14	0.07	0.03	0.25	0	0.4	0.3	0.1	0.0
ST-25	Pillow Basalt	10	0.48	0.05	0.10	0.67	0.45	0	1.0	0.1	0.1	1.0
ST-66	Fault Gouge	5	1.65	0.00	0.10	0.02	1.60	0	0.2	0.0	0.1	0.0
ST-94	Massive Flow	6	0.32	0.02	0.08	0.05	0.37	0	0.2	0.0	0.1	0.1
ST-103	Pillow Basalt	2	0.16	0.01	0.13	0.03	0.24	0	0.1	0.0	0.2	0.1
ST-112	Massive Flow	10	3.78	0.47	0.13	3.83	1.46	0	6.3	1.1	0.2	5.3
Relative Standard Deviations												
ST-65	Pillow Basalt	2	0.02	0.14	0.31	0.07	0.01	0	0.0	0.2	0.3	0.1
ST-96	Pillow Basalt	2	0.00	1.41	0.40	1.41	0.01	0	0.0	1.4	0.4	1.4
ST-25	Pillow Basalt	10	0.01	1.06	0.49	1.02	0.01	0	0.0	1.1	0.5	1.0
ST-66	Fault Gouge	5	0.03	2.24	0.79	0.45	0.03	0	0.0	2.2	0.8	0.4
ST-94	Massive Flow	6	0.01	0.75	0.54	0.67	0.01	0	0.0	0.7	0.5	0.7
ST-103	Pillow Basalt	2	0.00	0.10	0.32	0.33	0.01	0	0.0	0.1	0.3	0.3
ST-112	Massive Flow	10	0.07	0.84	0.97	0.79	0.04	0	0.1	0.8	0.9	0.8

Appendix 5: Sample Calculations and Error Propagations

In the following calculations, "E" refers to the absolute error, whereas "%E" refers to the relative error in percent.

Calculation of FeO and Fe_2O_3 from $Fe_2O_3^T$:

wt% FeO = wt% $Fe_2O_3^T$ × 0.8998 g FeO/g Fe_2O_3 × 0.85.
9.77 wt% FeO = 12.8 wt% $Fe_2O_3^T$ × 0.8998 g FeO/g Fe_2O_3 × 0.85.

$\%E_{FeO} = \%E_{Fe2O3T}$
$\%Acc_{FeO} = \%Acc_{Fe2O3T} = 1.0\%$

wt% Fe_2O_3 = wt% $Fe_2O_3^T$ × 0.15.
1.92 wt% Fe_2O_3 = 12.8 wt% $Fe_2O_3^T$ × 0.15.

$\%E_{Fe2O3} = \%E_{Fe2O3T}$
$\%Acc_{Fe2O3} = \%Acc_{Fe2O3T} = 1.0\%$

Recalculation of weight percent oxides to 100 wt% anhydrous total:

wt% $SiO_{2(anhyd)}$ = wt%$SiO_{2(hyd)}$/$total_{(hyd)}$ × 100%
52.1 wt% SiO_2 = 50.1 wt% SiO_2/96.11% × 100%

$\%E_{SiO2(anhyd)} = \%E_{SiO2(hyd)}$
$\%Acc_{SiO2(anhyd)} = \%Acc_{SiO2(hyd)} = 0.5\%$
This calculation applies to all major element weight percent oxides.

Calculation of Mg#:

Mg# = moles Mg/(moles Mg + moles Fe)
Mg# = wt% MgO/40.30 g/mol / (wt% MgO/40.30 g/mol + wt% FeO/71.85 g/mol)
0.52 = 6.25%/40.30 g/mol / (6.25%/40.30 g/mol + 10.2%/71.85 g/mol)

$$\%E_{Mg\#} = (\%E_{MgO}^2+(((E_{MgO}/40.30\ g/mol)^2+(E_{FeO}/71.85\ g/mol)^2)^{1/2}/ (MgO/40.30\ g/mol + FeO/71.85\ g/mol))^2)^{1/2}$$

$$\%Acc_{Mg\#} = (1\%^2+(((0.0625\ wt\%/40.30\ g/mol)^2+(0.102\ wt\%/71.85\ g/mol)^2)^{1/2}/ (6.25\ wt\%/40.30\ g/mol + 10.2\ wt\%/71.85\ g/mol))^2)^{1/2} = 1.24\%$$

Appendix 5: Sample Calculations and Error Propagations

Calculation of ΔNb:

$\Delta Nb = 1.74 + \log(Nb/Y) - 1.92 \times \log(Zr/Y)$
$\Delta Nb = 1.74 + \log(6\ ppm/29\ ppm) - 1.92 \times \log(95\ ppm/29\ ppm)$
$\Delta Nb = 0.06$

$E_{\Delta Nb} = ((0.434\times(\%E_{Nb}^2 + \%E_Y^2)^{½})^2 + (1.92\times0.434\times(\%E_{Zr}^2 + \%E_Y^2)^{½})^2)^{½}$
$Prec_{\Delta Nb} = ((0.434\times(1.6\%^2 + 0.01\%^2)^{½})^2 + (1.92\times0.434\times(0.5\%^2 + 0.01\%^2)^{½})^2)^{½}$
$Prec_{\Delta Nb} = 0.8$

Calculation of Europium anomaly:

$Eu^* = Eu_N/(Sm_N\times Gd_N)^{½} = 16.7/(21.6\times21.3)^{½} = 0.78$

$\%E_{Eu^*} = (\%E_{Eu}^2 + ((\%E_{Sm}^2 + \%E_{Gd}^2)^{½}/2)^2)^{½}$
$\%Acc_{Eu^*} = (4.9\%^2 + ((1.6\%^2 + 8.6\%^2)^{½}/2)^2)^{½} = 6.6\%$

Calculation of $(La/Sm)_N$:

$(La/Sm)_N = La_N/Sm_N = 20.0/21.6 = 0.93$

$\%E_{(La/Sm)N} = (\%E_{La}^2 + \%E_{Sm}^2)^{½}$
$\%Acc_{(La/Sm)N} = (3.0\%^2 + 1.6\%^2)^{½} = 3.4\%$

The calculation of $(La/Yb)_N$ is identical.